THE UNIVERSITY
of EDINBURGH

EVOLUTION IN THE HIGH-ALTITUDE PÁRAMO ECOSYSTEM

MARÍA CAMILA GÓMEZ GUTIÉRREZ

PHD THESIS
THE UNIVERSITY OF EDINBURGH
2016

I declare that this thesis was composed by me. The work presented is my own unless otherwise acknowledged and has not been submitted for any other degree.

Edinburgh, 22/04/2016

ACKNOWLEDGEMENTS

I would like to warmly thank the following individuals/institutions for their support.

The School of Biological Sciences Scholarship (The University of Edinburgh) for funding my studies and this project.

My supervisors James Richardson, Toby Pennington and Richard Milne for their guidance and unconditional support. I also want to thank Santiago Madriñán for his contributions to this project.

The herbaria at Aarhus University, Universidad de los Andes, National Herbarium of the Netherlands (Leiden and Utrecht) and New York Botanical Garden, for providing me with samples. In particular, I would like to thank Fabián Michelangeli (NYBG) for his expert advice on Melastomataceae.

The STS laboratory staff at the Royal Botanic Garden Edinburgh for all their technical support. Linda Neaves for her expert advice on population genetics.

Suzanne Harris, Max Coleman and rbgeColombia with whom I have collaborated in various science communication events, working with them greatly helped me improve my science communication skills and find my career path.

My dear friends Karina, Eugenio and Julieth for devoting their time discussing with me ideas related to this project and for supporting me with their friendship during difficult (and not so difficult) times.

Boni, Natalia and Rocío for being my family in Edinburgh.

My beloved family, that is, my parents and sisters for being who they are! A special thanks to my sister Toté for helping me with the edition of all figures.

And finally, Andreas for being my life's soundtrack.

ABSTRACT

The Páramo ecosystem is the most diverse high-altitude ecosystem on Earth with more than 4000 species of vascular plants. A naturally fragmented ecosystem, it also houses one of the youngest and fastest evolving biota. In this thesis, molecular data from the South American species of *Oreobolus* (Cyperaceae) and Páramo representatives within the Melastomeae tribe (Melastomataceae) were used to investigate the impact of Andean orogeny and recent climatic fluctuations on diversification processes.

Chapter Two highlights the role of Andean uplift in the diversification of Páramo species of *Oreobolus* as shown by their faster diversification rates compared to other southern hemisphere species. It is suggested that *Oreobolus* may have reached South America from Australia during the Pliocene through two independent long-distance dispersal events to the northern and southern Andes. This strong north-south geographic structure is evident in the species phylogeny. Chapter Three is a phylogeographic study of the South American species of *Oreobolus* that reveals complex relationships between and within species. Levels of haplotype sharing, measures of genetic distinctiveness and recent divergence times point to incomplete lineage sorting confounding species boundaries. Additionally, the role in species diversification of the contraction and expansion of Páramo islands during the climatic fluctuations of the Quaternary is supported by genetic data. Chapter Four showed that colonisation of Páramo within the largely Neotropical Melastomeae

tribe occurred repeatedly during the Pliocene. Species-poor Páramo lineages such as *Castratella* may highlight a possible role for extinction in some taxa. In Chapter Four I also suggested that frost adapted temperate lineages may have had an adaptative advantage that may have contributed towards a greater number of species at higher elevations.

LAY SUMMARY

The Páramo ecosystem in northwest South America is the most diverse high-altitude ecosystem on Earth housing more than 4000 species of vascular plants, of which 60% cannot be found anywhere else. A young ecosystem, the Páramo appeared following the final uplift of the Andes mountain range c. five million years (Ma) before the present. Given its young geological age but massive diversity, it has been hypothesised that both mountain uplift and recent climatic fluctuations (ice cycles of the Quaternary) had a positive impact on the formation of Páramo species. The aim of this thesis is to determine the effects of these abiotic events on Páramo representatives of *Oreobolus* R.Br., a genus in the sedge family (Cyperaceae), and the largely tropical Melastomaeae tribe in the family Melastomaceae. I used DNA to reconstruct genetic relationships amongst Páramo and southern temperate species of *Oreobolus* and other closely related genera. Additionally, I used the age of fossil relatives to provide a time-scale for evolutionary events and thus infer the impact of geological events. To provide further insight into the genetic relationships between and within the Páramo species of *Oreobolus*, I used a population genetics approach that allowed for comparison of multiple individuals per species across their entire distribution range. The study of populations assessed the impact of recent climatic events (from 2 Ma) as these would have influenced their current distribution. I also reconstructed the genetic relationships of Páramo representatives within the Melastomeae tribe and assigned a time-scale to these. Finally, I tested statistically if

frost-resistant plant lineages were more diverse at higher altitudes than non-resistant ones. For both the Páramo species of *Oreobolus* and Páramo representatives of Melastomeae, species formation is associated with Andean uplift. *Oreobolus* Páramo species showed higher rates of diversification than their southern temperate counterparts, while in the Melastomeae species-poor Páramo lineages highlight the importance of extinction in the diversification process. Similarly, current distribution of *Oreobolus* populations and complex genetic relationships between and within species are largely associated with recent climatic events. Frost-resistant and non-resistant lineages were found to be equally diverse at higher altitudes.

TABLE OF CONTENTS

LIST OF TABLES

LIST OF FIGURES

CHAPTER ONE. REVIEW

1.1 SPECIES DIVERSIFICATION

Species concepts are still widely debated. At least 25 different concepts exist of which Mayr's (1995) Biological Species Concept (BSC) is the most accepted. This author defined species as "groups of interbreeding natural populations that are reproductively isolated from other such groups". This definition was subsequently amended by Coyne and Orr (2004) who defined distinct species as "characterised by substantial but not necessarily complete reproductive isolation". Such reproductive isolation is fundamentally based on isolating barriers – i.e. biological characteristics of organisms that restrain the exchange of genetic material with individuals from other populations (Coyne & Orr, 2004). These include premating isolating barriers (i.e. behavioural isolation, ecological isolation or mechanical isolation), postmating prezygotic isolating barriers (i.e. gametic isolation) and postmating postzygotic isolating barriers (i.e. extrinsic or intrinsic inviability). While the BSC is the most widely accepted species concept, it shows limitations when applied to hybridisation and uniparental organisms (i.e. apomictic plant species) (Coyne & Orr, 2004).

Various processes may lead to the formation of a new species. The most controversial one is sympatric speciation, the process by which co-occurring populations become isolated by cause of intrinsic biological features promoting the appearance of a reproductive barrier that may lead to the formation of new species

through mutation, reinforcement and/or genetic drift (Coyne & Orr, 2004). A commonly cited example of sympatric speciation in plants arises from the palm family (Arecaceae). Savolainen et al. (2006) suggested that two co-occurring species of *Howea* from an oceanic island evolved in sympatry as a result of substrate specialisation and differences in flowering times. An important mechanism in sympatric speciation is allopolyploidization as polyploid organisms are usually unable to interbreed with their ancestors because of differences in ploidy numbers (Coyne & Orr, 2004; Abbott et al., 2013). A second mode of speciation, parapatric speciation, is commonly related to adaptation to local habitats. This process refers to the formation of species as a consequence of partial reproductive isolation between populations with no apparent geographic barrier (Coyne & Orr, 2004). In allopatric speciation the appearance of geographical barriers such as rivers or mountains divides a once continuous population into two or more smaller populations. These will be geographically isolated which will eventually lead to their genetic differentiation through mutation, genetic drift and/or natural selection (Coyne & Orr, 2004).

1.2 GEOLOGICAL HISTORY

1.2.1 The isolation of the South American continent

The super-continent of Gondwana occupied the southern hemisphere from the Palaeozoic to the mid-Mesozoic encompassing the modern landmasses of South America, Africa, Madagascar, the Arabian Peninsula, India, Australia, New Zealand and Antarctica (McLoughlin, 2001). Gondwana and the northern hemisphere super-

continent of Laurasia (North America and Eurasia) formed a unique landmass, Pangaea until their separation during the mid-Jurassic c. 180 - 165 Ma (Dietz & Holden, 1970). Since the Jurassic, between 180 and 35 Ma, the major stages of Gondwanan break-up occurred (Fig. 1.1; McLoughlin, 2001). An initial fracture into West (South America and Africa) and East Gondwana along the southern and eastern coasts of the contemporary African continent occurred during the Middle to Upper Jurassic, c. 165 – 162 Ma (Fig. 1.1; McLoughlin, 2001). With the expansion of the South Atlantic Ocean c. 135 – 130 Ma, continental breakup followed gradually, although the equatorial section of the two continents was connected until 119 – 105 Ma (Fig. 1.1; McLoughlin, 2001). Subsequently, South America separated from west Antarctica during the late Eocene c. 35 – 30.5 Ma (Fig. 1.1; McLoughlin, 2001). However, a deep marine passage was not established until the Oligocene, c. 32 – 28 Ma hence the Antarctic peninsula may have played an important role as a corridor for terrestrial vascular plants between Australia and South America until early Oligocene times (Raven & Axelrod, 1974; McLoughlin, 2001; Hoorn et al., 2010).

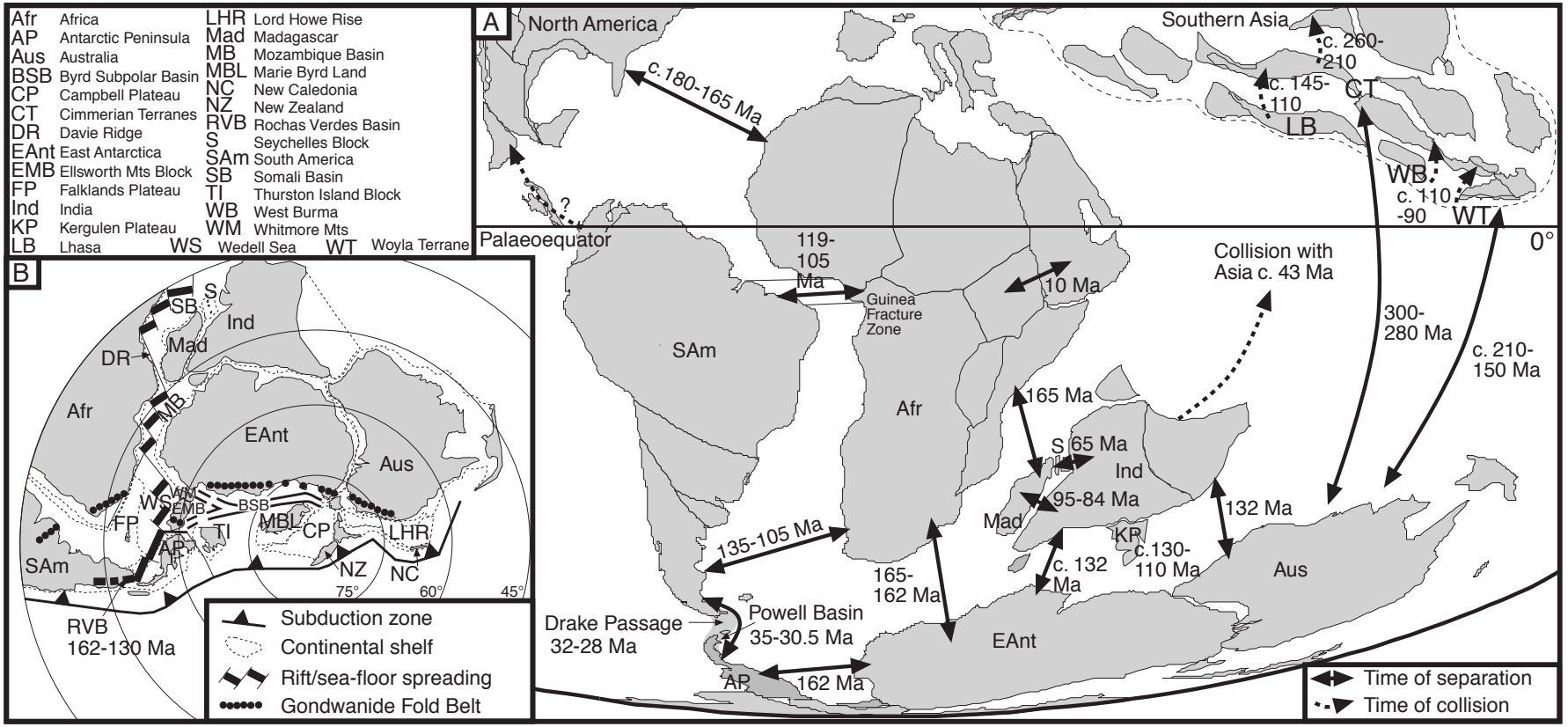

Figure 1.1. Summary of Gondwana breakup episodes and their estimated age (from McLoughlin, 2001).

1.2.2 The Andes orogeny

The Andean orogeny was crucial for diversification processes in Neotropical regions, affecting dispersal and promoting allopatric speciation, ecological displacement and habitat heterogeneity (e.g. Antonelli et al., 2009; Hoorn et al., 2010).

The Andean uplift started from the late Cretaceous with the collision between a volcanic arc and the western margin of the South American continent (Gregory-Wodzicki, 2000; Mora et al., 2010). Since then and mostly during the late Cenozoic (c. 30 Ma), there was a gradual uplift resulting from the subduction of the Nazca plate beneath the South American plate (Fig. 1.2) (Gregory-Wodzicki, 2000; Graham, 2009; Mora et al., 2010).

The southern Andes section (55ºS – 47ºS) is the lowest in elevation (average elevation of 1km) as well as the oldest. Its origin goes back to the early Mesozoic, partially as a consequence of the opening of the Atlantic Ocean and principally as the result of the subduction of the Antarctic Plate beneath the South American Plate (Fig. 1.2; Graham, 2009). By the mid-Miocene c. 17 – 14 Ma, this section had reached its current elevation (Graham, 2009). The uplift of the central Andes section (47ºS – 2ºN) started during the Cenozoic as a result of the subduction of the Nazca Plate beneath the South American Plate (Fig. 1.2) (Graham, 2009; Mora et al., 2010). The uplift of this section was a west to east process and by the mid-Miocene c. 15 Ma, half of its current altitude (1500 – 2000 km) had been reached (Fig. 1.3) (Graham, 2009; Mora et al., 2010). Since then, the western slope of the central Andes has had an arid climate partially as a consequence of the development of a rain shadow (Gregory-Wodzicki, 2000; Garzione et al., 2008). A final period of intense uplift

followed during the late Miocene – early Pliocene, c. 10 – 6 Ma (Gregory-Wodzicki, 2000; Garzione et al., 2008).

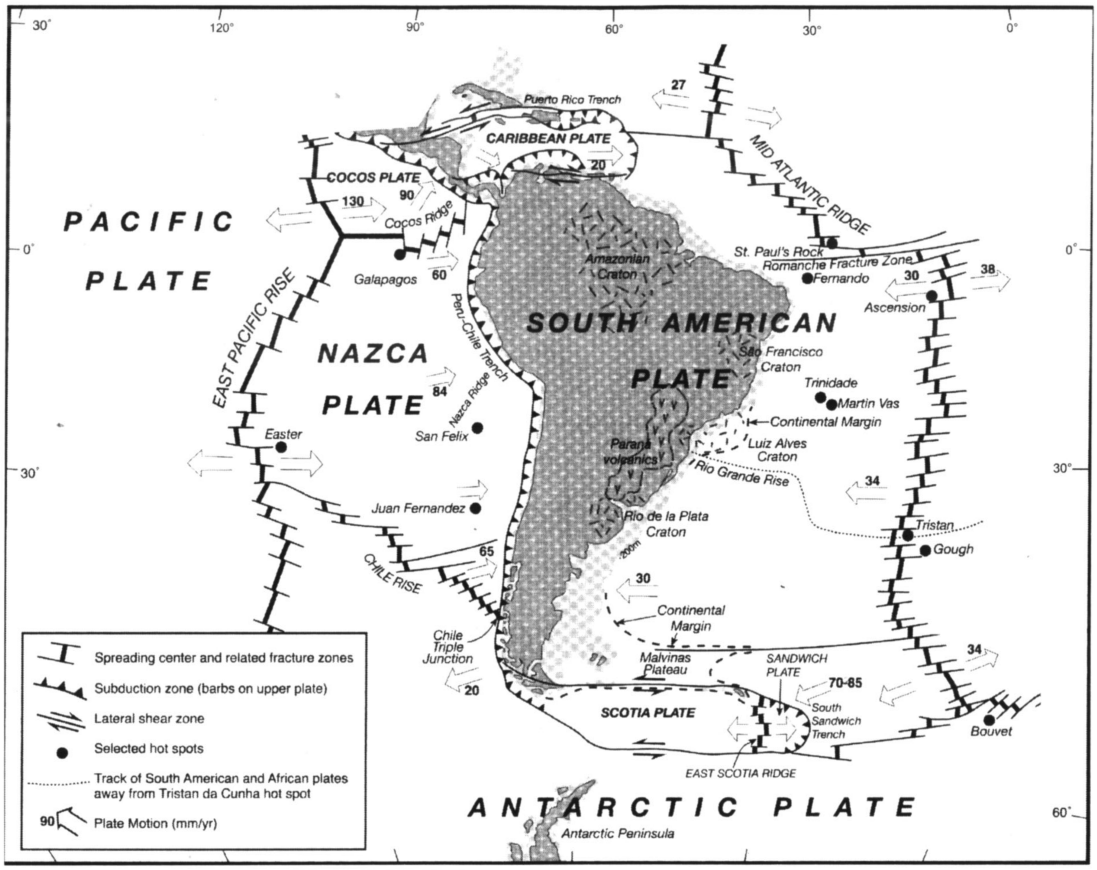

Figure 1.2. Tectonic plates acting on southern Central America and South America (from Graham, 2009).

The northern Andes section (2ºS – 12ºN) is the youngest and it branches into three Cordilleras – Eastern, Central and Western – above the Equator (Fig. 1.3) (Graham, 2009). The uplift of the three cordilleras was not contemporaneous, while uplift of the Central and Western Cordilleras began in the Paleocene, uplift of the Eastern Cordillera occurred mostly during the Pliocene (Gregory-Wodzicki, 2000; Hooghiemstra et al., 2006). By the mid-Miocene c. 14 Ma, the latter had reached no

more than 40% of its current altitude and was located in the tropical vegetation belt (van der Hammen, 1974; Gregory-Wodzicki, 2000; Hooghiemstra et al., 2006; Graham, 2009; Mora et al., 2010). Following a final episode of intense and rapid mountain building during the Pliocene c. 5 – 2 Ma, the Eastern Cordillera reached its modern altitude (Fig. 1.3) (Gregory-Wodzicki, 2000; Hooghiemstra & van der Hammen, 2004; Hoorn et al., 2010).

All sections of the Andes had reached their current altitude when the climatic fluctuations of the Quaternary started. In the Tropics, changes in the distribution of biota have been associated with these climatic events (e.g. Haffer, 1969; Hewitt, 2004). However, contrary to the latitudinal movements of vegetation belts observed in temperate regions, in the tropics migration was rather altitudinal (van der Hammen, 1974; Simpson, 1975; Gregory-Wodzicki, 2000; Hooghiemstra & van der Hammen, 2004; Garzione et al., 2008; Graham, 2009; Mora et al., 2010).

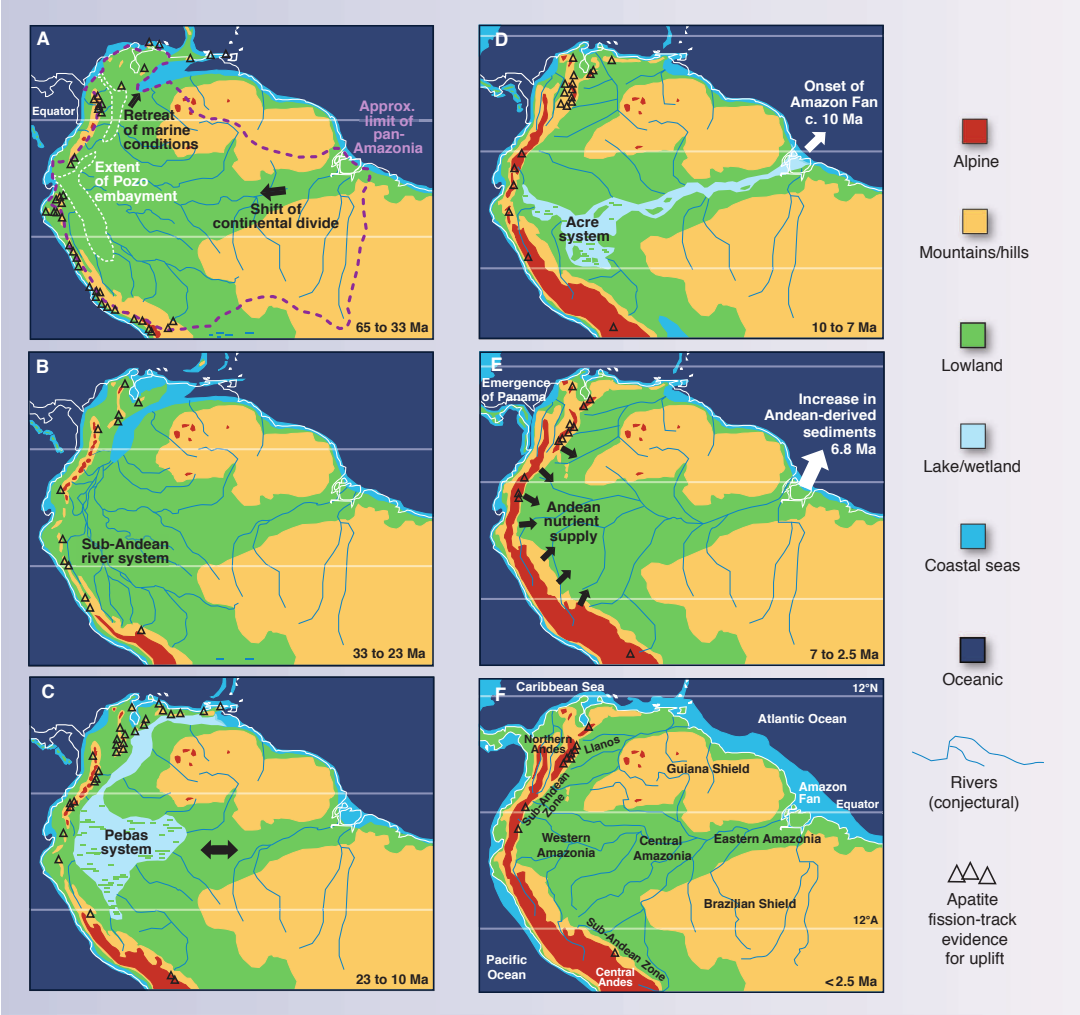

Figure 1.3. Palaeogeographic reconstruction of the stages of Andean uplift (from Hoorn et al., 2010).

1.3 USING MOLECULAR DATA TO TEST BIOGEOGRAPHIC HYPOTHESES

1.3.1 Molecular phylogenetics

Since the 1990s huge advances have been made in phylogenetic reconstruction largely through the introduction of techniques such as PCR and automated sequencing. These facilitated the production of large amounts of DNA sequence data providing hundreds to thousands of markers, e.g. APGIII (2009). The principal

advantage of DNA sequence data is not only the huge number of characters that can be generated but also the fact that many of those characters will be under minimal selection pressure. These molecular data are available in a number of different compartments within the plant cell some of which are inherited in different ways. While nuclear genes are biparentally inherited, chloroplast genes are generally maternally inherited in Angiosperms but paternally inherited in Gymnosperms (Ennos, 1994). The use of molecular data from chloroplast genes will allow the assessment of dispersal patterns whereas the nuclear genes allow for better circumscription of taxa as they are generally more variable (e.g. Naciri & Linder, 2015).

Phylogenies may be reconstructed following the principle of parsimony that state that the best fitted phylogenetic hypothesis will be the one with the least number of changes (Camin & Sokal, 1965). Following criticism that evolution may not be parsimonious, methods based on probabilistic models appeared. First, the maximum likelihood algorithm (ML) proposed a set of evolutionary models within which nucleotide and amino acid evolution could be framed and based on those the most likely phylogenetic hypothesis given the data can be reconstructed (Felsenstein, 1981). More recently, Bayesian statistics were applied to construct phylogenetic hypotheses. Making use of the same set of evolutionary models of ML, BI infers the posterior distribution of the phylogenetic tree and the model given the likelihood of the data (Huelsenbeck et al., 2001). Partly as a result of being more computationally efficient, BI is widely used in molecular phylogenetics.

Molecular phylogenies are widely used in the study of biogeography through the estimation of divergence times of lineages. Molecular dating relies on a modified

version of the molecular clock theory postulated by Zuckerkandl and Pauling (1962), that is the idea that all molecules evolved at the same rate in a clock-like fashion. The relaxed molecular clock theory integrated the caveat that many molecules did not evolve in a clock like fashion by permitting differential rates amongst lineages for the same molecule (Huelsenbeck et al., 2000). Sanderson (1997) incorporated this idea into the phylogenetic framework with the Non-Parametric Rate Smoothing (NPRS) and Penalized Likelihood (PL) algorithms. Sanderson (1997) postulated that, assuming there are differential rates across the branches of a phylogenetic tree, if one or various calibration points are set, a divergence time can be estimated for that particular set of taxa. Bayesian approaches are now implemented using Markov chain Monte Carlo (MCMC) for the same purpose (Drummond & Rambaut, 2007). Importantly, the Bayesian approach allowed for the incorporation of uncertainty through the establishment of parametric distributions on calibrated nodes (Ho & Phillips, 2009).

Four types of calibration can be used for molecular dating including the use of substitution rates, fossils, geological events (i.e. such as the splitting of continents or the emergence of oceanic islands) and secondary calibrations (Sauquet, 2013). Of these, fossil calibrations are the most widely used. These are placed at specific nodes in the phylogeny that contain all extant species sharing similar morphological characters with the fossil, providing an estimate age for that clade. However, it is important to consider this technique's limitations. Fossils only provide minimum age estimates as the taxon of the fossil may have evolved much earlier than the time at which the fossil was preserved. Molecular dating from fossil calibrations may give equivocal results if they are incorrectly placed in the phylogeny or not correctly

dated (Gandolfo et al., 2008). These limitations can be overcome with the inclusion of multiple fossil calibrations as well as expert knowledge of the group under study (Renner, 2005; Gandolfo et al., 2008). Furthermore, it is critical to include the uncertainty of evolutionary rates and calibration times through selection of models that adequately fit the data (Drummond et al., 2006).

The molecular dating approach as a way to estimate divergence times has had a massive impact on the study of biogeography, allowing for the comparison of the timing of divergence of lineages with the timing of geological events. In this manner hypotheses related to the impact of deep-time geological events on the diversification and distribution of taxa can be tested. An excellent example is the effect of the Andean orogeny on the contemporary distribution of plant diversity in South America. Through the comparison of Andean geological history with the estimated divergence times of numerous plant groups, researchers have demonstrated that the uplift of the Andes has acted both as a vicariant barrier and as a north-south dispersal corridor besides providing new high-altitude habitats (reviewed in Luebert & Weigend, 2014).

In addition to the estimation of divergence times, the directionality of migration can also be estimated from molecular phylogenies, addressing another fundamental question in biogeographic research related to the ancestral origin and pattern of migration of taxa. Methods to reconstruct ancestral areas have developed with molecular phylogenetics, and range from parsimony-based methods such as Dispersal-Vicariance Analysis (DIVA; Ronquist, 1997), to likelihood-based methods such as the Dispersal-Extinction Cladogenesis (DEC) model implemented in LAGRANGE (Ree et al., 2005; Ree & Smith, 2008) and finally to Bayesian-based

methods like those implemented in BayArea (Landis et al., 2013) or in RASP (Bayesian Binary Model; Yu et al., 2015).

Another use of molecular phylogenies is to estimate changes in diversification rates which could be either associated with extrinsic (e.g. geological, ecological) or intrinsic (e.g. floral adaptations, changes photosynthetic pathway) events. Changes can be identified across the phylogeny showing faster or slower evolutionary rates explaining differences in species diversity (Magallón & Sanderson, 2001; Rabosky & Lovette, 2008; Donoghue & Sanderson, 2015).

1.3.2 Phylogeography

Phylogeography reconciles the disciplines of phylogenetics and population genetics bringing together micro- and macro-evolutionary processes (Avise, 2009). Avise (2000) defined it as the study of "the principles and processes governing the geographic distributions of genealogical lineages, especially those within and among closely related species". This approach is particularly relevant when testing the impact of recent ecological and/or climatic events (e.g. climatic fluctuations of the Quaternary) on the genetic structure and distribution of taxa, allowing exploration of relationships amongst biogeographic areas and assessment of the recent history of species and/or populations (Avise et al., 1987; Bermingham & Moritz, 1998; Avise, 2000; Petit et al., 2003; Beheregaray, 2008; Avise, 2009). Numerous studies have used a phylogeographic approach to try to infer the relationships and history of populations but most of this work has focused on temperate regions (e.g. Dumolin-Lapègue et al., 1997; Hewitt, 2004). Studies on South America taxa are relatively few (e.g. Honorio Coronado et al., 2014; reviewed in Turchetto-Zolet et al., 2013)

and there have been no studies for high altitude plant taxa in northern South America.

1.4 THE PÁRAMO ECOSYSTEM

1.4.1 Geographic distribution and ecology

Páramo is a high-altitude ecosystem that is discontinuously distributed between 11ºN and 8ºS, and between 83ºW and 70ºW; it is mostly concentrated in Colombia, Venezuela and Ecuador, although some outliers are found in Costa Rica, Panamá and northern Peru (Fig. 1.4) (Smith & Cleef, 1988; Luteyn, 1999). This ecosystem is naturally fragmented, occupying the mountaintops of the northern segment of the Andes Mountain Range and the Talamanca Cordillera in southern Central America, between (2800-) 3000 and 5000 m.a.s.l. (Luteyn, 1999). It extends from the upper limit of the continuous forest up to the permanent snowline, covering an approximate area of 37,500 km^2 (Buytaert et al., 2010).

Páramo has been traditionally divided into three altitudinal vegetation zones, namely Subpáramo (2800 – 3500 m), Páramo (3500 – 4400 m) and Superpáramo (4000 – 5000 m) and there is a general trend to lower growing vegetation as altitude increases (Cuatrecasas, 1958; van der Hammen, 1974; Hooghiemstra & van der Hammen, 2004; Buytaert et al., 2010). The Subpáramo zone is characterised by a shrub forest mostly dominated by species in the Ericaceae, Melastomataceae and Asteraceae (Luteyn, 1999). The Páramo zone is dominated by tussock grasses of *Calamagrostis* species (Poaceae) on the dry slopes and species of *Chusquea* (Poaceae) on the wet slopes (Luteyn, 1999). In the Superpáramo, the vegetation is scarce and sparse

possibly due to the adverse conditions of frequent frosts and unstable soil caused by frost heaving (van der Hammen, 1974; van der Hammen & Cleef, 1986; Hooghiemstra et al., 2006; Madriñán et al., 2013).

Figure 1.4. Geographic delimitation of the Páramo ecosystem (light red) in northwest South America and southern Central America (from Madriñán et al., 2013).

Páramos are in general cold and wet, but local microclimates are the norm (Sarmiento, 1986). For instance, precipitation ranges from 500 mm in the driest parts of Ecuadorian and Peruvian páramos to 3000 mm in Colombia, these patterns are

mainly due to the irregular topography and elevation as well as the influence of different air masses (Sarmiento, 1986; Luteyn, 1999; Buytaert et al., 2010). An outstanding characteristic of páramos is what has been described as "summer every day and winter every night" (Hedberg, 1964) with daily temperature variation ranging from below freezing to as much as 30ºC (Sarmiento, 1986). Furthermore, with a difference of 9ºC in average daily temperature between Subpáramo and Superpáramo, it is temperature that largely determines the zonation of the vegetation belts (Sarmiento, 1986; Hooghiemstra & van der Hammen, 2004; Hooghiemstra et al., 2006). This temperature variation imposes a huge constraint on Páramo plants (Luteyn, 1999). Plants require adaptations to cold, including frost tolerance, and assimilation of nutrients is slow as a consequence of insufficient light and low temperatures (Sarmiento, 1986; Beck, 1994). Despite these difficult conditions, the Páramo flora is the most diverse high-altitude flora in the world with as much as 60% of its c. 4000 plant species, endemic (van der Hammen & Cleef, 1986; Smith & Cleef, 1988; Sklenář et al., 2014).

1.4.2 The palaeopalynological record

The historical assembly and origin of the Páramo flora has been a fundamental question in Neotropical biogeography. Chorological and palaeopalynological studies have suggested a composite origin, with locally recruited plants (Neotropical) that adapted to the new available habitat and diversified, and temperate immigrants that colonised through long-distance dispersal and profited from a new habitat with similar conditions to those they were pre-adapted to (van der Hammen & Cleef, 1986; Smith & Cleef, 1988; Simpson & Todzia, 1990; Donoghue, 2008).

Interestingly, studies have suggested a trend towards a higher percentage of temperate elements and lower endemic elements in the higher Superpáramo regions while in the lower Subpáramo region the dominant elements were of Neotropical origin (van der Hammen & Cleef, 1986; Hooghiemstra & van der Hammen, 2004; Hooghiemstra et al., 2006).

Records from the late Miocene to the late Pliocene showed a change in the plant composition of Páramo areas from tropical lowland taxa to pre-montane and montane taxa (Gregory-Wodzicki, 2000; Hooghiemstra & van der Hammen, 2004; Hooghiemstra et al., 2006). For instance, the occurrence of pollen from Poaceae, Asteraceae and *Hypericum* are indicative of vegetation developed above the tree line (Hooghiemstra et al., 2006). From the Plio-Pleistocene transition, c. 2 – 4 Ma, some of the oldest records of pollen from Páramo vegetation are found, including representatives of Poaceae, Cyperaceae, Ranunculaceae, Asteraceae, Ericaceae as well as genera such as *Valeriana*, *Hypericum*, *Miconia*, *Plantago* and *Aragoa*, amongst others (van der Hammen, 1974; van der Hammen & Cleef, 1986; Hooghiemstra & van der Hammen, 2004; Hooghiemstra et al., 2006). It is worth noting that by this time, records show taxa of both temperate (e.g. Ranunculaceae) and tropical (e.g. *Miconia*) origin, indicating the likely expansion of upper forest populations into montane areas as well as the existence of dispersal corridors from temperate regions (i.e. Panama Isthmus and the Andes) (van der Hammen & Cleef, 1986; Hooghiemstra et al., 2006; Graham, 2009).

During the Pleistocene a repeated alternation of forest and Páramo elements is evident at specific altitudes in the palaeopalynological record, registering the climatic fluctuations of the Quaternary (van der Hammen, 1974; van der Hammen &

Cleef, 1986). Cycles of shifting vegetation belts were repeated throughout the Pleistocene with Páramo areas being reduced to isolated islands during interglacial periods and expanding during glacial ones (van der Hammen, 1974; van der Hammen & Cleef, 1986). Pollen data from the Last Glacial Maximum has showed a downward migration of the lower Páramo limit by 1300 – 1500 m expanding to a much larger area and likely merging previously isolated Páramo islands (Fig. 1.5) (Hooghiemstra & van der Hammen, 2004; Hooghiemstra et al., 2006; Flantua et al., 2014).

It has been suggested that the altitudinal migration of vegetation belts during the climatic fluctuations of the Quaternary has been a predominant force in shaping present-day Páramo plant diversity and high levels of endemism (van der Hammen, 1974; Simpson, 1975; Madriñán et al., 2013; Luebert & Weigend, 2014). On the one hand, the possibilities for dispersal from higher latitudes were greater during glacial periods as were the possibilities for migration between Páramo islands, while during interglacial periods Páramo islands were isolated possibly promoting allopatric speciation (van der Hammen, 1974; Simpson, 1975; van der Hammen & Cleef, 1986).

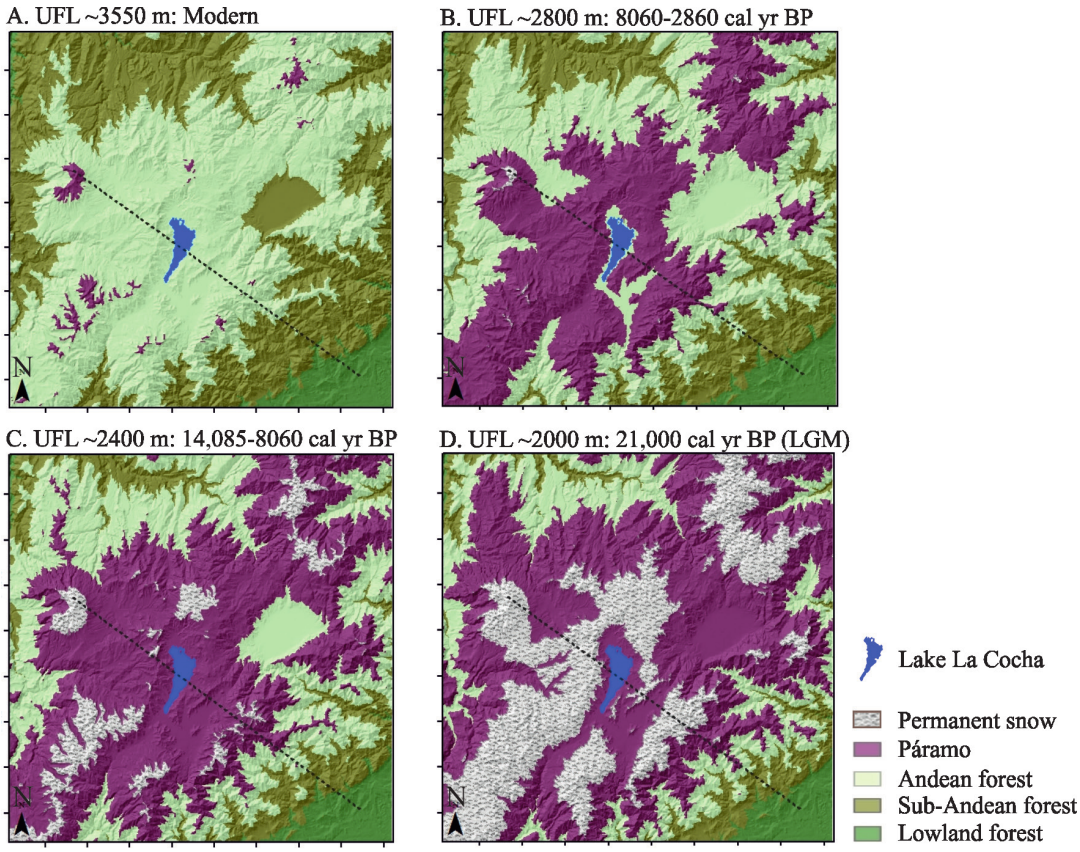

Figure 1.5. Distribution of vegetation belts and permanent snow since the Last Glacial Maximum in the area of Lake La Cocha, Southern Colombia (from Flantua et al., 2014).

1.4.3 Current knowledge from molecular phylogenetics

Chorological studies have been the starting point for a significant amount of molecular based studies of Páramo plant taxa. These have aimed to propose possible biogeographic and evolutionary scenarios for the origin and assembly of this flora (e.g. Rauscher, 2002; Kadereit & Hagen, 2003; Bell & Donoghue, 2005; Chacón et al., 2006; Hughes & Eastwood, 2006; reviewed in Sklenář et al., 2011 and Luebert & Weigend, 2014). Many of these studies were included in a meta-analysis of dated phylogenies of Páramo taxa that compared rates of speciation within this biome with those of other fast evolving biomes from other parts of the world, including Hawai'i,

the Cape Floras of South Africa, the Mediterranean region and Southwest Australia (Madriñán et al., 2013). These authors demonstrated that the Páramo flora has diversified more rapidly than any other on Earth. In addition, they indicated that a high percentage of species diversified during the Pleistocene. It was suggested that the climatic fluctuations during that epoch resulted in changing distributions of Páramo vegetation, which effectively acted as a species pump as populations repeatedly contracted and expanded (Madriñán et al., 2013).

1.5 STUDY TAXA

Based on the availability of phylogenetic information, appropriate distributions, their different ancestral ecologies and opposing breeding systems, *Oreobolus* R.Br. and Páramo representatives within Melastomeae (Melastomataceae) were selected as study taxa.

1.5.1 Oreobolus

Oreobolus (Cyperaceae) has 17 species with a southern Gondwanan, amphi-Pacific distribution, occupying mesic grasslands in southern temperate regions and high-altitude tropical areas (Mora-Osejo, 1987; Seberg, 1988). Twelve Pacific species extend across Australia, New Zealand, Malaysia and Hawai'i, while the five South American species are restricted to the southern and northern sections of the Andes Mountain Range (Fig. 1.6) (Seberg, 1988; Chacón et al., 2006). These sedges are low cushion perennial plants, growing in bogs and mesic habitats and, like most of the

family they are wind-pollinated and their seeds are dispersed by wind (Fig. 1.7) (Seberg, 1988).

Molecular phylogenetic analyses at the family and tribe level indicated that the genus is monophyletic (Muasya et al., 2009; Viljoen et al., 2013). Additionally, Chacón et al. (2006) suggested that the South American representatives form a monophyletic group. Furthermore, according to these authors' dated phylogeny, the South American clade diverged during the Pliocene c. 6 – 5.5 Ma. It was then suggested that *Oreobolus* may have reached the southern portion of South America from Australasia via long distance dispersal, and subsequently used the Andes as a corridor for northward migration (Chacón et al., 2006). However, this hypothesis was not supported in an ancestral area reconstruction for the tribe (Viljoen et al., 2013).

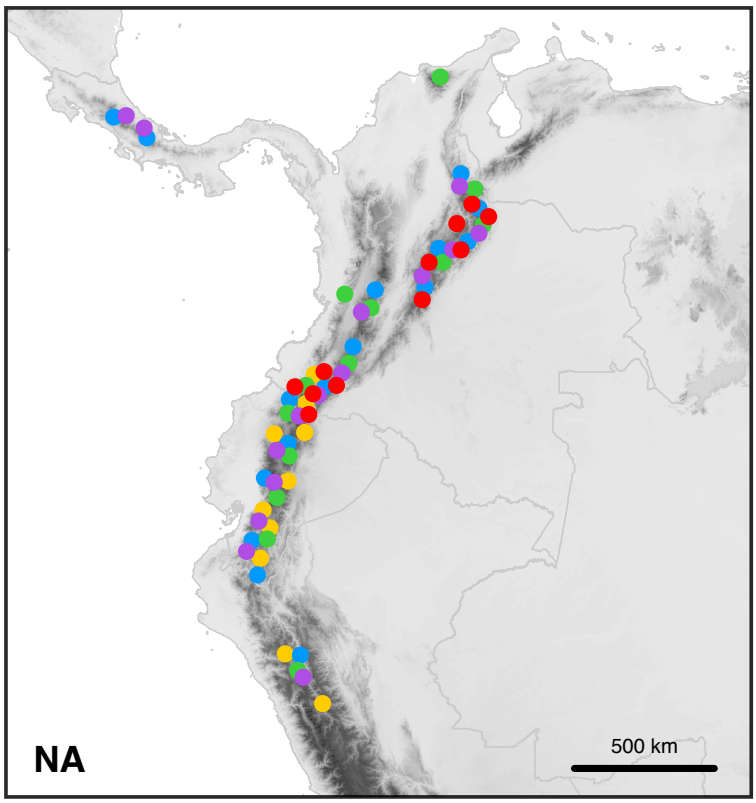

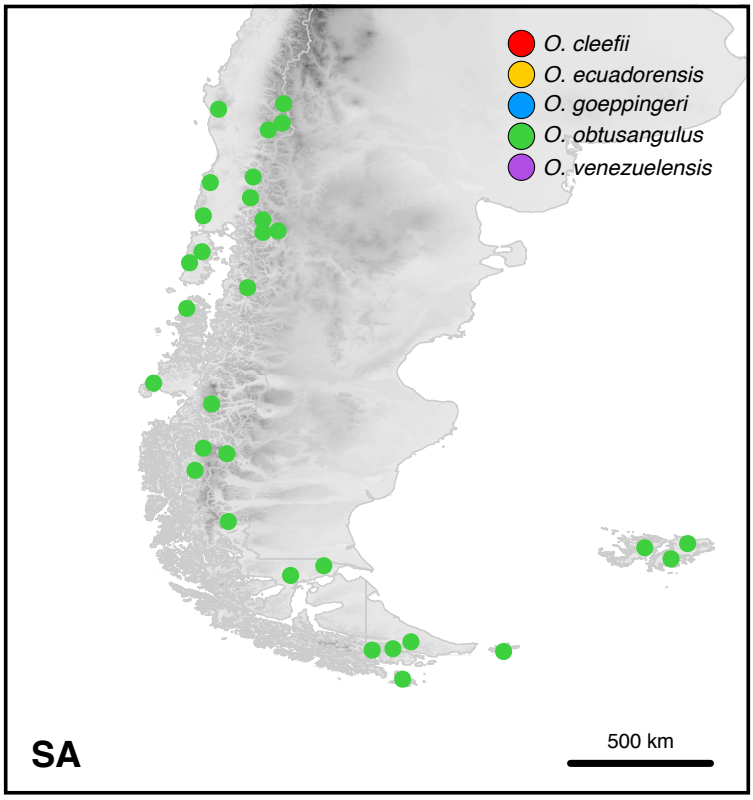

Figure 1.6. General distribution map of the South American species of *Oreobolus*. NA, northern Andes; SA, southern Andes.

Figure 1.7. (a, b) *Oreobolus goeppingeri* and (c) *O. cleefii*. Photo credit: Flora Ilustrada del Páramo de Chingaza (http://chingaza.uniandes.edu.co)

1.5.2 Melastomeae

The largely Neotropical Melastomeae (Melastomataceae) has more than 870 species in 47 genera (Michelangeli et al., 2013). The vast majority of species are distributed in South America (c. 570 species in 30 genera) with the rest distributed in the Palaeotropics (Renner, 1993; Michelangeli et al., 2013). Interestingly, Neotropical representatives occupy numerous habitats ranging from lowland forest to the high-altitude Páramo ecosystem, although the greatest number of species is found in the lowlands (Michelangeli et al., 2013). Páramo species are found within six genera including the endemic *Castratella* Naudin, the near-endemic *Bucquetia* DC., as well

as *Brachyotum* Triana, *Chaetolepis* Miq., *Monochaetum* Naudin and *Tibouchina* Aubl. (Luteyn, 1999; Michelangeli et al., 2013).

Castratella is of particular interest (Fig. 1.8). This genus has two species, *C. piloselloides* and *C. rosea*, endemic to the páramos of Colombia and Venezuela. They are rhizomatous perennial herbs with a rosulate habit (Fritsch et al., 2004; Sklenář et al., 2005; Michelangeli et al., 2013). Their flower colour and morphology, yellow to pink petals with very exposed stamens, suggests pollination by insects, and although this has yet to be confirmed, this is common in the family (Michelangeli et al., 2013). Though traditionally placed in Microlicieae, based on molecular and morphological characters, Fritsch et al. (2004) proposed a new placement within Melastomeae. Subsequently, one species within the genus, *C. piloselloide*s was included in a phylogenetic study of this tribe (Michelangeli et al., 2013). Furthermore there is no molecular evidence of *C. piloselloides* and *C. rosea* being sister taxa as no molecular data has been gathered for the latter. The aforementioned might be due to the difficulty of finding *C. rosea*, which until the 1970s was known only from the holotype, and even now collections are very limited.

Figure 1.8. (a) *Castratella rosea* and (b, c) *C. piloselloides*. Photo credits: (a) A. M. Cleef and (b, c) Flora Ilustrada del Páramo de Chingaza (http://chingaza.uniandes.edu.co)

1.6 THESIS AIM AND OBJECTIVES

1.6.1 Aim

This thesis investigates the patterns and processes underlying the diversification of plants in the Páramo ecosystem, through studies of representative species of *Oreobolus* (Cyperaceae) and Melastomeae (Melastomataceae).

1.6.2 Objectives

Objective 1: to investigate the impact of the Andes orogeny on the timing, directionality and diversification rates of the South American species of *Oreobolus* (Chapter Two).

a. Re-evaluate the monophyly of the South American clade of *Oreobolus,* and of each of the five South American species within the genus

b. Estimate dates of species divergence

c. Assess the likely direction of migration

d. Compare diversification rates of the South American species with Pacific ones and with the other genera within the *Oreobolus* clade.

Objective 2: to examine the genetic structure between and within the South American species of *Oreobolus* in order to understand the influences of more recent geological, climatic and ecological factors (Chapter Three).

a. Estimate the species tree of the South American species of *Oreobolus*

b. Assess the population and genetic structure at the inter- and intra-specific level

c. Investigate the impact of Quaternary glacial-interglacial cycles in shaping populations of *Oreobolus*.

Objective 3: to investigate the impact of the Andes orogeny on the diversification history of the Páramo species of the largely Neotropical Melastomeae tribe (Chapter Four).

a. Re-assess the phylogeny of the tribe under a Bayesian framework in order to re-evaluate the phylogenetic position of Páramo species

b. Estimate dates of divergence in Páramo species of Melastomeae

c. Infer the phylogenetic and phylogeographic relationships of *Castratella piloselloides*

Objective 4: to determine whether there were differences in species numbers of Páramo lineages of different geographic origin (Chapter Four).

a. Explore species richness patterns for the complete Páramo flora to assess if there is a relationship between species richness of Páramo clades and their geographic origin (temperate versus tropical)

b. Explore species richness patterns for the complete Páramo flora to assess if there is a relationship between geographic origin and altitudinal distribution

CHAPTER TWO. PHYLOGENY AND BIOGEOGRAPHY OF THE SOUTH AMERICAN SPECIES OF *OREOBOLUS* R. Br. (CYPERACEAE)

2.1 ABSTRACT

This study investigates the impact of Andean orogeny on the timing, directionality and diversification of the five South American species of *Oreobolus*, within the context of the tribe Schoeneae. *Oreobolus* is a genus of 17 species with a southern Gondwanan amphi-Pacific distribution, restricted to mesic grasslands in southern temperate regions and high-altitude tropical areas. Fifteen out of 17 species in the genus were sampled including an exhaustive sampling of 235 individuals from the five South American species covering for their entire distribution range. Phylogenetic analyses under maximum parsimony, maximum likelihood and Bayesian inference were undertaken for a combined matrix of chloroplast and nuclear ribosomal sequence data (*trn*L-F and ITS). Bayesian divergence time estimation and ancestral area reconstruction analyses were performed. Diversification rates were calculated for *Oreobolus* and allied genera. New results reported here include that *Oreobolus* is not monophyletic. Its South American species were recovered as a monophyletic group and show strong geographic structure the northern Andean species (NAC) from the southern Andean ones (SAC)

each forming separate clades. However, relationships amongst northern Andean species could not be resolved, possibly reflecting ongoing gene flow and/or incomplete lineage sorting. Ancestors of the South American species may have reached the continent through two independent long-distance dispersal events to the northern and southern Andes during the Pliocene. The arid central Andes have been a major ecological barrier to dispersal. Subsequent ice cycles of the Quaternary may have been key in the diversification of the northern Andean *Oreobolus*. Finally, habitat heterogeneity rather than the latitudinal gradient has a more important role in driving diversification rates, possibly by promoting niche partitioning and greater biotic interactions.

2.2 INTRODUCTION

Understanding and explaining patterns of global plant diversity across the planet has been a central question in biodiversity research. Plant diversity is concentrated in the tropical regions of the world and various explanations have been put forward to account for this. It may simply be a matter of regions with a tropical climate occupying a greater area for a longer period of time (Rosenzweig, 1995), as higher temperatures may previously have allowed tropical elements to occupy higher latitudes (Zachos et al., 2001). However, as temperatures fell, these elements may have been restricted to smaller tropical regions (Zachos et al., 2001). Alternatively, tropical regions may be more diverse because of greater energy input to support populations (Wright, 1983; Hurlbert & Stegen, 2014). Additionally, evolutionary rates in the tropics may be faster because of the greater temperature (Rohde, 1992;

Allen & Gillooly, 2006). Moreover, diversity may promote diversity with the increased importance of biotic interactions (Schemske, 2009). On the other hand, diversity outside the tropics may have been constrained by the younger ages of biomes, leading to both a smaller number of successful colonisation events, and limited time for diversification (Wiens et al., 2010; Romdal et al., 2012). The colonisation impediment may be the result of niche conservatism with limited capacity for tropical groups to overcome extreme physiological barriers, such as frost, in order to colonise temperate regions (Donoghue, 2008). It has also been suggested that tropical regions have not been subjected to major disturbances such as repeated glaciations, which have led to higher extinction rates in temperate to polar latitudes (Lomolino et al., 2006; Weir & Schluter, 2007).

There is also significant variation in biodiversity within the tropics, with the Neotropics being considerably more species-rich than Asian or African regions (Gentry, 1982; Antonelli & Sanmartín, 2011). Explanations have included increased extinction rates in Africa (Richards, 1973; White, 1981) and higher speciation rates in the Neotropics (Gentry, 1982). Overall, the explanation must lie in increased net diversification rates in the Neotropics, defined as the rate at which extant lineages arose (Coyne & Orr, 2004) from "the interplay of speciation and extinction" (Magallón & Castillo, 2009). Gentry (1982) famously attributed the greater diversity of the Neotropics to being an "Accident of the Andean orogeny", with the idea that the orogeny of the Andes Mountain Range has created opportunities for elevated rates of speciation.

Deep time geological events have been suggested as playing an important role in the evolution of ecosystems and their biodiversity (e.g. Hoorn et al., 2010; Antonelli &

Sanmartín, 2011). Mountain building and uplift could have had an impact on plant diversification generating niche heterogeneity across altitudinal gradients (Donoghue, 2008). This would have been the case with the Andes Mountain Range: following the final uplift of the northern Andes during the Pliocene, c. 5 Ma, new habitats became available, such as the Andean Páramo ecosystem (Donoghue, 2008). Similarly, vicariance events such as plate tectonics and the breakup of super-continents like Gondwana may explain past and present plant distributions (e.g. Sanmartín & Ronquist, 2004). However, the importance of long-distance dispersal in shaping plant distributions has been equally established (e.g. Pennington & Dick, 2004; Christenhusz & Chase, 2013). Dated molecular phylogenies can be used to reconstruct diversification histories of taxa to understand the relative influences of earth history and dispersal, and to determine the origin of lineages, as well as the timing and direction of particular migration events (e.g. Pennington & Dick, 2004; Särkinen et al., 2011). In addition, differences in diversification rates may also be identified and related to critical geological, climatic or ecological events (e.g. Hoorn et al., 2010).

The Páramo is distributed in a series of "sky islands" above 3000 m.a.s.l. along the mountain tops of the northern section of the Andes Mountain Range, occupying an approximate area of 37,500 km^2 (Buytaert et al., 2010). It is the most species-rich high-altitude ecosystem in the world (Smith & Cleef, 1988; Sklenář et al., 2014), with up to 4000 species of vascular plants, of which c. 60% are endemic (Luteyn, 1999). The huge diversity and comparatively young age of this ecosystem suggested that the rates of speciation there might have been exceptionally high. This idea was tested by Madriñán et al. (2013) who indicated that the Páramo ecosystem had a rate

of speciation that was higher than any other biodiversity hotspot on earth. Part of the diversity of the Páramo may also be due to recent immigration of lineages from temperate latitudes, which found an available niche with similar conditions to those they were already adapted to, and diversified within (Donoghue, 2008; Rull, 2011). According to the palaeopalynological record and previous floristic studies, 14% of the Páramo flora has a presumed Austral origin (van der Hammen, 1974; van der Hammen & Cleef, 1986), because migration from the south might have been facilitated by the almost continuous corridor of temperate-like habitats along the Andes Mountain Range (Sklenář et al., 2011).

The schoenoid sedge *Oreobolus* R. Br. (Cyperaceae: Schoeneae) is an ideal model system to study questions related to Páramo biogeography, both in terms of migration of lineages from other regions, and of in-situ diversification. *Oreobolus* contains 17 species and has a southern Gondwanan, amphi-Pacific distribution, occupying mesic grasslands in southern temperate regions and high-altitude tropical areas (Mora-Osejo, 1987; Seberg, 1988). The 12 Pacific species extend across Australia, New Zealand, Malaysia and Hawai'i, whilst the five South American species are restricted to the southern and northern sections of the Andes Mountain Range (Seberg, 1988; Chacón et al., 2006), providing an optimal distribution pattern to assess the impact of the Andes orogeny on its diversification. Additionally, *Oreobolus* is nested within the '*Oreobolus* clade' of the Schoeneae tribe (Viljoen et al., 2013), a lineage of closely related taxa with a southern hemisphere distribution. This clade is ideal for the comparison of diversification rates across a varied geographic range comprising different continents that were formerly connected as Gondwanaland.

The Schoeneae tribe has an almost entirely southern hemisphere distribution, being particularly diverse in Australia and South Africa, whereas just three out of 22 genera reach South America (Verboom, 2006; Viljoen et al., 2013). According to Viljoen et al. (2013), the tribe originated in the early Eocene in Australia where it diverged into its six main lineages c. 50 Ma (*Caustis* clade, *Lepidosperma* clade, *Tricostularia* clade, *Oreobolus* clade, *Gahnia* clade and *Schoenus* clade). The *Oreobolus* clade is unique among these in that its extant species diversified less than c. 10 Ma, during the late Miocene (Viljoen et al., 2013). Moreover, even though the clade is distributed across all main southern Gondwana landmasses, the individual species are regional endemics (Viljoen et al., 2013).

The current study focuses on the five South American species of *Oreobolus*. These species are found only in the high-altitude Páramo ecosystem, restricted to temperate-like environments in the northern section of the Tropical Andes and in southern Central America (Fig. 1.6 page 21) (Seberg, 1988; Chacón et al., 2006). Only the South American species, *O. obtusangulus*, has a disjunct distribution within the continent, occupying also the subantarctic region in the southern Andes (Seberg, 1988; Chacón et al., 2006). Furthermore, these southern Andes populations have been separated as subspecies *O. obtusangulus* subsp. *unispicus* (Seberg, 1988).

A previous study estimated a dated molecular phylogeny for *Oreobolus* based on ITS sequences of 14 out of the 17 species within the genus, including one sample of each of the five South American species (Chacón et al., 2006). The authors suggested that *Oreobolus* may have arrived from the south during the final uplift of the northern Andes in the Pliocene c. 5 Ma, reaching the newly available Páramo ecosystem and diversifying within it. However, the use of a geological event as calibration point, the

emergence of one of the islands of the Hawaiian Archipelago, is a weak method of calibration. First, the use of point calibrations ignores the error associated with the estimated date of the geological event (Ho & Phillips, 2009). The Hawaiian archipelago is a series of islands that might have been successively emerging and submerging since before any of the extant islands emerged; thus the use of the age of dispersal of a species to one of those islands may be erroneous as dispersal may have occurred earlier onto an island that is now submerged. Additionally, biogeographic calibrations bias towards younger divergence times and make strong assumptions about the role of vicariance and dispersal on the diversification pattern of the group under study (Ho & Phillips, 2009). Similarly, even though 14 out the 17 species were sampled in the analysis, only one outgroup was used (*Costularia laxa*) and therefore the monophyly of the genus was not tested.

Viljoen et al. (2013) proposed a dated phylogeny for the Schoeneae tribe based on two nuclear ribosomal markers (ITS and ETS) and three chloroplast markers (*rbc*L, *rps*16 and *trn*L), sampling each genus within the tribe proportionally to their size (i.e. number of species) and biogeographic distribution. In addition, at least one taxon of each major Cyperaceae lineage outside the tribe was sampled as outgroups (Viljoen et al., 2013). However, only five of the 17 species of *Oreobolus* were sampled in this study, of which one sample of *O. obtusangulus* from the southern Andes was included as a South American representative. By not including *Oreobolus* samples from the northern Andes, the authors may have been excluding an important biogeographic region from their analyses, considering that just three out of 22 species within Schoeneae reach South America (Verboom, 2006; Viljoen et al., 2013). Possibly as a result, Viljoen et al. (2013) were unable to resolve *Oreobolus* as

a monophyletic genus and they obtained an ambiguous reconstruction of the ancestral area for the '*Oreobolus* clade'.

The reconstruction of a dated molecular phylogeny, including a comprehensive set of species from the Schoeneae and an exhaustive sampling of the South American species of *Oreobolus,* including several samples per species, would allow a better appraisal of the monophyly of the genus, as well as an estimation of the timing of divergence and direction of migration within the '*Oreobolus* clade'. Furthermore, this will allow comparison of diversification rates within the clade, making possible the assessment of the impact of geological events on diversification patterns.

Hypotheses on diversity gradients can, to an extent, be tested individually by looking at a variety of groups with varied distributions. For example, would a temperate group that has recently moved into tropical regions, and that may be pre-adapted to temperate conditions, have a faster rate of diversification than its temperate sister clades? This may begin to address questions related to the effects of, for example, greater energy input in the tropics being the principal cause of faster diversification rates (Wright, 1983; Hurlbert & Stegen, 2014).

This chapter investigates the impact of the Andes orogeny on the timing, directionality and diversification rates of the South American species of *Oreobolus* within the context of its tribe. The specific aims are 1) to re-evaluate the monophyly of the South American clade of *Oreobolus,* and of each of the five South American species within the genus by including multiple samples per species; 2) to estimate dates of species divergence; 3) to assess the likely direction of migration; and 4) to

compare diversification rates of Andean species with Pacific ones and with the other genera within the *Oreobolus* clade.

2.3 METHODS

2.3.1 Species sampling

This study focuses on the Andean species of *Oreobolus* (*O. cleefii*, *O. ecuadorensis*, *O. goeppingeri*, *O. obtusangulus* and *O. venezuelensis*) within the phylogenetic context of the Schoeneae tribe (Cyperaceae). For that reason, a dataset was produced comprising multiple samples per species and sampling extensively across their entire distribution range, using both field-collected and herbarium samples (U, L, AAU, RNG). In order to incorporate my sampling into the existing phylogeny of the Schoeneae tribe (Viljoen et al., 2013) and include previously published data for the remaining species of *Oreobolus* (Chacón et al., 2006), sequence data for the nuclear ribosomal DNA Internal Transcribed Spacers (ITS) and the plastid region *trn*L-F were produced. As in Viljoen et al. (2013), a comprehensive set of species from the main non-Schoeneae lineages within the Cyperoideae subfamily and samples from the Mapanioideae subfamily were included as outgroups, allowing the use of calibration points using fossils. Table S2.1 presents the complete list of samples used in this study (Supplementary information, pages 199 – 213).

2.3.2 DNA extraction, amplification and sequencing

Both silica-dried fresh leaf samples and herbarium material were pulverised using a Mixer Mill (Retsch, Haan, Germany). Total genomic DNA from herbarium material

was isolated following the CTAB method (Doyle & Doyle, 1990) and from silica-dried samples with the DNeasy® Plant Mini Kit (QIAGEN, Manchester, UK) following the manufacturer's protocol. The chloroplast region *trn*L-F was amplified and sequenced using primers *trn*Lc and *trn*Lf for silica-dried material, and in combination with internal primers *trn*Ld and *trn*Le for herbarium material (Taberlet et al., 1991). For silica-dried material, the ITS region was amplified and sequenced only with external primers ITS5P and ITS8P (Möller & Cronk, 1997). For herbarium material, owing to the increased likelihood of the DNA being degraded, amplification and sequencing were performed using internal primers ITS5P and ITS8P in combination with internal primers ITS2P and ITS3P (Möller & Cronk, 1997), in order to amplify the shorter ITS1 and ITS2 regions in separate reactions. For both reactions, 20 µl PCR reactions used the following proportions: 1 µl of unquantified DNA, 1x Buffer (Bioline, London, UK), 1mM dNTPs, 1.5 mM $MgCl_2$ (Bioline, London, UK), 0.75 µM of each forward and reverse primer, 4µl of combinatorial enhancer solution (CES) and 0.05 U of *Taq* polymerase (Bioline, London, UK). The amplification cycle for *trn*L-F consisted of 2 min at 94 ºC, followed by 30 cycles of 1 min at 94 ºC, 1 min at 52 ºC and 1 min at 72 ºC, finalising with 7 min at 72 ºC. For ITS, the amplification cycle consisted of 3 min at 94 ºC, followed by 30 cycles of 1 min at 94 ºC, 1 min at 55 ºC and 90 sec at 72 ºC, finalising with 5 min at 72 ºC. PCR products were purified with 2 µl of ExoSAP-IT® (USB Corporation, High Wycombe, UK) for 5 µl of product. Sequencing reactions for each primer used the BigDye® Terminator v3.1 chemistry (Applied Biosystems™, Paisley, UK) and the manufacturer's protocol. Sequencing was performed at the Edinburgh Genomics facility of the University of Edinburgh.

2.3.3 Matrix assembly and sequence alignment

Contigs of forward and reverse sequences were assembled in Sequencher version 5.2 (Gene Codes Corporation, Ann Arbor, Michigan, USA). 231 ITS sequences and 169 *trn*L-F sequences were generated for this study (Table S2.1). The sequences were manually aligned using Mesquite v2.75 (Maddison & Maddison, 2014) with previously published sequences downloaded from GenBank (Table S2.1). Ambiguously aligned positions were discarded from the *trn*L-F alignment.

2.3.4 Phylogeny reconstruction

Phylogenies for each region were reconstructed using Maximum Parsimony (MP), Maximum Likelihood (ML) and Bayesian Inference (BI).

MP analyses were performed using the Willi Hennig Society edition of TNT version 1.1 (Goloboff et al., 2008). Characters were unordered and equally weighted, gaps were considered as missing data. Heuristic searches were conducted with 1000 Parsimony Ratchet replicates (Nixon, 1999) with 200 iterations per ratchet saving up to 20 trees per replicate, followed by tree bisection-reconnection (TBR) branch swapping. Clade support was assessed with a 1000 replicates, non-parametric bootstrap analysis (MP-BS). A strict consensus tree was calculated and one of the most parsimonious trees was annotated with bootstrap values and nodes that collapse in the strict consensus tree.

Evolutionary model testing was performed for each region using JModelTest 2.1.6 (Guindon & Gascuel, 2003; Darriba et al., 2012) with default settings. Based on the Bayesian Information Criterion (BIC; Schwarz, 1978), the best-fitting models were

GTR+I+Γ for ITS and TPM1uf+Γ for *trn*L-F. Maximum Likelihood (ML) reconstruction was performed using RAxML version 8 (Stamatakis, 2014). One hundred independent ML searches were carried out under a GTR + Gamma model, followed by a 1000 replicate non-parametric bootstrap search (ML-BS). Bootstrap values were summarised on the tree with the best likelihood score.

Bayesian Inference was performed using MrBayes v. 3.2.2 (Ronquist et al., 2012) run on the CIPRES Science Gateway v.3.3 (Miller et al., 2010). Four independent runs of 30,000,000 generations were performed, with three hot chains and one cold chain at a temperature of 0.1, sampling 10^4 parameter estimates in each run. Appropriate mixing, parameter and topological convergence were assessed with Tracer v1.6.0 (Rambaut et al., 2013). 75% of the samples from each run were discarded as burn-in and a maximum clade credibility (MCC) tree from the combined 10,000 trees was annotated with posterior probability support values (PP), median heights and 95% Highest Posterior Density (HPD) values using TreeAnnotator v2.1.2 (Rambaut & Drummond, 2015). Annotated trees were visualised and exported as graphics using FigTree v1.4.2 (Rambaut, 2014).

Non-parametric bootstrap values (MP-BS and ML-BS) of above 80% are considered to be high, 50% to 80% to be good and below 50% to be poor. With respect to posterior probability (PP), support values of above 90% are considered to be high, 60% to 90% to be good and below 60% to be poor. The difference in the set intervals derives from the general tendency of PP support values to be higher than their corresponding bootstrap values (e.g. Douady et al., 2003; Erixon et al., 2003).

Statistical assessment of topological congruence between phylogenetic trees (i.e. incongruence length difference test – ILD) has been rejected as an unbiased measure of phylogenetic congruence and combinability (e.g. Darlu & Lecointre, 2002; Barker & Lutzoni, 2002; Ramírez, 2006). Consequently, congruence between the chloroplast and nuclear tree topologies was visually assessed, which revealed no strongly supported conflict. The two matrices were therefore concatenated and partitioned by gene for the ML and BI analyses, resulting in a matrix of 333 taxa and 2610 bp. MP, ML and BI analyses were performed as described in the previous paragraphs.

2.3.5 Divergence Time estimation

To estimate divergence times, BEAST v2.1.3 (Bouckaert et al., 2014) was used. Missing data and duplicated sequences significantly increase computing time and have been shown to cause error in dating analyses (Drummond & Bouckaert, 2015). Consequently, only Andean *Oreobolus* samples with both regions successfully sequenced were included in the analysis. Similarly, to avoid duplicated sequences, where multiple individuals within a species had identical sequences, only one of them was included in the analysis. The data were partitioned as for the Bayesian analyses, and each partition was analysed under a GTR model with a gamma distribution with four rate categories, which is the minimum number to get a good approximation of the continuous function (Yang, 1994). The model of lineage-specific substitution rate variation was set as an uncorrelated lognormal relaxed clock model with estimated clock rates, and a exponential prior distribution with mean equals to 10. The diversification model was set to a birth death model

(Gernhard, 2008), which is an appropriate model to infer divergence times between species (Drummond & Bouckaert, 2015). Mapanioideae and Cyperoideae were constrained to each be monophyletic, because they constitute the two subfamilies within Cyperaceae recognised as sister monophyletic groups by Muasya et al. (2009). The crown node of the Cyperaceae was calibrated as a prior with a normal distribution defined by μ=75.1 Ma and σ=7.7 Ma, using the age and error range estimated for this node from a dated phylogeny of the Poales, calibrated with six fossils, by Besnard et al. (2009). *Hypolytrum nemorum* (Vahl) Spreng. and *Mapania cuspidata* (Miq.) Uittien were constrained to be a monophyletic group representing the Hypolytreae tribe (subfamily Mapanioideae). The mid Eocene fossil *Volkeria messelensis* S. Y. Smith et al. (Smith et al., 2009) was used to set a lognormal distribution with μ=6 Ma, and a minimum bound for the highest posterior density distribution of 38 Ma on the crown age of Hypolytreae because it has fruits, pollen and infructescence structure that attribute it to this clade. The standard deviation was set to 0.93, yielding a 95% HPD between 38 and 56 Ma, corresponding to the upper age limit of the mid-Eocene, and the lower age limit of the Eocene respectively (Cohen et al., 2013 updated). A normal distribution was used on the root because it is the most appropriate for secondary calibrations (Ho & Phillips, 2009). This type of distribution locates most of the probability density around the mean and allows for symmetrical decrease towards the tails accounting for the age error (Ho & Phillips, 2009). In contrast, a lognormal distribution is the most appropriate for a fossil calibration (Ho & Phillips, 2009). In this case, the fossil sets a hard minimum bound to the distribution with its highest probability density older than the fossil (Ho & Phillips, 2009). This calibration strategy biases in favour of an older age estimate,

which is recommended because fossils represent minimum age estimates, because they were likely to have formed after the evolution of the clade that they represent. The remaining priors were left at their default settings.

Four independent MCMC runs of 10^8 generations each, sampling every 10^4 were performed. Adequate mixing and convergence were assessed using Tracer v1.6.0 (Rambaut et al., 2013). 75% of the samples from each run were discarded as burn-in, and a MCC tree from the combined tree sets was annotated with median heights and 95% HPD node ages on TreeAnnotator v2.1.2 (Rambaut & Drummond, 2015).

2.3.6 Ancestral area reconstruction

To reconstruct the likely ancestral areas of the Schoeneae tribe, the Bayesian Binary Model (BBM; Ronquist & Huelsenbeck, 2003) was implemented in RASP v3.2 (Yu et al., 2015). BBM permits the assignment of multiple areas to the tree terminals and reconstructs, for each node, possible ancestral areas and their probability (Yu et al., 2015). The MCC chronogram estimated with BEAST v.2.1.3 (Bouckaert et al., 2014) was used as an input, and the analysis was run under the following parameters: 5,000,000 cycles, 10 chains, sampling every 100 cycles, with a temperature of 0.1 and a maximum of four areas for all nodes. All the remaining parameters were left at their default settings.

A total of 11 biogeographic regions were delimited according to the modern distribution of the Schoeneae taxa and the geological history of those regions (Fig. 2.4). Seven of these regions were defined following Sanmartín & Ronquist (2004): Africa, Madagascar, Australia (including Tasmania and New Guinea), New Zealand,

New Caledonia, South East Asia and Pacific Islands (Hawai'i). These areas correspond to either 1) Gondwanan landmasses that have been historically persistent, 2) composite areas (i.e. New Zealand) that split from Gondwana as a unit, or 3) oceanic archipelagos or small landmasses with a similar biota or recent land connections during the Pleistocene (Sanmartín & Ronquist, 2004). Four additional regions were defined for Central and South America: southern Central America, northern Andes (12ºN – 5ºS at the Amotape Cross), central Andes (5ºS at the Amotape Cross – 47ºS at the Gulf of Penas) and southern Andes (47ºS at the Gulf of Penas – 55ºS). The three Andean regions reflect differential temporal tectonic histories along the mountain range with more northern mountains rising later while southern Central America corresponds to the Caribbean Plate (Graham, 2009). Widespread taxa that occupy multiple areas introduce ambiguity in the data set and therefore may bias ancestral area reconstruction analysis (Sanmartín & Ronquist, 2004; Yu et al., 2015). In my dataset only *Schoenus nigricans* had such a wide distribution including Africa, Eurasia, North America, the Arabian Peninsula and India. The latter four regions were not defined in the analysis presented here. Areas were assigned to taxa following Brummitt et al. (2001).

2.3.7 Diversification rates estimation

To estimate diversification rates (r), the simple estimator of Kendall (1949) and Moran (1951) was used, where $r = [\ln(N) - \ln(N_0)]/T$ (where N = standing diversity, N_0 = initial diversity, here taken as = 1, and T = inferred clade age). This estimates a pure-birth model of diversification, with a constant rate and no extinction. Extinction is anticipated to have had a minimal effect on the diversification of the *Oreobolus*

clade, because a young age for its crown node (mid-Miocene) is expected, as calculated by Viljoen et al. (2013). Diversification rates were calculated for the well-supported clades within the *Oreobolus* clade.

2.4 RESULTS

This study presents the most complete taxon sampling of *Oreobolus* species to date, including 15 out of 17 species in the genus compared to 13 sampled by Chacón et al. (2006), and five sampled by Viljoen et al. (2013). An exhaustive sampling of 235 accessions of the five South American species of *Oreobolus* resulted in the addition of 169 *trn*L-F sequences and 231 ITS sequences to the data of Chacón et al. (2006) and Viljoen et al. (2013). My taxon sampling is the first to account for the entire distribution range of the South American species, as well as for possible within-species genetic variation. Additionally, two new Pacific *Oreobolus* sequences were added, one generated in this study (*O. ambiguus*) and one downloaded from GenBank (*O. kuekenthalii*).

2.4.1 Phylogenetic reconstruction

Figures 2.1 to 2.3 show the trees for the combined matrix in the following order: one of the most parsimonious trees annotated with bootstrap values (MP-BS, Fig. 2.1), the tree with the best likelihood score annotated with bootstrap values (ML-BS, Fig. 2.2) and the MCC tree from the Bayesian analysis annotated with posterior probability values (PP, Fig. 2.3). Trees for individual DNA regions are presented in Figures S2.4 to S2.7 (Supplementary information, page 214).

The Schoeneae (*sensu* Viljoen et al., 2013) was recovered as monophyletic with low support in MP and ML analyses (Fig. 2.1, MP-BS<50%; Fig. 2.2, ML-BS<50%) but well supported in BI (Fig. 2.3, PP=81%). In the MP analysis, the *Carpha* clade was recovered within the Schoeneae, poorly supported as sister to the *Schoenus* clade (MP-BS<50%). However, in ML it appeared poorly supported as sister clade to the entire Schoeneae (ML-BS<50%) while in BI it appeared forming a grade with the other Cyperoideae (PP=85%). Within Schoeneae, relationships at deeper nodes were poorly resolved, and the only strongly supported sister relationship was between the *Lepidosperma* and *Gahnia* clades in BI (PP=0.79), although this was poorly supported in ML (ML-BS<50%). Otherwise, no well supported relationships between the six main clades (*sensu* Viljoen et al., 2013) could be inferred. The six main clades consistently included the same species and were fully recovered as monophyletic groups (Figs. 2.1 – 2.3): *Schoenus* clade (MP-BS=99%, ML-BS=100%, PP=100%), *Tricostularia* clade (MP-BS=100%, ML-BS=100%, PP=100%), *Lepidosperma* clade (MP-BS=100%, ML-BS=100%, PP=100%), *Caustis* clade (MP-BS=64%, ML-BS=73%, PP=100%), *Gahnia* clade (MP-BS=87%, ML-BS=96%, PP=100%) and *Oreobolus* clade (MP-BS=98%, ML-BS=100%, PP=100%).

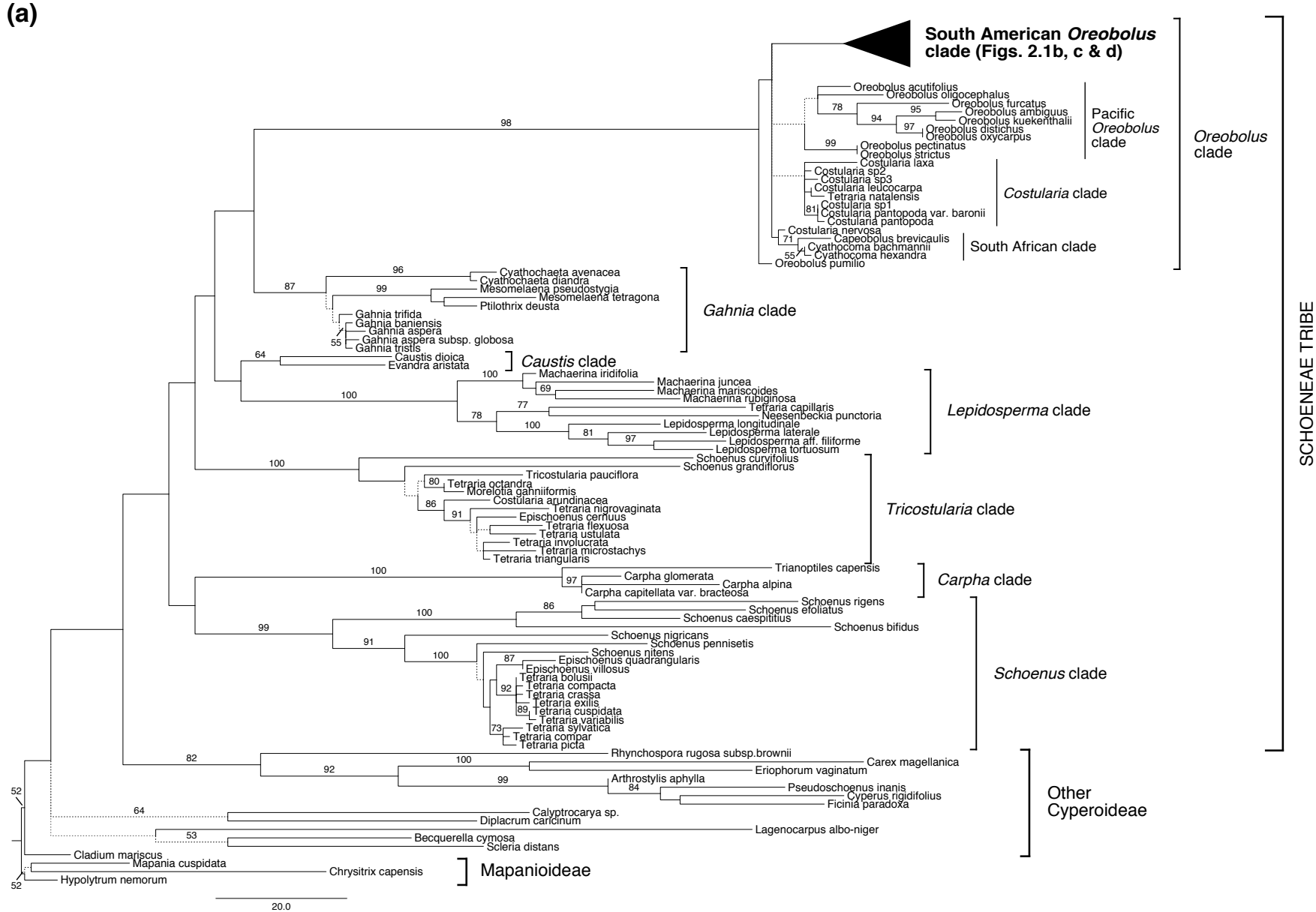
(a)
South American Oreobolus clade (Figs. 2.1b, c & d)
Oreobolus acutifolius
Oreobolus oligocephalus
Oreobolus furcatus
Oreobolus ambiguus
Oreobolus kuekenthalii
Oreobolus distichus
Oreobolus oxycarpus
Oreobolus pectinatus
Oreobolus strictus
Costularia laxa
Costularia sp2
Costularia sp3
Costularia leucocarpa
Tetraria natalensis
Costularia sp1
Costularia pantopoda var. baronii
Costularia pantopoda
Costularia nervosa
Capeobolus brevicaulis
Cyathocoma bachmannii
Cyathocoma hexandra
Oreobolus pumilio
Pacific Oreobolus clade
Costularia clade
South African clade
Oreobolus clade
Cyathochaeta avenacea
Cyathochaeta diandra
Mesomelaena pseudostygia
Mesomelaena tetragona
Ptilothrix deusta
Gahnia trifida
Gahnia baniensis
Gahnia aspera
Gahnia aspera subsp. globosa
Gahnia tristis
Gahnia clade
Caustis dioica
Evandra aristata
Caustis clade
Machaerina iridifolia
Machaerina juncea
Machaerina mariscoides
Machaerina rubiginosa
Tetraria capillaris
Neesenbeckia punctoria
Lepidosperma longitudinale
Lepidosperma laterale
Lepidosperma aff. filiforme
Lepidosperma tortuosum
Lepidosperma clade
Schoenus curvifolius
Schoenus grandiflorus
Tricostularia pauciflora
Tetraria octandra
Morelotia gahniiformis
Costularia arundinacea
Tetraria nigrovaginata
Epischoenus cernuus
Tetraria flexuosa
Tetraria ustulata
Tetraria involucrata
Tetraria microstachys
Tetraria triangularis
Tricostularia clade
Trianoptiles capensis
Carpha glomerata
Carpha alpina
Carpha capitellata var. bracteosa
Carpha clade
Schoenus rigens
Schoenus efoliatus
Schoenus caespititius
Schoenus bifidus
Schoenus nigricans
Schoenus pennisetis
Schoenus nitens
Epischoenus quadrangularis
Epischoenus villosus
Tetraria bolusii
Tetraria compacta
Tetraria crassa
Tetraria exilis
Tetraria cuspidata
Tetraria variabilis
Tetraria sylvatica
Tetraria compar
Tetraria picta
Schoenus clade
Rhynchospora rugosa subsp.brownii
Carex magellanica
Eriophorum vaginatum
Arthrostylis aphylla
Pseudoschoenus inanis
Cyperus rigidifolius
Ficinia paradoxa
Calyptrocarya sp.
Diplacrum carlcinum
Lagenocarpus albo-niger
Becquerella cymosa
Scleria distans
Other Cyperoideae
Cladium mariscus
Mapania cuspidata
Chrysitrix capensis
Hypolytrum nemorum
Mapanioideae
20.0
SCHOENEAE TRIBE

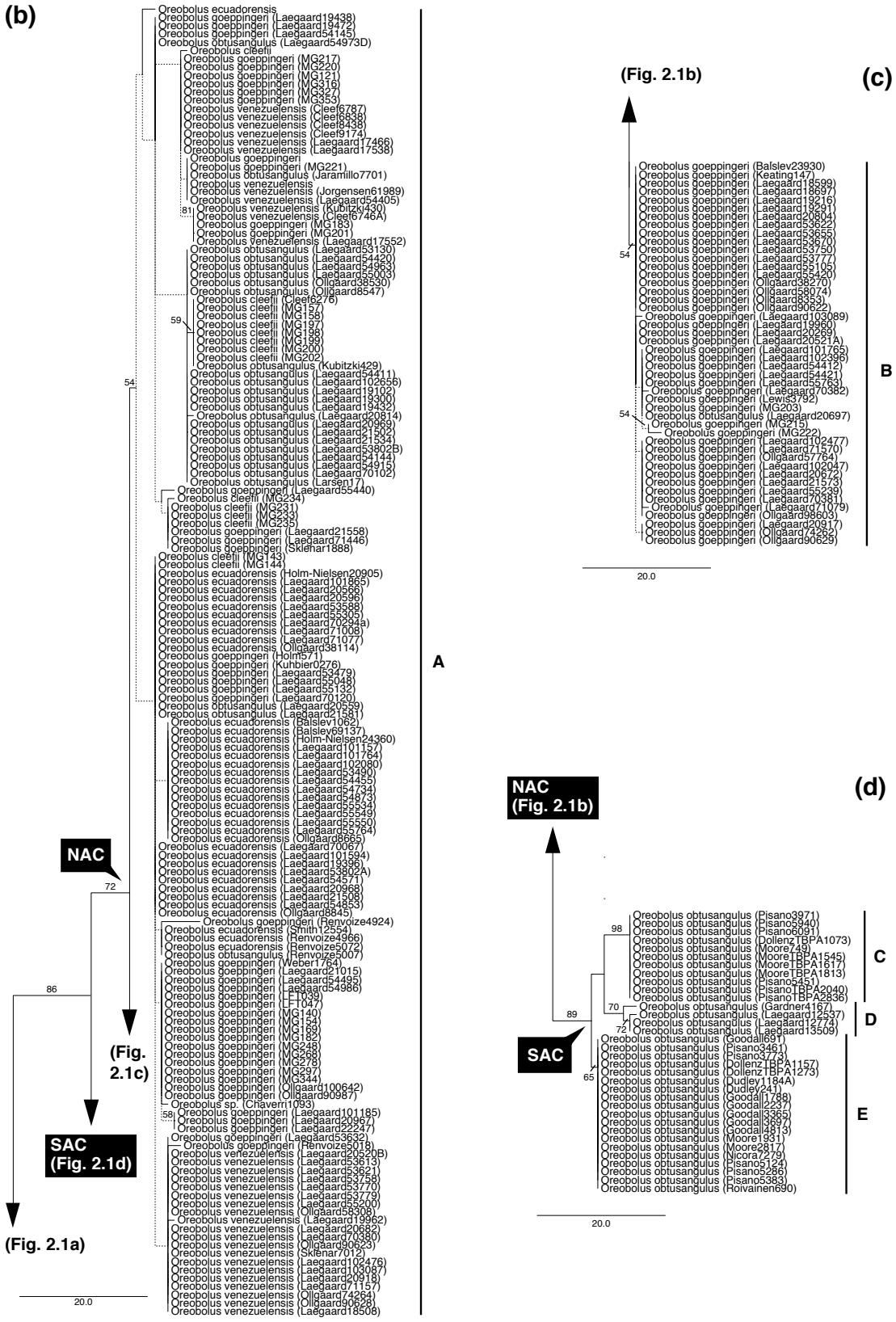

Figure 2.1. (a – d) One of the most parsimonious trees obtained from the combined matrix of ITS and *trn*L-F. Numbers above the branches represent bootstrap values (MP-BS < 0.50, not shown). Dashed lines indicate nodes that collapsed in the strict consensus tree.

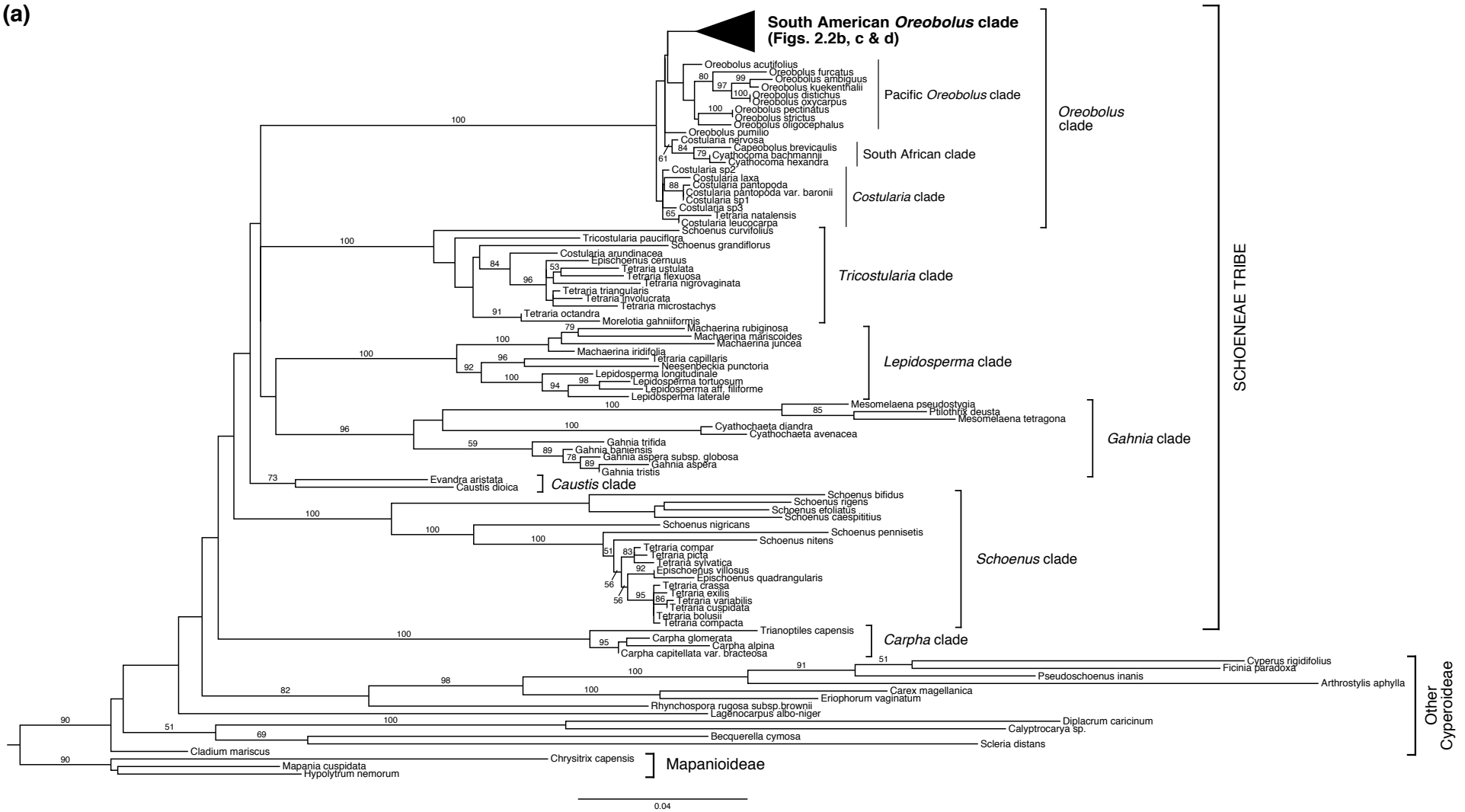
(a)
South American Oreobolus clade
(Figs. 2.2b, c & d)
Oreobolus acutifolius
Oreobolus furcatus
Oreobolus ambiguus
Oreobolus kuekenthalii
Oreobolus distichus
Oreobolus oxycarpus
Oreobolus pectinatus
Oreobolus strictus
Oreobolus oligocephalus
Oreobolus pumilio
Pacific Oreobolus clade
Costularia nervosa
Capeobolus brevicaulis
Cyathocoma bachmannii
Cyathocoma hexandra
South African clade
Costularia sp2
Costularia laxa
Costularia pantopoda
Costularia pantopoda var. baronii
Costularia sp1
Costularia sp3
Costularia clade
Oreobolus clade
Tetraria natalensis
Costularia leucocarpa
Schoenus curvifolius
Tricostularia pauciflora
Schoenus grandiflorus
Costularia arundinacea
Tricostularia clade
Epischoenus cernuus
Tetraria ustulata
Tetraria flexuosa
Tetraria nigrovaginata
Tetraria triangularis
Tetraria involucrata
Tetraria microstachys
Tetraria octandra
Morelotia gahniiformis
Machaerina rubiginosa
Machaerina mariscoides
Machaerina juncea
Machaerina iridifolia
Tetraria capillaris
Neesenbeckia punctoria
Lepidosperma longitudinale
Lepidosperma tortuosum
Lepidosperma aff. filiforme
Lepidosperma laterale
Lepidosperma clade
Mesomelaena pseudostygia
Ptilothrix deusta
Mesomelaena tetragona
Cyathochaeta diandra
Cyathochaeta avenacea
Gahnia trifida
Gahnia baniensis
Gahnia aspera subsp. globosa
Gahnia aspera
Gahnia tristis
Gahnia clade
Evandra aristata
Caustis dioica
Caustis clade
Schoenus bifidus
Schoenus rigens
Schoenus efoliatus
Schoenus caespititius
Schoenus nigricans
Schoenus pennisetis
Schoenus nitens
Tetraria compar
Tetraria picta
Tetraria sylvatica
Epischoenus villosus
Epischoenus quadrangularis
Tetraria crassa
Tetraria exilis
Tetraria variabilis
Tetraria cuspidata
Tetraria bolusii
Tetraria compacta
Schoenus clade
Trianoptiles capensis
Carpha glomerata
Carpha alpina
Carpha capitellata var. bracteosa
Carpha clade
SCHOENEAE TRIBE
Cyperus rigidifolius
Ficinia paradoxa
Pseudoschoenus inanis
Arthrostylis aphylla
Carex magellanica
Eriophorum vaginatum
Rhynchospora rugosa subsp.brownii
Lagenocarpus albo-niger
Diplacrum caricinum
Calyptrocarya sp.
Becquerella cymosa
Scleria distans
Other Cyperoideae
Cladium mariscus
Chrysitrix capensis
Mapania cuspidata
Hypolytrum nemorum
Mapanioideae
0.04

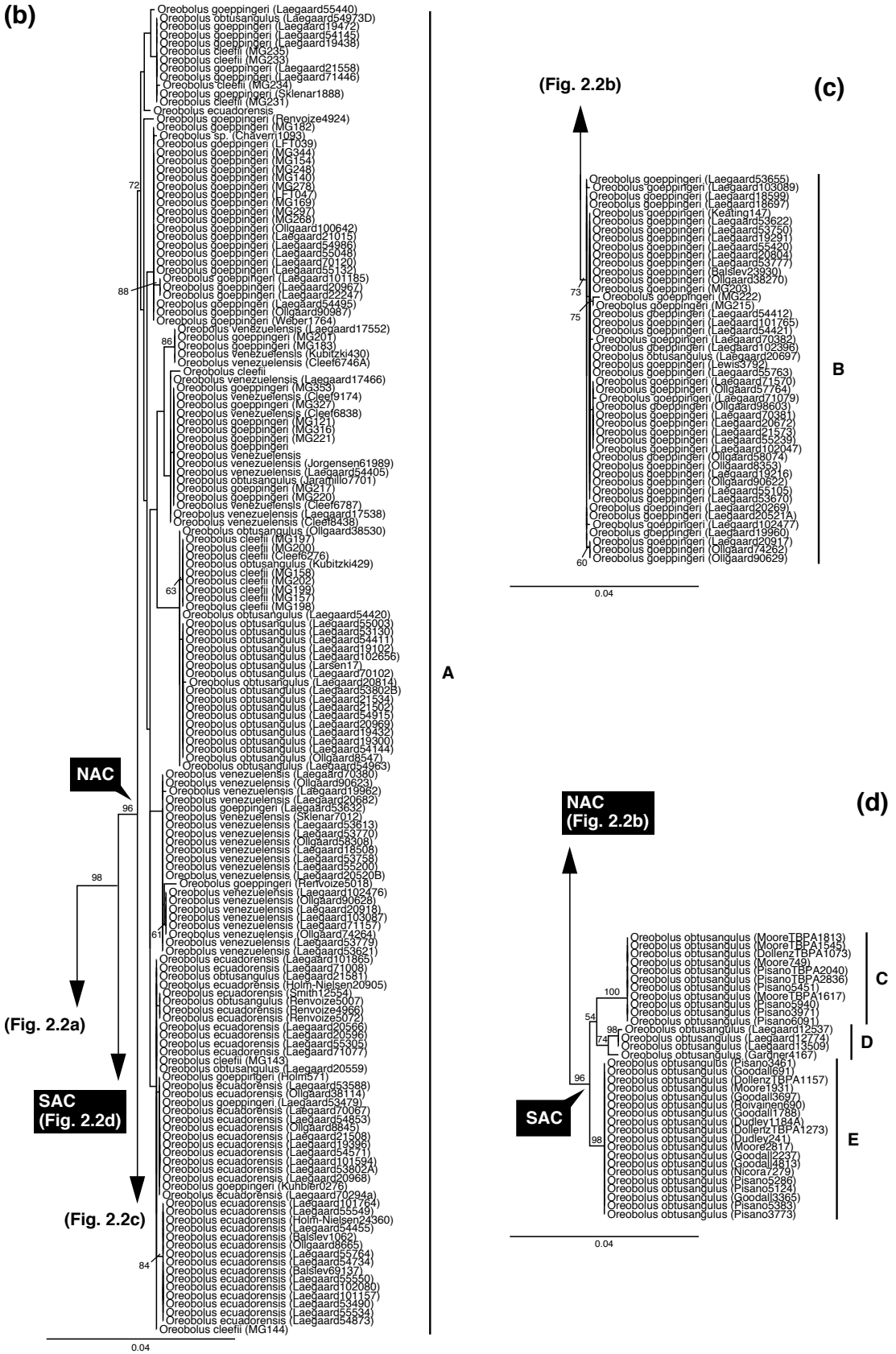

Figure 2.2. (a – d) Tree with the best likelihood score obtained from the combined matrix of ITS and *trn*L-F. Numbers above the branches represent bootstrap values (ML-BS < 0.50, not shown).

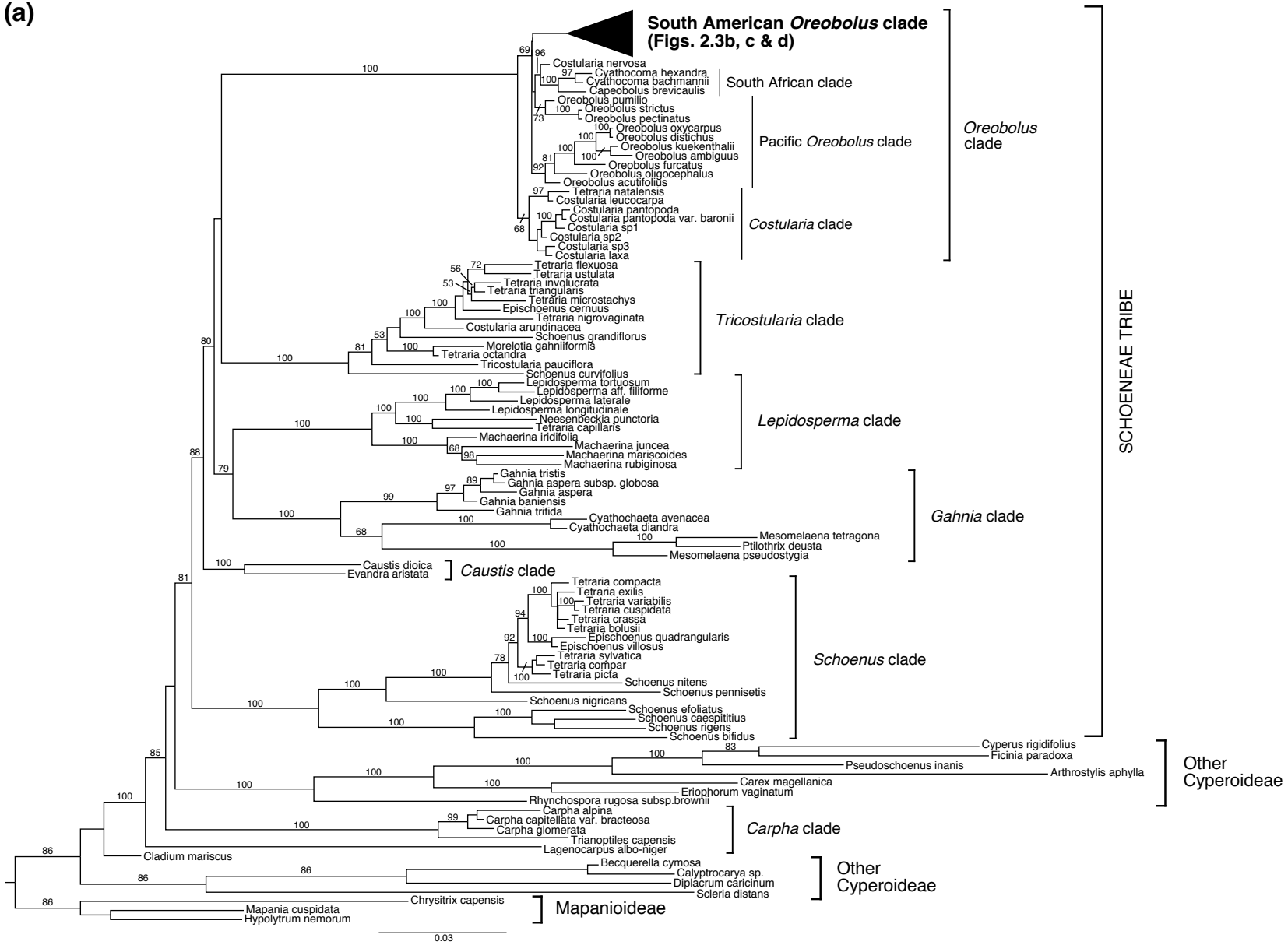
(a)
South American Oreobolus clade
(Figs. 2.3b, c & d)
Costularia nervosa
Cyathocoma hexandra
Cyathocoma bachmannii
Capeobolus brevicaulis
South African clade
Oreobolus pumilio
Oreobolus strictus
Oreobolus pectinatus
Oreobolus oxycarpus
Oreobolus distichus
Oreobolus kuekenthalii
Oreobolus ambiguus
Oreobolus furcatus
Oreobolus oligocephalus
Oreobolus acutifolius
Pacific Oreobolus clade
Tetraria natalensis
Costularia leucocarpa
Costularia pantopoda
Costularia pantopoda var. baronii
Costularia sp1
Costularia sp2
Costularia sp3
Costularia laxa
Costularia clade
Oreobolus clade
Tetraria flexuosa
Tetraria ustulata
Tetraria involucrata
Tetraria triangularis
Tetraria microstachys
Epischoenus cernuus
Tetraria nigrovaginata
Costularia arundinacea
Schoenus grandiflorus
Morelotia gahniiformis
Tetraria octandra
Tricostularia pauciflora
Tricostularia clade
Schoenus curvifolius
Lepidosperma tortuosum
Lepidosperma aff. filiforme
Lepidosperma laterale
Lepidosperma longitudinale
Neesenbeckia punctoria
Tetraria capillaris
Machaerina iridifolia
Machaerina juncea
Machaerina mariscoides
Machaerina rubiginosa
Lepidosperma clade
Gahnia tristis
Gahnia aspera subsp. globosa
Gahnia aspera
Gahnia baniensis
Gahnia trifida
Cyathochaeta avenacea
Cyathochaeta diandra
Mesomelaena tetragona
Ptilothrix deusta
Mesomelaena pseudostygia
Gahnia clade
Caustis dioica
Evandra aristata
Caustis clade
Tetraria compacta
Tetraria exilis
Tetraria variabilis
Tetraria cuspidata
Tetraria crassa
Tetraria bolusii
Epischoenus quadrangularis
Epischoenus villosus
Tetraria sylvatica
Tetraria compar
Tetraria picta
Schoenus nitens
Schoenus pennisetis
Schoenus nigricans
Schoenus efoliatus
Schoenus caespititius
Schoenus rigens
Schoenus bifidus
Schoenus clade
SCHOENEAE TRIBE
Cyperus rigidifolius
Ficinia paradoxa
Pseudoschoenus inanis
Arthrostylis aphylla
Carex magellanica
Eriophorum vaginatum
Rhynchospora rugosa subsp.brownii
Other Cyperoideae
Carpha alpina
Carpha capitellata var. bracteosa
Carpha glomerata
Trianoptiles capensis
Lagenocarpus albo-niger
Carpha clade
Cladium mariscus
Becquerella cymosa
Calyptrocarya sp.
Diplacrum caricinum
Scleria distans
Other Cyperoideae
Chrysitrix capensis
Mapania cuspidata
Hypolytrum nemorum
Mapanioideae
0.03

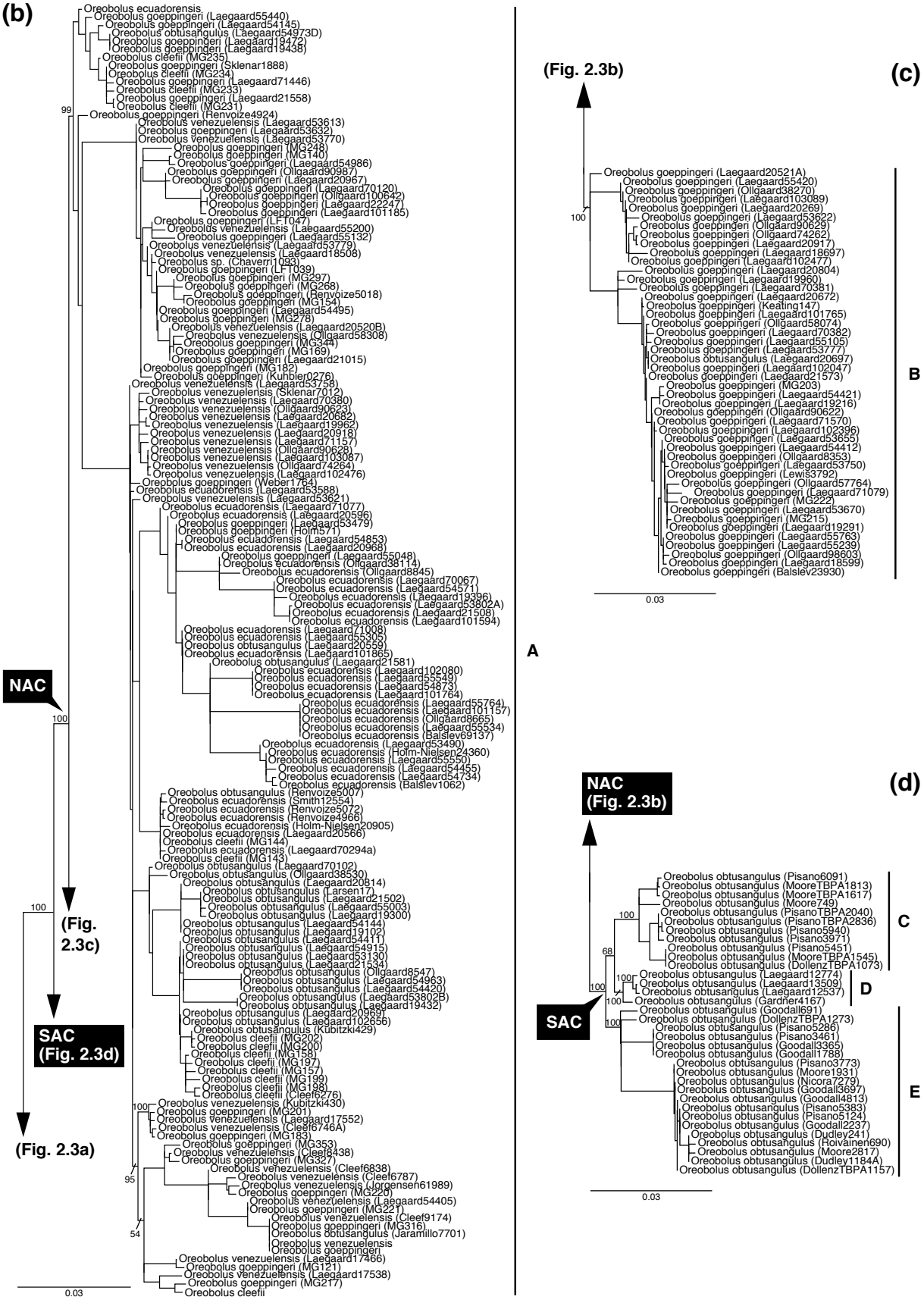

Figure 2.3. (a – d) Maximum clade credibility tree obtained from the Bayesian analysis based on the combined matrix of ITS and *trn*L-F. Numbers above the branches represent posterior probability values (PP < 0.50, not shown).

Within the *Oreobolus* clade, no well-supported relationships at between-genus level or above were recovered. Nevertheless, four sub-clades were consistently recovered in MP and ML (Figs. 2.1 and 2.2), while BI recovered five (Fig. 2.3). A *Costularia* clade was recovered with moderate support including all sampled African and Madagascan species of *Costularia* but neither of the New Caledonian ones (*C. nervosa* and *C. arundinacea*). However, *Tetraria natalensis* was also nested within this clade (MP-BS<50%, ML-BS<50%, PP=68%). *C. arundinacea* was recovered within the *Tricostularia* clade. The *Costularia* clade appeared as sister to the rest of the species within the *Oreobolus* clade, a relationship with low support in ML (ML-BS<50%), good support in BI (PP=68%) but not recovered in MP. The South African species (*Capeobolus brevicaulis*, *Cyathocoma bachmannii* and *Cyathocoma hexandra*) formed a well-supported clade (MP-BS=71%, ML-BS=84%, PP=100%) with *Costularia nervosa* consistently appearing as its sister taxon, poorly supported in MP and ML (MP-BS<50%, ML-BS=61%) but highly supported in BI (PP=96%). *Oreobolus* was not recovered as a monophyletic genus (Figs. 2.1 – 2.3); however the South American species of *Oreobolus* were recovered as a highly supported monophyletic group (MP-BS=86%, ML-BS=98%, PP=100%). Nine of the ten Pacific *Oreobolus* species sampled in this study (*O. ambiguus, O. acutifolius, O. kuekenthalii, O. distichus, O. oxycarpus, O. furcatus, O. oligocephalus, O. pectinatus* and *O. strictus*) formed a monophyletic group poorly supported in MP and ML (MP-BS<50%, ML-BS<50%) but not present in BI. In BI two well-supported clades with all ten Pacific species were formed: a first one including *O. pectinatus*, *O. strictus* and *O. pumilio* (PP=73%), and a second one including the rest of the species (PP=92%). The position of *Oreobolus pumilio* was inconsistent across analyses:

appearing as sister taxon to the rest of the *Oreobolus* clade in MP (MP-BS<50%), while in ML it was recovered as forming a polytomy with the South African clade, *C. nervosa* and the South American clade (ML-BS<50%).

None of the five South American species of *Oreobolus* were resolved as monophyletic (Figs. 2.1 – 2-3). However, the same backbone was consistently recovered across analyses. There was a distinct geographic pattern within the group, and two highly supported clades split at the crown node: a southern Andean clade (MP-BS=89%, ML-BS=96%, PP=100%) and a northern Andean clade (MP-BS=72%, ML-BS=96%, PP=100%). The southern Andean clade (SAC) was solely composed of samples of *O. obtusangulus*, the only species to be present in that region. Within the SAC, three well-supported subclades appeared with a strong geographic structure (clades C – E). The northern Andean clade (NAC) had two major well-supported sub-clades (A and B): clade B is formed by 46 samples of *O. goeppingeri* from Ecuador and the southern region of Colombia, plus one sample of *O. obtusangulus* from the same region (MP-BS=54%, ML-BS=73%, PP=100%). Clade B was sister to clade A, which was formed by the rest of the northern Andean samples (MP-BS=54%, ML-BS=72%, PP=99%). The support and resolution for smaller groupings diminishes towards the tips.

2.4.2 Divergence Time estimation

The BEAST analysis recovered the same well-supported clades as the phylogenetic reconstruction analyses (Fig. 2.4). The Schoeneae tribe diverged c. 50 Ma during the early Eocene (95% HPD [33.85 – 65.64] Ma). Of the six clades comprising Schoeneae, all but *Oreobolus* clade began to diversify during the late Eocene – early

Miocene: *Schoenus* clade c. 35 Ma (95% HPD [20.68 – 50.16] Ma), *Tricostularia* clade c. 20 Ma (95% HPD [9.65 – 32.31] Ma), *Lepidosperma* clade c. 21 Ma (95% HPD [10.9 – 31.16] Ma), *Caustis* clade c. 23 Ma (95% HPD [5.44 – 44.99] Ma) and *Gahnia* clade c. 27 Ma (95% HPD [15.07 – 40.63] Ma). The *Oreobolus* clade diverged during the late Miocene, c. 9 Ma (95% HPD [5.04 – 13.43] Ma). The four sub-clades within the *Oreobolus* clade were estimated to originate during the early Pliocene: South African + *C. nervosa* clade c. 4 Ma (95% HPD [1.34 – 7.55] Ma) with the South African species originating at c. 2 Ma (95% HPD [0.58 – 4.53] Ma), *Costularia* clade c. 4 Ma (95% HPD [1.49 – 7.41] Ma), Pacific *Oreobolus* clade (minus *O. pumilio*) c. 5 Ma (95% HPD [2.95 – 8.03] Ma) and the South American *Oreobolus* clade c. 5 Ma (95% HPD [2.79 – 7.47] Ma). The SAC and NAC originated within the same timeframe c. 3 Ma (95% HPD [1.37 – 4.71] Ma) and (95% HPD [1.80 – 4.79] Ma) respectively, during the late Pliocene. In the NAC, rapid diversification occurred within the last two million years during the Pleistocene. Table 2.1 presents nodes ages and 95% HPD for key nodes.

Figure 2.4. (a – c) Chronogram from the BEAST time divergence analysis for the combined matrix of ITS and *trn*L-F annotated with the ancestral areas reconstructed on RASP. Nodes 1 – 14 are referred to in Table 2.1. Node bars indicate 95% HPD age ranges. Lineages are coloured according to their reconstructed distribution. Coloured circles accompanying taxa indicate their current distribution. Pie charts represent the percentage PP of the ancestral reconstructed area at the selected node. Map inset indicates the 11 geographical regions defined. S. Afr. Cl., South African clade; Pac. *Oreob.* cl., Pacific *Oreobolus* clade.

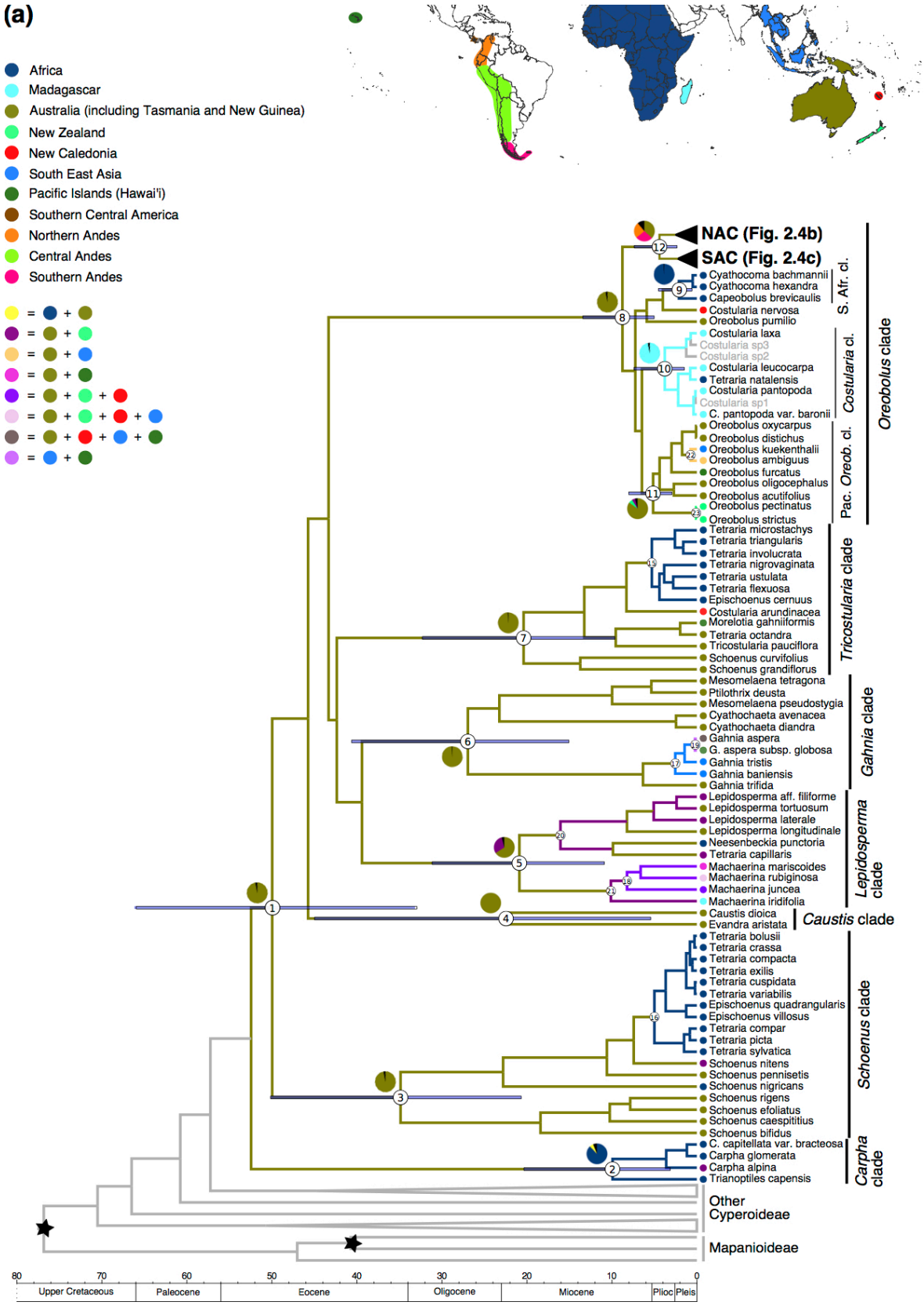
(a)
Africa
Madagascar
Australia (including Tasmania and New Guinea)
New Zealand
New Caledonia
South East Asia
Pacific Islands (Hawai'i)
Southern Central America
Northern Andes
Central Andes
Southern Andes
NAC (Fig. 2.4b)
SAC (Fig. 2.4c)
Cyathocoma bachmannii
Cyathocoma hexandra
Capeobolus brevicaulis
Costularia nervosa
Oreobolus pumilio
Costularia laxa
Costularia sp3
Costularia sp2
Costularia leucocarpa
Tetraria natalensis
Costularia pantopoda
Costularia sp1
C. pantopoda var. baronii
Oreobolus oxycarpus
Oreobolus distichus
Oreobolus kuekenthalii
Oreobolus ambiguus
Oreobolus furcatus
Oreobolus oligocephalus
Oreobolus acutifolius
Oreobolus pectinatus
Oreobolus strictus
Tetraria microstachys
Tetraria triangularis
Tetraria involucrata
Tetraria nigrovaginata
Tetraria ustulata
Tetraria flexuosa
Epischoenus cernuus
Costularia arundinacea
Morelotia gahniiformis
Tetraria octandra
Tricostularia pauciflora
Schoenus curvifolius
Schoenus grandiflorus
Mesomelaena tetragona
Ptilothrix deusta
Mesomelaena pseudostygia
Cyathochaeta avenacea
Cyathochaeta diandra
Gahnia aspera
G. aspera subsp. globosa
Gahnia tristis
Gahnia baniensis
Gahnia trifida
Lepidosperma aff. filiforme
Lepidosperma tortuosum
Lepidosperma laterale
Lepidosperma longitudinale
Neesenbeckia punctoria
Tetraria capillaris
Machaerina mariscoides
Machaerina rubiginosa
Machaerina juncea
Machaerina iridifolia
Caustis dioica
Evandra aristata
Tetraria bolusii
Tetraria crassa
Tetraria compacta
Tetraria exilis
Tetraria cuspidata
Tetraria variabilis
Epischoenus quadrangularis
Epischoenus villosus
Tetraria compar
Tetraria picta
Tetraria sylvatica
Schoenus nitens
Schoenus pennisetis
Schoenus nigricans
Schoenus rigens
Schoenus efoliatus
Schoenus caespititius
Schoenus bifidus
C. capitellata var. bracteosa
Carpha glomerata
Carpha alpina
Trianoptiles capensis
Other Cyperoideae
Mapanioideae
S. Afr. cl.
Costularia cl.
Pac. Oreob. cl.
Oreobolus clade
Tricostularia clade
Gahnia clade
Lepidosperma clade
Caustis clade
Schoenus clade
Carpha clade
80
70
60
50
40
30
20
10
0
Upper Cretaceous
Paleocene
Eocene
Oligocene
Miocene
Plioc
Pleis

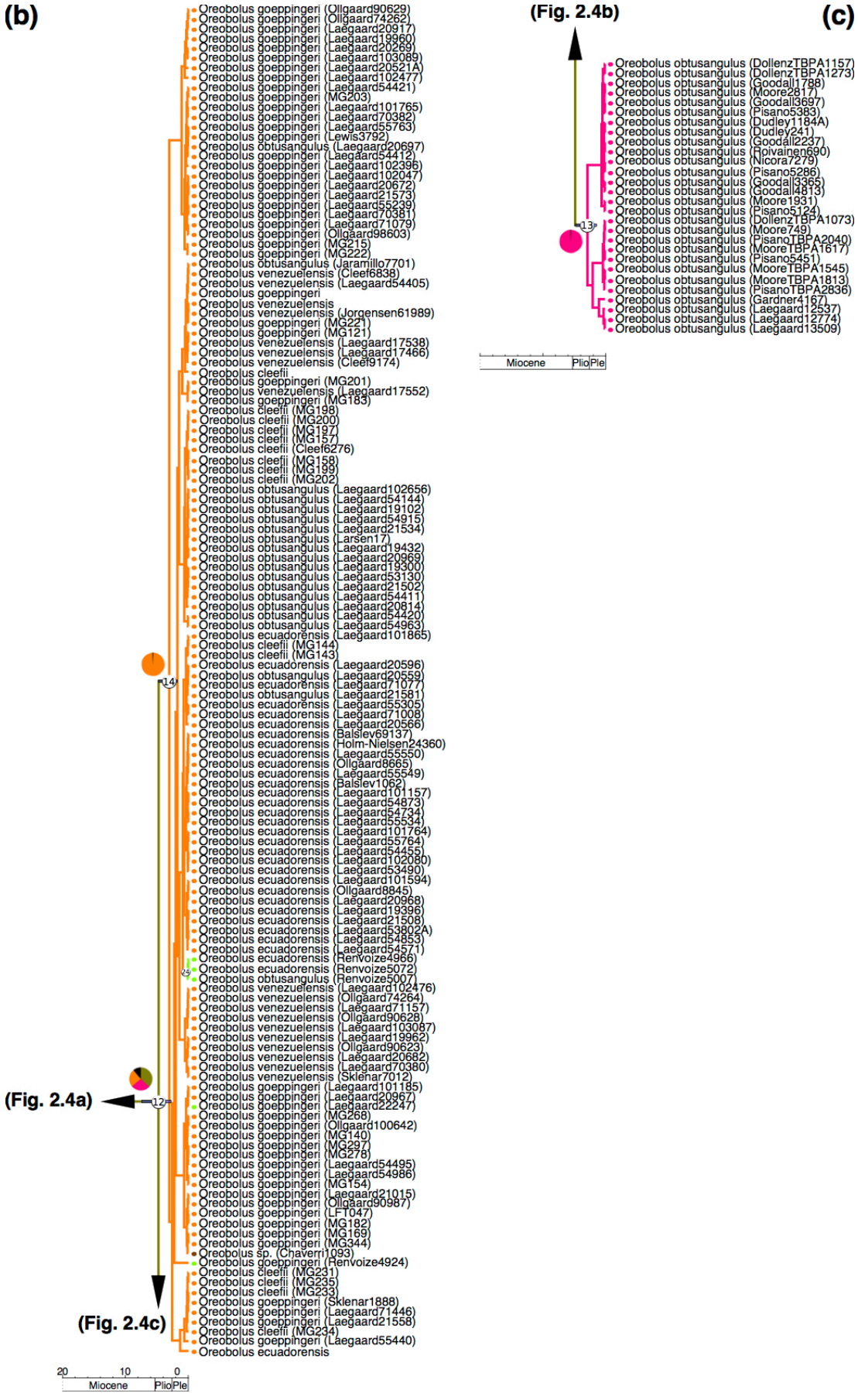
(b)
(c)
(Fig. 2.4b)
(Fig. 2.4a)
(Fig. 2.4c)
Oreobolus goeppingeri (Ollgaard90629)
Oreobolus goeppingeri (Ollgaard74262)
Oreobolus goeppingeri (Laegaard20917)
Oreobolus goeppingeri (Laegaard19960)
Oreobolus goeppingeri (Laegaard20269)
Oreobolus goeppingeri (Laegaard103089)
Oreobolus goeppingeri (Laegaard20521A)
Oreobolus goeppingeri (Laegaard102477)
Oreobolus goeppingeri (Laegaard54421)
Oreobolus goeppingeri (MG203)
Oreobolus goeppingeri (Laegaard101765)
Oreobolus goeppingeri (Laegaard70382)
Oreobolus goeppingeri (Laegaard55763)
Oreobolus goeppingeri (Lewis3792)
Oreobolus obtusangulus (Laegaard20697)
Oreobolus goeppingeri (Laegaard54412)
Oreobolus goeppingeri (Laegaard102396)
Oreobolus goeppingeri (Laegaard102047)
Oreobolus goeppingeri (Laegaard20672)
Oreobolus goeppingeri (Laegaard21573)
Oreobolus goeppingeri (Laegaard55239)
Oreobolus goeppingeri (Laegaard70381)
Oreobolus goeppingeri (Laegaard71079)
Oreobolus goeppingeri (Ollgaard98603)
Oreobolus goeppingeri (MG215)
Oreobolus goeppingeri (MG222)
Oreobolus obtusangulus (Jaramillo7701)
Oreobolus venezuelensis (Cleef6838)
Oreobolus venezuelensis (Laegaard54405)
Oreobolus goeppingeri
Oreobolus venezuelensis
Oreobolus venezuelensis (Jorgensen61989)
Oreobolus goeppingeri (MG221)
Oreobolus goeppingeri (MG121)
Oreobolus venezuelensis (Laegaard17538)
Oreobolus venezuelensis (Laegaard17466)
Oreobolus venezuelensis (Cleef9174)
Oreobolus cleefii
Oreobolus goeppingeri (MG201)
Oreobolus venezuelensis (Laegaard17552)
Oreobolus goeppingeri (MG183)
Oreobolus cleefii (MG198)
Oreobolus cleefii (MG200)
Oreobolus cleefii (MG197)
Oreobolus cleefii (MG157)
Oreobolus cleefii (Cleef6276)
Oreobolus cleefii (MG158)
Oreobolus cleefii (MG199)
Oreobolus cleefii (MG202)
Oreobolus obtusangulus (Laegaard102656)
Oreobolus obtusangulus (Laegaard54144)
Oreobolus obtusangulus (Laegaard19102)
Oreobolus obtusangulus (Laegaard54915)
Oreobolus obtusangulus (Laegaard21534)
Oreobolus obtusangulus (Larsen17)
Oreobolus obtusangulus (Laegaard19432)
Oreobolus obtusangulus (Laegaard20969)
Oreobolus obtusangulus (Laegaard19300)
Oreobolus obtusangulus (Laegaard53130)
Oreobolus obtusangulus (Laegaard21502)
Oreobolus obtusangulus (Laegaard54411)
Oreobolus obtusangulus (Laegaard20814)
Oreobolus obtusangulus (Laegaard54420)
Oreobolus obtusangulus (Laegaard54963)
Oreobolus ecuadorensis (Laegaard101865)
Oreobolus cleefii (MG144)
Oreobolus cleefii (MG143)
Oreobolus ecuadorensis (Laegaard20596)
Oreobolus obtusangulus (Laegaard20559)
Oreobolus ecuadorensis (Laegaard71077)
Oreobolus obtusangulus (Laegaard21581)
Oreobolus ecuadorensis (Laegaard55305)
Oreobolus ecuadorensis (Laegaard71008)
Oreobolus ecuadorensis (Laegaard20566)
Oreobolus ecuadorensis (Balslev69137)
Oreobolus ecuadorensis (Holm-Nielsen24360)
Oreobolus ecuadorensis (Laegaard55550)
Oreobolus ecuadorensis (Ollgaard8665)
Oreobolus ecuadorensis (Laegaard55549)
Oreobolus ecuadorensis (Balslev1062)
Oreobolus ecuadorensis (Laegaard101157)
Oreobolus ecuadorensis (Laegaard54873)
Oreobolus ecuadorensis (Laegaard54734)
Oreobolus ecuadorensis (Laegaard55534)
Oreobolus ecuadorensis (Laegaard101764)
Oreobolus ecuadorensis (Laegaard55764)
Oreobolus ecuadorensis (Laegaard54455)
Oreobolus ecuadorensis (Laegaard102080)
Oreobolus ecuadorensis (Laegaard53490)
Oreobolus ecuadorensis (Laegaard101594)
Oreobolus ecuadorensis (Ollgaard8845)
Oreobolus ecuadorensis (Laegaard20968)
Oreobolus ecuadorensis (Laegaard19396)
Oreobolus ecuadorensis (Laegaard21508)
Oreobolus ecuadorensis (Laegaard53802A)
Oreobolus ecuadorensis (Laegaard54853)
Oreobolus ecuadorensis (Laegaard54571)
Oreobolus ecuadorensis (Renvoize4966)
Oreobolus ecuadorensis (Renvoize5072)
Oreobolus obtusangulus (Renvoize5007)
Oreobolus venezuelensis (Laegaard102476)
Oreobolus venezuelensis (Ollgaard74264)
Oreobolus venezuelensis (Laegaard71157)
Oreobolus venezuelensis (Ollgaard90628)
Oreobolus venezuelensis (Laegaard103087)
Oreobolus venezuelensis (Laegaard19962)
Oreobolus venezuelensis (Ollgaard90623)
Oreobolus venezuelensis (Laegaard20682)
Oreobolus venezuelensis (Laegaard70380)
Oreobolus venezuelensis (Sklenar7012)
Oreobolus goeppingeri (Laegaard101185)
Oreobolus goeppingeri (Laegaard20967)
Oreobolus goeppingeri (Laegaard22247)
Oreobolus goeppingeri (MG268)
Oreobolus goeppingeri (Ollgaard100642)
Oreobolus goeppingeri (MG140)
Oreobolus goeppingeri (MG297)
Oreobolus goeppingeri (MG278)
Oreobolus goeppingeri (Laegaard54495)
Oreobolus goeppingeri (Laegaard54986)
Oreobolus goeppingeri (MG154)
Oreobolus goeppingeri (Laegaard21015)
Oreobolus goeppingeri (Ollgaard90987)
Oreobolus goeppingeri (LFT047)
Oreobolus goeppingeri (MG182)
Oreobolus goeppingeri (MG169)
Oreobolus goeppingeri (MG344)
Oreobolus sp. (Chaverri1093)
Oreobolus goeppingeri (Renvoize4924)
Oreobolus cleefii (MG231)
Oreobolus cleefii (MG235)
Oreobolus cleefii (MG233)
Oreobolus goeppingeri (Sklenar1888)
Oreobolus goeppingeri (Laegaard71446)
Oreobolus goeppingeri (Laegaard21558)
Oreobolus cleefii (MG234)
Oreobolus goeppingeri (Laegaard55440)
Oreobolus ecuadorensis
14
12
24
13
20
10
0
Miocene
Plio
Ple
Oreobolus obtusangulus (DollenzTBPA1157)
Oreobolus obtusangulus (DollenzTBPA1273)
Oreobolus obtusangulus (Goodall1798)
Oreobolus obtusangulus (Moore2817)
Oreobolus obtusangulus (Goodall3697)
Oreobolus obtusangulus (Pisano5383)
Oreobolus obtusangulus (Dudley1184A)
Oreobolus obtusangulus (Dudley241)
Oreobolus obtusangulus (Goodall2237)
Oreobolus obtusangulus (Roivainen690)
Oreobolus obtusangulus (Nicora7279)
Oreobolus obtusangulus (Pisano5286)
Oreobolus obtusangulus (Goodall3365)
Oreobolus obtusangulus (Goodall4813)
Oreobolus obtusangulus (Moore1931)
Oreobolus obtusangulus (Pisano5124)
Oreobolus obtusangulus (DollenzTBPA1073)
Oreobolus obtusangulus (Moore749)
Oreobolus obtusangulus (PisanoTBPA2040)
Oreobolus obtusangulus (MooreTBPA1617)
Oreobolus obtusangulus (Pisano5451)
Oreobolus obtusangulus (MooreTBPA1545)
Oreobolus obtusangulus (MooreTBPA1813)
Oreobolus obtusangulus (PisanoTBPA2836)
Oreobolus obtusangulus (Gardner4167)
Oreobolus obtusangulus (Laegaard12537)
Oreobolus obtusangulus (Laegaard12774)
Oreobolus obtusangulus (Laegaard13509)
13
Miocene
Plio
Ple

2.4.3 Ancestral area reconstruction

Figure 2.4 shows the dated phylogeny with the reconstructed areas. Table 2.1 presents the reconstructed areas with support for key nodes. The results presented here support those of Viljoen et al. (2013), with the Schoeneae tribe originating in Australia during the early Eocene. Similarly, all six clades within the tribe (nodes 3 to 8) were reconstructed as diverging within Australia and dispersing from there since the early Miocene. In the five clades (nodes 3 to 7) other than the *Oreobolus* clade, four dispersal events to Africa were evident (nodes 15 and 16, *Neesenbeckia punctoria* and *Schoenus nigricans*), two to South East Asia (node 17 and *Machaerina rubiginosa*), three to the Pacific Islands (node 19, *Morelotia gahniiformis* and *Machaerina mariscoides*), three to New Zealand (nodes 20 and 21, and *Schoenus nitens*), three to New Caledonia (node 18, *Costularia arundinacea* and *Gahnia aspera*) and one to Madagascar (*Machaerina iridifolia*).

Within the *Oreobolus* clade, dispersal from Australia was reconstructed as commencing during the late Miocene. A single dispersal event to Africa was supported for the South African clade (node 9). Similarly, one dispersal event to Madagascar was recovered for the *Costularia* clade (node 10), with a subsequent colonisation of Africa by the *Tetraria natalensis* lineage. Within the Pacific *Oreobolus* clade, a single dispersal event was reconstructed to each of the following areas: South East Asia (node 22), New Zealand (node 23) and the Pacific Islands (*Oreobolus furcatus*). The South American *Oreobolus* clade was reconstructed as originating in Australia, although with low support values (PP=0.37, node 12), and having colonised South America twice during the early Pliocene (nodes 13 and 14).

Alternative reconstructions suggested dispersal from Australia during the late Miocene (node 8) followed by either an early Pliocene origin in the southern Andes region with a subsequent dispersal to the northern Andes (PP=0.27), or an early Pliocene origin in the northern Andes with a subsequent dispersal to the southern Andes (PP=0.25). From the northern Andes, colonisation of the northernmost part of the central Andes region occurred at least twice during the Pleistocene (node 24 and *Oreobolus goeppingeri* (Renvoize4924)). Similarly, colonisation of southern Central America occurred at least once (*Oreobolus sp.* (Chaverri1093)).

Table 2.1. Node ages and reconstructed areas for key nodes. Node numbers correspond to those on Fig. 2.4. PP: posterior probability, HPD: highest posterior density, S. Am.: South American

Node	PP	Clade	Mean divergence age (95% HPD) Ma	Ancestral area (PP)	Epoch (HPD)
1	0.62	Schoeneae	49.95 (33.85 - 65.64)	Australia (0.97)	Eocene (Paleocene - Eocene)
2	1.00	*Carpha*	9.91 (3.15 - 20.36)	Africa (0.88)	Miocene (Miocene - Pliocene)
3	1.00	*Schoenus*	34.85 (20.68 - 50.16)	Australia (0.97)	Eocene (Eocene - Miocene)
4	1.00	*Caustis*	22.45 (5.44 - 44.99)	Australia (1.00)	Miocene (Eocene - Miocene)
5	1.00	*Lepidosperma*	20.87 (10.9 -31.16)	Australia (0.66)	Miocene (Oligocene - Miocene)
6	1.00	*Gahnia*	26.93 (15.07 - 40.63)	Australia (0.99)	Oligocene (Eocene - Miocene)
7	1.00	*Tricostularia*	20.38 (9.65 - 32.31)	Australia (0.99)	Miocene (Oligocene - Miocene)
8	1.00	*Oreobolus*	8.75 (5.04 - 13.43)	Australia (0.97)	Miocene (Miocene - Pliocene)
9	1.00	South African	2.10 (0.58 - 4.53)	Africa (0.99)	Pleistocene (Pliocene - Pleistocene)
10	0.76	*Costularia*	3.77 (1.49 - 7.41)	Madagascar (0.97)	Pliocene (Miocene - Pleistocene)
11	0.80	Pacific *Oreobolus*	5.14 (2.95 - 8.03)	Australia (0.85)	Pliocene (Miocene - Pliocene)
12	1.00	S. Am. *Oreobolus*	4.76 (2.79 - 7.47)	Australia (0.37), Southern Andes (0.27), Northern Andes (0.25)	Pliocene (Miocene - Pliocene)
13	1.00	SAC	2.80 (1.37 - 4.71)	Southern Andes (0.99)	Pliocene (Pliocene - Pleistocene)
14	1.00	NAC	3.07 (1.80 - 4.79)	Northern Andes (0.99)	Pliocene (Pliocene - Pleistocene)

2.4.4 Diversification rates estimation

Table 2.2 summarises the results for net diversification rates within the *Oreobolus* clade. Net diversification rate was highest in the *Costularia* clade (0.718 speciation events per million years, Myr^{-1}), followed by the South African clade (0.660 Myr^{-1}), then the Northern Andean clade (NAC) (0.524 Myr^{-1}), and finally the Pacific *Oreobolus* clade (0.467 Myr^{-1}). The net diversification rate for the South American *Oreobolus* clade is the lowest of all (0.338 Myr^{-1}), likely caused by the zero net diversification rate of SAC explained by this clade containing a single species.

Table 2.2. Net diversification rates (*r*) of lineages within the *Oreobolus* clade. Min and Max represent the lower and upper limits of the 95% HPD.

		Crown node age (Ma)			Net diversification Rate (*r*)		
Clade	*N*	Max	Mean	Min	Max	Mean	Min
South American *Oreobolus*	5	7.47	4.76	2.79	0.577	0.338	0.215
Northern Andean (NAC)	5	4.79	3.07	1.80	0.894	0.524	0.336
Southern Andean (SAC)	1	4.71	2.80	1.37	0.000	0.000	0.000
Pacific *Oreobolus*	11	8.03	5.14	2.95	0.813	0.467	0.299
South African (*Capeobolus* + *Cyathocoma*)	4	4.53	2.10	0.58	2.390	0.660	0.306
Costularia	15	7.41	3.77	1.49	1.817	0.718	0.365

2.5 DISCUSSION

This study examines the phylogenetics and biogeography of the South American species of *Oreobolus* within the context of its tribe. The taxon sampling in the study presented here allows, for the first time, a robust assessment of the monophyly of *Oreobolus* and of its South American species. Furthermore, it allows proper

investigation of the impact of the Andean orogeny on the timing of the diversification events and directionality of migration events, and is the first study to compare speciation rates amongst diversely distributed lineages in the *Oreobolus* clade.

2.5.1 Phylogenetics of Schoeneae

The systematics of the Schoeneae have proven difficult, because in addition to the variable support for the tribe in phylogenetic studies, there is a lack of unambiguous morphological synapomorphies to characterise it (Verboom, 2006). Furthermore, relationships between schoenoid clades have been invariably poorly recovered, and hence the need for further phylogenetic studies with representative sampling within each has been established (Verboom, 2006; Muasya et al., 2009; Viljoen et al., 2013). Here, the Schoeneae *sensu* Viljoen et al. (2013) was recovered as monophyletic across all three analyses with varied support (MP-BS and ML-BS<50%, PP=81%). This result supports previous studies (Verboom, 2006; Jung & Choi, 2013 see Schoeneae part 1; Viljoen et al., 2013). Genera in the *Carpha* clade (*Carpha* and *Trianoptiles*) have been traditionally included in the Schoeneae (Bruhl, 1995; Goetghebeur, 1998). However, subsequent studies have suggested their re-classification as a separate Carpheae tribe, sister to Schoeneae, based on their molecular systematics and distinct embryo types (Viljoen et al., 2013). The uncertainty in the position of the *Carpha* clade in the current study neither supports nor rejects its placement, either as sister to the tribe or as part of it. Moreover, the six main clades within the tribe (*Schoenus* clade, *Caustis* clade, *Gahnia* clade, *Lepidosperma* clade, *Tricostularia* clade and *Oreobolus* clade) were each recovered

as monophyletic but relationships amongst them could not be inferred confidently. Verboom (2006) suggested that the lack of resolution might reflect early rapid cladogenesis in the tribe, a hypothesis further supported by the results obtained by Viljoen et al. (2013) and those presented here. Importantly, given the greatly increased taxon sampling for the South American *Oreobolus* clade in the current study, support for monophyly is especially robust for the *Oreobolus* clade.

There is an evident need for a re-assessment of generic limits within the Schoeneae incorporating both established morphological classification as well as new phylogenetic evidence. To accomplish this, a better sampling of under-represented clades, both in terms of geographical distribution and taxonomy, is urgently needed. The present study adds significant new evidence to the phylogenetics of the under-represented South American *Oreobolus* clade of the *Oreobolus* making an important contribution to the systematics of schoenoid sedges.

The *Oreobolus* clade was fully recovered as a monophyletic group and four (or five) sub-clades were consistently recovered (Figs. 2.1 – 2.3), but relationships amongst them were poorly resolved. First, a *Costularia* clade including four out of six of the sampled *Costularia* species appeared as sister to the rest of the *Oreobolus* clade (Figs. 2.2 and 2.3). Importantly, the *Costularia* clade contains all sampled Madagascan species, in addition to the African *Tetraria natalensis*. These results support previous studies that have demonstrated the polyphyly of both *Costularia* and *Tetraria* (Zhang et al., 2004; Verboom, 2006; Muasya et al., 2009; Viljoen et al., 2013). Furthermore, based on similarity in floral characters, Koyama (1961) suggested *Costularia* should be treated as a subgenus of *Tetraria*. Additionally, all *Costularia* species recovered within the *Oreobolus* clade (*Costularia* clade and *C.*

nervosa) are classified under subgenus *Costularia* except *C. arundinacea* that belongs to subgenus *Lophoschoenus* and was recovered within the *Tricostularia* clade (Figs. 2.1 – 2.3). Despite *C. nervosa* consistently appearing as sister taxon to a well-supported clade formed by the South African species *Cyathocoma* and *Capeobolus*, the differential clustering of *Costularia* subgenera is in accordance with the hypothesis put forward by Seberg (1988) that species within subgenus *Costularia* might be closely related to *Oreobolus*.

Oreobolus was not recovered as monophyletic, contrary to results previously reported by Chacón et al. (2006). This resolved the inconsistency in the results of Viljoen et al. (2013), whose different analytical methods (Maximum Likelihood and Bayesian Inference) showed both a poorly supported monophyletic group and a paraphyletic one, respectively. The contrast between the results presented here and these previous studies reflects the difference in the number of outgroups included in each. Chacón et al (2006) used only one species of *Costularia* (*C. laxa*) as an outgroup to *Oreobolus* therefore did not test the monophyly of the genus. However, the current study included multiple outgroups from a representative sample of the tribe. The Pacific *Oreobolus* species appeared forming one (MP, Figs. 2.1; ML, 2.2) or two (BI, Fig. 2.3) clades but not a grade as postulated by Chacón et al. (2006). The strong geographic structure observed in the phylogeny of Chacón et al. (2006) was also evident in the current study, with co-distributed species appearing as sister taxa (e.g. New Zealand: *O. pectinatus* and *O. strictus*; Malaysia: *O. kuekenthalii* and *O. ambiguus*). Furthermore, the inclusion of the two aforementioned Malaysian species may have caused differences between my topology and that of Chacón et al. (2006), with *O. furcatus* and *O. acutifolius* not recovered as sister taxa and not forming a

clade with *O. pumilio* and the South American species. Instead, *O. furcatus* and *O. acutifolius* appeared nested with the rest of the Pacific *Oreobolus* species. Nonetheless, the results presented here support the prediction of Chacón et al. (2006) that the Malaysian species would group with the rest of the Pacific species. In the case of *O. pumilio*, even though its position is uncertain (Figs. 2.1 – 2.3), none of the current study's analyses recovered it as sister taxon to the South American species of *Oreobolus* (contra Chacón et al., 2006). Further exploration of these differences will require sequencing more accessions per species, because as for the rest of the Pacific *Oreobolus* species, the ITS and *trn*L-F sequences of *O. pumilio* used in the current study were taken from Chacón et al. (2006), and therefore possible sources of sequencing error for single accessions are impossible to assess.

2.5.1.1 Phylogenetics of the South American Oreobolus

The five South American species of *Oreobolus* formed a highly supported clade consistently recovered across analyses (MP-BS=86%, ML-BS=98%, PP=100%). Additionally, strong geographic structure within the South American clade was evident and two highly supported sub-clades diverged at the crown node: a southern Andean clade (SAC) solely composed of samples of *O. obtusangulus* (the only species in the region), and a northern Andean clade (NAC) containing samples from all five species. Because *O. obtusangulus,* uniquely, was present in both regions and both clades, it was recovered as polyphyletic (Figs. 2.1 – 2.3). Seberg (1988) recognised two subspecies within *O. obtusangulus*, namely subsp. *obtusangulus* restricted to the southern Andean region and subsp. *unispicus* restricted to the northern Andean region. Apart from minimal differences in floral and fruit

characters, these two subspecies were mainly differentiated on the basis of their disjunct distribution (Seberg, 1988). Chacón et al. (2006) examined only a single sample of *O. obtusangulus* from the southern Andean region and hence could not test the monophyly of the species. They recovered their sample as sister taxon to the rest of the South American species, a result that is in line with the position of the SAC in the current study. Given the phylogenetic separation and limited morphological differentiation of *O. obtusangulus* subsp. *obtusangulus* and *O. obtusangulus* subsp. *unispicus*, it may be suggested that these two subspecies are in fact morphologically cryptic species. Examples of cryptic species have been demonstrated within the Schoeneae (Britton et al., 2014) as well as in other sedge taxa (Derieg et al., 2013). It may be that the observed genetic differences are the result of local adaptation or genetic drift due to the allopatric distribution of the two subspecies, but their degree of reproductive isolation if in sympatry would be difficult to assess (Bickford et al., 2007).

The other South American species within the NAC (*O. cleefii*, *O. ecuadorensis*, *O. goeppingeri* and *O. venezuelensis*) were not monophyletic. Furthermore, relationships between them were unclear and few sub-clades were well supported (Figs. 2.1 – 2.3). Plausible explanations for the observed pattern include ongoing gene flow among species and/or incomplete lineage sorting. Whilst there are no studies of wind pollination in Páramo, wind-pollinated plants (such as *Oreobolus*) have higher between-species gene flow rates than those pollinated by animal vectors (Ellstrand, 2014). Furthermore, continuing interspecific gene flow has already been suggested to occur in the sedge family, e.g. between closely related species in the genus *Carex* (e.g. Escudero et al., 2014). Given the archipelagic nature of the Páramo

ecosystem, and the anemochorous pollination and dispersal systems of *Oreobolus*, the possibility of successful pollen and seed dispersal to nearby Páramo islands and even over longer distances seems reasonable.

An alternative (but not exclusive) explanation may be incomplete lineage sorting. Indeed, retention and stochastic sorting of ancestral polymorphisms may conceal relationships between species, in which case gene genealogies or gene trees do not necessarily reflect the species tree (Maddison, 1997; Maddison & Knowles, 2006; Knowles & Carstens, 2007). Furthermore, the probability of retaining ancestral polymorphisms increases with shorter divergence times (Jakob & Blattner, 2006; Degnan & Rosenberg, 2009). The confounding role of incomplete lineage sorting, in the reconstruction of phylogenetic relationships among closely related species, has been demonstrated in groups such as *Gentiana* section *Criminalis* (Christe et al., 2014), *Solidago* subsect. *Humiles* (Peirson et al., 2013) and the Arundinarieae tribe (Zhang et al., 2012).

Both gene flow and incomplete lineage sorting may be affecting the reconstruction of phylogenetic relationships within the NAC (Figs. 2.1 – 2.3). However, distinguishing between them can prove difficult as both processes produce incongruence between the phylogeny and the current taxonomy (Naciri & Linder, 2015). In order to understand the phylogenetic relationships amongst the five South American species of *Oreobolus*, while accounting for non-hierarchical tree building as well as possible persistent polymorphism and/or gene flow, analyses under a coalescent-based approach should be pursued (Knowles & Carstens, 2007; Marko & Hart, 2011; Naciri et al., 2012; Naciri & Linder, 2015).

2.5.2 Out-of-Australia and the colonisation of South America

The Schoeneae tribe originated in Australia and diverged during the early Eocene, c. 50 Ma. Its six main clades (*Schoenus* clade, *Caustis* clade, *Lepidosperma* clade, *Gahnia* clade, *Tricostularia* clade and *Oreobolus* clade) diverged from one another within Australia during the late Eocene – late Miocene period, and dispersed multiple times from there from the early Miocene onwards. At the time, continents were approaching their current geographic positions (McLoughlin, 2001) and consequently, present-day Schoenoid distributions are unlikely to be the result of vicariance events (i.e. plate tectonics). Therefore my results further support the hypothesis first postulated by Verboom (2006) and later corroborated by Viljoen et al. (2013) that colonisation of other southern hemisphere landmasses by the Schoeneae was likely accomplished through multiple long-distance dispersal events. Furthermore, the geographic distances covered varied from a few several thousand kilometres (e.g. Australia to New Caledonia, New Zealand and South East Asia) to transcontinental distances (e.g. Australia to South Africa, Madagascar and South America). This dispersal process was probably facilitated by the anemochorous dispersal system of the Schoenoid sedges. Indeed, long distance dispersal has been established as an important process in plant distribution patterns (e.g. Pennington & Dick, 2004; Christenhusz & Chase, 2013) as well as in southern hemisphere plant biogeography (e.g. Sanmartín & Ronquist, 2004; Crisp et al., 2009; Winkworth et al., 2015). Examples of long-distance dispersal between southern hemisphere landmasses have been shown in numerous plant groups e.g. *Nothofagus* (Knapp et al., 2005), the *Monttea*/*Ourisia* clade of the Angelonieae tribe (Martins et al., 2014), the

Hennecartia-Mollinedia clade in Monimiaceae (Renner et al., 2010), Schistochilaceae (Sun et al., 2014) and Proteaceae (Barker et al., 2007).

The South American *Oreobolus* clade diverged during the early Pliocene (c. 5 Ma), and the most likely reconstruction of colonisation of South America is two independent arrivals to the northern and southern Andes during the same epoch (PP = 0.37, Table 2.1). Alternative but less probable reconstructions suggested dispersal from Australia during the late Miocene followed by either an early Pliocene origin in the southern Andes region with a subsequent dispersal to the northern Andes (PP=0.27, Table 2.1) or and early Pliocene origin in the northern Andes with a subsequent dispersal to the southern Andes (PP=0.25, Table 2.1). In all cases, wind and ocean currents may have facilitated eastward dispersal to South America. Following the mid-Miocene climatic optimum (c. 15 Ma) a period of gradual cooling was set by the expansion of the eastern Antarctic ice sheet (Zachos et al., 2001). By the late Miocene, the complete glaciation of Antarctica strengthened and finalised the establishment of the circumpolar circulation systems (i.e. Antarctic Circumpolar Current and West Wind Drift) which may have facilitated eastward dispersal (Pagani et al., 2000; Shevenell et al., 2004). Sanmartín et al. (2007) used a set of 23 plant phylogenies with a southern hemisphere distribution to test hypotheses about plant dispersal mechanisms. According to their results, eastward dispersal was inferred more frequently between Australia and South America supporting the circumpolar circulation systems as an important dispersal mechanism. A second mechanism may have been stepping-stone dispersal along the Antarctic coast. Notwithstanding limited dispersal through Antarctica because of significant ice-sheet expansion by the late Miocene (Markgraf et al., 1995; Zachos et al., 2001; Siegert, 2008) various

authors have suggested that forest on the coastline may have existed as late as the Pliocene (Swenson & Bremer, 1997; Renner et al., 2000; Sanmartín et al., 2007). Therefore colonisation of South America through Antarctica may have been possible.

A colonisation scenario with two independent arrivals to the northern and southern Andes during the early Pliocene is the favoured reconstruction not only because it has the highest support (PP=0.37) but also because of the strong ecological barrier to dispersal imposed by the central Andes and leeward side (east) of the southern Andes. Indeed, since the mid Miocene (c. 15 Ma) these regions have had an arid to hyper-arid climate (Hartley, 2003; Blisniuk et al., 2005). *Oreobolus* is consistently distributed in mesic open-vegetation biomes with a temperate climate (Seberg, 1988). Furthermore, Viljoen et al. (2013) established a perennially wet and open-vegetation type as ancestral for the genus. Consequently, successful dispersal through the central Andes and leeward side (east) of the southern Andes may have been unlikely.

Independent arrivals to the northern and southern Andean regions are consistent with the likely role of niche conservatism in the diversification of Schoenoid sedges (Verboom, 2006; Viljoen et al., 2013). Successful establishment following long-distance dispersal events has been often associated with niche conservatism – the concept that species should more easily establish in a biome to which they are already pre-adapted (e.g. Donoghue, 2008; Crisp et al., 2009). By the Pliocene, both the southern and northern Andes provided a mesic temperate environment suitable for the ecological requirements of an ancestral *Oreobolus*. The southern Andes had reached their current elevation in the mid Miocene imposing a strong rain shadow effect that caused aridity on the east side of the range while the west was

characterised by a wet, temperate climate (Markgraf et al., 1995; Blisniuk et al., 2005; Graham, 2009). It is on the west (windward) side of the range that *O. obtusangulus* is presently distributed, and to where it probably dispersed in the Pliocene. The northern Andes were half their current elevation by the mid Miocene, and the final uplift of the northernmost Eastern Cordillera occurred during the Pliocene (Gregory-Wodzicki, 2000; Graham, 2009). It is in this epoch that the first palynological records of Páramo-like vegetation appeared: as the northern Andes rose, a newly available open vegetation type with temperate-like climate extended above the forest line (van der Hammen & Cleef, 1986; Hooghiemstra et al., 2006).

The strong phylogenetic differentiation consistently recovered between the northern and southern *O. obtusangulus,* in addition to the contemporaneous divergence of the SAC and NAC could reflect two independent colonisation events and therefore independent origin of morphologically similar populations, currently recognised as subspecies. However, the second and third scenarios of dispersal of *O. obtusangulus* from the SAC to the NAC or vice versa, suggest that the morphological similarity of the subspecies is due to common ancestry. Under the second scenario, given the recent divergence of all species of the NAC (c. 3 Ma), if the northern subspecies of *O. obtusangulus* is the ancestor of the other species in the clade one might expect it to share ancestral polymorphisms with the other species as shown in the phylogeny (Figs. 2.1 – 2.3). However it needs to be established if the retention of ancestral polymorphisms is the likely process behind the observed phylogenetic pattern. On the other hand, under the third scenario, if the northern subspecies of *O. obtusangulus* is the ancestor of the southern one, shared ancestral polymorphisms might also be expected but this is not recovered in any of the phylogenies presented

here (Figs. 2.1 – 2.3). However, these shared ancestral polymorphisms may have been lost as a consequence of bottlenecks and low effective population sizes in the southern *O. obtusangulus*.

In summary, though I favour a scenario of two independent dispersal events based upon its higher probability and the difficulty of dispersal along the Andes, the data are consistent with all scenarios. An option to assess better the relationships within the NAC and thus have an ancestral area reconstruction with higher support for the South American ancestor, would be to use a mixed diversification model on BEAST v2.1.3 (Bouckaert et al., 2014). A mixed model allows setting different diversification models along a phylogeny consequently a coalescent model could be defined for the South American *Oreobolus* clade and a birth death model for the rest of the phylogeny.

Under all scenarios, rapid diversification within the NAC occurred since the Pleistocene. Moreover, recent colonisation of the northernmost part of the central Andes and southern Central America from the northern Andes region also occurred (Fig. 2.4). The Quaternary ice cycles played a major role in the current distribution of Páramo plants (van der Hammen, 1974; van der Hammen & Cleef, 1986; Hooghiemstra & van der Hammen, 2004; Hooghiemstra et al., 2006). While in the northern hemisphere these climatic fluctuations promoted latitudinal migration of vegetation belts, in the tropical regions migration was altitudinal (van der Hammen, 1974; Hooghiemstra & van der Hammen, 2004; Mora et al., 2010). Consequently vegetation belts underwent repeated episodes of vertical contraction and expansion that provided an opportunity for high-altitude Páramo populations to expand and contract (van der Hammen & Cleef, 1986; Hooghiemstra & van der Hammen, 2004).

Flantua et al. (2014) reconstructed the change in biome distribution from a pollen record of a 7559 km^2 area in the Eastern Cordillera of Colombia. These authors estimated a loss of 96% of the Páramo biome area since the Last Glacial Maximum (c. 20 Ka) as well as reduced connectivity between Páramo patches as the upper forest line reached elevations higher than 3100 m.a.s.l. Therefore, during periods of contraction, Páramo populations may have been isolated, promoting allopatric speciation and/or genetic differentiation within species. In contrast, during periods of expansion, populations may have come into contact allowing for species dispersal and possible genetic exchange. Such Quaternary dynamics may explain the observed phylogenetic pattern recovered for the northern Andean *Oreobolus* (NAC) in the last two million years (Fig. 2.4). In the SAC, genetic differentiation within *O. obtusangulus* was also indicated to have occurred since the Pleistocene (Fig. 2.4). In the southern Andes, the Quaternary ice cycles produced complete glaciation across extensive areas generating massive fragmentation and restriction in the distribution of plants (Markgraf et al., 1995). Southern populations of *O. obtusangulus* may have been isolated during this period promoting genetic differentiation within the species.

2.5.3 Diversification rates

Net diversification rates were highest in the *Costularia* clade (0.718 speciation events per million years, Myr^{-1}), the South African clade (0.660 Myr^{-1}) and the NAC (0.524 Myr^{-1}) (Table 2.2). When compared with the background diversification rate for the Cyperaceae family (Escudero & Hipp, 2013), the results presented here indicate values an order of magnitude higher. Similarly, the results obtained here show a net diversification rate three times that found for the Schoenoid sedge

Tetraria (Slingsby et al., 2014). Macroevolutionary theory anticipates a positive correlation between clade age and species richness as older clades would have had more time to diversify than younger ones (Rabosky et al., 2012). This hypothesis is corroborated by the Cyperaceae family, where among-clade variance in species richness is mostly explained by clade age (Escudero & Hipp, 2013). However, diversification in the four sub-clades of the *Oreobolus* clade occurred within the same timeframe (late Pliocene – early Pleistocene) and therefore clade age does not explain differences in species diversity. For example, both the SAC and NAC diverged during the late Pliocene (c. 3 Ma) but the NAC diversified into five species, while the SAC only has one.

If greater energy input was the reason for greater speciation rates in tropical regions we would expect tropical clades to have higher diversification rates than temperate ones. In the case of Schoeneae the results are not conclusive. Madagascan *Costularia* (tropical) has the fastest diversification rate, but the South African clade has a faster rate than the tropical NAC. However the tropical NAC does have a faster diversification rate than the temperate SAC.

The *Costularia* clade, South African clade and NAC are distributed in biodiversity hotspots: Madagascar, the Cape Floristic Region and the Andean Páramo, respectively (Myers et al., 2000). These areas have high numbers of species and endemism associated with complex biogeographical histories (van der Hammen & Cleef, 1986; Wilmé et al., 2006; Verboom et al., 2014). An understanding of the ecosystem heterogeneity and climatic history may explain the observed diversification rates. Firstly, in Madagascar, volcanic activity during the Pliocene and Pleistocene may have increased habitat heterogeneity (Piqué, 1999) opening newly

available niches. Furthermore, during the Quaternary ice cycles, glacial periods imposed cooler and drier regimes, resulting in habitat fragmentation and the repeated contraction and expansion of species distribution ranges, which may have contributed to allopatric speciation (Wilmé et al., 2006). Similarly, in the Cape Floristic Region, the climatic fluctuations of the Quaternary promoted the altitudinal and geographical migration of vegetation belts with repeated cycles of contraction and expansion that may have provided an opportunity for allopatric speciation (Midgley et al., 2005; Verboom et al., 2014). However, climatic fluctuations in the Cape Floristic Region were mild (Dynesius & Jansson, 2000; Midgley et al., 2005), so such speciation might have been accompanied by population persistance and low extinction rates (Dynesius & Jansson, 2000; Verboom et al., 2014). Lastly, the final uplift of the northern Andes during the Pliocene caused the Páramo, a naturally fragmented ecosystem, to extend across the mountaintops above the treeline (van der Hammen & Cleef, 1986). Subsequently, the climatic fluctuations of the Quaternary caused repeated cycles of altitudinal contraction and expansion of the vegetation belts that may have isolated species in the Páramo islands, promoting allopatric speciation (van der Hammen, 1974; van der Hammen & Cleef, 1986; Hooghiemstra & van der Hammen, 2004; Hooghiemstra et al., 2006). Population dynamics as a response to climatic fluctuations, coupled with habitat heterogeneity could be concluded to have had a positive impact on the diversification of lineages.

The results presented here for the SAC and NAC support the hypothesis that a group that has recently moved into tropical regions with a temperate-like environment, to which they may be pre-adapted, has faster rates of diversification than its temperate sister clades. However, when also considering the *Costularia* and South African

clades, the results are not definite. Indeed, in this particular case, greater energy inputs may not be the principal cause of faster diversification rates as proposed by Wright (1983) and Hurlbert & Stegen (2014). However, it is important to note that faster diversification rates were found in biodiversity hotspots which could result from the increased importance of biotic interactions (Schemske, 2009). Moreover, the latter could in turn be the result of increased niche partitioning as a consequence of habitat heterogeneity, further supporting the conclusion of its positive impact on the diversification of lineages.

2.6 CONCLUSION

The purpose of the current study was to determine the impact of the Andes orogeny on the timing, directionality and diversification rates of the South American species of *Oreobolus* within the context of its tribe. Novel results reported here include: (i) the non-monophyly of the genus *Oreobolus;* (ii) the monophyly of the South American *Oreobolus* species as a group; (iii) the rapid diversification of this clade, and the species within it, as evidenced by their unresolved phylogenetic relationships; (iv) the colonisation of South America from Australia from two long-distance dispersal events to (or in one case, perhaps within) the Andes during the Pliocene and (v) the likely role of habitat heterogeneity on the diversification of lineages in the *Oreobolus* clade. In relation to biogeography in the Andes, the arid central Andes may be a major ecological barrier to dispersal, questioning the south to north dispersal hypothesis often invoked to explain Austral immigrants to the Páramo flora (e.g. Sklenář et al., 2011). Finally, the climatic fluctuations of the Quaternary

and the increasingly important role of habitat heterogeneity, rather than latitude, may have been significant drivers for the diversification of *Oreobolus* and allies.

Further work needs to be done under a coalescent-based approach in order to establish the phylogenetic relationships between the five South American species of *Oreobolus* and whether these are obscured by ongoing gene flow and/or persistent polymorphisms. Moreover, this will allow for greater exploration of the phylogeography of these five species. The current study provides the framework to undertake this investigation in Chapter Three.

CHAPTER THREE. PHYLOGEOGRAPHY OF THE SOUTH AMERICAN SPECIES OF OREOBOLUS R. Br. (CYPERACEAE)

3.1. ABSTRACT

This study examines genetic relationships between and within the South American species of *Oreobolus* and assesses the impact of recent climatic and ecological events on their diversification. A total of 197 individuals were scored for ITS haplotypes while 118 individuals were scored for cpDNA (*trn*L-F, *trn*H-*psb*A and *rpl*32-*trn*L) haplotypes, covering the distribution range of most of these species. Haplotype networks and measures of genetic diversity for both regions were calculated at the species and population levels. Additional tests for possible phylogeographic structure were undertaken. Furthermore, species relationships were recovered under a coalescent-based approach. Results indicate complex relationships between the five South American species of *Oreobolus*, likely confounded by incomplete lineage sorting. Nonetheless, hybridisation cannot be completely discarded, particularly between the northern populations of *O. obtusangulus* and *O. cleefii*. I report a case of cryptic speciation in *O. obtusangulus* where northern and southern populations of morphologically similar species are in fact genetically distinct in all analyses and this likely causes the strong phylogeographic structure at the continental scale that was recovered. At the population level, I present the first genetic evidence to support the

role in diversification of the contraction and expansion of the Páramo islands during the climatic fluctuations of the Quaternary, highlighting their fundamental role in shaping modern diversity.

3.2. INTRODUCTION

Phylogeography studies the spatial distribution of gene genealogies, allowing for the assessment of diversification patterns as well as the evaluation of the possible impact of recent climatic or ecological events that might have shaped those distributions (Avise, 2000). Furthermore, it simultaneously examines the role of possible ongoing genetic exchange between taxa (Schaal et al., 1998). Such studies are particularly relevant in the context of geologically young but megadiverse plant ecosystems where recent climatic and/or geological events may have shaped the extant populations but, at the same time, ongoing gene flow may still exist between recently diverged taxa.

This is the case of the Páramo, a putatively young ecosystem that appeared following the final uplift of the northern section of the Andes Mountain Range during the Pliocene, c. 5 Ma (van der Hammen, 1974; van der Hammen & Cleef, 1986; Hooghiemstra et al., 2006; Graham, 2009). The Páramo occupies an area of 37500 km^2 and is distributed in a series of sky islands with c. 4000 species of which 60% are endemic (Luteyn, 1999; Buytaert et al., 2010). It has been proposed that the glacial-interglacial cycles of the Quaternary may have played an important role in shaping Páramo plant populations (van der Hammen, 1974; Simpson, 1975). The continuous contraction and expansion of altitudinal vegetation belts may have

promoted the contact of Páramo islands during glacial periods, enabling the migration and exchange of otherwise isolated taxa (van der Hammen & Cleef, 1986). Conversely, during interglacial periods, Páramo islands may have been isolated, promoting speciation (van der Hammen & Cleef, 1986). Furthermore, previous studies have demonstrated that Páramo lineages have significantly higher speciation rates than any other biodiversity hotspot on Earth (Madriñán et al., 2013). Recent divergence times among Páramo plant lineages might have enormous implications, both at the phenotypic and genotypic level, because morphological diversity and differentiation may not reflect complete genetic divergence between and within closely related taxa (Schaal et al., 1998).

The five South American species of the schoenoid sedge *Oreobolus* R. Br. (*O. cleefii*, *O. ecuadorensis*, *O. goeppingeri*, *O. obtusangulus* and *O. venezuelensis*) are an ideal model system for a phylogeographic study. These species, with the exception of *O. obtusangulus* subspecies *obtusangulus*, are restricted to wet, temperate-like environments in the northern section of the Tropical Andes and in the Talamanca Cordillera in southern Central America, found only in the high-altitude Páramo ecosystem (Seberg, 1988; Chacón et al., 2006). *Oreobolus cleefii* is restricted to the Eastern Cordillera and the southern Andean region of Colombia; *O. ecuadorensis* is found in southern Colombia, Ecuador and northern Peru; *O. goeppingeri* is distributed in the Talamanca Cordillera in southern Central America, Colombia and Ecuador; *O. obtusangulus* has two subspecies with a disjunct distribution: subspecies *unispicus* is distributed in Colombia, Ecuador and northern Peru while subspecies *obtusangulus* occupies the subantarctic region of Chile, Argentina and the Falkland Islands; finally, *O. venezuelensis* occupies all Páramo

regions (Talamanca Cordillera, Venezuela, Colombia, Ecuador and northern Peru). The distributions of all *Oreobolus* Páramo species overlap with those of at least one other congeneric species. Figure 1.6 on page 21 presents a distribution map of the five South American species. All Páramo species are found between 3000 and 4300 m.a.s.l. while in the subantarctic regions, the altitude at which *O. obtusangulus* is found decreases with increasing latitude, from 2400 m.a.s.l. to sea level (Seberg, 1988).

The five South American species are clearly differentiated in terms of morphology, and in common with most Cyperaceae, *Oreobolus* is both wind pollinated and dispersed (Seberg, 1988). Little is known about ploidy levels and chromosome numbers in *Oreobolus* and only Moore (1967) has studied chromosome numbers in *O. obtusangulus* ssp. *obtusangulus* (2n = 48).

Previous studies have supported the monophyly of the South American clade of *Oreobolus* and dated its divergence to c. 5 Ma, coinciding with the appearance of the Páramo ecosystem (Chacón et al., 2006). Results from the second chapter of this thesis supported both findings but indicated that none of the five species was monophyletic for the markers examined (ITS and *trn*L-F). A phylogeographic approach may allow us to estimate the likely effect of recent climatic events (i.e. glacial cycles of the Quaternary) on the population structure of the South American species of *Oreobolus* by examining the genetic structure of populations across all species.

A handful of phylogeographic studies for similar high-altitude tropical ecosystems in Africa have been published in recent years (Kebede et al., 2007; Assefa et al., 2007;

Gizaw et al., 2013; Kadu et al., 2013; Wondimu et al., 2013). However, to my knowledge, none has been presented for the Páramo flora. The aims of this study are to 1) estimate the species phylogeny of the South American species of *Oreobolus*; 2) assess the population and genetic structure at the inter- and intra-specific level, 3) investigate the impact of Quaternary glacial-interglacial cycles in shaping populations of *Oreobolus*.

3.3. METHODS

3.3.1. Study species and sampling

The five South American species of *Oreobolus* (*O. cleefii*, *O. ecuadorensis*, *O. goeppingeri*, *O. obtusangulus* and *O. venezuelensis*) were extensively sampled across their entire distribution range (Fig. 1.6, page 21). A total of 269 samples from 32 populations were obtained from both field collections (10 populations) and herbarium material (22 populations) (Table 3.1 and Fig. 3.1). From each of the ten field populations, all within Colombia, two to ten fresh leaf samples per species were collected, and their location was recorded using a handheld GPS (Fig. 3.1, populations 2 – 11). For populations in Costa Rica, Ecuador, Peru, Chile and Argentina (Fig. 3.1, populations 1 and 12 – 32), herbarium material was acquired from the Utrecht (U) and Leiden University (L) branches of the National Herbarium of the Netherlands, Aarhus University Herbarium (AAU) and the University of Reading Herbarium (RNG). For herbarium material, between one and ten individuals per species were sampled from each population. Coordinates were recorded from the herbarium specimens and checked for accuracy using the NGA GEOnet Names

Server (GNS) (http://geonames.nga.mil). Populations are numbered 1 to 32 in a north to south direction. Populations 1 to 23 will be referred to as northern Andes (Costa Rica, Colombia, Ecuador and Peru) and 24 to 32 populations as southern Andes (Chile and Argentina). Previously published sequence data for *O. cleefii*, *O. goeppingeri* and *O. venezuelensis* (Chacón et al., 2006) were also incorporated and assigned to their corresponding population. Table S3.1 presents the complete list of samples used in this study (Supplementary Information, pages 215 – 224).

Table 3.1. Geographic coordinates and corresponding cluster of the populations sampled.

Nº	POPULATION NAME	CLUSTER	LATITUDE	LONGITUDE
1	CHIRRIPO	A	9.48411000	-83.48861000
2	COCUY	B	6.41211667	-72.33128333
3	LA RUSIA	C	5.93951667	-73.07583333
4	IGUAQUE	C	5.68610000	-73.44773333
5	TOTA-BIJAGUAL	B	5.48143333	-72.85540000
6	RABANAL	C	5.40818333	-73.54915000
7	GUERRERO	C	5.22618333	-74.01788333
8	CHINGAZA	D	4.52848333	-73.75866667
9	SUMAPAZ	D	4.28958333	-74.20781667
10	PURACE	E	2.36088333	-76.35038333
11	AZUFRAL	F	1.09543333	-77.68711667
12	VOLCAN CHILES	F	0.80000000	-77.93333333
13	MIRADOR	F	0.56666667	-77.65000000
14	COTOCACHI	F	0.36666667	-78.33333333
15	COTOPAXI	G	-0.66666667	-78.36666667
16	LLANGANATI	G	-1.15000000	-78.30000000
17	ALAO-HUAMBOYA	G	-1.80000000	-78.43333333
18	PARAMO DE LAS CAJAS	H	-2.81666667	-79.26666667
19	CUENCA-LIMON	H	-3.00000000	-78.66666667
20	CUENCA-LOJA	H	-3.16666667	-79.03333333
21	PODOCARPUS	I	-4.40000000	-79.10000000
22	CAJAMARCA	J	-7.05000000	-78.58333333
23	HUASCARAN	J	-9.45000000	-77.26666000
24	VALDIVIA	K	-40.18333333	-73.51666666
25	FIORDO PEEL	L	-50.50000000	-73.73333333
26	MALVINAS	N	-51.64297000	-59.89473000
27	PNN NAHUEL HUAPI	L	-51.73333333	-71.50000000
28	MAGALLANES	L	-53.45000000	-71.76666700
29	TIERRA DEL FUEGO	M	-54.76666666	-67.40000000
30	ISLA DE LOS ESTADOS	M	-54.80000000	-64.31666666
31	ISLA NAVARINO	M	-55.07553100	-67.65539600
32	CABO DE HORNOS	M	-55.94407800	-67.28092500

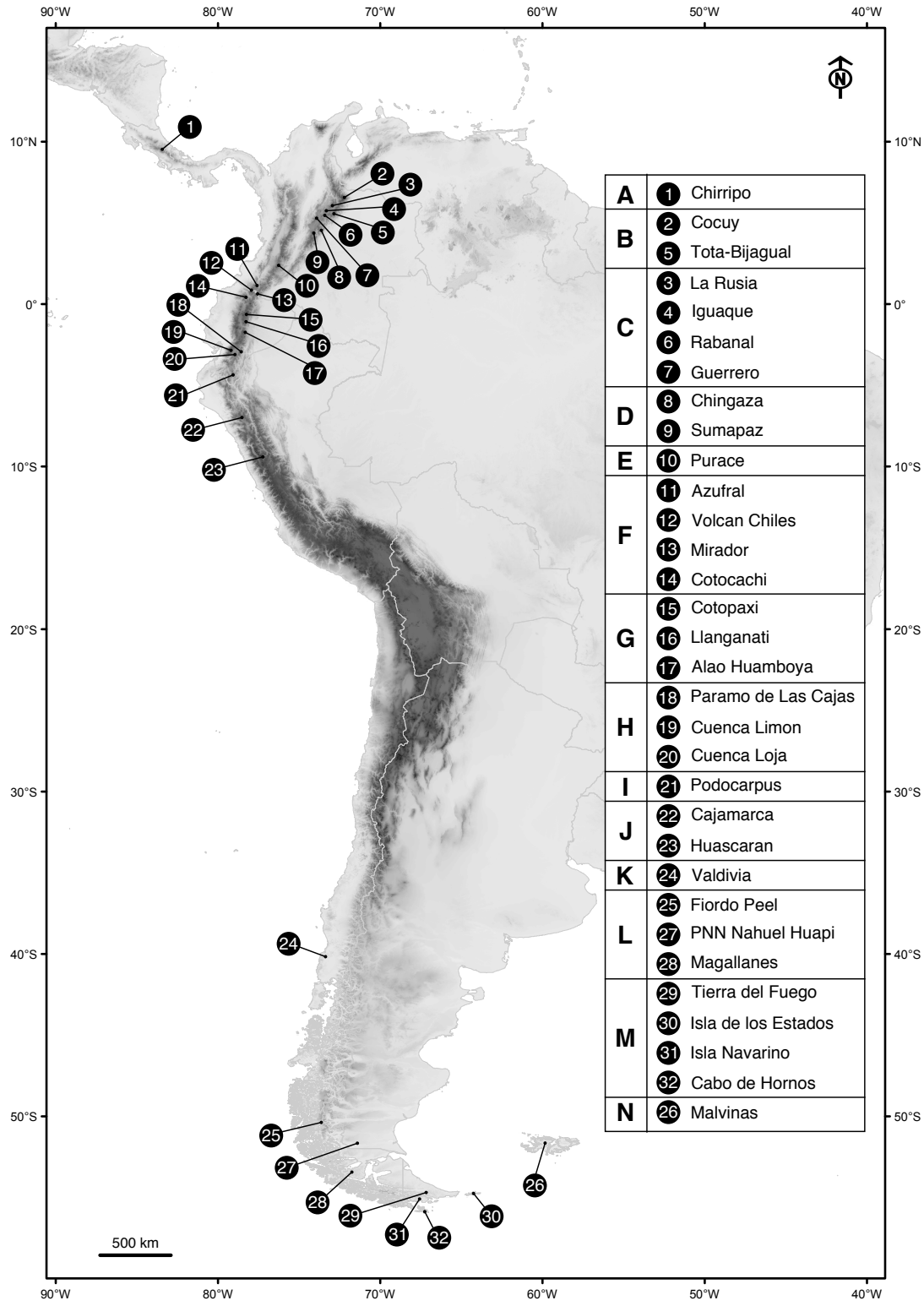

Figure 3.1. Map of populations sampled (1 – 32) and their corresponding cluster (A – N).

3.3.2. DNA extraction, amplification and sequencing

Both silica-dried fresh leaf samples and herbarium material were pulverised using a Mixer Mill (Retsch, Haan, Germany). Total genomic DNA from herbarium material was isolated following the CTAB method of Doyle and Doyle (1990) and from silica-dried samples with the DNeasy® Plant Mini Kit (QIAGEN, Manchester, UK) following the manufacturer's protocol. The nuclear ribosomal DNA internal transcribed spacers (ITS) and the chloroplast *trn*L regions were amplified and sequenced as detailed in Chapter Two (page 36). The chloroplast regions *trn*H-*psb*A and *rpl*32-*trn*L were amplified and sequenced using primer pairs *trn*H^{GUG} (Tate & Simpson, 2003)/*psb*A (Sang et al., 1997) and *trn*L$^{(UAG)}$/*rpl*32-F (Shaw et al., 2007), respectively. All PCR reactions were performed as described in Chapter Two (page 36). The amplification cycle for both chloroplast regions (*trn*H-*psb*A and *rpl*32-*trn*L) consisted of 2 min at 94°C, followed by 30 cycles of 1 min at 94°C, 1 min at 52°C and 1 min at 72°C, and a final extension step of 7 min at 72°C. PCR products were purified and sequenced as reported in Chapter Two (page 36). No double peaks were observed in the chromatograms of the ITS region and therefore it was not necessary to clone.

3.3.3. Matrix assembly and sequence alignment

Contigs of forward and reverse sequences were assembled in Sequencher version 5.2 (Gene Codes Corporation, Ann Arbor, Michigan, USA). 230 ITS sequences, 169 *trn*L-F sequences, 128 *trn*H-*psb*A sequences and 190 *rpl*32-*trn*L sequences were generated for this study (Table S3.1). The sequences were manually aligned using

Mesquite v2.75 (Maddison & Maddison, 2014). Table 3.2 describes number of individuals successfully sequenced per species per cluster/population.

Table 3.2. Number of individuals successfully sequenced per species per cluster/population for ITS and cpDNA (*trn*L-L-F, *trn*H-*psb*A and *rpl32*-*trn*L). Areas where species are not distributed are noted as n.d.

CLUSTER/Population	*O. cleefii*		*O. ecuadorensis*		*O. goeppingeri*		*O. obtusangulus*		*O. venezuelensis*	
	ITS	cpDNA	ITS	cpDNA	ITS	cpDNA	ITS	cpDNA	ITS	cpDNA
CLUSTER A	n.d.	n.d.	n.d.	n.d.	2	-	n.d.	n.d.	-	-
(1) Chirripo					2					
CLUSTER B	7	5	n.d.	n.d.	5	5	-	-	-	-
(2) Cocuy	5	4			3	4				
(5) Tota-Bijagual	2	1			2	1				
CLUSTER C	3	2	n.d.	n.d.	5	2	-	-	2	1
(4) Iguaque					1	1				
(3) La Rusia	2	2			1				2	1
(6) Rabanal					2	1				
(7) Guerrero	1				1					
CLUSTER D	1	-	n.d.	n.d.	6	3	1	-	6	3
(8) Chingaza	1				3	1			2	1
(9) Sumapaz					3	2	1		4	2
CLUSTER E	n.d.	n.d.	n.d.	n.d.	3	3	-	-	-	-
(10) Purace					3	3				
CLUSTER F	4	2	2	3	11	5	6	6	1	1
(11) Azufral	4	2			1	1				
(12) Volcan Chiles			1	1	5		5	4		
(13) Mirador					2	2	1	2	1	1
(14) Cotocachi	n.d.	n.d.	1	2	3	2				
CLUSTER G	n.d.	n.d.	12	16	7	-	4	3	-	1
(15) Cotopaxi			9	13	2		2	2		1
(16) Llanganati				1	2		2	1		
(17) Alao-Huamboya			3	2	3					
CLUSTER H	n.d.	n.d.	7	8	15	5	10	9	2	3

(18) Paramo De Las Cajas			3	4	2	2	4	3		
(19) Cuenca-Limon					2		3	3		
(20) Cuenca-Loja			4	4	11	3	3	3	2	3
CLUSTER I	n.d.	n.d.	-	-	18	4	1	1	15	4
(21) Podocarpus					18	4	1	1	15	4
CLUSTER J	n.d.	n.d.	3	2	3	-	1	1	-	-
(22) Cajamarca			1	1	3		1	1		
(23) Huascaran			2	1						
CLUSTER K	n.d.	n.d.	n.d.	n.d.	n.d.	n.d.	1	1	n.d.	n.d.
(24) Valdivia							1	1		
CLUSTER L	n.d.	n.d.	n.d.	n.d.	n.d.	n.d.	15	8	n.d.	n.d.
(25) Fiordo Peel							2			
(27) PNN Nahuel Huapi							2	1		
(28) Magallanes							11	7		
CLUSTER M	n.d.	n.d.	n.d.	n.d.	n.d.	n.d.	16	9	n.d.	n.d.
(29) Tierra Del Fuego							10	5		
(30) Isla De Los Estados							2	1		
(31) Isla Navarino							1			
(32) Cabo De Hornos							3	3		
CLUSTER N	n.d.	n.d.	n.d.	n.d.	n.d.	n.d.	1	1	n.d.	n.d.
(26) Malvinas							1	1		
TOTAL	15	9	24	29	75	27	56	39	27	14

3.3.4. Haplotype definition and networks

Haplotypes were identified independently for the nuclear ribosomal region (ITS) and the concatenated plastid regions (*trn*L-F, *trn*H-*psb*A and *rpl*32-*trn*L) in Microsoft Excel (Microsoft Corporation, Washington DC, USA) using the Chloroplast PCR-RFLP Excel macro (French, 2003). For ITS, only samples successfully sequenced for the whole region were included (Table S3.1). Likewise, for the concatenated plastid regions, only samples successfully sequenced for all three regions were considered (Table S3.1). Informative insertion/deletion events were included in the analysis and coded as absent (0) or present (1). Poly-T and poly-A length polymorphisms, bi-nucleotide repeats and ambiguously aligned regions were excluded from subsequent analyses for all regions. Haplotype connection lengths were calculated using Arlequin ver3.5 (Excoffier & Lischer, 2010) and a minimum-spanning tree was produced in Hapstar v0.5 (Teacher & Griffiths, 2011).

3.3.5. Statistical analyses

Populations were combined into clusters to increase the likelihood of detecting a phylogeographic signal (Table 3.1 and 3.2; Fig. 3.1). Clusters were defined regardless of species classification; this approach is justified by the results presented in Chapter Two that showed poor phylogenetic resolution amongst the South American species of *Oreobolus*. Fourteen clusters (A – N) were defined according to geographic distance and ensuring the absence of any significant geographic barrier between populations within each cluster, i.e. deep inter-Andean valleys.

Haplotype (h) and nucleotide (π) diversities were calculated independently for each cluster and each species in Arlequin ver3.5 (Excoffier & Lischer, 2010). Additionally, haplotype richness (hr) was estimated for each species using HIERFSTAT (Goudet, 2005) in R version 3.2.3 (R Core Team, 2015). This package uses a rarefaction procedure set to 100 runs to correct for bias due to unequal sample sizes. ITS sample size was standardised to 15 individuals while cpDNA sample size was standardised to nine. Additionally, F_{ST} values between cluster pairs and species pairs were calculated independently for ITS and the concatenated plastid regions using Arlequin ver3.5 (Excoffier & Lischer, 2010). For the cluster pairs, clusters A, K and N were excluded from the analysis due to their low sample numbers ($N < 2$). In the case of the species pairs, calculations were first undertaken considering *O. obtusangulus* as one species and then with the northern and southern populations considered as two different species.

To analyse the geographical structure of genetic variation, a spatial analysis of molecular variance (SAMOVA) was performed for the nuclear and concatenated plastid datasets, independently (Dupanloup et al., 2002). SAMOVA identifies groups of populations/clusters that are geographically homogeneous as well as maximising genetic differentiation amongst them (Dupanloup et al., 2002). One hundred annealing simulations for each number of groups (ITS, $K = 2 – 13$; cpDNA, $K = 2 – 12$) were undertaken. The minimum number of groups (K) maximising the genetic differentiation amongst them (F_{CT}) was chosen. Similarly, to test if the phylogeographic structure had a phylogenetic component, two measures of genetic differentiation amongst clusters were estimated using PERMUTCPSSR 2.0 (Pons & Petit, 1996; Burban et al., 1999). A distance matrix was calculated based on the

number of mutational steps between haplotypes (N_{ST}) and on haplotype frequencies (G_{ST}). Ten thousand permutations were performed to assess if N_{ST} was significantly higher than G_{ST}.

Additionally, variation in the genetic structure was further examined for 1) all species, 2) all clusters, 3) all northern Andes clusters, 4) clusters grouped by region (northern Andes, southern Andes) and 5) SAMOVA groups using an analysis of molecular variance (AMOVA) in Arlequin ver3.5 (Excoffier & Lischer, 2010).

3.3.6. Species tree and phylogenetic networks

Results from the Chapter Two were consistent with either incomplete lineage sorting or ongoing gene flow affecting the reconstruction of phylogenetic relationships amongst the five South American species of *Oreobolus*. Therefore the multispecies coalescent model implemented in *BEAST (Heled & Drummond, 2010) was used to examine the relationships between these five species. Additionally, this approach effectively combines plastid and nuclear sequence data. *BEAST estimates phylogenetic relationships between species as well as their divergence time and estimated population size, assuming incomplete lineage sorting as the main source of incongruence between gene trees and species trees (Heled & Drummond, 2010). Under this model, all gene trees are contained within the species tree and comply with the species tree constraint, which is that the common ancestor of a gene cannot be younger than the speciation event (Heled & Drummond, 2010; Drummond & Bouckaert, 2015). The model assumes there is no significant gene flow between species hence if the data do not fit this model incomplete lineage sorting rather than

reticulate evolution is the favoured explanation for the lack of clear genetic differentiation amongst species.

All sequences generated for this study, both complete and incomplete, were used for the species tree estimation (ITS, *trn*L-F, *trn*H-*psb*A and *rpl*32-*trn*L; Table S3.1). Evolutionary model testing was performed for each region using jModelTest 2.1.6 (Guindon & Gascuel, 2003; Darriba et al., 2012) with default settings. Based on the Bayesian Information Criterion (BIC; Schwarz, 1978), the best-fitting models were TN93 for ITS, JC69+Γ for *trn*L-F and *rpl*32-*trn*L, and JC69 for *trn*H-*psb*A. Phylogenetic reconstruction and divergence time estimations were performed using BEAST v2.1.3 (Bouckaert et al., 2014). Each dataset was analysed using the above substitution models. Additionally, for *trn*L-F and *rpl*32-*trn*L a gamma distribution with four rate categories was defined, which is the minimum number required to get a good approximation of the continuous function (Yang, 1994). The tree model was linked for the three plastid regions, as cpDNA does not undergo recombination. The model of lineage-specific substitution rate variation was set as an uncorrelated lognormal relaxed clock model for each dataset. A *BEAST analysis requires each taxon to be associated with a species or taxonomic unit (Taxon Sets). These were defined following current taxonomy but with *O. obtusangulus* divided into northern and southern taxa based on the separation of these taxa in the phylogenetic analyses presented in Chapter Two (Figs. 2.1 – 2.3, pages 45 – 50). The diversification model for the species tree was set to a birth death model (Gernhard, 2008), an appropriate model to infer divergence times between species (Drummond & Bouckaert, 2015). Similarly, the population size model for the species tree was set as piece-wise linear with constant root, which allows linear change in population sizes within each branch

of the species tree but keeps a constant population size for the ancestral population at the root (Drummond & Bouckaert, 2015). For calibration purposes, sequence data for ITS and *trn*L-F of *Capeobolus brevicaulis* (Viljoen et al., 2013) were included as outgroups. The crown node of the '*Oreobolus*' clade was calibrated in the ITS and *trn*L-F gene trees using a prior with a normal distribution defined by a mean (μ) of 8.75 Ma and a standard deviation (σ) of 2.8 Ma. The age and error range correspond to those estimated for the crown node of the '*Oreobolus*' clade from the dated phylogeny of the Schoeneae tribe presented in Chapter Two. A normal distribution was used on the root because it is the most suitable for secondary calibrations (Ho & Phillips, 2009). This type of distribution allocates most of the probability density around the mean and allows for symmetrical decrease towards the tails accounting for age error (Ho & Phillips, 2009). All other priors were left at their default settings.

Twenty independent MCMC runs of 50 million generations each, sampling every 5000 generations were performed. Ten percent of the samples from each run were discarded as burn-in and a combined log file was produced. Adequate mixing and convergence were assessed using Tracer v1.6.0 (Rambaut et al., 2013). A maximum clade credibility tree (MCC) from the combined tree sets was annotated with median heights, 95% HPD node ages and posterior probability values (PP) on TreeAnnotator v2.1.2 (Rambaut & Drummond, 2015).

Phylogenetic trees typically assume bifurcating relationships between taxa, which may not be appropriate for this study group, as demonstrated in Chapter Two. Therefore, a NeighborNet network (NN; Bryant & Moulton, 2004) was constructed for both nuclear and concatenated plastid haplotypes using Splitstree 4 (Huson & Bryant, 2006). This method allows representation of conflicting signals in the data,

which might be a due to incomplete lineage sorting or reticulate evolution (Bryant & Moulton, 2004; Huson & Bryant, 2006). In the resulting network, conflicts are represented by parallel edges connecting taxa. The NN networks used uncorrected-p distances, which calculate the number of changes between each pair of haplotypes. Similarly, a NN network for both nuclear and concatenated plastid regions was constructed from the F_{ST} values previously calculated between species pairs.

3.4. RESULTS

3.4.1. Haplotype definition and networks

3.4.1.1. Nuclear ribosomal DNA

A total of 197 individuals from 14 clusters (A – N) were scored for ITS haplotypes, including individuals for all five species across their entire distribution range (Table 3.2). After exclusion of poly-T and poly-A length polymorphisms, bi-nucleotide repeats and ambiguously aligned regions, 523 bp of aligned sequences remained. Thirty-nine polymorphic sites comprising 38 nucleotide substitutions and one indel defined thirty haplotypes. Of these, 22 (73.3%) were species-specific while eight (26.7%) were shared among species (Table 3.3). The haplotypes were distributed as follows: *O. cleefii* (Hn1), *O. ecuadorensis* (Hn6, Hn7), *O. goeppingeri* (Hn11, Hn12, Hn13, Hn14, Hn15, Hn17, Hn18, Hn19), *O. obtusangulus* (Hn20, Hn21, Hn22, Hn23, Hn24, Hn25), *O. venezuelensis* (Hn26, Hn27, Hn28, Hn29, Hn30) and shared (Hn2, Hn3, Hn4, Hn5, Hn8, Hn9, Hn10, Hn16). The minimum-spanning tree (MST) showed no clear clustering according to taxonomy (Fig. 3.2). The NeighborNet network (NN) corroborated this result (Fig. 3.3).

At a continental scale, haplotypes were geographically restricted with no shared haplotypes between the northern Andes (NA) region and the southern Andes (SA) (Table 3.3). This geographic structure was evident in both the minimum-spanning tree (Fig. 3.2) and the NN network (Fig. 3.3). Within the northern Andean populations, patterns were a little more complicated. There are eight shared haplotypes evident in the MST (Figure 3.2) and many edges in the NN Network (Figure 3.3). Of the eight shared haplotypes, seven occur in *O. goeppingeri*. Furthermore Hn9, a haplotype shared between *O. goeppingeri* and *O. obtusangulus*, is located in the middle of the MST connecting the SA haplotypes to the NA ones (Fig. 3.2). The haplotypes Hn12 and Hn14 found in *O. goeppingeri* are closer to those found in other species than they are to other haplotypes of the same species as are Hn28 and Hn30 in *O. venezuelensis*.

Table 3.3. ITS haplotype (Hn) occurrence across clusters and species. Clusters (A – N) as described in Figure 3.1 and Table 3.1. cle: *O. cleefii*, ecu: *O. ecuadorensis*, goe: *O. goeppingeri*, obt: *O. obtusangulus* and ven: *O. venezuelensis*.

		NORTHERN ANDES										SOUTHERN ANDES			
		A	B	C	D	E	F	G	H	I	J	K	L	M	N
Hn1	*cle*	.	.	.	1	.	.	.	.	.	.	.	.	.	.
	ecu	.	.	.	.	.	.	.	.	.	.	.	.	.	.
	goe	.	.	.	.	.	.	.	.	.	.	.	.	.	.
	obt	.	.	.	.	.	.	.	.	.	.	.	.	.	.
	ven	.	.	.	.	.	.	.	.	.	.	.	.	.	.
Hn2	*cle*	.	7	1	.	.	.	.	.	.	.	.	.	.	.
	ecu	.	.	.	.	.	.	.	.	.	.	.	.	.	.
	goe	.	.	.	.	.	.	.	.	.	.	.	.	.	.
	obt	.	.	.	1	.	.	.	.	.	.	.	.	.	.
	ven	.	.	.	.	.	.	.	.	.	.	.	.	.	.
Hn3	*cle*	.	.	2	.	.	.	.	.	.	.	.	.	.	.
	ecu	.	.	.	.	.	2	11	8	.	.	.	.	.	.
	goe	.	.	.	.	.	.	.	.	.	.	.	.	.	.
	obt	.	.	.	.	.	.	.	.	1	.	.	.	.	.
	ven	.	.	.	.	.	.	.	.	.	.	.	.	.	.
Hn4	*cle*	.	.	.	.	.	3	.	.	.	.	.	.	.	.
	ecu	.	.	.	.	.	.	.	.	.	.	.	.	.	.
	goe	.	.	.	.	.	2	3	.	1	.	.	.	.	.
	obt	.	.	.	.	.	1	.	.	.	.	.	.	.	.
	ven	.	.	.	.	.	.	.	.	.	.	.	.	.	.
Hn5	*cle*	.	.	.	.	.	1	.	.	.	.	.	.	.	.
	ecu	.	.	.	.	.	.	.	.	.	.	.	.	.	.
	goe	.	.	.	.	.	.	.	.	.	.	.	.	.	.
	obt	.	.	.	.	.	2	1	.	.	.	.	.	.	.
	ven	.	.	.	.	.	.	.	.	.	.	.	.	.	.
Hn6	*cle*	.	.	.	.	.	.	.	.	.	.	.	.	.	.
	ecu	.	.	.	.	.	.	1	.	.	.	.	.	.	.
	goe	.	.	.	.	.	.	.	.	.	.	.	.	.	.
	obt	.	.	.	.	.	.	.	.	.	.	.	.	.	.
	ven	.	.	.	.	.	.	.	.	.	.	.	.	.	.
Hn7	*cle*	.	.	.	.	.	.	.	.	.	.	.	.	.	.
	ecu	.	.	.	.	.	.	.	.	.	2	.	.	.	.
	goe	.	.	.	.	.	.	.	.	.	.	.	.	.	.
	obt	.	.	.	.	.	.	.	.	.	.	.	.	.	.
	ven	.	.	.	.	.	.	.	.	.	.	.	.	.	.
Hn8	*cle*	.	.	.	.	.	.	.	.	.	.	.	.	.	.
	ecu	.	.	.	.	.	.	.	.	.	1	.	.	.	.
	goe	.	.	.	.	.	.	.	.	.	.	.	.	.	.
	obt	.	.	.	.	.	.	.	.	.	1	.	.	.	.
	ven	.	.	.	.	.	.	.	.	.	.	.	.	.	.
Hn9	*cle*	.	.	.	.	.	.	.	.	.	.	.	.	.	.
	ecu	.	.	.	.	.	.	.	.	.	.	.	.	.	.
	goe	.	.	.	.	2	6	3	5	13	.	.	.	.	.
	obt	.	.	.	.	.	.	.	1	.	.	.	.	.	.
	ven	.	.	.	.	.	.	.	.	.	.	.	.	.	.
Hn10	*cle*	.	.	.	.	.	.	.	.	.	.	.	.	.	.
	ecu	.	.	.	.	.	.	.	.	.	.	.	.	.	.
	goe	.	1	1	3	1	.	.	.	.	.	.	.	.	.
	obt	.	.	.	.	.	.	1	.	.	.	.	.	.	.
	ven	.	1	1	2	.	1	.	.	.	.	.	.	.	.
Hn11	*cle*	.	.	.	.	.	.	.	.	.	.	.	.	.	.
	ecu	.	.	.	.	.	.	.	.	.	.	.	.	.	.

	goe	.	2	4	3	.	3	.	3	.	1	.	.	.	.
	obt	.	.	.	.	.	.	.	.	.	.	.	.	.	.
	ven	.	.	.	.	.	.	.	.	.	.	.	.	.	.
	cle	.	.	.	.	.	.	.	.	.	.	.	.	.	.
	ecu	.	.	.	.	.	.	.	.	.	.	.	.	.	.
Hn12	*goe*	.	.	.	.	.	.	.	7	2	.	.	.	.	.
	obt	.	.	.	.	.	.	.	.	.	.	.	.	.	.
	ven	.	.	.	.	.	.	.	.	.	.	.	.	.	.
	cle	.	.	.	.	.	.	.	.	.	.	.	.	.	.
	ecu	.	.	.	.	.	.	.	.	.	.	.	.	.	.
Hn13	*goe*	.	.	.	.	.	.	.	.	1	.	.	.	.	.
	obt	.	.	.	.	.	.	.	.	.	.	.	.	.	.
	ven	.	.	.	.	.	.	.	.	.	.	.	.	.	.
	cle	.	.	.	.	.	.	.	.	.	.	.	.	.	.
	ecu	.	.	.	.	.	.	.	.	.	.	.	.	.	.
Hn14	*goe*	.	.	.	.	.	.	.	.	1	.	.	.	.	.
	obt	.	.	.	.	.	.	.	.	.	.	.	.	.	.
	ven	.	.	.	.	.	.	.	.	.	.	.	.	.	.
	cle	.	.	.	.	.	.	.	.	.	.	.	.	.	.
	ecu	.	.	.	.	.	.	.	.	.	.	.	.	.	.
Hn15	*goe*	.	.	.	.	.	.	1	.	.	.	.	.	.	.
	obt	.	.	.	.	.	.	.	.	.	.	.	.	.	.
	ven	.	.	.	.	.	.	.	.	.	.	.	.	.	.
	cle	.	.	.	.	.	.	.	.	.	.	.	.	.	.
	ecu	.	.	.	.	.	.	.	.	.	.	.	.	.	.
Hn16	*goe*	.	2	.	.	.	.	.	.	.	.	.	.	.	.
	obt	.	.	.	.	.	.	.	.	.	.	.	.	.	.
	ven	.	.	.	2	.	.	.	.	.	.	.	.	.	.
	cle	.	.	.	.	.	.	.	.	.	.	.	.	.	.
	ecu	.	.	.	.	.	.	.	.	.	.	.	.	.	.
Hn17	*goe*	.	.	.	.	.	.	.	.	.	1	.	.	.	.
	obt	.	.	.	.	.	.	.	.	.	.	.	.	.	.
	ven	.	.	.	.	.	.	.	.	.	.	.	.	.	.
	cle	.	.	.	.	.	.	.	.	.	.	.	.	.	.
	ecu	.	.	.	.	.	.	.	.	.	.	.	.	.	.
Hn18	*goe*	.	.	.	.	.	.	.	.	.	1	.	.	.	.
	obt	.	.	.	.	.	.	.	.	.	.	.	.	.	.
	ven	.	.	.	.	.	.	.	.	.	.	.	.	.	.
	cle	.	.	.	.	.	.	.	.	.	.	.	.	.	.
	ecu	.	.	.	.	.	.	.	.	.	.	.	.	.	.
Hn19	*goe*	2	.	.	.	.	.	.	.	.	.	.	.	.	.
	obt	.	.	.	.	.	.	.	.	.	.	.	.	.	.
	ven	.	.	.	.	.	.	.	.	.	.	.	.	.	.
	cle	.	.	.	.	.	.	.	.	.	.	.	.	.	.
	ecu	.	.	.	.	.	.	.	.	.	.	.	.	.	.
Hn20	*goe*	.	.	.	.	.	.	.	.	.	.	.	.	.	.
	obt	.	.	.	.	.	.	.	.	.	.	.	10	.	1
	ven	.	.	.	.	.	.	.	.	.	.	.	.	.	.
	cle	.	.	.	.	.	.	.	.	.	.	.	.	.	.
	ecu	.	.	.	.	.	.	.	.	.	.	.	.	.	.
Hn21	*goe*	.	.	.	.	.	.	.	.	.	.	.	.	.	.
	obt	.	.	.	.	.	.	.	.	.	.	.	1	1	.
	ven	.	.	.	.	.	.	.	.	.	.	.	.	.	.
	cle	.	.	.	.	.	.	.	.	.	.	.	.	.	.
	ecu	.	.	.	.	.	.	.	.	.	.	.	.	.	.
Hn22	*goe*	.	.	.	.	.	.	.	.	.	.	.	.	.	.
	obt	.	.	.	.	.	.	.	.	.	.	.	2	15	.
	ven	.	.	.	.	.	.	.	.	.	.	.	.	.	.
Hn23	*cle*	.	.	.	.	.	.	.	.	.	.	.	.	.	.
	ecu	.	.	.	.	.	.	.	.	.	.	.	.	.	.

	goe	.	.	.	.	.	.	.	.	.	.	.	.	.	.
	obt	.	.	.	.	.	.	.	.	.	.	1	.	.	.
	ven	.	.	.	.	.	.	.	.	.	.	.	.	.	.
	cle	.	.	.	.	.	.	.	.	.	.	.	.	.	.
	ecu	.	.	.	.	.	.	.	.	.	.	.	.	.	.
Hn24	*goe*	.	.	.	.	.	.	.	.	.	.	.	.	.	.
	obt	.	.	.	.	.	3	2	8	.	.	.	.	.	.
	ven	.	.	.	.	.	.	.	.	.	.	.	.	.	.
	cle	.	.	.	.	.	.	.	.	.	.	.	.	.	.
	ecu	.	.	.	.	.	.	.	.	.	.	.	.	.	.
Hn25	*goe*	.	.	.	.	.	.	.	.	.	.	.	.	.	.
	obt	.	.	.	.	.	.	.	.	.	.	.	2	.	.
	ven	.	.	.	.	.	.	.	.	.	.	.	.	.	.
	cle	.	.	.	.	.	.	.	.	.	.	.	.	.	.
	ecu	.	.	.	.	.	.	.	.	.	.	.	.	.	.
Hn26	*goe*	.	.	.	.	.	.	.	.	.	.	.	.	.	.
	obt	.	.	.	.	.	.	.	.	.	.	.	.	.	.
	ven	.	.	1	.	.	.	.	.	.	.	.	.	.	.
	cle	.	.	.	.	.	.	.	.	.	.	.	.	.	.
	ecu	.	.	.	.	.	.	.	.	.	.	.	.	.	.
Hn27	*goe*	.	.	.	.	.	.	.	.	.	.	.	.	.	.
	obt	.	.	.	.	.	.	.	.	.	.	.	.	.	.
	ven	.	.	.	1	.	.	.	.	.	.	.	.	.	.
	cle	.	.	.	.	.	.	.	.	.	.	.	.	.	.
	ecu	.	.	.	.	.	.	.	.	.	.	.	.	.	.
Hn28	*goe*	.	.	.	.	.	.	.	.	.	.	.	.	.	.
	obt	.	.	.	.	.	.	.	.	.	.	.	.	.	.
	ven	.	.	.	.	.	.	.	1	15	.	.	.	.	.
	cle	.	.	.	.	.	.	.	.	.	.	.	.	.	.
	ecu	.	.	.	.	.	.	.	.	.	.	.	.	.	.
Hn29	*goe*	.	.	.	.	.	.	.	.	.	.	.	.	.	.
	obt	.	.	.	.	.	.	.	.	.	.	.	.	.	.
	ven	.	.	.	1	.	.	.	.	.	.	.	.	.	.
	cle	.	.	.	.	.	.	.	.	.	.	.	.	.	.
	ecu	.	.	.	.	.	.	.	.	.	.	.	.	.	.
Hn30	*goe*	.	.	.	.	.	.	.	.	.	.	.	.	.	.
	obt	.	.	.	.	.	.	.	.	.	.	.	.	.	.
	ven	.	.	.	.	.	.	.	1	.	.	.	.	.	.

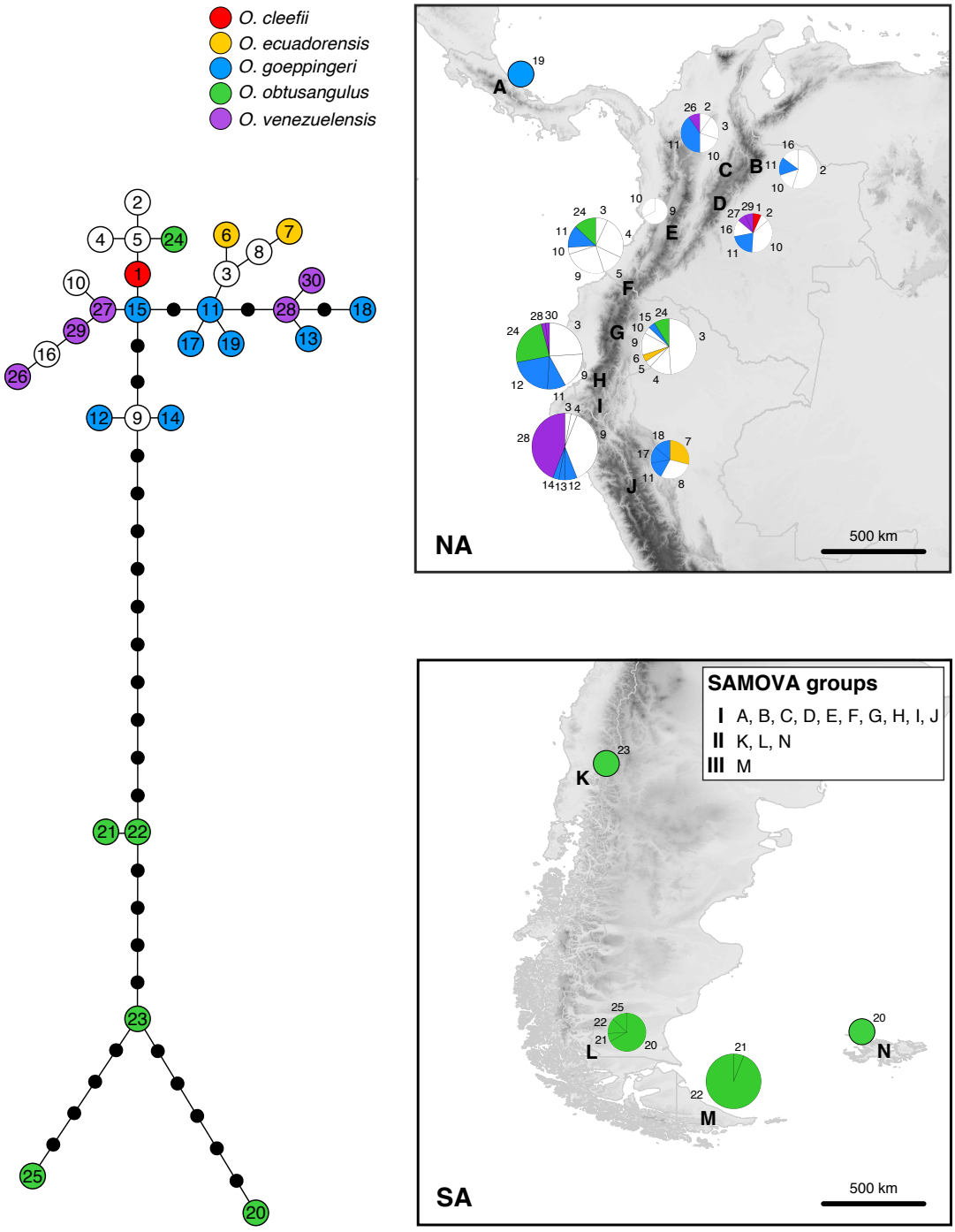

Figure 3.2. MST and distribution of ITS haplotypes. Numbers refer to haplotypes listed in Table 3.3. Haplotypes are coloured according to species. Shared haplotypes are shown in white. Detail of species sharing haplotypes is given in Fig. 3.3. Hypothetical haplotypes are represented by filled black circles, numbers within indicate their number when more than one. Letters on the map refer to clusters as described in Table 3.1 and Figure 3.1. Pie charts are proportional to sample size for each cluster (N = 1 – 34). Numbers next to each segment refer to haplotype number. NA: northern Andes, SA: southern Andes.

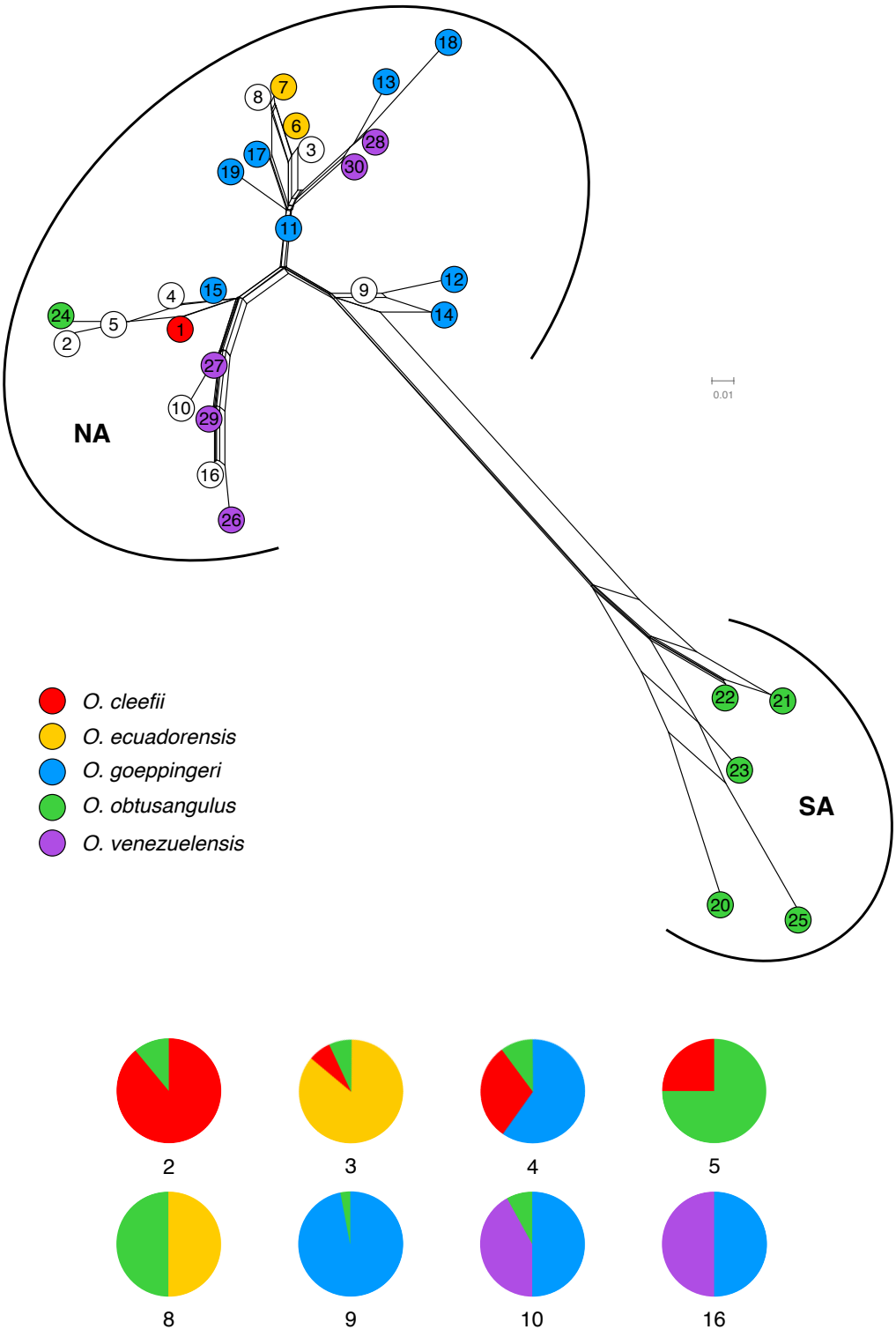

Figure 3.3. NeighborNet network for the ITS haplotypes based on the uncorrected-p distances. Haplotypes are coloured according to species. Shared haplotypes are shown in white. Pie charts are labelled with haplotype number and indicate frequency per species. NA: northern Andes, SA: southern Andes.

3.4.1.2. Plastid DNA

A total of 118 individuals from 13 clusters (B – N) were successfully sequenced for all three plastid markers (*trn*L-F, *trn*H-*psb*A and *rpl*32-*trn*L), including individuals from all five species across most of their distribution range (Table 3.2). A concatenated matrix of 2465 bp of aligned sequences (*trn*L-F, 1040 bp; *trn*H-*psb*A, 676 bp; *rpl*32-*trn*L, 749 bp) resulted after the exclusion of poly-T and poly-A length polymorphisms, bi-nucleotide repeats and ambiguously aligned regions. Forty haplotypes were identified based on 141 polymorphic sites (*trn*L-F, 53; *trn*H-*psb*A, 14; *rpl*32-*trn*L, 74) including 112 nucleotide substitutions and 28 indels. Thirty-four haplotypes (85%) were species-specific while six (15%) were shared among species (Table 3.4), these were distributed as follows: *O. cleefii* (Hc1, Hc3), *O. ecuadorensis* (Hc5, Hc7, Hc8, Hc9), *O. goeppingeri* (Hc10, Hc11, Hc12, Hc15, Hc16, Hc17, Hc18, Hc19), *O. obtusangulus* (Hc20, Hc21, Hc22, Hc23, Hc25, Hc26, Hc27, Hc28, Hc29, Hc30, Hc31, Hc32, Hc33, Hc34, Hc35), *O. venezuelensis* (Hc36, Hc37, Hc38, Hc39, Hc40) and shared (Hc2, Hc4, Hc6, Hc13, Hc14, Hc24). Both the MST and NN network showed some degree of clustering according to taxonomy for three of the species, namely *O. ecuadorensis*, *O. goeppingeri* and *O. venezuelensis* (Fig. 3.4 – 3.5).

Similar to the results obtained for ITS, there were no shared haplotypes between the northern Andes (NA) region and the southern Andes (SA) (Table 3.4). This geographic structure was evident in both the MST and the NN network (Fig. 3.4 – 3.5). There was low support for groupings in the cpDNA network in the relationships amongst northern Andean groups compounded by the large number of possible

unsampled haplotypes compared with ITS. The results of the cpDNA analysis were similar to those of ITS in showing a large number of edges and of shared haplotypes.

Table 3.4. cpDNA (*trn*L-F, *trn*H-*psb*A and *rpl*32-*trn*L) haplotype (Hc) occurrence across clusters and species. Clusters (B – N) as described in Figure 3.1 and Table 3.1. cle: *O. cleefii*, ecu: *O. ecuadorensis*, goe: *O. goeppingeri*, obt: *O. obtusangulus* and ven: *O. venezuelensis*.

		NORTHERN ANDES									SOUTHERN ANDES			
		B	C	D	E	F	G	H	I	J	K	L	M	N
Hc1	*cle*	.	2	.	.	.	.	.	.	.	.	.	.	.
	ecu	.	.	.	.	.	.	.	.	.	.	.	.	.
	goe	.	.	.	.	.	.	.	.	.	.	.	.	.
	obt	.	.	.	.	.	.	.	.	.	.	.	.	.
	ven	.	.	.	.	.	.	.	.	.	.	.	.	.
Hc2	*cle*	4	.	.	.	.	.	.	.	.	.	.	.	.
	ecu	.	.	.	.	.	.	.	.	.	.	.	.	.
	goe	.	.	.	.	.	.	.	.	.	.	.	.	.
	obt	.	.	.	.	3	.	.	.	.	.	.	.	.
	ven	.	.	.	.	.	.	.	.	.	.	.	.	.
Hc3	*cle*	1	.	.	.	.	.	.	.	.	.	.	.	.
	ecu	.	.	.	.	.	.	.	.	.	.	.	.	.
	goe	.	.	.	.	.	.	.	.	.	.	.	.	.
	obt	.	.	.	.	.	.	.	.	.	.	.	.	.
	ven	.	.	.	.	.	.	.	.	.	.	.	.	.
Hc4	*cle*	.	.	.	.	2	.	.	.	.	.	.	.	.
	ecu	.	.	.	.	.	.	.	.	.	.	.	.	.
	goe	.	.	.	.	.	.	.	1	.	.	.	.	.
	obt	.	.	.	.	.	.	.	.	.	.	.	.	.
	ven	.	.	.	.	.	.	.	.	.	.	.	.	.
Hc5	*cle*	.	.	.	.	.	.	.	.	.	.	.	.	.
	ecu	.	.	.	.	3	9	.	.	.	.	.	.	.
	goe	.	.	.	.	.	.	.	.	.	.	.	.	.
	obt	.	.	.	.	.	.	.	.	.	.	.	.	.
	ven	.	.	.	.	.	.	.	.	.	.	.	.	.
Hc6	*cle*	.	.	.	.	.	.	.	.	.	.	.	.	.
	ecu	.	.	.	.	.	2	5	.	1	.	.	.	.
	goe	.	.	.	.	.	.	.	.	.	.	.	.	.
	obt	.	.	.	.	.	.	1	1	1	.	.	.	.
	ven	.	.	.	.	.	.	.	.	.	.	.	.	.
Hc7	*cle*	.	.	.	.	.	.	.	.	.	.	.	.	.
	ecu	.	.	.	.	.	4	3	.	.	.	.	.	.
	goe	.	.	.	.	.	.	.	.	.	.	.	.	.
	obt	.	.	.	.	.	.	.	.	.	.	.	.	.
	ven	.	.	.	.	.	.	.	.	.	.	.	.	.
Hc8	*cle*	.	.	.	.	.	.	.	.	.	.	.	.	.
	ecu	.	.	.	.	.	1	.	.	.	.	.	.	.
	goe	.	.	.	.	.	.	.	.	.	.	.	.	.
	obt	.	.	.	.	.	.	.	.	.	.	.	.	.
	ven	.	.	.	.	.	.	.	.	.	.	.	.	.
Hc9	*cle*	.	.	.	.	.	.	.	.	.	.	.	.	.
	ecu	.	.	.	.	.	.	.	.	1	.	.	.	.
	goe	.	.	.	.	.	.	.	.	.	.	.	.	.
	obt	.	.	.	.	.	.	.	.	.	.	.	.	.
	ven	.	.	.	.	.	.	.	.	.	.	.	.	.
Hc10	*cle*	.	.	.	.	.	.	.	.	.	.	.	.	.
	ecu	.	.	.	.	.	.	.	.	.	.	.	.	.
	goe	.	.	.	.	.	.	.	1	.	.	.	.	.
	obt	.	.	.	.	.	.	.	.	.	.	.	.	.
	ven	.	.	.	.	.	.	.	.	.	.	.	.	.

	cle	.	.	.	.	.	.	.	.	.	.	.	.	.
	ecu	.	.	.	.	.	.	.	.	.	.	.	.	.
Hc11	*goe*	.	.	.	.	2	.	2	.	.	.	.	.	.
	obt	.	.	.	.	.	.	.	.	.	.	.	.	.
	ven	.	.	.	.	.	.	.	.	.	.	.	.	.
	cle	.	.	.	.	.	.	.	.	.	.	.	.	.
	ecu	.	.	.	.	.	.	.	.	.	.	.	.	.
Hc12	*goe*	2	1	2	.	2	.	3	.	.	.	.	.	.
	obt	.	.	.	.	.	.	.	.	.	.	.	.	.
	ven	.	.	.	.	.	.	.	.	.	.	.	.	.
	cle	.	.	.	.	.	.	.	.	.	.	.	.	.
	ecu	.	.	.	.	.	.	.	.	.	.	.	.	.
Hc13	*goe*	1	.	1	1	.	.	.	.	.	.	.	.	.
	obt	.	.	.	.	.	.	.	.	.	.	.	.	.
	ven	.	1	2	.	.	.	.	.	.	.	.	.	.
	cle	.	.	.	.	.	.	.	.	.	.	.	.	.
	ecu	.	.	.	.	.	.	.	.	.	.	.	.	.
Hc14	*goe*	2	.	.	.	.	.	.	.	.	.	.	.	.
	obt	.	.	.	.	.	.	.	.	.	.	.	.	.
	ven	.	.	1	.	.	.	.	.	.	.	.	.	.
	cle	.	.	.	.	.	.	.	.	.	.	.	.	.
	ecu	.	.	.	.	.	.	.	.	.	.	.	.	.
Hc15	*goe*	.	.	.	1	.	.	.	.	.	.	.	.	.
	obt	.	.	.	.	.	.	.	.	.	.	.	.	.
	ven	.	.	.	.	.	.	.	.	.	.	.	.	.
	cle	.	.	.	.	.	.	.	.	.	.	.	.	.
	ecu	.	.	.	.	.	.	.	.	.	.	.	.	.
Hc16	*goe*	.	.	.	1	.	.	.	.	.	.	.	.	.
	obt	.	.	.	.	.	.	.	.	.	.	.	.	.
	ven	.	.	.	.	.	.	.	.	.	.	.	.	.
	cle	.	.	.	.	.	.	.	.	.	.	.	.	.
	ecu	.	.	.	.	.	.	.	.	.	.	.	.	.
Hc17	*goe*	.	.	.	.	1	.	.	.	.	.	.	.	.
	obt	.	.	.	.	.	.	.	.	.	.	.	.	.
	ven	.	.	.	.	.	.	.	.	.	.	.	.	.
	cle	.	.	.	.	.	.	.	.	.	.	.	.	.
	ecu	.	.	.	.	.	.	.	.	.	.	.	.	.
Hc18	*goe*	.	1	.	.	.	.	.	.	.	.	.	.	.
	obt	.	.	.	.	.	.	.	.	.	.	.	.	.
	ven	.	.	.	.	.	.	.	.	.	.	.	.	.
	cle	.	.	.	.	.	.	.	.	.	.	.	.	.
	ecu	.	.	.	.	.	.	.	.	.	.	.	.	.
Hc19	*goe*	.	.	.	.	.	.	.	2	.	.	.	.	.
	obt	.	.	.	.	.	.	.	.	.	.	.	.	.
	ven	.	.	.	.	.	.	.	.	.	.	.	.	.
	cle	.	.	.	.	.	.	.	.	.	.	.	.	.
	ecu	.	.	.	.	.	.	.	.	.	.	.	.	.
Hc20	*goe*	.	.	.	.	.	.	.	.	.	.	.	.	.
	obt	.	.	.	.	.	.	.	.	.	.	5	.	1
	ven	.	.	.	.	.	.	.	.	.	.	.	.	.
	cle	.	.	.	.	.	.	.	.	.	.	.	.	.
	ecu	.	.	.	.	.	.	.	.	.	.	.	.	.
Hc21	*goe*	.	.	.	.	.	.	.	.	.	.	.	.	.
	obt	.	.	.	.	.	.	.	.	.	.	1	4	.
	ven	.	.	.	.	.	.	.	.	.	.	.	.	.
	cle	.	.	.	.	.	.	.	.	.	.	.	.	.
	ecu	.	.	.	.	.	.	.	.	.	.	.	.	.
Hc22	*goe*	.	.	.	.	.	.	.	.	.	.	.	.	.
	obt	.	.	.	.	.	.	.	.	.	1	.	.	.
	ven	.	.	.	.	.	.	.	.	.	.	.	.	.

	cle	.	.	.	.	.	.	.	.	.	.	.	.	.	.
	ecu	.	.	.	.	.	.	.	.	.	.	.	.	.	.
Hc23	*goe*	.	.	.	.	.	.	.	.	.	.	.	.	.	.
	obt	.	.	.	.	.	.	.	.	.	.	.	.	1	.
	ven	.	.	.	.	.	.	.	.	.	.	.	.	.	.
	cle	.	.	.	.	.	.	.	.	.	.	.	.	.	.
	ecu	.	.	.	.	.	.	.	.	.	.	.	.	.	.
Hc24	*goe*	.	.	.	.	.	.	.	.	.	.	.	.	.	.
	obt	.	.	.	.	.	1	.	.	.	.	.	.	.	.
	ven	.	.	.	.	1	.	.	.	.	.	.	.	.	.
	cle	.	.	.	.	.	.	.	.	.	.	.	.	.	.
	ecu	.	.	.	.	.	.	.	.	.	.	.	.	.	.
Hc25	*goe*	.	.	.	.	.	.	.	.	.	.	.	.	.	.
	obt	.	.	.	.	.	.	1	.	.	.	.	.	.	.
	ven	.	.	.	.	.	.	.	.	.	.	.	.	.	.
	cle	.	.	.	.	.	.	.	.	.	.	.	.	.	.
	ecu	.	.	.	.	.	.	.	.	.	.	.	.	.	.
Hc26	*goe*	.	.	.	.	.	.	.	.	.	.	.	.	.	.
	obt	.	.	.	.	.	.	.	.	.	.	1	.	.	.
	ven	.	.	.	.	.	.	.	.	.	.	.	.	.	.
	cle	.	.	.	.	.	.	.	.	.	.	.	.	.	.
	ecu	.	.	.	.	.	.	.	.	.	.	.	.	.	.
Hc27	*goe*	.	.	.	.	.	.	.	.	.	.	.	.	.	.
	obt	.	.	.	.	1	2	2	.	.	.	.	.	.	.
	ven	.	.	.	.	.	.	.	.	.	.	.	.	.	.
	cle	.	.	.	.	.	.	.	.	.	.	.	.	.	.
	ecu	.	.	.	.	.	.	.	.	.	.	.	.	.	.
Hc28	*goe*	.	.	.	.	.	.	.	.	.	.	.	.	.	.
	obt	.	.	.	.	.	.	1	.	.	.	.	.	.	.
	ven	.	.	.	.	.	.	.	.	.	.	.	.	.	.
	cle	.	.	.	.	.	.	.	.	.	.	.	.	.	.
	ecu	.	.	.	.	.	.	.	.	.	.	.	.	.	.
Hc29	*goe*	.	.	.	.	.	.	.	.	.	.	.	.	.	.
	obt	.	.	.	.	.	.	1	.	.	.	.	.	.	.
	ven	.	.	.	.	.	.	.	.	.	.	.	.	.	.
	cle	.	.	.	.	.	.	.	.	.	.	.	.	.	.
	ecu	.	.	.	.	.	.	.	.	.	.	.	.	.	.
Hc30	*goe*	.	.	.	.	.	.	.	.	.	.	.	.	.	.
	obt	.	.	.	.	.	.	1	.	.	.	.	.	.	.
	ven	.	.	.	.	.	.	.	.	.	.	.	.	.	.
	cle	.	.	.	.	.	.	.	.	.	.	.	.	.	.
	ecu	.	.	.	.	.	.	.	.	.	.	.	.	.	.
Hc31	*goe*	.	.	.	.	.	.	.	.	.	.	.	.	.	.
	obt	.	.	.	.	.	.	2	.	.	.	.	.	.	.
	ven	.	.	.	.	.	.	.	.	.	.	.	.	.	.
	cle	.	.	.	.	.	.	.	.	.	.	.	.	.	.
	ecu	.	.	.	.	.	.	.	.	.	.	.	.	.	.
Hc32	*goe*	.	.	.	.	.	.	.	.	.	.	.	.	.	.
	obt	.	.	.	.	2	.	.	.	.	.	.	.	.	.
	ven	.	.	.	.	.	.	.	.	.	.	.	.	.	.
	cle	.	.	.	.	.	.	.	.	.	.	.	.	.	.
	ecu	.	.	.	.	.	.	.	.	.	.	.	.	.	.
Hc33	*goe*	.	.	.	.	.	.	.	.	.	.	.	.	.	.
	obt	.	.	.	.	.	.	.	.	.	.	.	.	3	.
	ven	.	.	.	.	.	.	.	.	.	.	.	.	.	.
	cle	.	.	.	.	.	.	.	.	.	.	.	.	.	.
	ecu	.	.	.	.	.	.	.	.	.	.	.	.	.	.
Hc34	*goe*	.	.	.	.	.	.	.	.	.	.	.	.	.	.
	obt	.	.	.	.	.	.	.	.	.	.	1	.	.	.
	ven	.	.	.	.	.	.	.	.	.	.	.	.	.	.

	cle	.	.	.	.	.	.	.	.	.	.	.	.	.
	ecu	.	.	.	.	.	.	.	.	.	.	.	.	.
Hc35	*goe*	.	.	.	.	.	.	.	.	.	.	.	.	.
	obt	.	.	.	.	.	.	.	.	.	.	.	1	.
	ven	.	.	.	.	.	.	.	.	.	.	.	.	.
	cle	.	.	.	.	.	.	.	.	.	.	.	.	.
	ecu	.	.	.	.	.	.	.	.	.	.	.	.	.
Hc36	*goe*	.	.	.	.	.	.	.	.	.	.	.	.	.
	obt	.	.	.	.	.	.	.	.	.	.	.	.	.
	ven	.	.	.	.	.	1	.	.	.	.	.	.	.
	cle	.	.	.	.	.	.	.	.	.	.	.	.	.
	ecu	.	.	.	.	.	.	.	.	.	.	.	.	.
Hc37	*goe*	.	.	.	.	.	.	.	.	.	.	.	.	.
	obt	.	.	.	.	.	.	.	.	.	.	.	.	.
	ven	.	.	.	.	.	.	1	1	.	.	.	.	.
	cle	.	.	.	.	.	.	.	.	.	.	.	.	.
	ecu	.	.	.	.	.	.	.	.	.	.	.	.	.
Hc38	*goe*	.	.	.	.	.	.	.	.	.	.	.	.	.
	obt	.	.	.	.	.	.	.	.	.	.	.	.	.
	ven	.	.	.	.	.	.	2	.	.	.	.	.	.
	cle	.	.	.	.	.	.	.	.	.	.	.	.	.
	ecu	.	.	.	.	.	.	.	.	.	.	.	.	.
Hc39	*goe*	.	.	.	.	.	.	.	.	.	.	.	.	.
	obt	.	.	.	.	.	.	.	.	.	.	.	.	.
	ven	.	.	.	.	.	.	.	3	.	.	.	.	.
	cle	.	.	.	.	.	.	.	.	.	.	.	.	.
	ecu	.	.	.	.	.	.	.	.	.	.	.	.	.
Hc40	*goe*	.	.	.	.	.	.	.	.	.	.	.	.	.
	obt	.	.	.	.	.	.	.	.	.	.	.	.	.
	ven	.	.	.	.	.	.	.	1	.	.	.	.	.

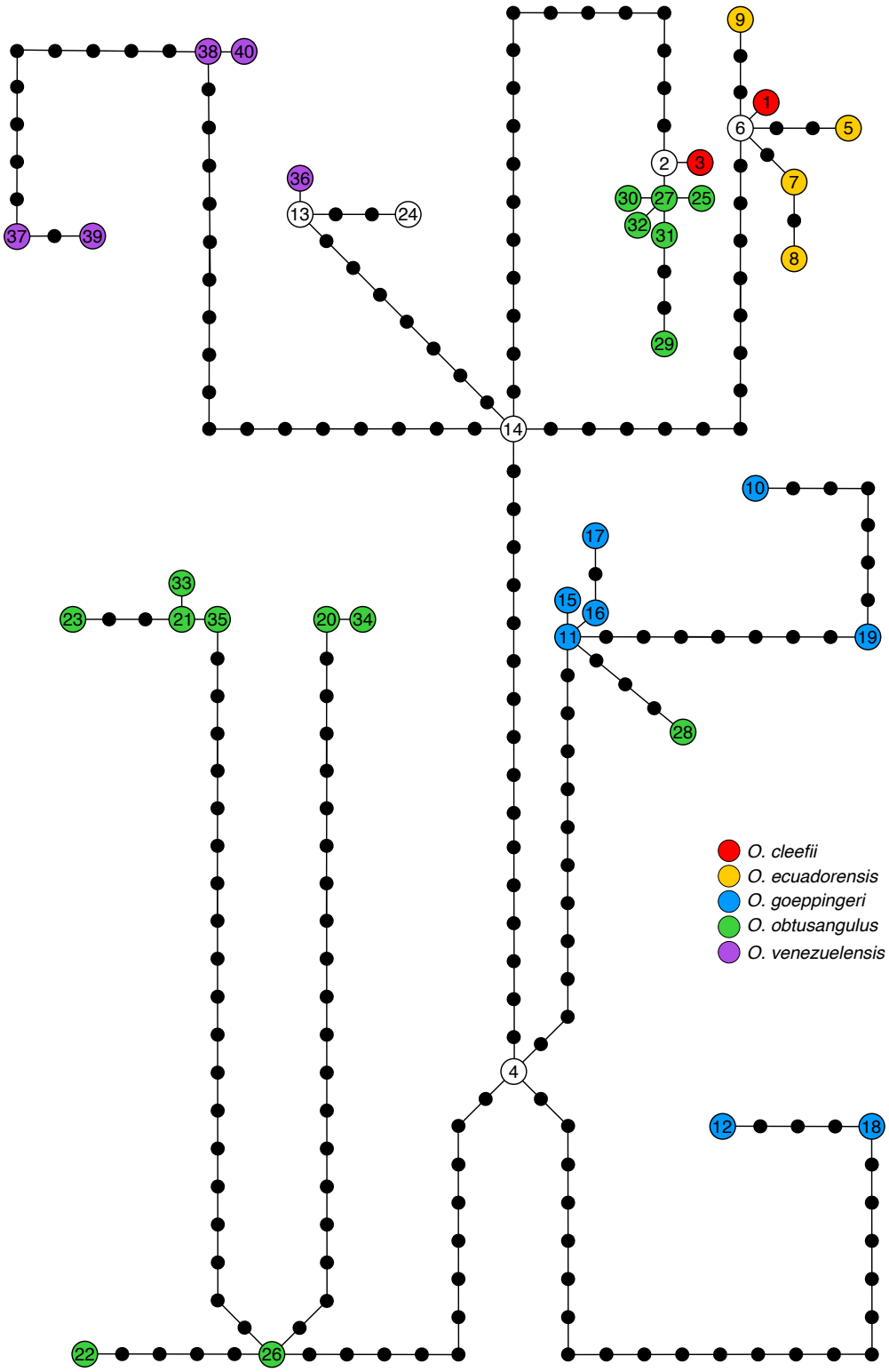
9
1
6
5
38
40
2
3
36
7
13
24
30
27
25
32
31
37
39
8
29
14
10
17
33
15
16
23
21
35
20
34
11
19
28
O. cleefii
O. ecuadorensis
O. goeppingeri
O. obtusangulus
O. venezuelensis
4
12
18
22
26

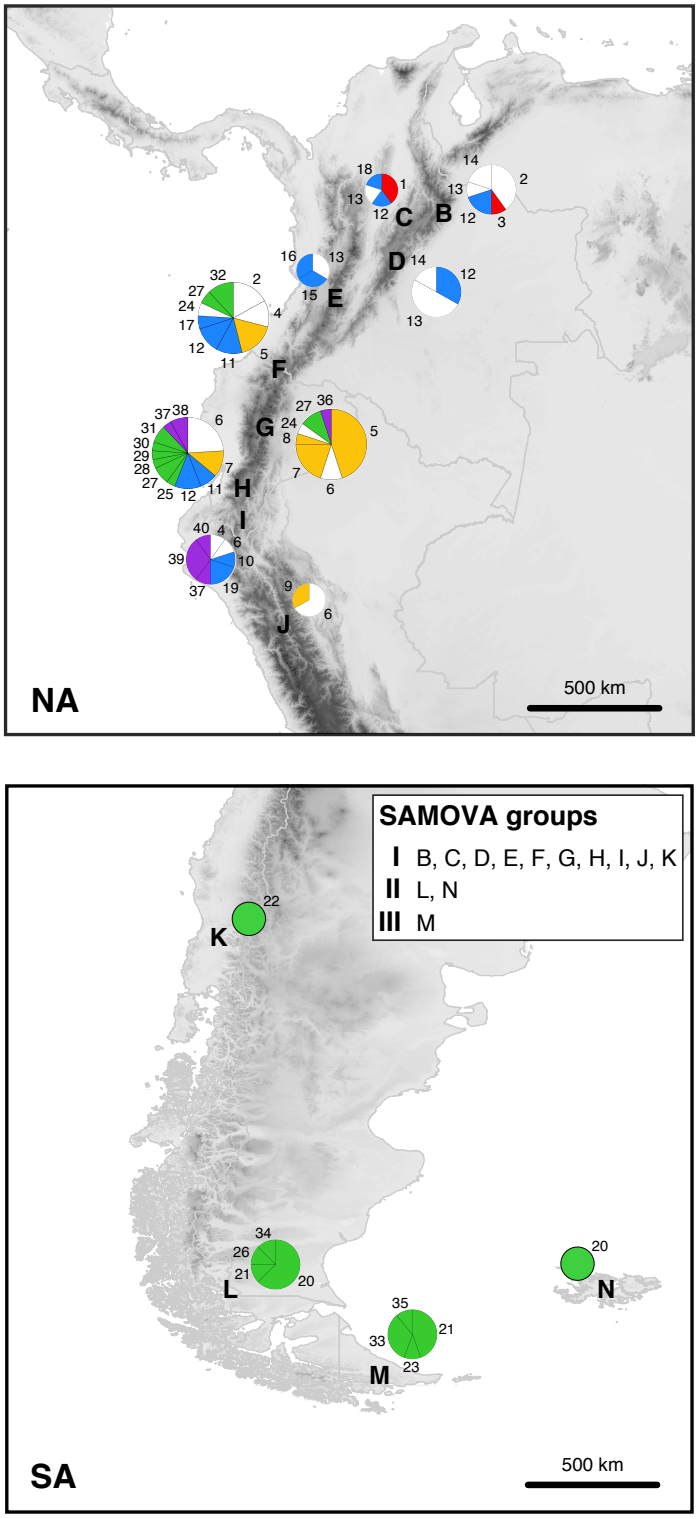

Figure 3.4. MST and distribution of cpDNA (*trn*L-F, *trn*H-*psb*A and *rpl*32-*trn*L) haplotypes. Numbers refer to haplotypes listed in Table 3.4. Haplotypes are coloured according to species. Shared haplotypes are shown in white. Detail of species sharing haplotypes is given in Fig. 3.5. Hypothetical haplotypes are represented by filled black circles. Letters on the map refer to clusters as described in Table 3.1 and Figure 3.1. Pie charts are proportional to sample size for each cluster (N = 1 – 25). Numbers next to each segment refer to haplotype number. NA: northern Andes, SA: southern Andes.

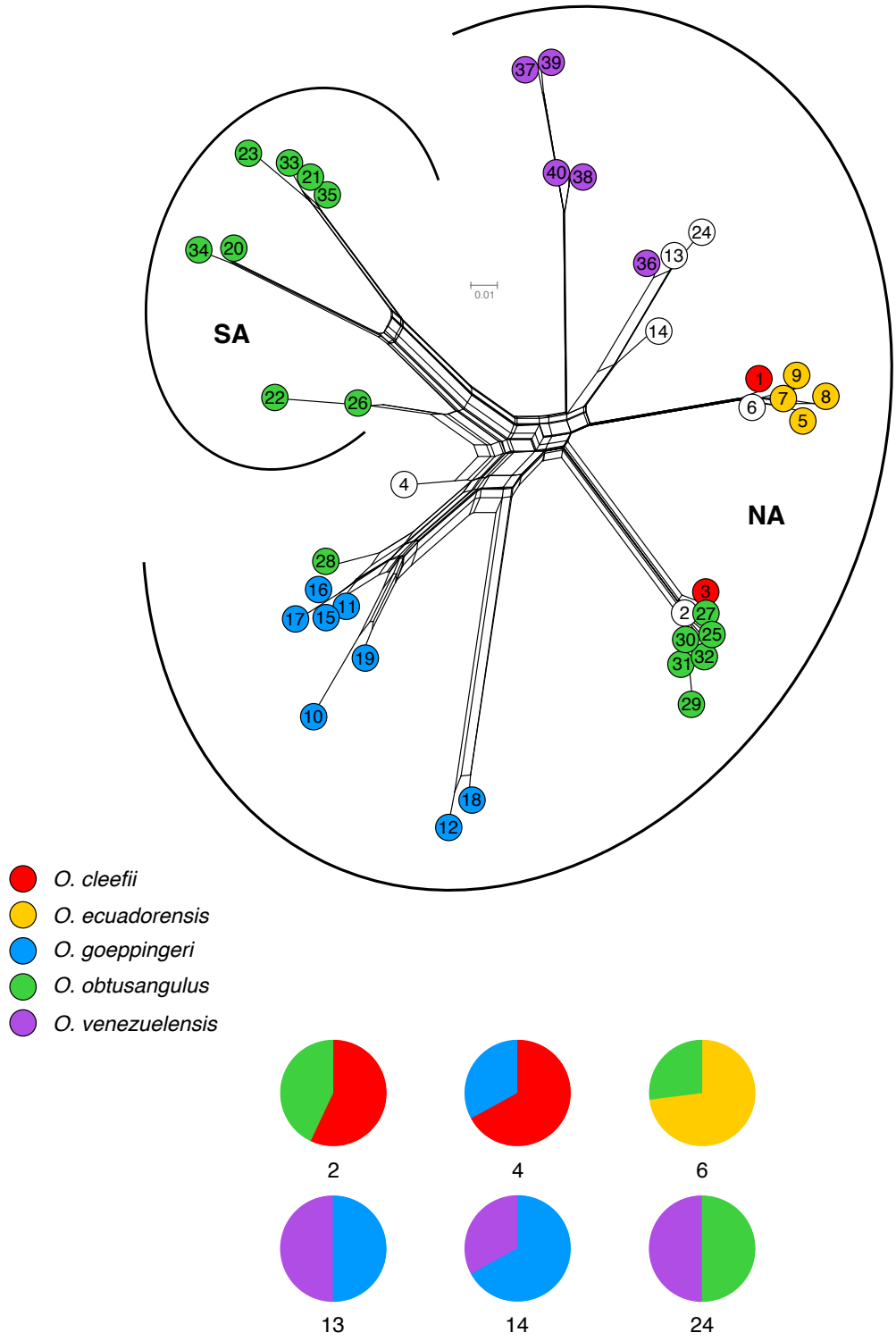

Figure 3.5. NeighborNet network for the cpDNA (*trn*L-F, *trn*H-*psb*A and *rpl*32-*trn*L) haplotypes based on the uncorrected-p distances. Haplotypes are coloured according to species. Shared haplotypes are shown in white. Pie charts are labelled with haplotype number and indicate frequency per species. NA: northern Andes, SA: southern Andes.

3.4.2. Statistical analyses

3.4.2.1. Cluster genetic structure

Table 3.5 presents the results for the molecular diversity indices calculated for ITS and cpDNA. In ITS, haplotype diversity was lowest in cluster M (h = 0.13 ± 0.11) and highest in cluster J (h = 0.91 ± 0.10), while in cpDNA it was lowest in cluster L (h = 0.64 ± 0.18) and highest in cluster E (h = 1.00 ± 0.27). Nucleotide diversity in ITS was lowest in cluster J (π x 100 = 0.56 ± 0.39) and highest in cluster C (π x 100 = 2.95 ± 1.63) while in cpDNA it was lowest in cluster M (π x 100 = 0.06 ± 0.05) and highest in cluster C (π x 100 = 3.95 ± 2.41). In the AMOVA analyses, genetic differentiation amongst all clusters was high (ITS, $F_{ST} = 0.43$, $p < 0.001$; cpDNA, $F_{ST} = 0.37$, $p < 0.001$) although 57% (ITS) and 63% (cpDNA) of the variation was contained within clusters (Table 3.8). When only including northern Andean (NA) clusters, genetic differentiation was moderate (ITS, $F_{ST} = 0.15$, $p < 0.01$; cpDNA, $F_{ST} = 0.21$, $p < 0.001$), and 86% (ITS) and 79% (cpDNA) of the variation was within clusters (Table 3.8). For ITS, 53% of the pairwise F_{ST} values calculated amongst clusters showed significant differentiation ($p < 0.05$). Clusters E and C were the least differentiated ($F_{ST} = -0.073$) and clusters M and G the most ($F_{ST} = 0.718$) (Table 3.6). For cpDNA, 50% of the F_{ST} values showed significant differentiation ($p < 0.05$) with clusters G and J being the least differentiated ($F_{ST} = -0.080$) and clusters J and M the most ($F_{ST} = 0.989$) (Table 3.6). Typically, sites with low levels of differentiation were geographically proximate, while those with high levels of differentiation were separated by large distances. There were however, some exceptions, such as between clusters B and D ($F_{ST} = 0.112$) or between clusters G and I ($F_{ST} = 0.452$), in both cases for the plastid regions.

Table 3.5. Molecular diversity indices for ITS and cpDNA (*trn*L-L-F, *trn*H-*psb*A and *rpl32*-*trn*L) for each cluster. Clusters (A – N) as described in Figure 3.1 and Table 3.1. Metrics were not applicable (n.a.) for clusters with less than three individuals. N, number of individuals; h, haplotype diversity (± SD); π, nucleotide diversity (± SD).

	ITS				cpDNA			
	SAMOVA group	N	h	π x100	SAMOVA group	N	h	π x 100
A	I	2	n.a.	n.a.	-	-	-	-
B	I	13	0.69 ± 0.12	0.76 ± 0.46	I	10	0.82 ± 0.10	2.34 ± 1.25
C	I	10	0.82 ± 0.10	2.95 ± 1.63	I	5	0.90 ± 0.16	3.95 ± 2.41
D	I	14	0.85 ± 0.07	0.63 ± 0.39	I	6	0.73 ± 0.16	2.78 ± 1.62
E	I	3	0.67 ± 0.31	0.72 ± 0.63	I	3	1.00 ± 0.27	2.15 ± 1.62
F	I	24	0.86 ± 0.04	0.67 ± 0.40	I	17	0.93 ± 0.04	2.68 ± 1.36
G	I	23	0.76 ± 0.08	0.66 ± 0.40	I	20	0.77 ± 0.08	1.69 ± 0.86
H	I	34	0.83 ± 0.03	0.84 ± 0.48	I	25	0.92 ± 0.03	3.10 ± 1.55
I	I	34	0.67 ± 0.05	1.88 ± 0.98	I	10	0.91 ± 0.08	2.20 ± 1.18
J	I	7	0.91 ± 0.10	0.56 ± 0.39	I	3	0.67 ± 0.31	0.09 ± 0.08
K	II	1	n.a.	n.a.	I	1	n.a.	n.a.
L	II	15	0.55 ± 0.14	2.36 ± 1.27	II	8	0.64 ± 0.18	2.13 ± 1.18
M	III	16	0.13 ± 0.11	1.46 ± 0.80	III	9	0.75 ± 0.11	0.06 ± 0.05
N	II	1	n.a.	n.a.	II	1	n.a.	n.a.

Table 3.6. Pairwise F_{ST} values amongst clusters calculated from ITS and cpDNA (*trn*L-L-F, *trn*H-*psb*A and *rpl32*-*trn*L). Results for ITS are shown below the diagonal and cpDNA above. Bold numbers indicate significance at the 5% level.

	A	B	C	D	E	F	G	H	I	J	K	L	M	N	
A		-	-	-	-	-	-	-	-	-	-	-	-	-	A
B	-		0.134	0.112	0.136	0.001	**0.504**	**0.101**	**0.211**	**0.586**	-	**0.462**	**0.713**	-	B
C	-	**0.092**		0.028	0.050	0.038	**0.206**	-0.003	**0.157**	0.200	-	**0.417**	**0.690**	-	C
D	-	**0.141**	0.050		0.023	**0.166**	**0.530**	**0.220**	**0.264**	**0.597**	-	**0.470**	**0.740**	-	D
E	-	**0.290**	-0.073	0.200		0.048	**0.511**	0.113	0.076	0.712	-	**0.414**	**0.874**	-	E
F	-	**0.147**	**0.106**	**0.201**	0.101		**0.342**	0.000	**0.109**	**0.402**	-	**0.408**	**0.621**	-	F
G	-	**0.267**	0.061	**0.249**	0.206	**0.089**		**0.188**	**0.452**	-0.080	-	**0.646**	**0.794**	-	G
H	-	**0.258**	**0.120**	**0.258**	0.028	0.051	0.052		**0.095**	**0.207**	-	**0.406**	**0.581**	-	H
I	-	**0.232**	0.055	**0.202**	-0.046	**0.141**	**0.127**	**0.087**		**0.532**	-	**0.444**	**0.724**	-	I
J	-	**0.498**	**0.065**	**0.484**	**0.485**	**0.406**	**0.232**	**0.276**	**0.122**		-	**0.698**	**0.989**	-	J
K	-	-	-	-	-	-	-	-	-	-		-	-	-	K
L	-	**0.629**	**0.474**	**0.635**	**0.482**	**0.659**	**0.660**	**0.661**	**0.537**	**0.595**	-		**0.657**	-	L
M	-	**0.702**	**0.531**	**0.708**	**0.601**	**0.715**	**0.718**	**0.704**	**0.563**	**0.688**	-	**0.296**		-	M
N	-	-	-	-	-	-	-	-	-	-	-	-	-		N
	A	B	C	D	E	F	G	H	I	J	K	L	M	N	

Table 3.7 shows the results for the SAMOVA analysis. There is an overall pattern of increasing F_{CT} values as the number of groups (K) approaches the number of clusters sampled (K = 9). For both ITS and cpDNA, three groups (I – III; Table 3.5) were selected (ITS, $F_{CT} = 0.622$, $p < 0.001$; cpDNA, $F_{CT} = 0.426$, $p < 0.001$) as this was the number of K that maximised genetic differentiation amongst groups while minimising the number of single-cluster groups. For ITS, group I included all northern Andean clusters (A – J) while groups II (K, L, N) and III (M) included the southern Andean ones (Table 3.5). For cpDNA, group I included all northern Andean clusters plus the northernmost southern Andean cluster (K), while groups II (L, N) and III (M) included the rest (Table 3.5). SAMOVA groups explained slightly more of the genetic structure (ITS, $F_{CT} = 0.62$, $p < 0.001$; cpDNA, $F_{CT} = 0.43$, $p < 0.001$) than the pre-defined geographic regions (ITS, $F_{CT} = 0.60$, $p < 0.001$; cpDNA, $F_{CT} = 0.36$, $p < 0.001$) (Table 3.8). Significant phylogeographic structure was indicated by the significantly higher values of N_{ST} (ITS, $N_{ST} = 0.605$; cpDNA, $N_{ST} = 0.406$) compared to G_{ST} (ITS, $G_{ST} = 0.262$; cpDNA, $G_{ST} = 0.156$; $p < 0.01$). However most of the unexplained diversity is contained within clusters, which may be an artefact of combining species into clusters regardless of their classification.

Table 3.7. Spatial analysis of molecular variance (SAMOVA) results for ITS and cpDNA (*trn*L-L-F, *trn*H-*psb*A and *rpl32*-*trn*L) showing the variance amongst groups (F_{CT} values) for pre-defined K number of groups.

	K											
	2	3	4	5	6	7	8	9	10	11	12	13
F_{CT} ITS	0.595	0.622	0.608	0.608	0.603	0.581	0.505	0.507	0.468	0.481	0.504	0.639
F_{CT} cpDNA	0.417	0.426	0.417	0.414	0.412	0.406	0.405	0.410	0.441	0.502	0.675	-

Table 3.8. Analysis of molecular variance (AMOVA) results for ITS and cpDNA (*trn*L-L-F, *trn*H-*psb*A and *rpl32*-*trn*L).

Group level	Source of variation	Degrees of freedom		Sum of Squares		Variance components		Percentage of variation		Fixation indices	
		ITS	cpDNA	ITS	cpDNA	ITS	cpDNA	ITS	cpDNA	ITS	cpDNA
Species	Among species	4	4	260	2033	1.69	21.67	30.46	47.65	F_{ST} = 0.31***	F_{ST} = 0.48***
	Within species	192	113	741	2689	3.86	23.80	69.54	52.35		
Clusters (all clusters)	Among clusters	13	12	442	1925	2.30	15.54	42.95	36.84	F_{ST} = 0.43***	F_{ST} = 0.37***
	Within clusters	183	105	560	2798	3.06	26.65	57.05	63.16		
Clusters (northern Andes - NA)	Among clusters	9	8	88	885	0.46	7.88	14.50	21.34	F_{ST} = 0.15**	F_{ST} = 0.21***
	Within clusters	154	90	416	2612	2.70	29.03	85.50	78.66		
Regions	Among regions	1	1	309	746	5.38	19.89	59.49	35.54	F_{CT} = 0.60***	F_{CT} = 0.36***
	Among clusters within regions	12	11	133	1179	0.61	9.41	6.72	16.82	F_{SC} = 0.17**	F_{SC} = 0.26***
	Within clusters	183	105	560	2798	3.06	26.65	33.79	47.64	F_{ST} = 0.66***	F_{ST} = 0.52***
SAMOVA groups	Among groups	2	2	348	999	5.71	25.47	62.19	42.59	F_{CT} = 0.62***	F_{CT} = 0.43***
	Among clusters within groups	11	10	93	926	0.41	7.68	4.51	12.84	F_{SC} = 0.12*	F_{SC} = 0.22***
	Within clusters	183	105	560	2798	3.06	26.65	33.30	44.56	F_{ST} = 0.67***	F_{ST} = 0.55***

* significant at the 5% level; ** significant at the 1% level; *** significant at the 0.1% level

3.4.2.2. Species genetic structure

Table 3.9 presents the results of the molecular diversity indices calculated for ITS and cpDNA for the five *Oreobolus* species. For both ITS and cpDNA, haplotype diversity was lowest in *O. ecuadorensis* (ITS, h = 0.31 ± 0.12; cpDNA, h = 0.72 ± 0.05) and highest in *O. obtusangulus* (ITS, h = 0.82 ± 0.03; cpDNA, h = 0.94 ± 0.02). Likewise, nucleotide diversity was lowest in *O. ecuadorensis* (ITS, π x 100 = 0.01 ± 0.10; cpDNA, π x 100 = 0.11 ± 0.07) and highest in *O. obtusangulus* (ITS, π x 100 = 2.76 ± 1.39; cpDNA, π x 100 = 3.05 ± 1.49). Similarly, haplotypic richness was lowest in *O. ecuadorensis* (ITS, hr = 3.12; cpDNA = 3.54) and highest in *O. obtusangulus* (ITS, hr = 6.59; cpDNA = 7.12).

Table 3.9. Molecular diversity indices for ITS and cpDNA (*trn*L-L-F, *trn*H-*psb*A and *rpl32*-*trn*L) for each species. N, number of individuals; H, number of haplotypes; hr, haplotype richness (ITS, rarefied to a minimum sample of 15; cpDNA, rarefied to a minimum sample of 9); h, haplotype diversity (± SD); π, nucleotide diversity (± SD).

Species	N	H	hr	h	π x 100
	ITS				
O. cleefii	15	5	5.00	0.70 ± 0.11	0.45 ± 0.30
O. ecuadorensis	24	4	3.12	0.31 ± 0.12	0.01 ± 0.10
O. goeppingeri	75	12	6.09	0.79 ± 0.03	1.15 ± 0.61
O. obtusangulus	56	13	6.59	0.82 ± 0.03	2.76 ± 1.39
O. venezuelensis	27	7	5.02	0.63 ± 0.10	1.49 ± 0.80
	cpDNA				
O. cleefii	9	4	4.00	0.78 ± 0.11	1.96 ±1.07
O. ecuadorensis	29	5	3.54	0.72 ± 0.05	0.11 ± 0.07
O. goeppingeri	27	11	5.67	0.84 ± 0.06	2.36 ± 1.17
O. obtusangulus	39	18	7.12	0.94 ± 0.02	3.05 ± 1.49
O. venezuelensis	14	8	6.30	0.91 ± 0.05	2.23 ± 1.15

Genetic differentiation amongst species was high (ITS, $F_{ST} = 0.31$, $p < 0.001$; cpDNA, $F_{ST} = 0.48$, $p < 0.001$) although 69% (ITS) and 52% (cpDNA) of it was contained within species variation (Table 3.8). In ITS, F_{ST} values between all species pairs were significant ($p < 0.001$) with *O. goeppingeri* and *O. venezuelensis* being the least differentiated ($F_{ST} = 0.175$) and *O. cleefii* and *O. ecuadorensis* the most ($F_{ST} = 0.770$) (Table 3.10a). In cpDNA, F_{ST} values were also significant between all species pairs ($p < 0.05$) with *O. cleefii* and *O. obtusangulus* being the least differentiated ($F_{ST} = 0.098$) and *O. ecuadorensis* and *O. venezuelensis* the most ($F_{ST} = 0.801$) (Table 3.10a). When considering *O. obtusangulus* as two species, pairwise F_{ST} values for ITS were significant for all species pairs ($p < 0.01$) with *O. cleefii* and *O. obtusangulus* (NA) being the closest ($F_{ST} = 0.157$) and *O. cleefii* and *O. ecuadorensis* the furthest ($F_{ST} = 0.770$) (Table 3.10b). For cpDNA, *O. cleefii* and *O. obtusangulus* (NA) were the closest and non-significantly differentiated ($F_{ST} = -0.020$). All the other species pairs were significantly differentiated ($p < 0.01$) with the most different being *O. ecuadorensis* and *O. obtusangulus* (SA) ($F_{ST} = 0.819$) (Table 3.10b).

Table 3.10. Pairwise F_{ST} values amongst species calculated from ITS and cpDNA (*trn*L-L-F, *trn*H-*psb*A and *rpl32*-*trn*L) considering *O. obtusangulus* as (a) one species and (b) as two species. Values for ITS are below the diagonal and cpDNA above. Bold numbers denote significance at the 5% level. cle: *O. cleefii*, ecu: *O. ecuadorensis*, goe: *O. goeppingeri*, obt: *O. obtusangulus* and ven: *O. venezuelensis*.

(a)

	cle	ecu	goe	obt	ven	
cle		**0.797**	**0.283**	**0.098**	**0.317**	cle
ecu	**0.770**		**0.732**	**0.600**	**0.801**	ecu
goe	**0.284**	**0.307**		**0.229**	**0.288**	goe
obt	**0.269**	**0.360**	**0.289**		**0.256**	obt
ven	**0.314**	**0.328**	**0.175**	**0.291**		ven
	cle	ecu	goe	obt	ven	

(b)

	cle	ecu	goe	obt (NA)	obt (SA)	ven	
cle		**0.797**	**0.283**	-0.020	**0.487**	**0.317**	cle
ecu	**0.770**		**0.732**	**0.780**	**0.819**	**0.801**	ecu
goe	**0.284**	**0.307**		**0.363**	**0.430**	**0.288**	goe
obt (NA)	**0.157**	**0.710**	**0.294**		**0.547**	**0.399**	obt (NA)
obt (SA)	**0.595**	**0.649**	**0.578**	**0.620**		**0.478**	obt (SA)
ven	**0.314**	**0.328**	**0.175**	**0.339**	**0.551**		ven
	cle	ecu	goe	obt (NA)	obt (SA)	ven	

3.4.3. Species tree and phylogenetic networks

The *BEAST (Heled & Drummond, 2010) analysis using both ITS and cpDNA (*trn*L-F, *trn*H-*psb*A and *rpl*32-*trn*L) datasets did not reach convergence or adequate mixing after 100 x 10^7 generations. Similarly, the effective sample size (ESS) for most of the variables was lower than 100. Consequently, the divergence time estimation was not completed. This result was likely caused by the absence of sequenced data for the outgroup (*Capeobolus brevicaulis*) for two of the plastid regions (*trn*H-psbA and *rpl*32-trnL). A possible solution would be clock rooting the species tree in order to calibrate it.

As an approximation to the species tree, Fig. 3.6 shows the MCC tree for the combined tree sets (likelihood with ESS>100, posterior and species coalescent with ESS<100). *O. cleefii*, *O. ecuadorensis*, *O. goeppingeri* and *O. venezuelensis* are recovered as genetically distinct. The results support the genetic differentiation between *O. obtusangulus* from the northern Andes region (NA; Fig. 3.6) and *O. obtusangulus* from the southern Andes region (SA; Fig. 3.6), the latter being identified as a genetically isolated entity. *O. obtusangulus* (SA) appears as sister taxon to the rest of the species. In the northern Andean clade (NAC; PP=99%), *O. ecuadorensis*, *O. cleefii* and *O. obtusangulus* (NA) form a poorly supported clade (PP=44%) sister to another poorly supported clade composed of *O. goeppingeri* and *O. venezuelensis* (PP=39%). *O. cleefii* and *O. obtusangulus* (NA) are recovered as sister taxa with good support (PP=80%).

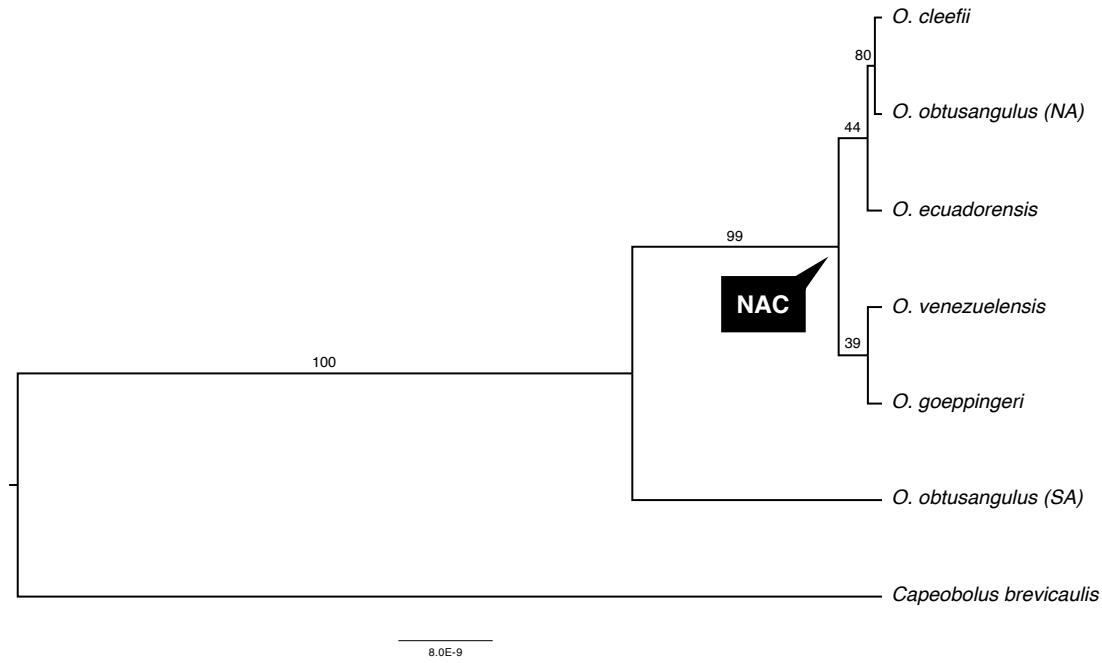

Figure 3.6. Maximum clade credibility tree from the *BEAST analysis based on ITS and cpDNA (*trn*L-F, *trn*H-*psb*A and *rpl*32-*trn*L). Numbers above the branches represent posterior probability values. NAC, northern Andean clade as described in Chapter Two; NA, northern Andes; SA, southern Andes.

Figures 3.7 and 3.8 show the resulting NN networks based on ITS and the concatenated plastid regions, respectively. *Oreobolus ecuadorensis* is consistently distinguished from the other species in both ITS and cpDNA. When considering *O. obtusangulus* as one species, it is reconstructed in the middle of the network and its placement is not well resolved in either ITS or cpDNA NN networks (Figs. 3.7a and 3.8a). On the contrary, when considering northern and southern groups separately, *O. obtusangulus* (SA) is clearly different from other *Oreobolus* species, whereas *O. obtusangulus* (NA) has affinities with *O. cleefii*. The conflicting signal between the latter two species (i.e. multiple parallel edges) is evident in both cpDNA and ITS NN networks (Figs. 3.7b and 3.8b). *Oreobolus goeppingeri* and *O. venezuelensis* are well differentiated in cpDNA but not in ITS where they appeared in the centre of the networks with multiple connections to the other species (Figs. 3.7 and 3.8). The latter

is consistent with the poor PP obtained in the MCC tree for the clade formed by these two species (Fig. 3.6).

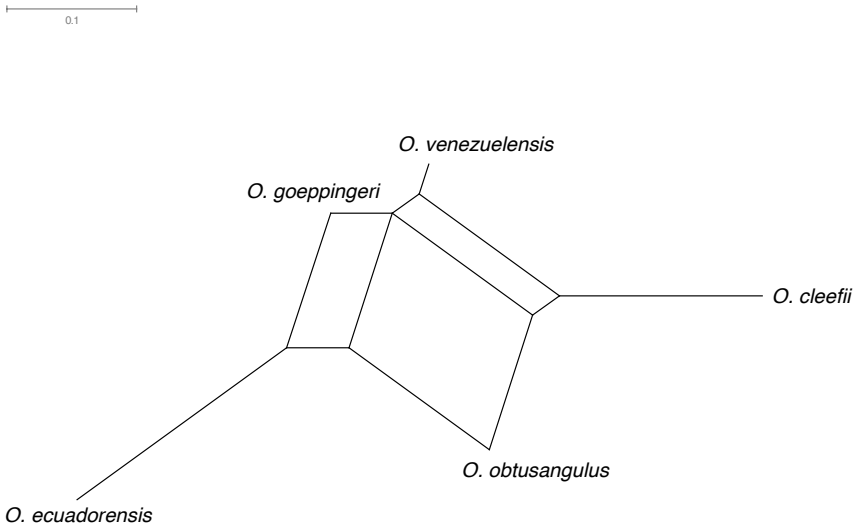

(a)

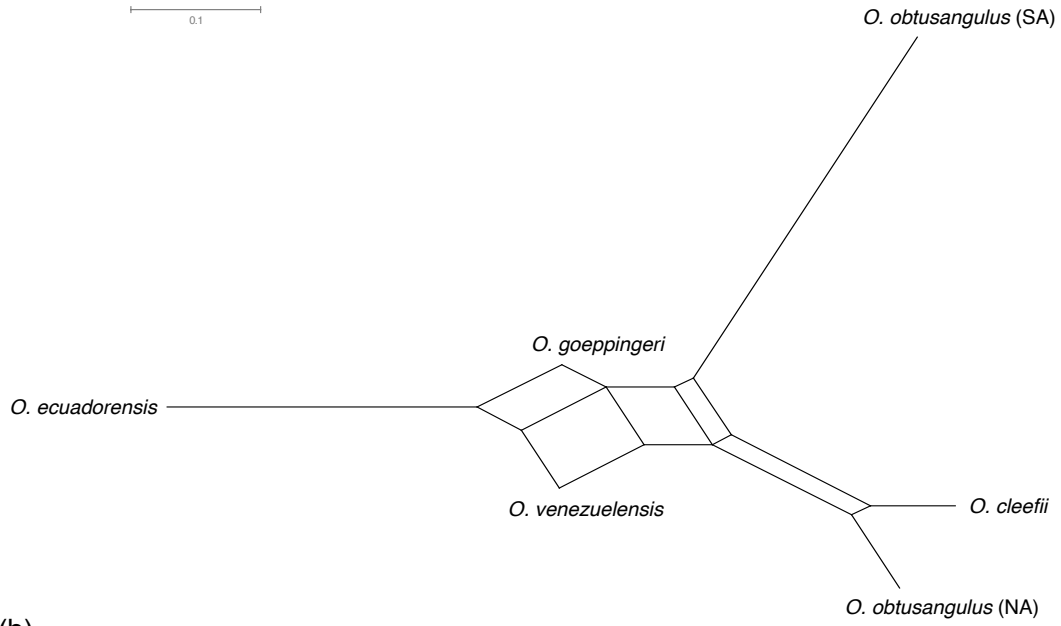

(b)

Figure 3.7. NeighborNet network showing genetic relatedness amongst the South American species of *Oreobolus* based on ITS F_{ST} pairwise values considering (a) *O. obtusangulus* as one species (b) *O. obtusangulus* as two species.

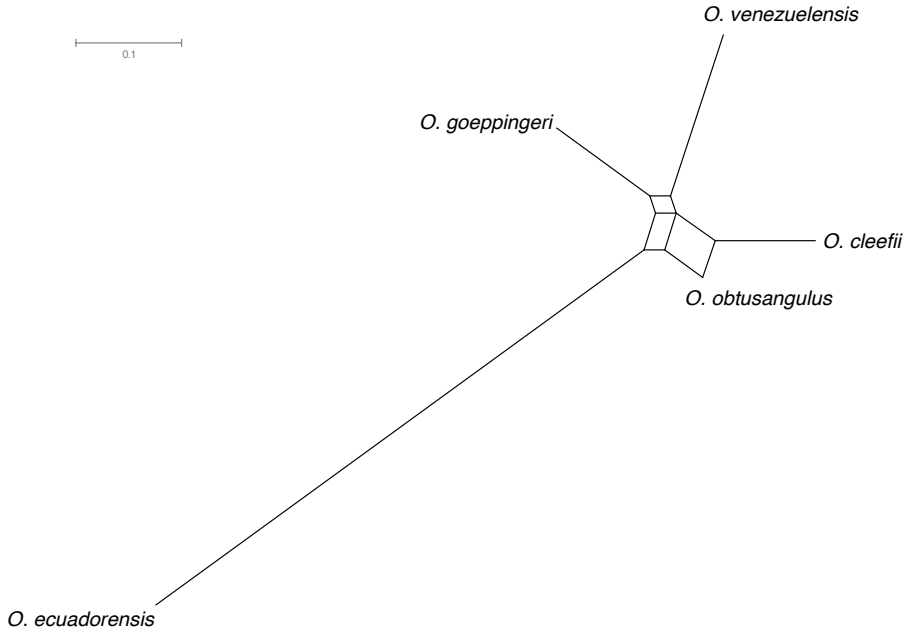

(a)

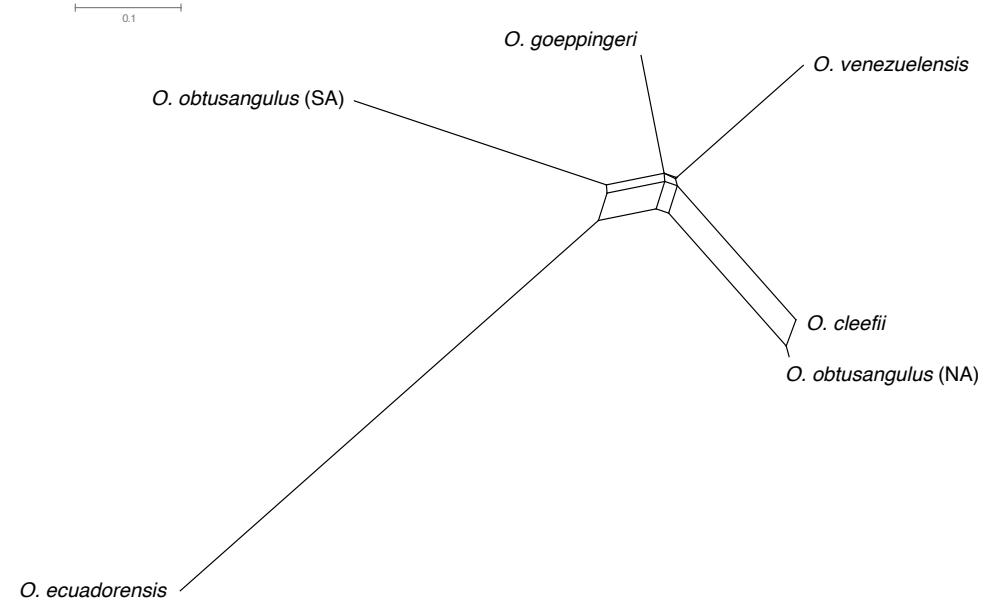

(b)

Figure 3.8. NeighborNet network showing genetic relatedness amongst the South American species of *Oreobolus* based on cpDNA (*trn*L-L-F, *trn*H-*psb*A and *rpl32*-*trn*L) F_{ST} pairwise values considering (a) *O. obtusangulus* as one species (b) *O. obtusangulus* as two species.

3.5. DISCUSSION

This is the first study to investigate the processes that might have shaped diversification both within and amongst species of Páramo plants. Furthermore, it provides insights into the phylogenetic and phylogeographic complexity of this system resulting from the interplay between contemporary topography, the Andean uplift and the glacial cycles of the Quaternary. The five South American species of *Oreobolus* presented complex relationships, with evidence of haplotype sharing. Moreover, there was evidence of phylogeographic patterns at a range of scales from continental to within northern and southern Andean clades, with significant F_{ST} values and SAMOVA results indicating these pattern were geographically defined. Several species also exhibited high levels of genetic diversity.

3.5.1. Species delimitation and relationships

The results obtained in this study reveal a complex evolutionary history for the five South American species of *Oreobolus*. Indeed, species relationships were difficult to estimate indicating either interspecific gene flow and/or shared ancestral polymorphisms (Naciri & Linder, 2015). Haplotype and nucleotide diversity were high for both ITS and cpDNA for all species except *O. ecuadorensis* (Table 3.9). Additionally, shared haplotypes were observed in both ITS (27%) and cpDNA (15%). This intricate history is also evident in the MST and NN networks for both ITS and cpDNA (Figs. 3.2 – 3.5 and 3.7 – 3.8) as well as in the low PP values recovered in the species tree (Fig. 3.6).

The high degree of complexity observed amongst these species, with shared haplotypes and poorly resolved phylogenetic relationships, contrasts with the morphological characters that distinguish them. Two possible but not mutually exclusive explanations could be put forward. Firstly, given the recent Pliocene diversification of both the northern and southern Andean clades of *Oreobolus* (Fig. 2.4 pages 54 – 55), lineage sorting may not have been fully completed. Alternatively, the species relationships may be obscured by ongoing gene flow.

The Páramo ecosystem is relatively young having appeared during the Pliocene c. 5 Ma (van der Hammen, 1974; van der Hammen & Cleef, 1986; Hooghiemstra et al., 2006; Graham, 2009). My results from Chapter Two indicated that the South American species of *Oreobolus* diverged within the same timeframe (Fig. 2.4 pages 54 – 55). Previous studies have indicated the importance of incomplete lineage sorting (ILS) in recently diverged groups particularly when effective population sizes are large (Maddison & Knowles, 2006; Jakob & Blattner, 2006; Degnan & Rosenberg, 2009; Cutter, 2013). Large populations are expected for *Oreobolus* given its rhizomatous herbaceous habit and wind-dispersed seeds that facilitate long-distance dispersal. Statistical genetic analyses provided additional evidence supporting ILS. Firstly, for both ITS and cpDNA a high percentage of haplotypes (73.3% and 85%, respectively) were species-specific. In particular, cpDNA better differentiated currently recognised taxonomic species than ITS for *O. ecuadorensis*, *O. goeppingeri* and *O. venezuelensis* (Figs. 3.2 – 3.5). Being haploid, plastid genes have a lower effective population size than nuclear genes and thus are expected to coalesce faster (Schaal & Olsen, 2000; Naciri & Linder, 2015). Additionally, four of the five species were recovered as monophyletic groups, with gene trees contained

within the species tree (Fig. 3.6). Likewise, genetic differentiation among species was high (Table 3.8) and F_{ST} values between all species pairs were significant for both ITS and cpDNA (Table 3.10a).

Ongoing gene flow impacting on the species relationships would be expected to result in heterozygosity in ITS and this was not observed. Furthermore, shared haplotypes were recovered in multiple pairs of individuals from all species suggestive of a stochastic process likely related to lineage sorting. Therefore, based on the recovered evidence, although gene flow cannot be ruled out, I suggest incomplete lineage sorting in a recently diversified group as the most likely explanation for the complex patterns observed in the South American species of *Oreobolus*. To the best of my knowledge there are no other phylogeographic studies of Páramo plants, making it impossible to compare the patterns observed in this study with previously published ones. Nevertheless, there are comparable studies in other parts of the world. For instance, a recent phylogeographic study of the Australian alpine *Poa* (Poaceae) describes a similar pattern of problematic recovery of species relationships associated with a putatively young ecosystem and a Pleistocene radiation following long-distance dispersal to Australia (Griffin & Hoffmann, 2014). This study also favoured ILS rather than ongoing gene flow as the likely process behind the observed pattern based on the widespread genetic similarity, recent divergence times and large effective population size.

Additional research would be required to more thoroughly distinguish between ILS and ongoing gene flow. Looking at additional markers may provide better resolution regarding species relationships. However, Griffin & Hoffmann (2014) showed that the addition of more informative markers added little extra information to the

resolution of the similarly complex phylogenies of Australian *Poa*. The potential for hybridisation could also be assessed using crossing experiments between *Oreobolus* species.

3.5.2. Genetic structure within species

High levels of genetic variation were found within species. For both nuclear and chloroplast regions, high levels of genetic diversity were better explained by intra-specific rather than inter-specific variation (ITS 69% and cpDNA 52%; Table 3.7). I discuss below results for each species.

3.5.2.1. Oreobolus obtusangulus

The data presented here indicate that the two subspecies of *O. obtusangulus* represent morphologically cryptic species. This further corroborates results from Chapter Two. Under the current taxonomy, this species showed the highest molecular diversity indices (Table 3.9), which is what you would expect for a polyphyletic species (Figs. 2.1 – 2.3, pages 45 – 50). Furthermore, its placement in the NN networks was not well resolved with conflicting signals for both ITS and cpDNA (Figs. 3.7a and 3.8a). However, when considered separately, both *O. obtusangulus* (SA) and *O. obtusangulus* (NA) were fully recovered as monophyletic in the species tree with PP=100% and PP=80%, respectively (Fig. 3.6). Moreover, *O. obtusangulus* (NA) was reconstructed as a derived taxon within the phylogeny, in contrast to *O. obtusangulus* (SA) which was recovered as sister to the northern Andean Clade. Additionally, *O. obtusangulus* (SA) was no more similar to its northern counterpart than to any other northern Andean species. This is evident in the

absence of shared haplotypes (Figs. 3.2 – 3.5) and the significant pairwise F_{ST} values obtained between *O. obtusangulus* (SA) and the rest of the species, including *O. obtusangulus* (NA) (Table 3.10b; Figs. 3.7b – 3.8b). Britton et al. (2014) have described another example of cryptic speciation within the Schoeneae in the South African species *Tetraria triangularis*. These authors found at least three lineages within the species that qualified as cryptic species based on their genetic distinctiveness and subtle morphological differentiation.

3.5.2.2. Oreobolus cleefii

Oreobolus cleefii and *O. obtusangulus* (NA) display a complicated relationship likely involving both hybridisation and ILS. Pairwise F_{ST} values between these species were significantly different for ITS but not for cpDNA (Table 3.10b). In this sense, one plastid haplotype (Hc2; Table 3.4) and two nuclear ones (Hn2 and Hn5; Table 3.3) are exclusively shared between these two species. Moreover, all individuals with shared haplotype Hc2 consistently have shared haplotypes Hn2 or Hn5. The position of Hc2 in the NN and MST networks is of particular interest, being grouped with private haplotypes of both *O. cleefii* and *O. obtusangulus* (Figs. 3.4 – 3.5). The aforementioned could be indicative of a pattern of hybridisation, probably due to chloroplast capture, and simultaneous nuclear introgression. Hybridisation is more likely to happen in closely related taxa (Abbott et al., 2013) and in this case both species were well recovered in the species tree as sister species (PP=80%; Fig. 3.6). The latter also supports the relevance of ILS in the divergence of these two species. Furthermore, they occur in sympatry (Fig. 1.6 page 21) and show an overlap in morphological characters (Seberg, 1988). Indeed, Seberg (1988)

suggested that *O. cleefii* should be reduced to synonymy under *O. obtusangulus unispicus*, the northern Andean subspecies of *O. obtusangulus*, based on the extensive overlap of specimens. Hybridisation is a frequent phenomenon in plants (Arnold, 1997) and in Cyperaceae it has been shown to be an important mechanism in shaping the population genetic structure of *Carex* (e.g. Escudero et al., 2014). Specifically, a study involving two co-occurring sister species of *Carex*, *C. monostachya* and *C. runssoroensis*, from a similar tropical alpine ecosystem in East Africa showed strong signals of hybridisation for these taxa (Gizaw et al., 2016). The authors suggested that following divergence, secondary contact zones likely formed from long-distance dispersal events. Subsequently, at least one of these zones could have led to interspecific hybridisation (Gizaw et al., 2016). The results presented here are consistent with a similar scenario. Populations of *O. cleefii* and *O. obtusangulus* (NA) may have come into secondary contact following isolation during interglacial periods in the Quaternary (van der Hammen, 1974). Afterwards, some of these sympatric populations may have hybridised.

3.5.2.3. Oreobolus ecuadorensis

Oreobolus ecuadorensis is one of the most geographically restricted species, distributed only in Ecuador and northern Peru (Fig. 1.6 page 21). This species showed the lowest haplotype and nucleotide diversities for both ITS and cpDNA indicating the presence of a few haplotypes with low divergence amongst them (Table 3.9). This pattern is evident in the MST for both ITS and cpDNA (Figs 3.2 and 3.4) where the species' geographically widespread and common haplotypes occupy a central position (ITS, Hn3; cpDNA, Hc6) with connections to localised and

less abundant haplotypes (ITS, Hn6, Hn7, Hn8; cpDNA, Hc5, Hc7, Hc8, Hc9). These findings are consistent with a scenario of a severe bottleneck followed by a population expansion likely imposed by the glacial cycles of the Quaternary (Templeton, 1998; Hewitt, 2004). Ecuador and Peru have the highest percentage of permanent snow and therefore interglacial periods may have greatly reduced the size of the populations of *O. ecuadorensis,* reducing the species' genetic diversity. Following the Last Glacial Maximum (LGM), population expansion may have occurred with new mutations likely accumulating as the species occupied new areas. New haplotypes were thereby produced, diverging from the founder population by only a few nucleotides. At the same time, the strong impact of interglacial periods is evident in the clear differentiation of *O. ecuadorensis* from the rest of the species (Table 3.10, Figs. 3.7 and 3.8). Indeed, during interglacial periods, isolation likely promoted allopatric speciation.

3.5.2.4. Oreobolus goeppingeri and O. venezuelensis

The two most widespread species in the Páramo, *O. goeppingeri* and *O. venezuelensis* (Fig. 1.6 page 21), also present the most complicated genetic patterns. Both species show high levels of molecular diversity, as would be expected from widespread taxa (Table 3.9) but their placement in the species tree is poorly resolved (PP=39%, Fig. 3.6). Additionally, they both share haplotypes with other northern Andean species (Figs. 3.3 and 3.5) and their placement in the species NN networks shows a conflicting signal (Figs. 3.7 – 3.8). This pattern may suggest that both species have retained ancestral haplotypes. Similar patterns have been observed in the New World species of the grass genus *Hordeum* (Jakob & Blattner, 2006). This

group of recently divergent species (c. 4 Ma) showed multiple plastid haplotypes shared between species as well as high genetic diversity indices. The authors suggest that a likely explanation could be large effective population sizes that would allow for the persistence of all haplotypes. This may also be an explanation for the observed pattern in *O. goeppingeri* and *O. venezuelensis*. Further evidence could be given by the estimation of divergence dates between haplotypes. This will allow for a better assessment of haplotype relationships and the possible ancestry of some of the haplotypes recovered in *O. goeppingeri* and *O. venezuelensis*. An alternative explanation is that the widespread nature of these species provided greater opportunities for mixing with each other, and other species, compared with those with more restricted ranges, which exhibit a similar pattern of haplotype sharing, albeit on a smaller scale (Figs. 3.3 and 3.5).

Likewise, it should be noted that these species also show some evidence of phylogeographic structure. For instance, *O. venezuelensis* exhibits two distinct haplotype groups, with no plastid haplotypes shared between the southern grouping of H+I, and all other clusters of this species (but see Biogeography section for further discussion) (Fig. 3.4). These patterns of divergent haplotype groups combined with haplotype sharing likely impacted on the low resolution in the species tree (Fig. 3.6).

3.5.3. Biogeography

Overall there is evidence of phylogeographic patterns in *Oreobolus* species. At the continental scale, haplotypes are geographically clustered, as evidenced by the MST and NN networks for both ITS and cpDNA (Figs. 3.2 – 3.5). Significant phylogeographic structure was also suggested by a higher value of N_{ST} compared to

G_{ST} ($p < 0.01$), indicating that haplotypes in the same cluster are on average more closely related than distinct haplotypes from different clusters. This genetic structure could be separated into three spatially defined groups ($F_{CT} = 0.60$, Table 3.7). For ITS, these groups separated clusters A to J (group I), K, L and N (group II), and M (group III) while for cpDNA groups were separated as follows, A to K (group I), L and N (group II), and M (group III) (Figs. 3.2 and 3.4). F_{ST} values also indicate geographical structure, with southern Andean clusters L and M significantly different from all northern Andean clusters (Table 3.6). In general, there appears to be a pattern of geographic congruence with F_{ST} values differing as geographic distance increases. This may be the result of isolation by distance or the presence of barriers to gene flow between NAC and SAC. As discussed in Chapter Two, the arid central Andes likely impose a strong barrier to dispersal and thus to gene flow. The results presented here further support this (but see below for discussion on possible long distance dispersal between NAC and SAC).

The clearest phylogeographic break apparent in *Oreobolus* is between the northern Andes (NA) haplotypes and southern Andes (SA) haplotypes. This pattern is evident in both chloroplast and nuclear regions, although the pattern is much stronger in cpDNA compared with ITS (Figs. 3.2 – 3.5). However, the exact position of this break is unclear. SAMOVA groups clearly identify the NA/SA disjunction in ITS but not in the plastid region where cluster K is grouped with the northern Andean clusters (Table 3.5; Figs. 3.2 and 3.4). The latter is also evident in the cpDNA NN where the distance between haplotypes is shorter than in the NN for ITS (Figs. 3.3 and 3.5). The incongruence between ITS and plastid regions could suggest this population is the result of mixing between the SAC and NAC resulting from long

distance dispersal events. Cluster K is separated from both NA clusters and other SA clusters by a substantial distance and possesses unique haplotypes at both ITS and plastid regions (Table 3.3 – 3.4). Nonetheless, further work investigating additional markers (e.g. microsatellite markers) would be required to assess the origin of this population and potential hybridisation.

3.5.3.1. Northern Andes

Additional structure is evident at regional scales within the NAC. This appears to be associated with putative geographic barriers to gene flow. Clusters B and J were significantly differentiated from all other sites, regardless of the geographic distances. Both clusters show F_{ST} values indicating a significant difference from other NA clusters for ITS while in cpDNA, F_{ST} values indicate a significant difference from most NA clusters (Table 3.6). These two clusters are separated from all other NA clusters by inter-Andean valleys of seasonally dry tropical forest. Cluster B is isolated from the rest by the dry Chicamocha Canyon while cluster J is separated from the other NA clusters by the Marañón Valley. Särkinen et al. (2012) suggested that biome heterogeneity across the Andes represented a strong barrier to dispersal within island-like ecosystems. This is particularly relevant when deep valleys section the mountain ranges as in this case. In addition, clusters H and I present ITS haplotypes distinct from the rest within their species, namely *O. venezuelensis* (Hn28 and Hn30) and *O. goeppingeri* (Hn12 and Hn14) (Figs. 3.2 – 3.3). These haplotypes are distributed in the southernmost part of these species' distribution and their differentiation from species-specific haplotypes distributed in

the northernmost areas further supports the observed phylogeographic structure and possible pattern of isolation by distance.

The dated phylogeny presented in Chapter Two (Fig. 2.4, pages 54 – 55), proposed that the most recent common ancestor of the South American *Oreobolus* may have diverged 4.76 Ma (95% HPD [2.79 – 7.47] Ma) during the late Miocene – early Pliocene. Subsequently, the southern Andean clade (SAC) and northern Andean clade (NAC) appear to have diverged during the late Pliocene, at 2.80 Ma (95% HPD [1.37 – 4.71] Ma) and 3.07 Ma (95% HPD [1.80 – 4.79] Ma) respectively. The NAC has diversified within the last two million years, during the Pleistocene. This suggests the expansion and contraction of Páramo islands during the glacial cycles of the Quaternary may have played a role in diversification (van der Hammen, 1974; Simpson, 1975; van der Hammen & Cleef, 1986; Hooghiemstra & van der Hammen, 2004). High levels of molecular diversity for both nuclear and plastid regions as well as the high number of unsampled cpDNA haplotypes apparent in my dataset are concordant with this scenario (Table 3.5, Fig. 3.4). Furthermore, variation amongst NA clusters was moderate and mostly explained by within cluster variation (ITS, 86%; cpDNA, 79%; Table 3.8). Vicariance events would allow for differentiation of populations and diversification, through selection and drift. If reproductive isolation is incomplete, subsequent expansion events may result in secondary contact and gene flow amongst nearby populations. Repeated vicariance and secondary contact, which would be expected from Quaternary glacial cycles, would generate complex phylogeographic patterns, with species sharing haplotypes. Such patterns are evident in *Oreobolus*, with a few widespread haplotypes amongst species apparently giving rise to geographically restricted haplotypes (Fig 3.2 and 3.4). Similar patterns have

been reported for the afro-alpine populations of *Arabis alpina* (Assefa et al., 2007). These authors suggest that several cycles of range contraction and expansion caused by the glacial cycles of the Quaternary may have shaped the distribution of genetic diversity observed in that species.

3.5.3.2. Southern Andes

SAMOVA analyses for both ITS and cpDNA, assigned cluster M as a divergent genetic group (Figs. 3.2 and 3.4). Molecular diversity indices for this cluster showed low haplotype diversity and high nucleotide diversity in ITS, and high haplotype diversity and low nucleotide diversity in cpDNA (Table 3.5). A possible explanation for this pattern might be that these populations underwent a bottleneck during isolation resulting in a low number of divergent haplotypes. During the glacial cycles of the Quaternary ice sheets covered extensive areas and generated massive fragmentation and restriction in the distribution of southern Andean plants producing pockets of refugial populations (e.g. Markgraf et al., 1995). Although a scenario of Pleistocene refugia has already been proposed for other southern Andean plants (e.g. *Hypochaeris incana*, Tremetsberger et al., 2009) further work would be required to assess the potential for refugial populations in *O. obtusangulus* (SA).

It is also worth noting that the absence of shared haplotypes between *O. obtusangulus* (SA) and the other four species (including its northern counterpart), the recent divergence of both the northern and southern Andean clades of *Oreobolus* as well as the fact that *O. obtusangulus* (NA) is not recovered as sister to the rest of the Páramo species strongly suggest that the likelihood of a south to north colonisation of *Oreobolus* is minimal.

The high levels of variation contained within clusters could be the result of not discriminating by species. This may mask some phylogeographic patterns within the species, and additional sampling would be required to assess the detailed phylogeographic patterns within each species. That said, the simultaneous assessment of all *Oreobolus* species, as I have employed here is critical to the identification (and accurate interpretation) of the numerous shared haplotypes found in the South American species of *Oreobolus*. The latter suggests potential hybridisation and recent speciation, which would confound patterns if each species was considered independently.

3.6. CONCLUSION

The present study is a contribution to the understanding of the historical assembly of the Páramo flora. It is the first to explore genetic relationships below the species level in a group of closely related and recently divergent species. I aimed to assess the genetic relationships between and within the South American species of *Oreobolus* as well as investigate the impact of the Quaternary ice cycles on the shaping of these populations. Based on the high percentage of private haplotypes, significantly different pairwise F_{ST} values between species, lack of heterozygosity in ITS and recent divergence times, I believe incomplete lineage sorting has played a major role in the diversification of the South American species of *Oreobolus*. However hybridisation cannot be discounted, as many of these species are sympatric. In particular, *O. cleefii* and *O. obtusangulus* (NA) are excellent candidates to further explore this. In relation to the Quaternary biogeography of these species, the role in

diversification of the contraction and expansion of Páramo islands during glacial cycles is for the first time supported by genetic data. Additional work incorporating more extensive sampling of individuals and assessing additional genetic data will be required to estimate patterns of historical demography, which could bring further insight into the population dynamics of Páramo plants.

CHAPTER FOUR. SPECIES POOR LINEAGES IN THE PÁRAMO ECOSYSTEM, A BIODIVERSITY HOTSPOT

4.1 ABSTRACT

A dated phylogeny using DNA sequence data was used to investigate the phylogenetic position and biogeography of Páramo species of Melastomeae. Páramo was colonised multiple times by different lineages of Melastomeae. Colonisation also occurred in different time frames with species poor lineages colonising from the mid-Miocene. Low levels of variability in chosen sequences meant that relationships amongst populations within *Castratella*, a genus with only one or two species, were poorly resolved. The low number of species in *Castratella* may have resulted from lower diversification or higher extinction rates. Castratella diverged from its nearest ancestor in the mid-Miocene but only appears to have diversified in the Páramo in the Pleistocene. *Castratella* may have persisted at lower altitudes until it dispersed to the Páramo more recently, and subsequently went extinct at lower altitudes. I also argue that effective seed dispersal may have maintained enough gene flow to prevent the reproductive isolation that would have resulted in speciation in the Páramo.

Lineages of temperate or tropical origin contributed equal numbers of species to the Páramo flora. Although the frost-resistance mechanism of temperate lineages might have played a role in their successful diversification at higher altitudes, the results

presented here cannot confirm this mechanism gave them a competitive advantage over tropical elements.

4.2 INTRODUCTION

The question of why some lineages are species rich and others are species poor has been a long-standing one in biodiversity research. Possible causes of species rich lineages might be related to changes in diversification rates across the tree of life associated with key geological events (e.g. *Inga*, Richardson et al., 2001), ecological shifts (e.g. *Lupinus*, Hughes & Eastwood, 2006; Drummond et al., 2012) or key morphological innovations (e.g. *Aquilegia*, Hodges & Arnold, 1994). Another possible explanation is the age of the clades, with older ones having had more time to accumulate more species (McPeek & Brown, 2007; Rabosky et al., 2012). Conversely, species poor lineages may result from higher extinction rates, a hypothesis particularly difficult to test due to the incompleteness of the fossil record (Magallón & Sanderson, 2001; Rabosky & Lovette, 2008; Donoghue & Sanderson, 2015). Alternatively, it could be the result of taxonomic delimitation with more (or fewer) species described than there actually exist (Scotland & Sanderson, 2004).

Such a debate is particularly relevant when species poor lineages occupy geologically young ecosystems (i.e. ecosystems formed from recent mountain orogeny) that were readily available for colonisation from geographically local lineages but were widely colonised by immigrants arriving from greater distances. This is the case of the Páramo, a young ecosystem that appeared following the final uplift of the northern section of the Andes Mountain Range during the Pliocene, from

c. 5 Ma and to which many lineages have arrived from distant, temperate biomes (van der Hammen, 1974; van der Hammen & Cleef, 1986; Hooghiemstra et al., 2006; Graham, 2009; Sklenář et al., 2011).

The Páramo occupies an area of 35000 km^2 and is distributed in a series of sky islands with c. 4000 plant species of which 60% are endemic (Luteyn, 1999; Buytaert et al., 2010). Because of its recent origin and massive diversity, it has been proposed that net speciation rates might have been exceptionally high, a hypothesis tested by Madriñán et al. (2013). These authors indicated that Páramo lineages had a speciation rate higher than any other biodiversity hotspot on earth.

However, the Páramo ecosystem imposes huge constraints on its biota. Because of its altitudinal range (above 3000 m.a.s.l.), frost is common and temperature fluctuates daily from freezing up to 25ºC (Sarmiento, 1986). This temperate-like environment may have contributed to some level of ecological filtering on lowland Neotropical taxa colonising and diversifying in the highlands (Donoghue, 2008). These taxa may have had to overcome intense physiological boundaries, in particular frost, in order to colonise upland areas successfully. Conversely, immigrants from temperate regions may have found similar conditions to those they were already adapted to, giving them a competitive advantage and enhancing the possibility of their diversification (van der Hammen & Cleef, 1986; Simpson & Todzia, 1990; Donoghue, 2008). The palaeopalynological record and previous floristic studies have estimated that approximately 50% of Páramo species have a likely temperate origin while the other 50% are of likely tropical origin (van der Hammen & Cleef, 1986; Sklenář et al., 2011). The high proportion of temperate elements in the Páramo flora may have arrived via suitable dispersal corridors (i.e. Isthmus of Panama) or may

have had to colonise following long-distance dispersal events (e.g. *Oreobolus*) (Simpson & Todzia, 1990; Donoghue, 2008; Sklenář et al., 2011).

The relative contributions of tropical and temperate lineages to species numbers in the Páramo will also depend on speciation rates within the ecosystem, and in particular, whether tropical lineages entering the Páramo have undergone less subsequent diversification (or higher extinction) than did temperate ones. If temperate taxa diversified more, a higher number of species would be expected compared to tropical ones. Furthermore, given that tropical taxa had to adapt to new conditions as the altitude increased while temperate taxa likely migrated through or from similar temperate-like environments, a relationship between species richness, geographic origin and altitude might also be expected. In this case, temperate taxa would be more species-rich at higher altitudes than tropical ones. The latter might be influenced by the frost-resistance mechanism adopted by Páramo plants. Sklenář et al. (2012) tested the hypothesis that Páramo plants will adopt different mechanisms according to their geographic origin. These authors found that plants with a north temperate origin mostly tolerated freezing by formation of extracellular ice while plants with tropical and south temperate origin avoided freezing by supercooling, i.e. preventing the formation of ice at temperatures below freezing point. However, the latter provides a solution for a short period of moderate frost but would be an inadequate mechanism against severe or permanent subfreezing temperatures (Beck, 1994). In that sense, freezing tolerance would provide a better solution to extreme cold and therefore might promote colonisation of higher altitudes by plants with a north temperate origin.

The Melastomeae tribe of the largely tropical family Melastomataceae is an ideal model group to approach some of these questions. With >870 species in 47 genera, the vast majority of species are in South America (c. 570 species in 30 genera) with the rest distributed in the Palaeotropics (Renner, 1993; Michelangeli et al., 2013). Furthermore, the Neotropical species occupy a wide variety of habitats from lowland forest to the high-altitude Páramo ecosystem, with the greatest number of species in the lowlands (Michelangeli et al., 2013). Additionally, there is a huge disparity in terms of species richness within the 30 Neotropical genera. On one hand the mostly lowland genus *Tibouchina* Aubl. has 241 species while endemic or near-endemic Páramo genera such as *Castratella* Naudin and *Bucquetia* DC. have two and three species, respectively (Luteyn, 1999; Michelangeli et al., 2013).

Castratella is of particular interest. One of the few endemic Páramo genera, it is confined to the páramos in the Eastern Cordillera of Colombia and Venezuela. Furthermore, *Castratella* has a herbaceous habit contrary to the bushy habit of the rest of the Páramo species within the tribe and the family (Sklenář et al., 2005). Although it has two species, *C. piloselloides* and *C. rosea*, the latter is only known from the type specimen plus some few additional collections and its validity as a species has been questioned (F. Michelangeli, *pers. comm.*). Little is known about the ploidy level and chromosome numbers in *Castratella*, however previous studies have shown that haploid numbers of $n = 9$, 10, 11 and 12 are common in the tribe as are dysploid or polyploid derivatives of these numbers (Solt & Wurdack, 1980; Almeda & Chuang, 1992). The question of why *Castratella* has so few species in comparison to most Páramo genera is of great interest. Information on the timing of

the evolution of this genus could provide insights into explaining why it has so few species.

In order to reconstruct diversification histories, dated molecular phylogenies can be used to estimate the timing of particular events. The current study investigates the impact of the Andes orogeny on the diversification history of the Páramo species of the largely Neotropical Melastomeae tribe. Specifically the aims of this study are 1) to re-assess the phylogeny of the tribe under a Bayesian framework in order to re-evaluate the phylogenetic position of the endemic Páramo genera *Castratella* and *Bucquetia*, as well as of the Páramo species within *Brachyotum*, *Chaetolepis*, *Monochaetum* and *Tibouchina*; 2) to estimate dates of divergence in Páramo species of Melastomeae; 3) to infer the phylogenetic and genealogical relationships within *Castratella piloselloides*; 4) to explore species richness patterns for the complete Páramo flora to assess if there is a relationship between species richness of Páramo clades and their geographic origin (temperate versus tropical), and if there is a relationship between geographic origin and altitudinal distribution (tropical elements may tend to occupy lower altitudes).

4.3 METHODS

4.3.1 Species sampling

To determine the phylogenetic framework of the Páramo taxa within Melastomeae, the dataset from Michelangeli et al. (2013) was re-analysed under Bayesian Inference. Their dataset includes 239 taxa sequenced for the nuclear ribosomal DNA internal transcribed spacers (ITS) and the plastid regions *acc*D-*psa*I and *psb*K-*psb*L.

This extensive sampling of the Melastomeae tribe (217 species) includes samples from Páramo species within *Castratella*, *Bucquetia*, *Brachyotum*, *Chaetolepis*, *Monochaetum* and *Tibouchina*. It also includes a comprehensive set of species from the tribes Microlicieae, Rhexieae, Miconieae and Merianieae that were incorporated as outgroups, allowing the use of calibration points using fossils.

To estimate the phylogenetic and genealogical relationships within the endemic Páramo species *Castratella piloselloides*, extensive sampling was undertaken across its entire distribution range). A total of 120 samples from eight populations were obtained from field collections (Table 4.1 and Fig. 4.1). From each population, two to ten fresh leaf samples were collected, and their location was recorded using a handheld GPS. Additionally, one sample of *Castratella rosea* was obtained from the Utrecht Herbarium (U) of the National Herbarium of the Netherlands. Populations were numbered 1 to 8 in a north to south direction. Additionally, samples of *Bucquetia glutinosa* also collected in Colombia and herbarium samples of *Chaetolepis cufodontisii*, *C. lindeniana* and *C. microphylla* obtained from the New York Botanical Garden (NY) were included as outgroups. Table S4.1 presents the complete list of samples used in this study (Supplementary Information, pages 225 – 238).

Table 4.1. Geographic coordinates of the populations sampled.

Nº	POPULATION NAME	LATITUDE	LONGITUDE
1	COCUY	6.41211667	-72.33128333
2	LA RUSIA	5.93951667	-73.07583333
3	IGUAQUE	5.68610000	-73.44773333
4	TOTA-BIJAGUAL	5.48143333	-72.85540000
5	RABANAL	5.40818333	-73.54915000
6	GUERRERO	5.22618333	-74.01788333
7	CHINGAZA	4.52848333	-73.75866667
8	SUMAPAZ	4.28958333	-74.20781667

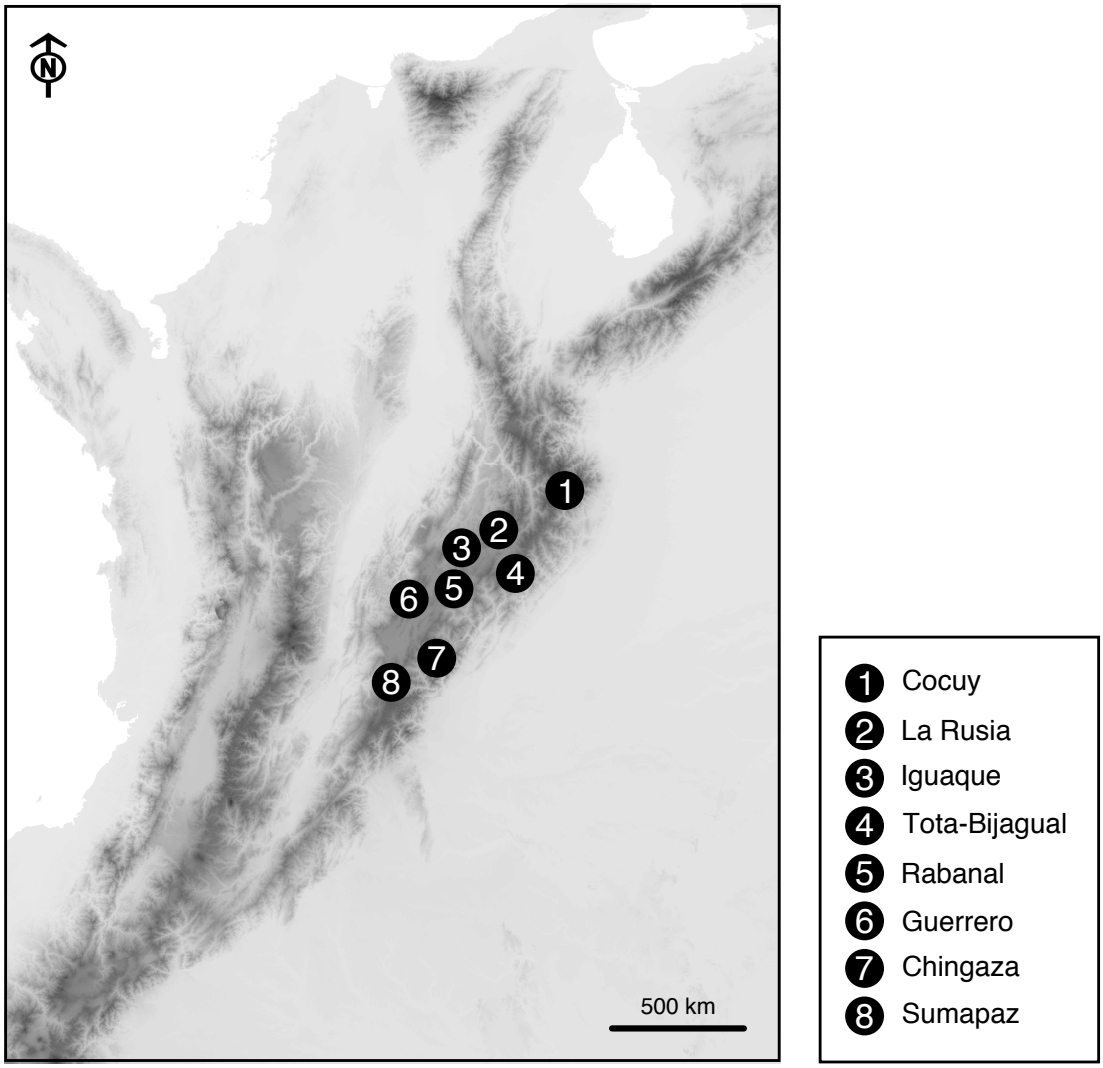

Figure 4.1. Map of the populations of *Castratella piloselloides* sampled.

4.3.2 DNA extraction, amplification and sequencing

Both silica-dried fresh leaf samples and herbarium material were pulverised using a Mixer Mill (Retsch, Haan, Germany). Total DNA from all samples was isolated following a modified protocol of the DNeasy® Plant Mini Kit (QIAGEN, Manchester, UK), which involved adding 30 µl of Proteinase K (Invitrogen™, Fisher Scientific, Loughborough, UK) plus 30 µl of ß-mercaptoethanol per extraction along with the lysis buffer (AP1), allowing for an incubation of 24 hours at 42ºC, with gentle rocking. This modified protocol has been shown to increase DNA quality and yield in Melastomataceae (Michelangeli et al., 2008; 2013). In order to include my *C. piloselloides* samples into the dataset of Michelangeli et al. (2013), the ITS and plastid regions *acc*D-*psa*I and *psb*K-*psb*L were amplified and sequenced as detailed in Chapter Two (page 36) using primers ITS5P/ITS8P (Möller & Cronk, 1997), accD/psaI-75R (Shaw et al., 2007) and psbK/psbL (Reginato et al., 2010), respectively. Additionally, to estimate genealogical relationships within *C. piloselloides*, the plastid regions *rpl32-trn*L and *trn*G were amplified and sequenced using primer pairs trnL$^{(UAG)}$/rpl32-F and trnG$^{(UUC)}$/trnG2G, respectively (Shaw et al., 2005; 2007). Similarly, the nuclear ribosomal external transcribed spacer (ETS) was amplified and sequenced with forward primer ETS-Mel specific to Melastomataceae (F. Michelangeli, *unp.*) and reverse primer 18S (Starr et al., 2003). All PCR reactions were performed as described in Chapter Two (page 36). The amplification cycle for all chloroplast regions consisted of 2 min at 94°C, followed by 30 cycles of 1 min at 94°C, 1 min at 52°C and 1 min at 72°C, finalising with 7 min at 72°C. For ITS and ETS, the amplification cycle consisted of 3 min at 94°C, followed by 30 cycles of 1

min at 94°C, 1 min at 55°C and 90 sec at 72°C, finalising with 5 min at 72°C. PCR products were purified and sequenced as reported in Chapter Two (page 36).

4.3.3 Matrix assembly and sequence alignment

Contigs of forward and reverse sequences were assembled in Sequencher version 5.2 (Gene Codes Corporation, Ann Arbor, Michigan, USA). Sequences from ITS, *acc*D-*psa*I and *psb*K-*psb*L were aligned with the dataset of Michelangeli et al. (2013) on Muscle v3.7 (Edgar, 2004) and then visually checked using Mesquite v2.75 (Maddison & Maddison, 2014). Sequences from ETS, *trn*G and *rpl32*-*trn*L were manually aligned using Mesquite v2.75 (Maddison & Maddison, 2014).

4.3.4 Phylogeny reconstruction

Evolutionary model testing was performed for each gene region using jModelTest 2.1.6 (Guindon & Gascuel, 2003; Darriba et al., 2012) with default settings. Based on the Bayesian Information Criterion (BIC, Schwarz, 1978), the best-fitting models were: GTR+I+Γ (ITS), TVM+Γ (*acc*D-*psa*I and *psb*K-*psb*L), TPM2uf+Γ (ETS) and TPM1uf (*trn*G and *rpl32*-*trn*L).

Phylogenies for each region were reconstructed using Bayesian Inference (BI) with MrBayes v. 3.2.2 (Ronquist et al., 2012) run on the CIPRES Science Gateway v.3.3 (Miller et al., 2010). For the Melastomeae datasets (ITS, *acc*D-*psa*I and *psb*K-*psb*L), four independent runs of 30,000,000 generations were performed, with three hot chains and one cold chain at a temperature of 0.1, sampling 10^4 parameter estimates in each run. For the *C. piloselloides* datasets (ETS, *trn*G and *rpl32*-*trn*L), four independent runs of 10,000,000 generations were performed with three hot chains

and one cold chain at a temperature of 0.1, sampling 10^4 parameter estimates in each run. Appropriate mixing, parameter and topological convergence were assessed with Tracer v1.6.0 (Rambaut et al., 2013). For each dataset, 75% of the samples from each run were discarded as burn-in and a maximum clade credibility (MCC) tree from the combined 10,000 trees was annotated with posterior probability support values (PP), median heights and 95% highest posterior density (HPD) values using TreeAnnotator v2.1.2 (Rambaut & Drummond, 2015). Annotated trees were visualised and exported as graphics using FigTree v1.4.2 (Rambaut, 2014). Posterior probability (PP) support values of above 90% are considered to be high, 60% to 90% to be good and below 60% to be poor.

Statistical assessment of topological congruence between phylogenetic trees (i.e. incongruence length difference test – ILD) has been rejected as an unbiased measure of phylogenetic congruence and combinability (e.g. Darlu & Lecointre, 2002; Barker & Lutzoni, 2002; Ramírez, 2006). Consequently, congruence between the chloroplast and nuclear tree topologies was visually assessed for each dataset, which revealed no strongly supported conflict in both cases. Two concatenated matrices were then produced and partitioned by gene. BI analyses were performed as described in the previous paragraphs.

4.3.5 Divergence time estimation

To estimate dates of divergence in Páramo species of Melastomeae, BEAST v2.1.3 (Bouckaert et al., 2014) was used on the combined Melastomeae dataset (ITS, *acc*D-*psa*I and *psb*K-*psb*L). The data were partitioned as for the Bayesian analyses and each partition was analysed under a GTR model with a gamma distribution with four

rate categories which is the minimum number to get a good approximation of the continuous function (Yang, 1994). The model of lineage-specific substitution rate variation was set as an uncorrelated lognormal relaxed clock model with estimated clock rates and a mean with an exponential prior distribution where the mean equals 10. The diversification model was set to a birth death model (Gernhard, 2008), an appropriate model to infer divergence times between species (Drummond & Bouckaert, 2015). Miconieae + Merianieae were constrained to be monophyletic as was recovered in the phylogeny presented in this study as well as by Michelangeli et al. (2013). Their crown node was calibrated with the oldest Melastomataceae fossil leaves from the Early Eocene of North Dakota (Hickey, 1977), which have been described as resembling the extant species of Miconieae and Merianieae (Hickey, 1977; Renner & Meyer, 2001). A prior with a lognormal distribution was set with a mean (μ) of 7 Ma, a standard deviation (σ) of 0.54 and a minimum bound for the highest posterior density distribution of 41.3 Ma. The standard deviation was set to 0.54 yielding a 95% highest posterior density (HPD) between 41.3 and 56 Ma that corresponds to the upper age limit of the Eocene and the lower age limit of the Early Eocene (Cohen et al., 2013 updated). The tribe Microlicieae was constrained to be monophyletic and a prior with a normal distribution was set at its crown node defined by μ=16 Ma, σ=0.6 Ma and a minimum bound for the highest posterior density distribution of 9.0 Ma. The age and 95% HPD correspond to that estimated by Renner (2004) for the crown node of the Microlicieae from a dated phylogeny of the Melastomataceae, calibrated with four fossils. Similarly, Rhexieae was constrained to be monophyletic and fossil seeds from the Early Miocene (23 to 26 Ma) across Europe (Dorofeev, 1960; 1963; 1988; Collinson & Pingen, 1992; Dyjor

et al., 1992; Fairon-Demaret, 1996; Mai, 2000) were used to set a lognormal distribution on its crown node with μ= 4 Ma, σ=0.81 Ma and a minimum bound for the highest posterior density distribution of 23 Ma. These fossil seeds have been identified to have a type of testa ornamentation synapomorphic for Rhexieae with a cochleate shape and multicellular tubercles (Renner & Meyer, 2001; Renner et al., 2001; Michelangeli et al., 2013). A normal distribution was used for Microlicieae because it is the most appropriate for secondary calibrations (Ho & Phillips, 2009). This type of distribution locates most of the probability density around the mean and allows for symmetrical decrease towards the tails accounting for the age error (Ho & Phillips, 2009). In contrast, a lognormal distribution is the most appropriate for a fossil calibration (Ho & Phillips, 2009). In this case, the fossil sets a hard minimum bound to the distribution with its highest probability density older than the fossil (Ho & Phillips, 2009). This calibration strategy biases in favour of an older age estimate that is recommended as fossils represent minimum age estimates as they were likely to have formed after the evolution of the clade that they represent. The remaining priors were left at their default settings.

Twelve independent MCMC runs of 25 x 10^6 generations each, sampling every 2500 were performed. Adequate mixing and convergence were assessed using Tracer v1.6.0 (Rambaut et al., 2013). Ten percent of the samples from each run were discarded as burn-in, and a MCC tree from the combined tree sets was annotated with median heights and 95% HPD node ages on TreeAnnotator v2.1.2 (Rambaut & Drummond, 2015).

4.3.6 Haplotype definition and network

Haplotypes were identified independently for the nuclear ribosomal region (ETS) and the concatenated plastid regions (*trn*G and *rpl32-trn*L) in Microsoft Excel (Microsoft Corporation, Washington DC, USA) using the Chloroplast PCR-RFLP Excel macro (French, 2003). For the concatenated plastid regions, only samples successfully sequenced for both regions were considered (Table S4.1). Haplotype connection lengths were calculated using Arlequin ver3.5 (Excoffier & Lischer, 2010) and a minimum-spanning tree was produced in Hapstar v0.5 (Teacher & Griffiths, 2011).

4.3.7 Species richness, geographic origin and altitudinal distribution

To assess if there is a relationship between species richness of Páramo clades and their geographic origin, as well as between geographic origin and altitudinal distribution for the complete Páramo flora, generic composition of the Páramo flora and their geographic origin was compiled from Sklenář et al. (2011). This included 380 genera within six geographic categories: (1) tropical: Páramo endemic, Neotropical, Pantropical and (2) temperate: Austral-Antarctic, Holarctic, Pantemperate. Information about number of species per genus in the Páramo and maximum altitudinal distribution in the Páramo was obtained from Luteyn (1999). The altitudinal categories were Subpáramo (2800 – 3500 m.a.s.l.), Páramo (3500 – 4400 m.a.s.l) and Superpáramo (4400 – 5000 m.a.s.l.). Table S4.2 (Supplementary Information, page 239) summarises the tabulated data. Boxplots of species richness versus geographic origin and species richness versus maximum altitudinal distribution were generated in R version 3.2.3 (R Core Team, 2015). In addition,

Kruskal-Wallis and Conover-Inman (Conover, 1999) tests were used to assess statistical differences between the different groups.

4.4 RESULTS

4.4.1 Matrix details

A total of 18 ITS, 22 ETS, 14 *acc*D-*psa*I, 16 *psb*K-*psb*L, 21 *rpl32*-*trn*L and 22 *trn*G sequences were generated for this study (Table S4.1). The concatenated matrix for the Melastomeae dataset totalled 250 taxa and 3219 bp of aligned sequences (ITS, 1119 bp; *acc*D-*psa*I, 1465 bp; *psb*K-*psb*L, 635 bp) with 73% (2340 bp) informative characters (ITS, 849 bp; *acc*D-*psa*I, 1038 bp; *psb*K-*psb*L, 453 bp). The *Castratella* dataset produced a concatenated matrix of 20 taxa and 1798 bp of aligned sequences (ETS, 608 bp; *trn*G, 754 bp; *rpl32*-*trn*L, 436 bp). Of these, 10% (184 bp) were informative (ETS, 118 bp; *trn*G, 37 bp; *rpl32*-*trn*L, 34 bp).

4.4.2 Phylogenetic relationships of the Melastomeae Páramo species

Figure 4.2 shows the MCC tree annotated with posterior probability values (PP) resulting from the Bayesian analysis for the combined matrix of Melastomeae (ITS, *acc*D-*psa*I and *psb*K-*psb*L).

The phylogeny presented in this study recovers the same major clades and relationships obtained by Michelangeli et al. (2013) from Maximum Parsimony and Maximum likelihood phylogenetic analyses, further confirming the results presented by these authors. All sampled Páramo species were reconstructed within a clade

sister to the '*Tibouchina* (*Pleroma*) + *Microlepis, Svitramia, Tibouchinopsis*' clade (PP = 80%; Fig. 4.2a), specifically within clades '*Brachyotum* and allies' (PP = 78%; Fig. 4.2b) and '*Monochaetum* and allies' (PP = 100%; Fig. 4.2b). In the former, three highly supported Páramo clades and one species were recovered: *Brachyotum ledifolium* + *B. lindenii* (PP = 100%); *B. confertum* + *B. fraternum* + *B. harlingii* + *B. fictum* (PP = 100%); *B. rostratum* (PP = 100%); and *Tibouchina grossa* + *T. mollis* (PP = 100%). Within the '*Monochaetum* and allies' clade, two Páramo clades and one species appeared. First, a highly supported Páramo clade formed by *Bucquetia glutinosa* + *Castratella piloselloides* + *Chaetolepis cufodontisii* + *C. microphylla* (PP = 100%) was recovered. In this Páramo clade, two species of the paraphyletic *Chaetolepis*, *C. cufodontisii* and *C. microphylla*, formed a highly supported clade sister to the rest (PP = 100%). Additionally, *B. glutinosa* appears as sister taxon to *C. piloselloides* with poor support (PP < 50%). Also, the monophyly of *C. piloselloides* is further confirmed (PP = 100%). Second, a Páramo clade formed by *Chaetolepis lindeniana* + *Monochaetum discolor* was reconstructed with high support (PP = 100%). Finally, the Páramo species *Monochaetum bonplandii* also appeared highly supported (PP = 97%).

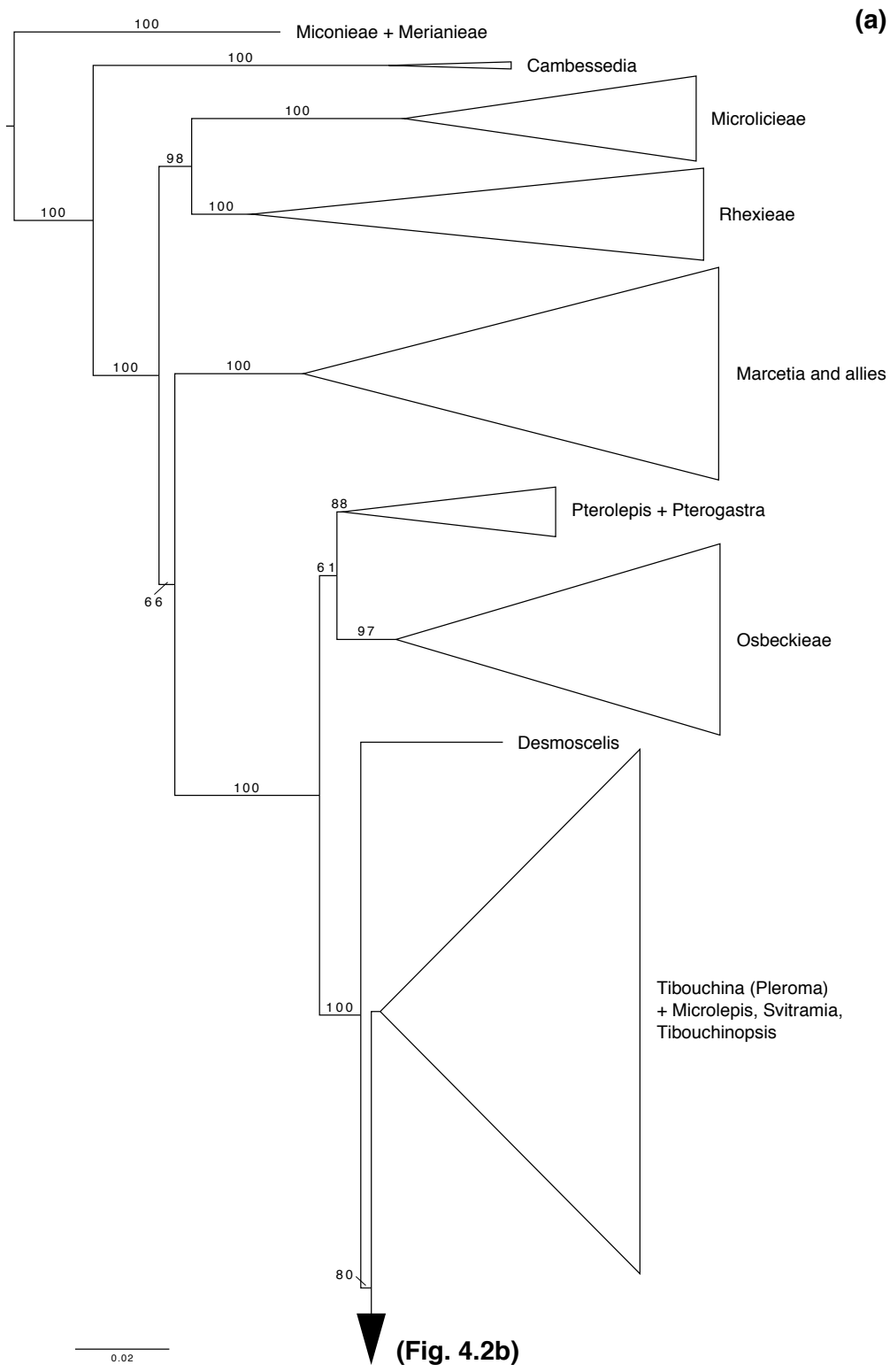
(a)
100
Miconieae + Merianieae
100
Cambessedia
100
Microlicieae
98
100
Rhexieae
100
100
100
Marcetia and allies
88
Pterolepis + Pterogastra
61
66
97
Osbeckieae
Desmoscelis
100
Tibouchina (Pleroma)
+ Microlepis, Svitramia,
Tibouchinopsis
100
80
0.02
(Fig. 4.2b)

(b)

(Fig. 4.2a)

Figure 4.2. (a – b) Maximum clade credibility tree of Melastomeae obtained from the Bayesian analysis based on the combined matrix of nuclear (ITS) and plastid regions (*acc*D-*psa*I and *psb*K-*psb*L). Clade names follow Michelangeli et al. (2013). Numbers above the branches represent posterior probability values (PP < 0.50, not shown). Páramo species are indicated in ***italics and bold***.

Figure 4.3 shows the MCC tree annotated with posterior probability values (PP) resulting from the Bayesian analysis for the combined matrix of the *Castratella* dataset (ETS, *trn*G and *rpl32-trn*L). *Castratella piloselloides* (including *C. rosea*)

was recovered as monophyletic (PP = 100%). Sister to the *Castratella* clade appeared a highly supported *Chaetolepis* clade (PP = 100%) including all three species sampled in this study. Additionally, *Bucquetia glutinosa* was recovered as sister taxon to the *Castratella* + *Chaetolepis* clade (PP = 100%). Within *Castratella*, resolution is poor but basally branching individuals tend to be distributed on the east of the Eastern Cordillera while more derived ones are distributed on the west. Of these, only two clades were highly supported: the first grouping samples MG345, LFT035, MG239, MG282 and MG352 (PP = 100%) and a second grouping the five previously listed samples in addition to MG247 and MG328 (PP = 93%).

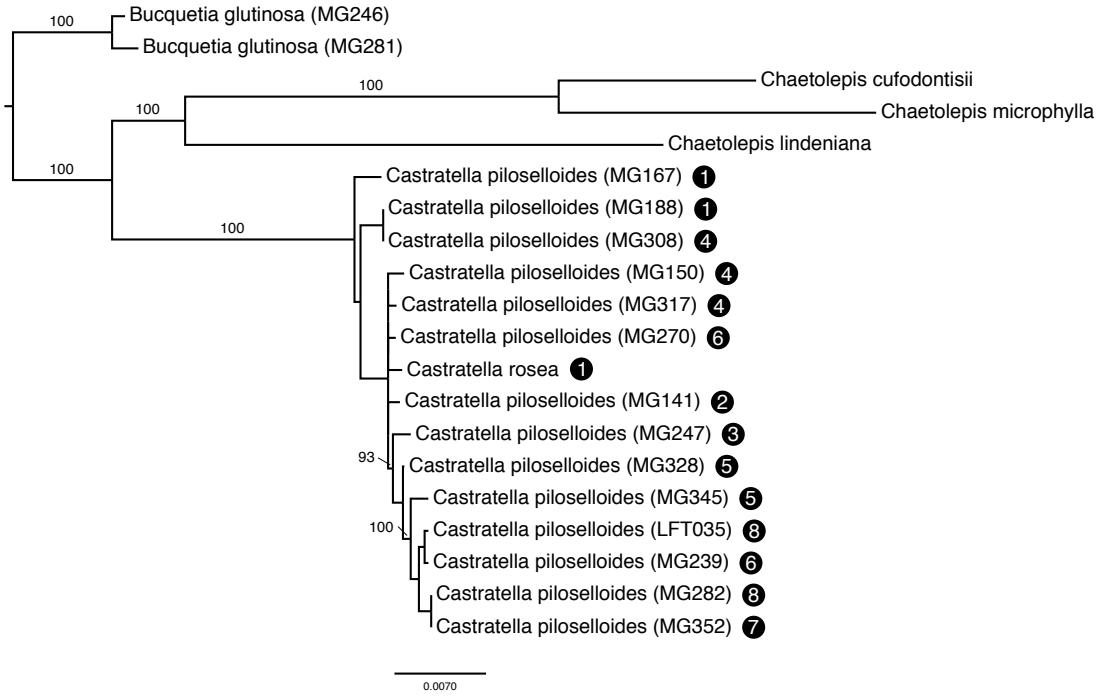

Figure 4.3. Maximum clade credibility tree of *Castratella piloselloides* obtained from the Bayesian analysis based on the combined matrix of nuclear (ETS) and plastid regions (*trn*G and *rpl32-trn*L). Circled numbers indicate population number as described in Figure 4.1 and Table 4.1. Numbers above the branches represent posterior probability values (PP < 0.50, not shown).

4.4.3 Divergence time estimation

The BEAST analysis recovered the same well-supported clades for Melastomeae as the Bayesian analysis (Fig. 4.4). The '*Brachyotum* and allies' and '*Heterocentron* and allies' clades (*sensu* Michelangeli et al, 2013) diverged during the early Miocene c. 23.61 Ma (95% HPD [16.75 – 32.51] Ma) and started diversifying from c. 19.18 Ma (95% HPD [10.81 – 28.11] Ma; node F) and c. 22.27 Ma (95% HPD [14.76 – 30.84] Ma; node G), respectively. Within the former, a well-supported clade formed by eleven species of *Tibouchina* diverged during the mid-Miocene c. 12.4 Ma (95% HPD [7.44 – 18.58] Ma; node E). Within the genus *Brachyotum*, Páramo lineages diverged from the Pliocene: *B. ledifolium* + *B. lindenii* c. 0.33 Ma (95% HPD [0 – 1.15] Ma; node A), *B. confertum* + *B. fictum* + *B. fraternum* + *B. harlingii* c. 2.07 (95% HPD [0.94 – 3.6] Ma; node B) and *B. rostratum* c. 4.71 (95% HPD [2.54 – 7.33] Ma; node C). Similarly, the clade formed by *Tibouchina* Páramo species *T. grossa* and *T. mollis* (node D) also diverged during the Pliocene c. 3.35 Ma (95% HPD [1.29 – 6.25] Ma).

The '*Monochaetum* and allies' clade (*sensu* Michelangeli et al., 2013) diverged during the late Oligocene c. 24.51 Ma (95% HPD [17.9 – 33.71] Ma) and started diversifying during the Miocene c. 17.96 Ma (95% HPD [12.34 – 24.89] Ma). The Páramo clade formed by *Bucquetia glutinosa*, *Castratella piloselloides*, *Chaetolepis cufodontisii* and *Chaetolepis microphylla* (node J) diverged during the Miocene c. 14.03 Ma (95% HPD [9.28 – 20.32] Ma). Subsequently, *B. glutinosa* and *C. piloselloides* diverged c. 11.66 Ma (95% HPD [6.03 – 17.69] Ma; node H) with the latter diversifying since c. 1.06 Ma (95% HPD [0.36 – 2.2] Ma; node I). Likewise, *C. cufodontisii* and *C. microphylla* diverged during the Pliocene c. 4.78 Ma (95% HPD

[1.87 – 9.16] Ma; node K). The *Monochaetum* clade (node N) diverged c. 17.96 Ma (95% HPD [12.34 – 24.89] Ma) and diversified from the mid-Miocene c. 13.47 Ma (95% HPD [8.91 – 19.32] Ma). Within the latter, a Páramo clade formed by *Chaetolepis lindeniana* and *Monochaetum discolor* (node L) diverged during the Pliocene c. 3.48 Ma (95% HPD [0.97 – 7.05] Ma), as did Páramo species *Monochaetum bonplandii* c. 4.69 Ma (95% HPD [2.22 – 8.01] Ma; node M).

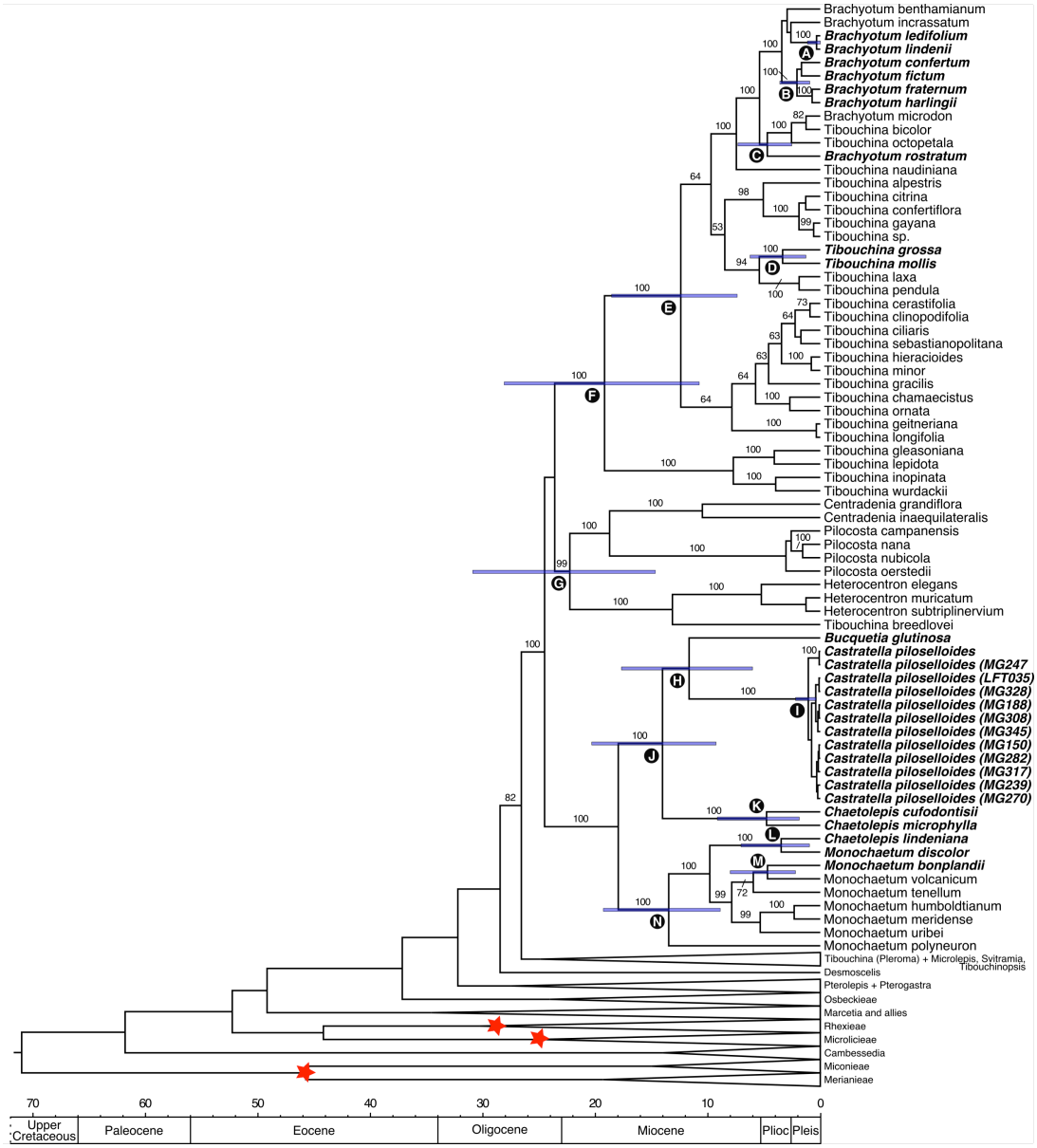

Figure 4.4. Chronogram from the BEAST analysis for the combined matrix of ITS and plastid regions (*acc*D-*psa*I and *psb*K-*psb*L). Stars indicate calibrated nodes. Node bars indicate 95% HPD age ranges. Nodes A – N are described and discussed in the text. Numbers above the branches represent posterior probability values (PP < 0.50, not shown). Páramo species are indicated in ***bold*** and ***italics***

4.4.4 Haplotype definition and network

Figure 4.5 presents the haplotype network and haplotype distribution map for both ETS and cpDNA. A total of 18 individuals from eight populations were scored for

ETS haplotypes, including individuals for both *C. piloselloides* and *C. rosea* (Table 4.2). Aligned sequences totalled 523 bp. One nucleotide substitution defined two haplotypes neither of which were species-specific. There was no evident geographic clustering with Hn1 (n = 16) common and widely distributed and Hn2 (n = 2) restricted to two populations. For the cpDNA, a total of 15 individuals from both species were successfully sequenced for both plastid markers (*trn*G and *rpl32-trn*L). The resulting concatenated matrix totalled 1172 bp of aligned sequences (*trn*G, 744 bp; *rpl32-trn*L, 428 bp). Five haplotypes were identified based on five polymorphic sites (*trn*G, 2; *rpl32-trn*L, 3). Of these, Hc5 is specific to *C. rosea*. Similarly to ETS, there was no evident geographic clustering. Hc3 (n = 6) and Hc1 (n = 5) were the most common haplotypes with the former located at the centre of the network. Hc2 and Hc4 were restricted to one and two populations, respectively.

Table 4.2. Number of individuals of *Castratella* spp. successfully sequenced per population for ETS and cpDNA (*trn*G and *rpl32-trn*L).

POPULATION	*C. piloselloides*		*C. rosea*	
	ETS	cpDNA	ETS	cpDNA
(1) COCUY	2	2	1	1
(2) LA RUSIA	1	1	-	-
(3) IGUAQUE	1	1	-	-
(4) TOTA-BIJAGUAL	3	3	-	-
(5) RABANAL	2	2	-	-
(6) GUERRERO	2	2	-	-
(7) CHINGAZA	3	1	-	-
(8) SUMAPAZ	3	2	-	-
TOTAL	17	14	1	1

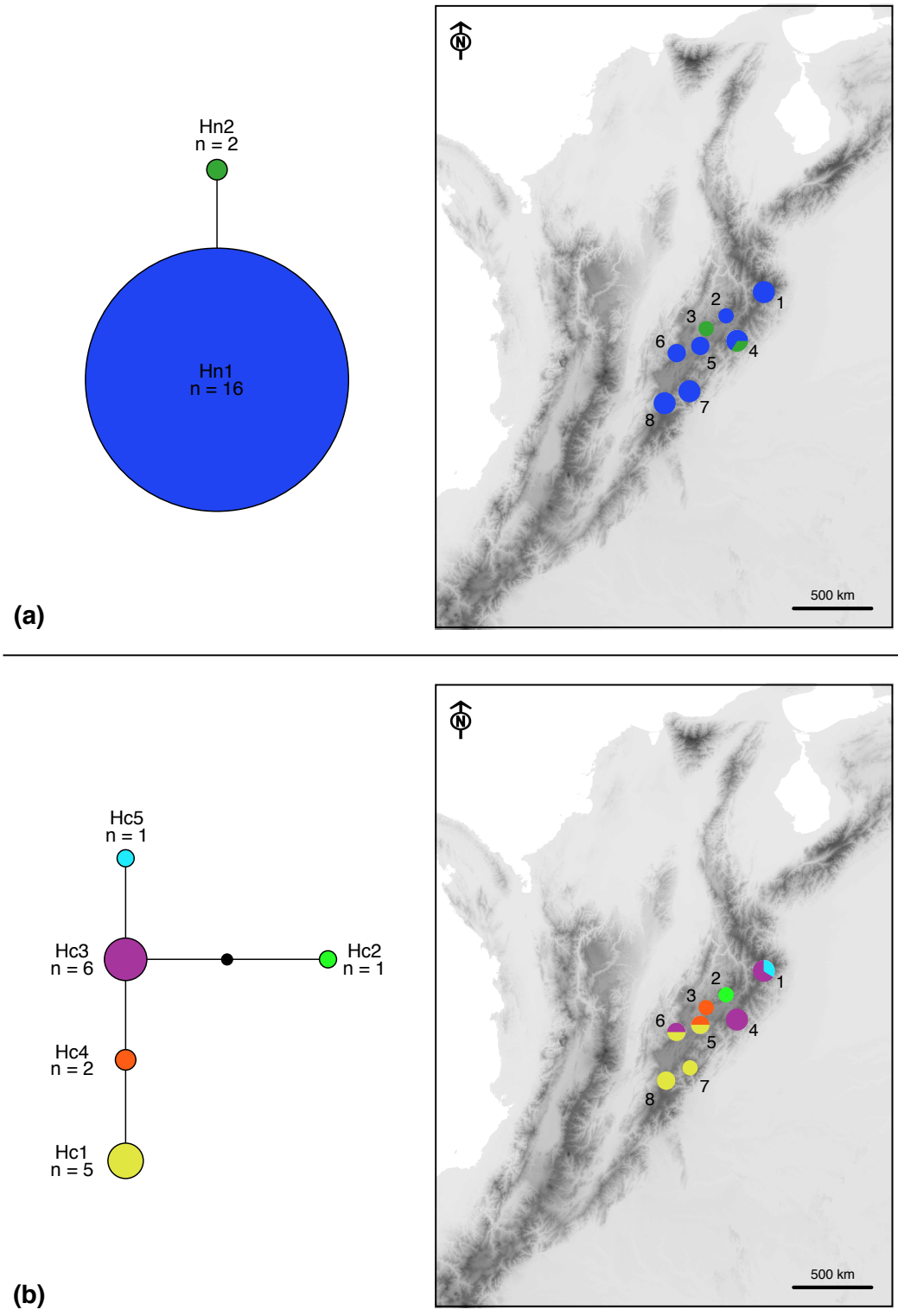

Figure 4.5. Haplotype network and distribution of (a) ETS and (b) cpDNA (*trn*G and *rpl32-trn*L) sequences for 18 *Castratella piloselloides* and one *C. rosea* accessions. Numbers in the map refer to populations described in Table 4.1 and Figure 4.1. Circle size is proportional to sample size for each population and for each haplotype. Hypothetical haplotypes are represented by filled black circles.

4.4.5 Species richness, geographic origin and altitudinal distribution

Figure 4.6 summarises the various comparisons between species richness, geographic origin and altitudinal distribution for the complete Páramo flora. No significant differences in species richness were found between tropical and temperate elements ($p > 0.05$; Fig. 4.6a). Similarly, when discriminating by geographic category within each element no significant differences were found amongst them ($p > 0.05$; Fig. 4.6b). When comparing species richness between tropical and temperate elements within each altitudinal category (Subpáramo, Páramo, Superpáramo), no significant differences were found within any of them ($p > 0.05$; Fig. 4.6c). Likewise, no significant differences were found amongst the six geographic categories when discriminating by altitudinal category ($p > 0.05$; Fig. 4.6d).

However, when comparing each element across altitudinal categories, species richness was significantly different for both temperate and tropical elements ($p < 0.05$; Fig. 4.6c). For temperate elements, differences were explained by higher species richness in the Superpáramo compared to both Subpáramo and Páramo. In the case of tropical elements, differences accounted for greater species richness in the Páramo compared to both Subpáramo and Superpáramo, as well as a more species-rich Superpáramo compared to Subpáramo. After discriminating by geographic category, results showed that differences in species richness were explained by elements of Neotropical, Pantropical, Holarctic and Pantemperate origin ($p < 0.05$; Fig. 4.6d). Differences were explained as follows. For Neotropical elements: (i) species richness was higher in the Páramo compared to both Subpáramo and Superpáramo, as well as higher in Superpáramo compared to Subpáramo; (ii) for Pantropical elements, Páramo was richer than Subpáramo; and (iii) for Holarctic and

Pantemperate elements, Superpáramo had a greater richness than Páramo. Table S4.3 presents test statistics and *p*-values for all comparisons undertaken (Supplementary Information, page 240 – 241).

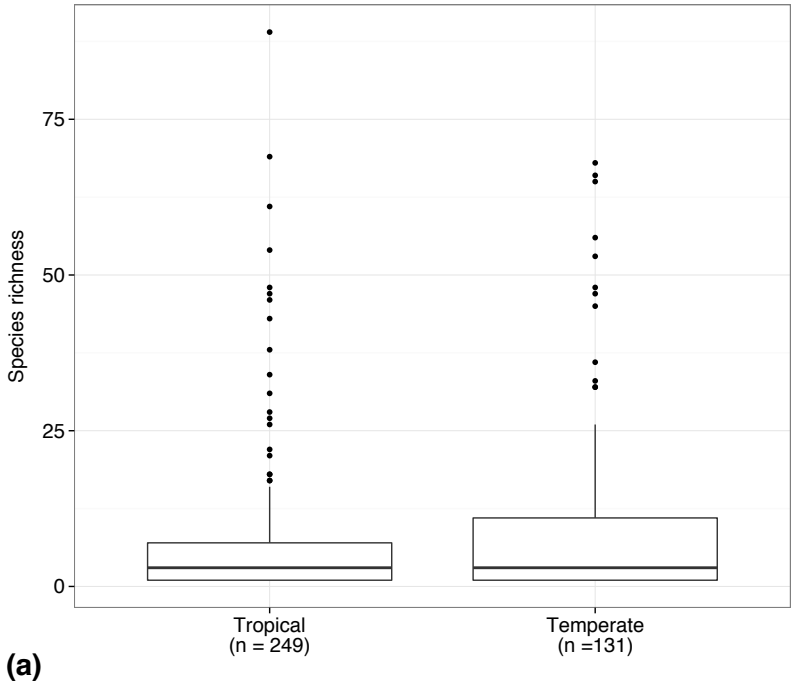
Species richness
75
50
25
0
Tropical
(n = 249)
Temperate
(n =131)

(a)

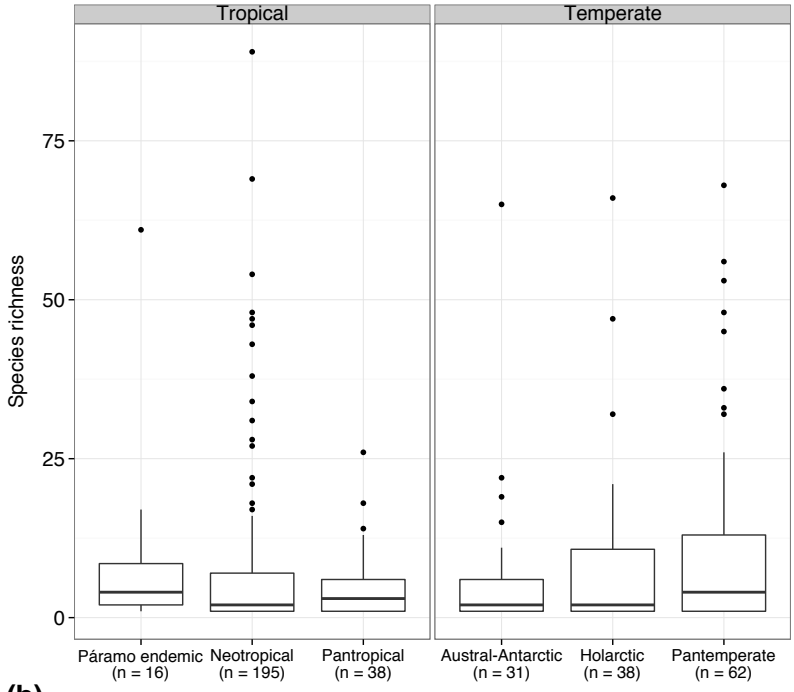
Tropical
Temperate
Species richness
75
50
25
0
Páramo endemic
(n = 16)
Neotropical
(n = 195)
Pantropical
(n = 38)
Austral-Antarctic
(n = 31)
Holarctic
(n = 38)
Pantemperate
(n = 62)

(b)

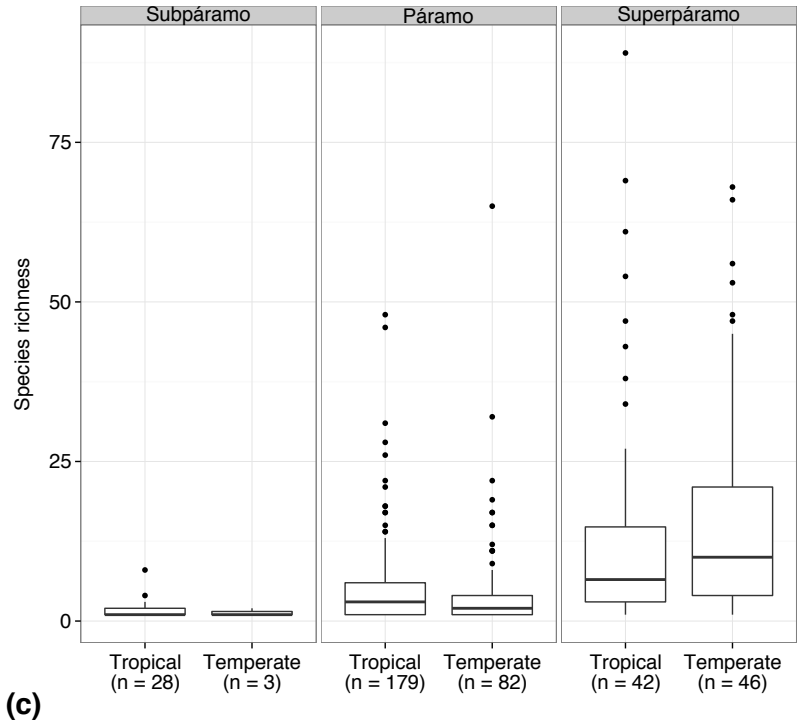

(c)

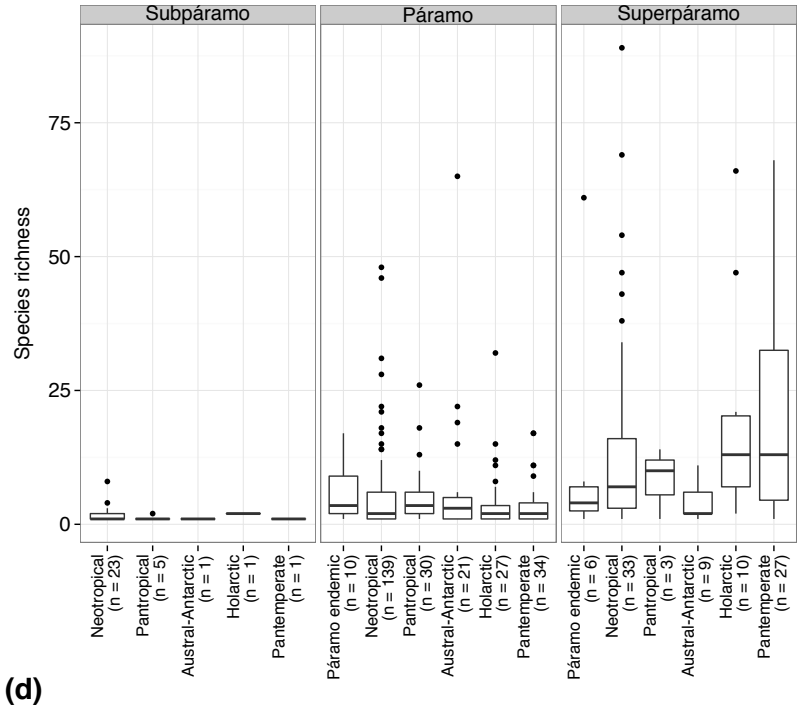

(d)

Figure 4.6. Boxplots for (a - b) species richness versus geographic origin and (c - d) species richness versus geographic origin discriminated by elevation.

4.5 DISCUSSION

4.5.1 Phylogeny and biogeography of the Melastomeae Páramo species

Páramo species of Melastomeae were phylogenetically restricted to one clade of the reconstructed phylogeny (Fig. 4.2). However, within this clade colonisation of Páramo occurred repeatedly in both the '*Brachyotum* and allies' and '*Monochaetum* and allies' clades. Within the former, four different lineages diversified into the Páramo from the Pliocene (Fig. 4.4). By then, the final uplift of the Andes had already taken place and the mountain range was at its current elevation (Gregory-Wodzicki, 2000; Graham, 2009; Mora et al., 2010). Species of *Brachyotum* and *Tibouchina* likely colonised the newly available Páramo ecosystem at this time, extending their distribution above the treeline. Páramo species of *Tibouchina*, *T. grossa* and *T. mollis*, and *Brachyotum ledifolium* and *B. lindenii* have a wider distribution across the páramos of Colombia and Ecuador (Luteyn, 1999; Michelangeli et al., 2013). This suggests effective dispersal after colonisation of Páramo. On the contrary, the clade formed by *Brachyotum confertum*, *B. fraternum*, *B. harlingii* and *B. fictum* is restricted to the páramos of Ecuador whereas *B. rostratum* extends from Ecuador to Peru. The limited distribution of the four Ecuadorian species might reflect more limited dispersal increasing the impact of the Quaternary ice cycles on their diversification history. Repeated episodes of expansion and contraction may have promoted allopatric speciation during periods of isolation.

Within '*Monochaetum* and allies', a Páramo clade formed by *Bucquetia glutinosa*, *Castratella piloselloides*, *Chaetolepis cufodontisii* and *Chaetolepis microphylla*

diverged from its most recent common ancestor (MRCA) in the mid Miocene c. 14.03 Ma (Fig. 4.4). At this time the Andes mountain range had reached half its current height, an altitude insufficient to support Páramo (van der Hammen & Cleef, 1986; Hooghiemstra & van der Hammen, 2004). *Bucquetia glutinosa* and *C. piloselloides*, two species restricted to the Eastern Cordillera of Colombia and Venezuela, the youngest section of the Andes, diverged shortly after c. 11.66 Ma (Gregory-Wodzicki, 2000; Graham, 2009; Mora et al., 2010). The estimated divergence time of these two species could suggest a progressive colonisation of the hilltops from the lowlands, a hypothesis also put forward for *Valeriana* (Bell & Donoghue, 2005). Subsequent divergence of *C. cufodontisii* and *C. microphylla* during the Pliocene c. 4.78 Ma is consistent with the formation of the Páramo ecosystem. Moreover, *C. cufodontisii* is endemic to the páramos of Costa Rica suggesting possible dispersal to Central America from the south. Further colonisations of the Páramo also occurred during the Pliocene by *Chaetolepis lindeniana*, *Monochaetum discolor* and *M. bonplandii*.

4.5.2 Phylogeography of *Castratella piloselloides*

Castratella was recovered as monophyletic in both the Melastomeae dataset and the *Castratella* dataset (PP = 100%; Figs. 4.2 – 4.3). However, reconstruction of the sister clade varied between datasets. In the Melastomeae phylogeny (Fig. 4.2), *Bucquetia glutinosa* appeared poorly supported as sister to *Castratella* (PP < 50%) whereas in the *Castratella* dataset (Fig. 4.3), a clade formed by the three sampled species of *Chaetolepis* was highly supported as its sister clade (PP = 100%). Furthermore, whereas *Chaetolepis* appeared as paraphyletic in the Melastomeae

phylogeny, it was highly supported as monophyletic in the *Castratella* phylogeny (PP = 100%). These differences highlight the importance of sample size and marker choice in phylogenetic reconstruction. A better reconstruction of the relationships between *Bucquetia*, *Castratella*, *Chaetolepis* and *Monochaetum* will require the thorough sampling of all species within these genera and the use of more variable markers. In the present study, only *Castratella* was sampled for both species, *C. piloselloides* and *C. rosea*, whereas only one out of three, three out of eleven and two out of forty species have been sampled for *Bucquetia*, *Chaetolepis* and *Monochaetum*, respectively.

Castratella rosea was nested within *C. piloselloides* (Fig. 4.3). Nevertheless, given the poor level of resolution within the clade, *C. rosea* cannot be confirmed or denied as a distinct species, and as mentioned in the introduction there are doubts about its morphological distinctiveness. Furthermore, because sequencing of regions used in the Melastomeae dataset (ITS, *acc*D-*psa*I and *psb*K-*psb*L) were unsuccessful for *C. rosea*, this species could not be incorporated into the broader tribal level phylogeny and therefore results about its phylogenetic status are inconclusive. Additional structure is evident within *Castratella*, even though only two clades are highly supported (Fig. 4.3). Southeastern individuals (populations 2, 3, 5 – 8) are nested within northwestern ones (populations 1 and 4) of the Eastern Cordillera that is consistent with the species originating in the more northwestern parts.

Genealogical relationships within *Castratella* indicated a pattern of one or two common haplotypes and one or two rare ones for both ETS and the plastid regions (Fig. 4.5). This is particularly evident in the ETS network where 89% of the samples presented Hn1 while only 11% had Hn2. In the case of the plastid network, two

haplotypes (Hc3 and Hc1) grouped 73% of the samples while Hc2 and Hc4 represented 20%. Furthermore, the resulting cpDNA network showed some degree of geographical structure, which might reflect the likely impact of the Quaternary ice cycles on the diversification history of *Castratella*. This genus diverged from its MRCA during the mid-Miocene c. 11.66 Ma, but diversification within extant populations of *C. piloselloides* only occurred from the Pleistocene c. 1.06 Ma (Fig. 4.4). By then, the likely contraction of Páramo islands during glacial periods (van der Hammen & Cleef, 1986; Hooghiemstra & van der Hammen, 2004; Flantua et al., 2014) might have promoted the isolation of refugial populations. Subsequently, during inter-glacial periods these Páramo islands might have come into contact, which, coupled with effective seed dispersal (wind), might have facilitated range expansion. The results obtained for ETS could be indicative of a lack of variation for this nuclear region. Furthermore, the difference in the number of base pairs sequenced for ETS (523 bp) compared to the concatenated plastid regions (1172 bp) could explain the higher polymorphism recovered in the cpDNA network. However, given the low samples sizes, these results are inconclusive and might also reflect a sampling artefact. *Castratella rosea* has a species-specific plastid haplotype (Hc5) although equally differentiated by a single mutational step.

4.5.3 Species richness, geographic origin and altitudinal distribution

General patterns of species richness in relation to geographic origin (tropical versus temperate) and maximum altitudinal distribution were assessed for the complete Páramo flora (Fig. 4.6). The results presented here support the palaeopalynological record and previous floristic studies in that temperate and tropical elements

contribute an equal proportion of species to this flora (van der Hammen & Cleef, 1986; Sklenář et al., 2011). Both elements may have diversified to the same extent in the recently formed Páramo ecosystem, profiting from this new and empty niche resulting from the final uplift of the northern Andes section during the Pliocene c. 5 Ma (van der Hammen, 1974; van der Hammen & Cleef, 1986; Hooghiemstra et al., 2006; Graham, 2009). Indeed, radiations in lineages of tropical origin (e.g. *Espeletia* complex, Madriñán et al., 2013) and temperate (e.g. *Lupinus*, Hughes & Eastwood, 2006) occurred during the Pliocene and Pleistocene broadly as a consequence of ecological opportunity (Sklenář et al., 2011; Madriñán et al., 2013; Luebert & Weigend, 2014; Hughes & Atchison, 2015). The proposed hypothesis that the frost-resistance mechanism possessed by plants with a north temperate origin (formation of extracellular ice) might provide a pre-adaptation that could promote more successful colonisation and diversification at higher altitudes when compared to tropical elements lacking such pre-adaptation could not be supported. Indeed, species richness showed a tendency to increase with increasing altitude for both tropical and temperate elements (Fig. 4.6c). However, the likely role that this frost-resistance mechanism might have played in the successful diversification of temperate taxa at higher altitudes cannot be discarded.

Nonetheless, the general pattern described in the previous paragraph should only be used as an approximation and more definite conclusions should be drawn from analyses of individual cases. I was able to compare relative diversification rates of Páramo lineages derived from within a predominantly cloud forest tropical one in a lineage of Melastomeae (Fig. 4.4). As described earlier, most Páramo lineages diverged during the Pliocene – Pleistocene with *Brachyotum* being the most diverse

(25/55 species). This greater number of species could be related to its different pollination syndrome. *Tibouchina*, *Chaetolepis*, *Bucquetia*, *Castratella* and *Monochaetum* are pollinated by insects but all species within *Brachyotum* are pollinated by bats and hummingbirds (Wurdack, 1953).

Castratella is of particular interest, having diverged from its MRCA during the mid-Miocene c. 11.66 Ma. *Castratella*, with just two species, is one of the few endemic Páramo genera (Luteyn, 1999; Sklenář et al., 2005) and the only Melastomeae Páramo representative to present a herbaceous perennial habit, the rest being bushes (Sklenář et al., 2005; Michelangeli et al., 2013). The clade comprising *Tibouchina cerastifolia* with a similar divergence time of c. 12.4 Ma diverged into eleven species within the same timeframe (node E; Fig 4.4). These species occupy the high-elevation areas of the Mata Atlantica in Eastern Brazil (Michelangeli et al., 2013) a region that had already reached its current altitude (c. 2000 – 3000 m.a.s.l.) by the mid Miocene (DeForest Safford, 2007). The reasons for the different evolutionary history of this clade and other more species rich lineages and *Castratella* are intriguing. They reflect different diversification or extinction rates. *Castratella* could have had a lower diversification rate or a greater extinction rate. A possible explanation for the obtained results might be that *Castratella* is a recent arrival to the Páramo ecosystem. Evidence for a definite date of arrival into the Páramo is provided only by the age of the crown node of the genus, which began diversifying during the Pleistocene c. 1.06 Ma (Fig. 4.4). Even though an ancient *Castratella* may have diverged from its MRCA during the mid-Miocene c. 11.66 Ma, it might have persisted as a small refugial population at a lowland location. Subsequent dispersal to the Páramo ecosystem may have occurred more recently and the refugial population

could then have gone extinct. This scenario is consistent with patterns in the haplotype networks presented above. Though scarcity of pollinators at higher altitudes might have limited effective pollen dispersal, effective seed dispersal (wind) might have compensated for this and allowed an increase in population sizes with high gene flow that would have reduced opportunities for reproductive isolation. Moreover, the development of a herbaceous rhizomatous rosette habit may have had a positive impact on effective population sizes.

Donoghue & Edwards (2014) hypothesised that the probability of a lineage shifting into a new biome could depend on the adjacency of the two biomes, the amount of time these two biomes have been connected and that greatest colonisation might occur when it is relatively empty. Furthermore, these authors suggested that evolutionary biome shifts would be phylogenetically clustered. All the aforementioned seem to be confirmed for the Páramo lineages of Melastomeae; phylogenetically clustered within one lineage, all Páramo lineages diverged from mostly mountainous clades occupying the forest below the treeline. Further analyses of diversification rates, climatic data and functional traits will greatly contribute to the understanding of the diversification within Melastomeae and to a better understanding of the diversification of the Páramo ecosystem.

4.6 CONCLUSION

Classification into tropical and temperate elements of the Páramo flora originally postulated by van der Hammen & Cleef (1986) provides a valuable basis from where to describe general patterns and formulate hypothesis related to the general assembly

of the Páramo flora. However, their method lacked the evolutionary evidence provided by molecular phylogenetics. Detailed studies of the molecular phylogenetics and biogeography of individual cases is therefore critical for a better understanding of the origin of the Páramo flora. Although much work has been done (reviewed in: Sklenář et al., 2011; Luebert & Weigend, 2014), a significant proportion is missing. Melastomeae is an excellent candidate to study evolutionary biome shifts and the impact of these on diversification histories as it has a significant amount of published phylogenetic information. I showed that colonisation of Páramo occurred repeatedly from the Pliocene in *Brachyotum*, *Tibouchina*, *Monochaetum* and *Chaetolepis*. Interestingly, the near-endemic and endemic, respectively, and least diverse genera, *Bucquetia* and *Castratella* diverged during the mid-Miocene. For the latter, I suggest that a refugial population may have persisted at a lowland location, then gone extinct but only after dispersing and diversifying in the Páramo ecosystem more recently.

Because of the potential scarcity of genetic divergence within the species of endemic Páramo genera, very few studies have been undertaken below the species level. I attempted to reconstruct the phylogeographic history of *Castratella piloselloides*, but sequence divergence was less than 0.4% for all regions. This history could potentially be reconstructed with the use of more informative data such as microsatellites or a greater quantity of DNA sequence data (Fig. 4.5) that will permit a better understanding of evolutionary processes within the species.

CHAPTER FIVE. CONCLUSIONS

5.1 RESEARCH SYNTHESIS

The Páramo ecosystem is one of the youngest and fastest evolving on Earth (Madriñán et al., 2013). As such it is a model for studying recent evolutionary diversification processes. With the evolution of the large numbers of species with a high percentage of endemism to the biome, this ecosystem is interesting on a number of levels. It has similarities to island ecosystems with its distinct climate differentiating it from surrounding lowland ecosystems in a series of sky islands. Its climate requires adaptation to extreme conditions with high diurnal temperature changes including in some cases night frosts and high UV radiation. Determining the origin of Páramo lineages, whether they be from temperate regions with similar climates or from warmer tropical regions, will indicate how important pre-adaptation is in successful colonisation and diversification. Successful colonisation could depend on phylogenetic niche conservatism (PNC), which is the tendency of species to retain their ancestral traits, resulting in closely related species being more ecologically similar than would be expected based on their phylogenetic relations (Wiens & Graham, 2005). This hypothesis has been supported at various spatial scales (Silvertown et al., 2006; Losos, 2008; Crisp et al., 2009).. In the case of the Páramo, based on PNC, we might expect more lineages to have had an origin in

temperate regions and also that those lineages would have diversified more successfully, in terms of the number of species per lineage.

This thesis examines the patterns and processes underlying the diversification of plants in the Páramo ecosystem, through studies of representative species of *Oreobolus* (Cyperaceae) and Melastomeae (Melastomataceae). The former has an origin in southern temperate regions and the latter originated in lowland tropical regions. The two groups were chosen for their different ancestral ecologies and also because they have different breeding systems. The main objectives were 1) to investigate the impact of the Andes orogeny on the timing, directionality and diversification rates of the South American species of *Oreobolus* (chapter two); 2) to examine the genetic structure between and within the South American species of *Oreobolus* in order to understand the influences of more recent geological, climatic and ecological factors (chapter three); 3) to investigate the impact of the Andes orogeny on the diversification history of the Páramo species of the largely Neotropical Melastomeae tribe (chapter four); and 4) to determine whether there were differences in species numbers of Páramo lineages of different geographic origin (chapter four).

Key research findings, implications and future directions are discussed below.

5.2 KEY RESEARCH FINDINGS

5.2.1 Timing, directionality and diversification rates of the South American species of a southern temperate lineage, Oreobolus (Cyperaceae).

Results from Chapter Two highlight the importance of long-distance dispersal events and habitat heterogeneity in the diversification of the South American species of *Oreobolus*. The most recent common ancestor (MRCA) of these species diverged during the early Pliocene in Australia. Subsequent long-distance dispersal events to South America occurred in the same epoch, colonising both the northern and southern Andes. Importantly, the arid central Andes appear to have a strong impact on the distribution of these species imposing a barrier to dispersal between north and south. Comparison of diversification rates between northern and southern Andean clades provided further support for the positive impact of the Andes orogeny on diversification, through habitat heterogeneity.

It is worth noting that phylogenetic analyses recovered unresolved relationships within the '*Oreobolus* clade' of the Schoeneae tribe, with uncertain taxonomic boundaries at the generic level. This may have had a small effect on biogeographic reconstructions influencing statistical supports recovered for the ancestral area reconstructions.

Notwithstanding these limitations, my study allowed for comparison of diversification patterns between sister clades with contrasting numbers of species but similar divergence times and origin. These results further support the role of Andean uplift in the promotion of diversity in the tropical Andes. Interestingly, it is apparent

that, given the right confluence of events, temperate taxa have the genotypic plasticity to quickly diversify.

5.2.2 Genetic structure between and within the South American species of Oreobolus (Cyperaceae)

My data indicated an example of cryptic speciation with the two morphologically similar southern and northern Andean subspecies of *O. obtusangulus* being genetically distinct in all analyses. Amongst the rest of the northern Andean Páramo *Oreobolus* species, a pattern of incomplete lineage sorting was evident. Incomplete lineage sorting is more likely to have confounded species boundaries than the alternative explanation of hybridisation based on the high percentage of private haplotypes, significantly different pairwise FST values between species, lack of heterozygosity in ITS and the recent divergence times of these species. However, hybridisation cannot be completely discarded because many of these species are sympatric providing opportunity for inter-specific gene flow. I suggest possible hybridisation between *O. cleefii* and the northern subspecies of *O. obtusangulus*.

My results were also consistent with the glacial cycles of the Quaternary playing a role in the diversification process of *Oreobolus*, not only promoting speciation, but also maintaining high levels of genetic diversity within species and populations. These results add genetic evidence that is consistent with hypotheses based on the palaeopalynological record that suggest cycles of contraction and expansion of Páramo islands promoted allopatric speciation but also gene flow amongst species via secondary contact (van der Hammen, 1974; Simpson, 1975).

5.2.3 Diversification history of the Páramo species of the largely Neotropical Melastomeae tribe

Results from Chapter four indicate multiple colonisations of the Páramo ecosystem within one clade of the Neotropical Melastomeae tribe. These diversification events occurred since the mid-Miocene for species-poor lineages such as *Castratella* and *Bucquetia*, but mostly during the Pliocene for species within *Brachyotum*, *Chaetolepis*, *Monochaetum* and *Tibouchina*.

I discussed the likely role of extinction in the lack of diversification of *Castratella*. *Castratella* did not undergo an explosive radiation as has been the case for most Páramo plant clades. Donoghue & Sanderson (2015) coined the term depauperon to refer to "significantly depauperate lineages", that show slower speciation or higher extinction rates compared to more species-rich lineages within the same group. I suggested a possible explanation for the pattern I observed of an old and species poor lineage that has only begun to diversify genetically since the Pleistocene. *Castratella* diverged from its MRCA c. 11 Ma during the mid-Miocene. It could then have remained at lower altitudes until the Andes reached a height sufficient to support the Páramo ecosystem. *Castratella* could then have dispersed into the Páramo, gone extinct at lower latitudes, and begun diversifying genetically but not sufficiently for new species to form. This could have been because its breeding system permitted gene flow amongst populations preventing divergence into morphologically distinct and reproductively isolated units.

I showed how the identification and study of Páramo depauperons could greatly contribute to a more comprehensive understanding of the historical assembly of the

Páramo flora as these studies will allow the incorporation of diversity patterns other than species-rich radiations.

5.2.4 Differences in species numbers of Páramo lineages of different geographic origin

Chapter four indicated that Páramo elements of tropical and temperate origin contribute equally to this flora. However, I also showed that elements with a north temperate origin contributed greater numbers to the higher altitude Superpáramo flora. This could be attributed to differences in frost resistance mechanisms, could give north temperate elements a competitive advantage. North temperate origin elements may be more likely to tolerate frost, whereas those of a tropical origin less so. It is worth noting that the general patterns described in this chapter only provide a first glance into the general assembly of the Páramo flora. In that sense, studies should focus on specific groups identified as good models to tackle biogeographic questions. Importantly, such investigations need to incorporate the use of molecular phylogenetics in order to estimate geographical origin and possible dispersal routes. Such phylogenetic studies can then be coupled with ecophysiological data.

5.3 RESEARCH IMPLICATIONS

5.3.1 Phylogenetic niche conservatism versus niche evolution

The comparison between patterns and processes in the biogeographic history of *Oreobolus* and Melastomeae are interesting. While phylogenetic niche conservatism can be invoked for *Oreobolus* as they appear to have only colonised within their

ancestral climatic niche, Melastomeae presents a history of limited niche evolution with multiple colonisations of temperate climates, though only a few times and within the same clade. Under a scenario of ecological opportunity, these results highlight important aspects of the natural history of each of these groups and bring attention to the impacts that these two strategies might have on plant diversification. If dispersal to a similar ecosystem is effective (PNC), taxa with a temperate origin are likely to quickly diversify, probably enabled by their pre-adaptations, as shown in *Oreobolus*. On the contrary, taxa with a tropical origin could face some degree of ecological filtering in that they need to adapt to new conditions, which might hinder their diversification, as may be the case in *Castratella*. Nonetheless, if these limitations are overcome, explosive radiations may occur as has been shown for the *Espeletia* complex (Rauscher, 2002).

5.3.2 Phylogeography of Páramo plant taxa

Phylogeographic studies of South American plant taxa are scarce and mostly focus on lowland species (Beheregaray, 2008; Turchetto-Zolet et al., 2013). Unfortunately, genetic diversity below the species level may be low in Páramo taxa, hindering such investigations. However, in order to understand speciation processes in the Páramo ecosystem, phylogeographic studies are necessary for closely related and recently divergent species, such as those in *Oreobolus*. In Chapter three I employ a phylogeographic approach providing novel evidence that reveals complex genetic relationships between and within the South American species of *Oreobolus*. Nonetheless, single-species phylogeographic studies may still prove difficult, as shown in Chapter four with the pilot study presented for *Castratella.*

Integrating phylogeography into studies of diversification within the Páramo ecosystem would greatly contribute to our understanding of the evolution of this flora. Current challenges imposed by the lack of molecular variability could be overcome by the incorporation of data from more variable markers such as chloroplast and nuclear microsatellites. Furthermore, the generation of large amounts of sequence data through Next Generation approaches could provide researchers with new opportunities to explore phylogeographic patterns. These data will permit us to better understand how Páramo taxa have responded to historical changes such as climatic cycles that may allow us to predict how they might react to future changes.

5.3.3 Conservation

Páramos are regional water towers, a role that is mostly facilitated by the plants within the ecosystem. However, mining activities, the expansion of the agricultural frontier and climate change are imposing great threats. Knowledge and understanding of the genetic diversity in Páramo plant species are critical to the conservation of this biodiversity hotspot. My results for the northern Andean species of *Oreobolus* showed that the Quaternary glacial cycles may have promoted speciation while maintaining high levels of genetic diversity. Coupling this genetic data with species distribution models that hindcast and forecast their distributions could provide further insight into their population dynamics. In this manner genetic diversity information could be incorporated into conservation management plans.

5.4 FUTURE RESEARCH DIRECTIONS

Further work needs to be done to resolve the molecular systematics of all species within the '*Oreobolus* clade' of the Schoeneae tribe. A thorough sampling of all species within the clade, including multiple samples per species would permit a better assessment of the phylogenetic relationships within it. Moreover, the inclusion of more sequence data from additional DNA regions could provide additional phylogenetic resolution. Phylogenetic evidence should also be combined with morphological data, as cryptic species are evident (i.e. *Oreobolus obtusangulus*, this study; *Tetraria triangularis*, Britton et al., 2014). Although work is being done in this area (Slingsby et al., 2014; Britton et al., 2014), it has primarily focused on South African representatives of the tribe.

Additionally, further work could focus on investigating possible hybridisation between *O. cleefii* and the northern subspecies of *O. obtusangulus*. To pursue this investigation, a larger sampling of individuals from sympatric populations where hybridisation might be underway would be required. Moreover, incorporation of both nuclear and chloroplast microsatellite data would allow further exploration of population genetic dynamics between these two species. Additionally, breeding experiments should be undertaken to assess if hybridisation might be ongoing or if the observed patterns are the result of gene flow during species divergence. The possibility of speciation by allopolyploidization should also be investigated. This would require cytogenetic studies of these species, and ideally of all species within the genus.

Additional research could also concentrate on the investigation of evolutionary biome shifts within the Melastomeae tribe. Particular focus should be paid to the cloud forest lineages crossing into the Páramo ecosystem. Given the significant amount of available phylogenetic information, estimation of diversification rates and ancestral area reconstructions could be undertaken. Additional studies on trait evolution and phenotypic plasticity along altitudinal gradients could provide further information that would allow us to better understand diversification processes. Identification of rate heterogeneity could lead to the formulation of hypotheses exploring which confluence (*sensu* Donoghue & Sanderson, 2015) of traits and/or combination of ecological, climatic or geological events might be responsible for key evolutionary events that have permitted lineages to enter the Páramo ecosystem.

REFERENCES

Abbott R., Albach D., Ansell S., Arntzen J.W., Baird S.J.E., Bierne N., Boughman J., Brelsford A., Buerkle C.A., Buggs R., Butlin R.K., Dieckmann U., Eroukhmanoff F., Grill A., Cahan S.H., Hermansen J.S., Hewitt G., Hudson A.G., Jiggins C., Jones J., Keller B., Marczewski T., Mallet J., Martinez-Rodriguez P., Möst M., Mullen S., Nichols R., Nolte A.W., Parisod C., Pfennig K., Rice A.M., Ritchie M.G., Seifert B., Smadja C.M., Stelkens R., Szymura J.M., Väinölä R., Wolf J.B.W., & Zinner D. (2013) Hybridization and speciation. *Journal of Evolutionary Biology*, **26**, 229–246.

Ahmed S., Compton S.G., Butlin R.K., & Gilmartin P.M. (2009) Wind-borne insects mediate directional pollen transfer between desert fig trees 160 kilometers apart. *Proceedings of the National Academy of Sciences of the United States of America*, **106**, 20342–20347.

Allen A.P. & Gillooly J.F. (2006) Assessing latitudinal gradients in speciation rates and biodiversity at the global scale. *Ecology Letters*, **9**, 947–954.

Almeda F. & Chuang T.I. (1992) Chromosome numbers and their systematic significance in some Mexican Melastomataceae. *Systematic Botany*, **17**, 583–593.

Antonelli A. & Sanmartín I. (2011) Why are there so many plant species in the Neotropics? *Taxon*, **60**, 403–414.

Antonelli A., Nylander J.A.A., Persson C., & Sanmartín I. (2009) Tracing the impact of the Andean uplift on Neotropical plant evolution. *Proceedings of the National Academy of Sciences of the United States of America*, **106**, 9749–9754.

APG III (2009) An update of the Angiosperm Phylogeny Group classification for the orders and families of flowering plants: APG III. *Botanical Journal of the Linnean Society*, **161**, 105–121.

Arnold M.L. (1997) *Natural hybridization and evolution.* Oxford University Press, New York.

Assefa A., Ehrich D., Taberlet P., Nemomissa S., & Brochmann C. (2007) Pleistocene colonization of afro-alpine "sky islands" by the arctic-alpine *Arabis alpina*. *Heredity*, **99**, 133–142.

Avise J.C. (2000) *Phylogeography.* Harvard University Press, Cambridge.

Avise J.C. (2009) Phylogeography: retrospect and prospect. *Journal of Biogeography*, **36**, 3–15.

Avise J.C., Arnold J., Ball R.M., Bermingham E., Lamb T., Neigel J.E., Reeb C.A., & Saunders N.C. (1987) Intraspecific phylogeography: the mitochondrial DNA bridge between population genetics and systematics. *Annual Review of Ecology and Systematics*, **18**, 489–522.

Barker F.K. & Lutzoni F.M. (2002) The utility of the incongruence length difference test. *Systematic Biology*, **51**, 625–637.

Barker N.P., Weston P.H., Rutschmann F., & Sauquet H. (2007) Molecular dating of the "Gondwanan" plant family Proteaceae is only partially congruent with the timing of the break-up of Gondwana. *Journal of Biogeography*, **34**, 2012–2027.

Beck E. (1994) Cold tolerance in tropical alpine plants. *Tropical Alpine Environments* (ed. by P.W. Rundel, A.P. Smith, and F.C. Meinzer), pp. 77–110. Cambridge University Press, Cambridge.

Beheregaray L.B. (2008) Twenty years of phylogeography: the state of the field and the challenges for the Southern Hemisphere. *Molecular Ecology*, **17**, 3754–3774.

Bell C.D. & Donoghue M.J. (2005) Phylogeny and biogeography of Valerianaceae (Dipsacales) with special reference to the South American valerians. *Organisms Diversity & Evolution*, **5**, 147–159.

Bermingham E. & Moritz C. (1998) Comparative phylogeography: concepts and applications. *Molecular Ecology*, **7**, 367–369.

Besnard G., Muasya A.M., Russier F., Roalson E.H., Salamin N., & Christin P.-A. (2009) Phylogenomics of C4 photosynthesis in sedges (Cyperaceae): multiple appearances and genetic convergence. *Molecular Biology and Evolution*, **26**, 1909–1919.

Bickford D., Lohman D.J., Sodhi N.S., Ng P.K.L., Meier R., Winker K., Ingram K.K., & Das I. (2007) Cryptic species as a window on diversity and conservation. *Trends in Ecology & Evolution*, **22**, 148–155.

Blisniuk P.M., Stern L.A., Chamberlain C.P., Idleman B., & Zeitler P.K. (2005) Climatic and ecologic changes during Miocene surface uplift in the Southern Patagonian Andes. *Earth and Planetary Science Letters*, **230**, 125–142.

Bouckaert R., Heled J., Kühnert D., Vaughan T., Wu C.-H., Xie D., Suchard M.A., Rambaut A., & Drummond A.J. (2014) BEAST 2: A Software Platform for Bayesian Evolutionary Analysis. *PLoS Computational Biology*, **10**, e1003537–6.

Britton M.N., Hedderson T.A., & Verboom G.A. (2014) Topography as a driver of cryptic speciation in the high-elevation cape sedge *Tetraria triangularis* (Boeck.) C. B. Clarke (Cyperaceae: Schoeneae). *Molecular Phylogenetics and Evolution*, **77**, 96–109.

Bruhl J.J. (1995) Sedge genera of the world: Relationships and a new classification of the Cyperaceae. *Australian Systematic Botany*, **8**, 125–305.

Brummitt R.K. (2001) *World geographical scheme for recording plant distributions.* Hunt Institute for Botanical Documentation, Pittsburgh.

Bryant D. & Moulton V. (2004) Neighbor-Net: An Agglomerative Method for the Construction of Phylogenetic Networks. *Molecular Biology and Evolution*, **21**, 255–265.

Burban C., Petit R., Carcreff E., & Jactel H. (1999) Rangewide variation of the maritime pine bast scale *Matsucoccus feytaudi* Duc. (Homoptera: Matsucoccidae) in relation to the genetic structure of its host. *Molecular Ecology*, **8**, 1593–1602.

Buytaert W., Cuesta-Camacho F., & Tobón C. (2010) Potential impacts of climate change on the environmental services of humid tropical alpine regions. *Global Ecology and Biogeography*, **20**, 19–33.

Camin J.H. & Sokal R.R. (1965) A method for deducing branching sequences in phylogeny. *Evolution*, **19**, 311–326.

Chacón J., Madriñán S., Chase M.W., & Bruhl J.J. (2006) Molecular phylogenetics of *Oreobolus* (Cyperaceae) and the origin and diversification of the American species. *Taxon*, **55**, 359–366.

Christe C., Caetano S., Aeschimann D., Kropf M., Diadema K., & Naciri Y. (2014) The intraspecific genetic variability of siliceous and calcareous *Gentiana* species is shaped by contrasting demographic and re-colonization processes. *Molecular Phylogenetics and Evolution*, **70**, 323–336.

Christenhusz M.J.M. & Chase M.W. (2013) Biogeographical patterns of plants in the Neotropics – dispersal rather than plate tectonics is most explanatory. *Botanical Journal of the Linnean Society*, **171**, 277–286.

Cohen K.M., Finney S.C., Gibbard P.L., & Fan J.-X. (2013) The ICS International Chronostratigraphic Chart. *Episodes*, **36**, 199–204.

Collinson M.E. & Pingen M. (1992) Seeds of the Melastomataceae from the Miocene of Central Europe. *Pan-European Palaeobotanical Conference*, pp. 129–139.

Conover W.J. (1999) *Practical Nonparametric Statistics.* John Wiley & Sons, New York.

Coyne J.A. & Orr H.A. (2004) *Speciation.* Sinauer Associates, Inc, Sunderland.

Crisp M.D., Arroyo M.T.K., Cook L.G., Gandolfo M.A., Jordan G.J., McGlone M.S., Weston P.H., Westoby M., Wilf P., & Linder H.P. (2009) Phylogenetic biome conservatism on a global scale. *Nature*, **458**, 754–756.

Cuatrecasas J. (1958) Aspectos de la vegetación natural de Colombia. *Revista de la Academia Colombiana de Ciencias Exactas*, **10**, 221–264.

Cutter A.D. (2013) Integrating phylogenetics, phylogeography and population genetics through genomes and evolutionary theory. *Molecular Phylogenetics and Evolution*, **69**, 1172–1185.

Darlu P. & Lecointre G. (2002) When does the incongruence length difference test fail? *Molecular Biology and Evolution*, **19**, 432–437.

Darriba D., Taboada G.L., Doallo R., & Posada D. (2012) jModelTest 2: more models, new heuristics and parallel computing. *Nature Methods*, **9**, 772.

DeForest Safford H. (2007) Brazilian Páramos IV. Phytogeography of the campos de altitude. *Journal of Biogeography*, **34**, 1701–1722.

Degnan J.H. & Rosenberg N.A. (2009) Gene tree discordance, phylogenetic inference and the multispecies coalescent. *Trends in Ecology & Evolution*, **24**, 332–340.

Derieg N.J., Weil S.J., Reznicek A.A., & Bruederle L.P. (2013) *Carex viridistellata* sp. nov. (Cyperaceae), a new cryptic species from Prairie Fens of the Eastern United States. *Systematic Botany*, **38**, 82–91.

Dietz R.S. & Holden J.C. (1970) Reconstruction of Pangaea: Breakup and dispersion of continents, Permian to Present. *Journal of Geophysical Research*, **75**, 4939–4956.

Donoghue M.J. (2008) A phylogenetic perspective on the distribution of plant diversity. *Proceedings of the National Academy of Sciences of the United States of America*, **105**, 11549–11555.

Donoghue M.J. & Edwards E.J. (2014) Biome Shifts and Niche Evolution in Plants. *Annual Review of Ecology, Evolution, and Systematics*, **45**, 547–572.

Donoghue M.J. & Sanderson M.J. (2015) Confluence, synnovation, and depauperons in plant diversification. *New Phytologist*, **207**, 260–274.

Dorofeev P.I. (1960) On the Tertiary flora of Belorussia. *Botanichesky Zhurnal*, **45**, 1418–1434.

Dorofeev P.I. (1963) *The Tertiary floras of western Siberia.* Izdatelstvo Akademii Nauk, Moskva-Leningrad.

Dorofeev P.I. (1988) *Miocene floras of the Tambov district.* Akademii Nauk, Leningrad.

Douady C.J., Delsuc F., Boucher Y., Doolittle W.F., & Douzery E.J.P. (2003) Comparison of Bayesian and Maximum Likelihood Bootstrap Measures of Phylogenetic Reliability. *Molecular Biology and Evolution*, **20**, 248–254.

Doyle J. & Doyle J.L. (1990) Isolation of plant DNA from fresh tissue. *Focus*, **12**, 13–15.

Drummond A.J. & Bouckaert R.R. (2015) *Bayesian Evolutionary Analysis with BEAST*. Cambridge University Press, Cambridge.

Drummond A.J. & Rambaut A. (2007) BEAST: Bayesian evolutionary analysis by sampling trees. *BMC Evolutionary Biology*, **7**, 214–8.

Drummond A.J., Ho S.Y.W., Phillips M.J., & Rambaut A. (2006) Relaxed Phylogenetics and Dating with Confidence. *PLoS Biology*, **4**, e88–12.

Drummond C.S., Eastwood R.J., Miotto S.T.S., & Hughes C.E. (2012) Multiple continental radiations and correlates of diversification in *Lupinus* (Leguminosae): testing for key innovation with incomplete taxon sampling. *Systematic Biology*, **61**, 443–460.

Dumolin-Lapègue S., Demesure B., Fineschi S., Le Corre V., & Petit R.J. (1997) Phylogeographic structure of white oaks throughout the European continent. *Genetics*, **146**, 1475–1487.

Dupanloup I., Schneider S., & Excoffier L. (2002) A simulated annealing approach to define the genetic structure of populations. *Molecular Ecology*, **11**, 2571–2581.

Dyjor S., Kvacek Z., & Lanucka-Srodoniowa M. (1992) The younger tertiary deposits in the Gozdnica Region (SW Poland) in the light of recent palaeobotanical research. *Polish Botanical Studies*, **3**, 1–129.

Dynesius M. & Jansson R. (2000) Evolutionary consequences of changes in species' geographical distributions driven by Milankovitch climate oscillations. *Proceedings of the National Academy of Sciences of the United States of America*, **97**, 9115–9120.

Edgar R.C. (2004) MUSCLE: multiple sequence alignment with high accuracy and high throughput. *Nucleic Acids Research*, **32**, 1792–1797.

Ellstrand N.C. (2014) Is gene flow the most important evolutionary force in plants? *American Journal of Botany*, **101**, 737–753.

Ennos R.A. (1994) Estimating the relative rates of pollen and seed migration among plant populations. *Heredity*, **72**, 250–259.

Erixon P., Svennblad B., Britton T., & Oxelman B. (2003) Reliability of Bayesian Posterior Probabilities and Bootstrap Frequencies in Phylogenetics. *Systematic Biology*, **52**, 665–673.

Escudero M. & Hipp A. (2013) Shifts in diversification rates and clade ages explain species richness in higher-level sedge taxa (Cyperaceae). *American Journal of Botany*, **100**, 2403–2411.

Escudero M., Eaton D.A.R., Hahn M., & Hipp A.L. (2014) Genotyping-by-sequencing as a tool to infer phylogeny and ancestral hybridization: A case study in *Carex* (Cyperaceae). *Molecular Phylogenetics and Evolution*, **79**, 359–367.

Excoffier L. & Lischer H.E.L. (2010) Arlequin suite ver 3.5: a new series of programs to perform population genetics analyses under Linux and Windows. *Molecular Ecology Resources*, **10**, 564–567.

Fairon-Demaret M. (1996) Les fruits et graines du Miocène de Bioul (Entre-Sambre-et-Meuse, Belgique). Etude qualitative, quantitative et considérations paléoécologiques. *Annales de la Société géologique de Belgique*, **117**, 277–309.

Felsenstein J. (1981) Evolutionary trees from DNA sequences: a maximum likelihood approach. *Journal of molecular evolution*, **17**, 368–376.

Flantua S.G., Hooghiemstra H., van Boxel J.H., Cabrera M., González-Carranza Z., & González-Arango C. (2014) Connectivity dynamics since the Last Glacial Maximum in the northern Andes: a pollen-driven framework to assess potential migration. *Paleobotany and biogeography: a festschrift for Alan*

Graham in his 80th year (ed. by P.H. Raven, O.M. Montiel, and W.D. Stevens), pp. 98–123. Missouri Botanical Garden, St. Louis

French G.C. (2003) *Conservation genetics of British Euphrasia L.* University of Edinburgh and Royal Botanic Garden Edinburgh, Edinburgh.

Fritsch P.W., Almeda F., Renner S.S., Martins A.B., & Cruz B.C. (2004) Phylogeny and circumscription of the near-endemic Brazilian tribe Microlicieae (Melastomataceae). *American Journal of Botany*, **91**, 1105–1114.

Gandolfo M.A., Nixon K.C., & Crepet W.L. (2008) Selection of fossils for calibration of molecular dating models. *Annals of the Missouri Botanical Garden*, **95**, 34–42.

Garzione C.N., Hoke G.D., Libarkin J.C., Withers S., MacFadden B., Eiler J., Ghosh P., & Mulch A. (2008) Rise of the Andes. *Science*, **320**, 1304–1307.

Gentry A.H. (1982) Neotropical floristic diversity: phytogeographical connections between Central and South America, Pleistocene climatic fluctuations, or an accident of the Andean orogeny? *Annals of the Missouri Botanical Garden*, **69**, 557–593.

Gernhard T. (2008) The conditioned reconstructed process. *Journal of Theoretical Biology*, **253**, 769–778.

Gizaw A., Kebede M., Nemomissa S., Ehrich D., Bekele B., Mirré V., Popp M., & Brochmann C. (2013) Phylogeography of the heathers *Erica arborea* and *E. trimera* in the afro-alpine "sky islands" inferred from AFLPs and plastid DNA sequences. *Flora*, **208**, 453–463.

Gizaw A., Wondimu T., Mugizi T.F., Masao C.A., Abdi A.A., Popp M., Ehrich D., Nemomissa S., & Brochmann C. (2016) Vicariance, dispersal, and hybridization in a naturally fragmented system: the afro-alpine endemics *Carex monostachya* and *C. runssoroensis* (Cyperaceae). *Alpine Botany*, **126**, 59–71.

Goetghebeur P. (1998) Cyperaceae. *Flowering Plants. Monocotyledons* (ed. by K. Kubitzki), pp. 141–190. Springer Berlin Heidelberg, Berlin.

Goloboff P.A., Farris J.S., & Nixon K.C. (2008) TNT, a free program for phylogenetic analysis. *Cladistics*, **24**, 774–786.

Goudet J. (2005) Hierfstat, a package for R to compute and test hierarchical F-statistics. *Molecular Ecology Notes*, **5**, 184–186.

Graham A. (2009) The Andes: a geological overview from a biological perspective. *Annals of the Missouri Botanical Garden*, **96**, 371–385.

Gregory-Wodzicki K.M. (2000) Uplift history of the Central and Northern Andes: A review. *Geological Society of America Bulletin*, **112**, 1091–1105.

Griffin P.C. & Hoffmann A.A. (2014) Limited genetic divergence among Australian alpine *Poa* tussock grasses coupled with regional structuring points to ongoing gene flow and taxonomic challenges. *Annals of Botany*, **113**, 953–965.

Guindon S. & Gascuel O. (2003) A Simple, fast, and accurate algorithm to estimate large phylogenies by maximum likelihood. *Systematic Biology*, **52**, 696–704.

Haffer J. (1969) Speciation in Amazonian forest birds. *Science*, **165**, 131–137.

Hartley A.J. (2003) Andean uplift and climate change. *Journal of the Geological Society*, **160**, 7–10.

Hedberg O. (1964) Features of Afroalpine plant ecology. *Acta Phytogeographica Suecica*, **48**, 1–144.

Heled J. & Drummond A.J. (2010) Bayesian inference of species trees from multilocus data. *Molecular Biology and Evolution*, **27**, 570–580.

Hewitt G.M. (2004) Genetic consequences of climatic oscillations in the Quaternary. *Philosophical Transactions of the Royal Society B: Biological Sciences*, **359**, 183–195.

Hickey L.J. (1977) *Stratigraphy and Paleobotany of the Golden Valley Formation (Early Tertiary) of Western North Dakota.* Geological Society of America, Boulder.

Ho S.Y.W. & Phillips M.J. (2009) Accounting for calibration uncertainty in phylogenetic estimation of evolutionary divergence times. *Systematic Biology*, **58**, 367–380.

Hodges S.A. & Arnold M.L. (1994) Columbines: a geographically widespread species flock. *Proceedings of the National Academy of Sciences*, **91**, 5129–5132.

Honorio Coronado E.N., Dexter K.G., Poelchau M.F., Hollingsworth P.M., Phillips O.L., & Pennington R.T. (2014) *Ficus insipida* subsp. *insipida* (Moraceae) reveals the role of ecology in the phylogeography of widespread Neotropical rain forest tree species. *Journal of Biogeography*, **41**, 1697–1709.

Hooghiemstra H. & van der Hammen T. (2004) Quaternary Ice-Age dynamics in the Colombian Andes: developing an understanding of our legacy. *Philosophical Transactions of the Royal Society B: Biological Sciences*, **359**, 173–181.

Hooghiemstra H., Wijninga V.M., & Cleef A.M. (2006) The paleobotanical record of Colombia: implications for biogeography and biodiversity. *Annals of the Missouri Botanical Garden*, **93**, 297–324.

Hoorn C., Wesselingh F.P., Steege ter H., Bermudez M.A., Mora A., Sevink J., Sanmartín I., Sanchez-Meseguer A., Anderson C.L., Figueiredo J.P., Jaramillo C., Riff D., Negri F.R., Hooghiemstra H., Lundberg J., Stadler T., Särkinen T., & Antonelli A. (2010) Amazonia through time: Andean uplift, climate change, landscape evolution, and biodiversity. *Science*, **330**, 927–931.

Huelsenbeck J.P., Larget B., & Swofford D. (2000) A compound poisson process for relaxing the molecular clock. *Genetics*, **154**, 1879–1892.

Huelsenbeck J.P., Ronquist F., Nielsen R., & Bollback J.P. (2001) Bayesian inference of phylogeny and its impact on evolutionary biology. *Science*, **294**, 2310–2314.

Hughes C. & Eastwood R. (2006) Island radiation on a continental scale: exceptional rates of plant diversification after uplift of the Andes. *Proceedings of the National Academy of Sciences of the United States of America*, **103**, 10334–10339.

Hughes C.E. & Atchison G.W. (2015) The ubiquity of alpine plant radiations: from the Andes to the Hengduan Mountains. *New Phytologist*, **207**, 275–282.

Hurlbert A.H. & Stegen J.C. (2014) When should species richness be energy limited, and how would we know? *Ecology Letters*, **17**, 401–413.

Huson D.H. & Bryant D. (2006) Application of phylogenetic networks in evolutionary studies. *Molecular Biology and Evolution*, **23**, 254–267.

Jakob S.S. & Blattner F.R. (2006) A chloroplast genealogy of *Hordeum* (Poaceae): long-term persisting haplotypes, incomplete lineage sorting, regional extinction, and the consequences for phylogenetic inference. *Molecular Biology and Evolution*, **23**, 1602–1612.

Jung J. & Choi H.-K. (2013) Recognition of two major clades and early diverged groups within the subfamily Cyperoideae (Cyperaceae) including Korean sedges. *Journal of Plant Research*, **126**, 335–349.

Kadereit J.W. & Hagen von K.B. (2003) The Evolution of Flower Morphology in Gentianaceae - Swertiinae and the Roles of Key Innovations and Niche Width for the Diversification of *Gentianella* and *Halenia* in South America. *International Journal of Plant Sciences*, **164**, S441–S452.

Kadu C.A.C., Konrad H., Schueler S., Muluvi G.M., Eyog-Matig O., Muchugi A., Williams V.L., Ramamonjisoa L., Kapinga C., Foahom B., Katsvanga C., Hafashimana D., Obama C., & Geburek T. (2013) Divergent pattern of nuclear genetic diversity across the range of the Afromontane *Prunus africana* mirrors variable climate of African highlands. *Annals of Botany*, **111**, 47–60.

Kebede M., Ehrich D., Taberlet P., Nemomissa S., & Brochmann C. (2007) Phylogeography and conservation genetics of a giant lobelia (*Lobelia giberroa*) in Ethiopian and Tropical East African mountains. *Molecular Ecology*, **16**, 1233–1243.

Kendall D.G. (1949) Stochastic processes and population growth. *Journal of the Royal Statistical Society Series B (Statistical Methodology)*, **11**, 230–264.

Knapp M., Stöckler K., Havell D., Delsuc F., Sebastiani F., & Lockhart P.J. (2005) Relaxed Molecular Clock Provides Evidence for Long-Distance Dispersal of *Nothofagus* (Southern Beech). *PLoS Biology*, **3**, 0038–0043.

Knowles L.L. & Carstens B.C. (2007) Delimiting Species without Monophyletic Gene Trees. *Systematic Biology*, **56**, 887–895.

Koyama T. (1961) Classification of the family Cyperaceae 1. *Journal of the Faculty of Science, University of Tokyo*, **8**, 37–148.

Landis M.J., Matzke N.J., Moore B.R., & Huelsenbeck J.P. (2013) Bayesian Analysis of Biogeography when the Number of Areas is Large. *Systematic Biology*, **62**, 789–804.

Lomolino M.V., Riddle B.R., & Brown J.H. (2006) *Biogeography.* Sinauer Associates, Inc, Sunderland.

Losos J.B. (2008) Phylogenetic niche conservatism, phylogenetic signal and the relationship between phylogenetic relatedness and ecological similarity among species. *Ecology Letters*, **11**, 995–1003.

Luebert F. & Weigend M. (2014) Phylogenetic insights into Andean plant diversification. *Frontiers in Ecology and Evolution*, **2**, 1–17.

Luteyn J.L. (1999) *Páramos: a checklist of plant diversity, geographical distribution, and botanical literature.* The New York Botanical Garden Press, New York.

Maddison W.P. (1997) Gene Trees in Species Trees. *Systematic Biology*, **46**, 523–536.

Maddison W.P. & Knowles L.L. (2006) Inferring phylogeny despite incomplete lineage sorting. *Systematic Biology*, **55**, 21–30.

Maddison W.P. & Maddison D.R. (2014) Mesquite: a modular system for evolutionary analysis version 2.75. Available at: http://mesquiteproject.org.

Madriñán S., Cortés A.J., & Richardson J.E. (2013) Páramo is the world's fastest evolving and coolest biodiversity hotspot. *Frontiers in Genetics*, **4**, 1–7.

Magallón S. & Castillo A. (2009) Angiosperm diversification through time. *American Journal of Botany*, **96**, 349–365.

Magallón S. & Sanderson M.J. (2001) Absolute diversification rates in Angiosperm clades. *Evolution*, **55**, 1762–1780.

Mai D.H. (2000) Die untermiozänen Floren aus der Spremberger Folge und dem II. Flözhorizont in der Lausitz. Teil III: Dialypetalae und Sympetalae. *Palaeontographica Abteilung B*, **253**, 1–106.

Markgraf V., McGlone M., & Hope G. (1995) Neogene paleoenvironmental and paleoclimatic change in southern temperate ecosystems—a southern perspective. *Trends in Ecology & Evolution*, **10**, 143–147.

Marko P.B. & Hart M.W. (2011) The complex analytical landscape of gene flow inference. *Trends in Ecology & Evolution*, **26**, 448–456.

Martins A.C., Scherz M.D., & Renner S.S. (2014) Several origins of floral oil in the Angelonieae, a southern hemisphere disjunct clade of Plantaginaceae. *American Journal of Botany*, **101**, 2113–2120.

Mayr E. (1995) Species, classification, and evolution. *Biodiversity and Evolution* (ed. by R. Arai, M. Kato, and Y. Doi), pp. 3–12. Biodiversity and Evolution. National Science Museum Foundation, Tokyo.

McLoughlin S. (2001) The breakup history of Gondwana and its impact on pre-Cenozoic floristic provincialism. *Australian Journal of Botany*, **49**, 271–300.

McPeek M.A. & Brown J.M. (2007) Clade Age and Not Diversification Rate Explains Species Richness among Animal Taxa. *The American Naturalist*, **169**, E97–E106.

Michelangeli F.A., Guimaraes P.J.F., Penneys D.S., Almeda F., & Kriebel R. (2013) Phylogenetic relationships and distribution of New World Melastomeae (Melastomataceae). *Botanical Journal of the Linnean Society*, **171**, 38–60.

Michelangeli F.A., Judd W.S., Penneys D.S., Skean J.D. Jr., Bécquer-Granados E.R., Goldenberg R., & Martin C.V. (2008) Multiple Events of Dispersal and Radiation of the Tribe Miconieae (Melastomataceae) in the Caribbean. *The Botanical Review*, **74**, 53–77.

Midgley G.F., Reeves G., & Klak C. (2005) Late Tertiary and Quaternary climate change and centres of endemism in the Southern African flora. *Phylogeny and Conservation* (ed. by A. Purvis, J.L. Gittleman, and T. Brooks), pp. 230–242. Cambridge University Press, New York.

Miller M.A., Pfeiffer W., & Schwartz T. (2010) Creating the CIPRES Science Gateway for inference of large phylogenetic trees. *Proceedings of the Gateway Computing Environments Workshop (GCE)*, 1–8.

Möller M. & Cronk Q.C.B. (1997) Origin and relationships of *Saintpaulia* (Gesneriaceae) based on ribosomal DNA internal transcribed spacer (ITS) sequences. *American Journal of Botany*, **84**, 956–965.

Moore D.M. (1967) Chromosome numbers of Falkland Islands Angiosperms. *British Antarctic Survey Bulletin*, **14**, 69–82.

Mora A., Baby P., Roddaz M., Parra M., Brusset S., Hermoza W., & Espurt N. (2010) Tectonic history of the Andes and sub-Andean zones: implications for the development of the Amazon drainage basin. *Amazonia: landscape and species evolution* (ed. by C. Hoorn and F.P. Wesselingh), pp. 38–60. Blackwell Publishing Ltd, Oxford.

Mora-Osejo L.E. (1987) *Estudios morfológicos, autoecológicos y sistemáticos en Angiospermas.* Academia Colombiana de Ciencias Exactas, Físicas y Naturales, Bogotá, DE.

Moran P.A. (1951) Estimation methods for evolutive processes. *Journal of the Royal Statistical Society Series B (Statistical Methodology)*, **13**, 141–146.

Muasya A.M., Simpson D.A., Verboom G.A., Goetghebeur P., Naczi R.F.C., Chase M.W., & Smets E. (2009) Phylogeny of Cyperaceae Based on DNA Sequence Data: Current Progress and Future Prospects. *The Botanical Review*, **75**, 2–21.

Myers N., Mittermeier R.A., Mittermeier C.G., da Fonseca G.A.B., & Kent J. (2000) Biodiversity hotspots for conservation priorities. *Nature*, **403**, 853–858.

Naciri Y. & Linder H.P. (2015) Species delimitation and relationships: The dance of the seven veils. *Taxon*, **64**, 3–16.

Naciri Y., Caetano S., & Salamin N. (2012) Plant DNA barcodes and the influence of gene flow. *Molecular Ecology Resources*, **12**, 575–580.

Nixon K.C. (1999) The parsimony ratchet, a new method for rapid parsimony analysis. *Cladistics*, **15**, 407–414.

Pagani M., Arthur M.A., & Freeman K.H. (2000) Variations in Miocene phytoplankton growth rates in the southwest Atlantic: evidence for changes in ocean circulation. *Paleoceanography*, **15**, 486–496.

Peirson J.A., Dick C.W., & Reznicek A.A. (2013) Phylogeography and polyploid evolution of North American goldenrods (*Solidago* subsect. *Humiles*, Asteraceae). *Journal of Biogeography*, **40**, 1887–1898.

Pennington R.T. & Dick C.W. (2004) The role of immigrants in the assembly of the South American rainforest tree flora. *Philosophical Transactions of the Royal Society B: Biological Sciences*, **359**, 1611–1622.

Petit R.J., Aguinagalde I., de Beaulieu J.-L., Bittkau C., Brewer S., Cheddadi R., Ennos R., Fineschi S., Grivet D., Lascoux M., Mohanty A., Müller-Starck G., Demesure-Musch B., Palmé A., Martín J.P., Rendell S., & Vendramin G.G. (2003) Glacial refugia: hotspots but not melting pots of genetic diversity. *Science*, **300**, 1563–1565.

Piqué A. (1999) L'évolution géologique de Madagascar et la dislocation du Gondwana: une introduction. *Journal of African Earth Sciences*, **28**, 919–930.

Pons O. & Petit R.J. (1996) Measuring and testing genetic differentiation with ordered versus unordered alleles. *Genetics*, **144**, 1237–1245.

R Core Team (2015) R: A language and environment for statistical computing. R Foundation for Statistical Computing, Vienna, Austria. Available at https://www.R-project.org/.

Rabosky D.L. & Lovette I.J. (2008) Explosive evolutionary radiations: decreasing speciation or increasing extinction through time? *Evolution*, **62**, 1866–1875.

Rabosky D.L., Slater G.J., & Alfaro M.E. (2012) Clade age and species richness are decoupled across the eukaryotic Tree of Life. *PLoS Biology*, **10**, e1001381.

Rambaut A. (2014) FigTree: Tree Figure Drawing Tool version 1.4.2. Available at: http://tree.bio.ed.ac.uk/software/figtree.

Rambaut A. & Drummond A.J. (2015) TreeAnnotator: MCMC Output Analysis version 2.3.0. Available at: http://tree.bio.ed.ac.uk/software/beast.

Rambaut A., Suchard M.A., Xie W., & Drummond A.J. (2013) Tracer: MCMC Trace Analysis Tool version 1.6.0. Available at: http://tree.bio.ed.ac.uk/software/tracer.

Ramírez M.J. (2006) Further problems with the incongruence length difference test: "hypercongruence" effect and multiple comparisons. *Cladistics*, **22**, 289–295.

Rauscher J.T. (2002) Molecular phylogenetics of the *Espeletia* complex (Asteraceae): evidence from nrDNA ITS sequences on the closest relatives of an Andean adaptive radiation. *American Journal of Botany*, **89**, 1074–1084.

Raven P.H. & Axelrod D.I. (1974) Angiosperm biogeography and past continental movements. *Annals of the Missouri Botanical Garden*, **61**, 539–673.

Ree R.H. & Smith S.A. (2008) Maximum Likelihood Inference of Geographic Range Evolution by Dispersal, Local Extinction, and Cladogenesis. *Systematic Biology*, **57**, 4–14.

Ree R.H., Moore B.R., Webb C.O., & Donoghue M.J. (2005) A likelihood framework for inferring the evolution of geographic range on phylogenetic trees. *Evolution*, **59**, 2299–2311.

Reginato M., Michelangeli F.A., & Goldenberg R. (2010) Phylogeny of *Pleiochiton* (Melastomataceae, Miconieae): total evidence. *Botanical Journal of the Linnean Society*, **162**, 423–434.

Renner S.S. (1993) Phylogeny and classification of the Melastomataceae and Memecylaceae. *Nordic Journal of Botany*, **13**, 519–540.

Renner S.S. (2004) Bayesian analysis of combined chloroplast loci, using multiple calibrations, supports the recent arrival of Melastomataceae in Africa and Madagascar. *American Journal of Botany*, **91**, 1427–1435.

Renner S.S. (2005) Relaxed molecular clocks for dating historical plant dispersal events. *Trends in Plant Science*, **10**, 550–558.

Renner S.S. & Meyer K. (2001) Melastomeae come full circle: biogeographic reconstruction and molecular clock dating. *Evolution*, **55**, 1315–1324.

Renner S.S., Clausing G., & Meyer K. (2001) Historical biogeography of Melastomataceae: the roles of Tertiary migration and long-distance dispersal. *American Journal of Botany*, **88**, 1290–1300.

Renner S.S., Foreman D.B., & Murray D. (2000) Timing transantarctic disjunctions in the Atherospermataceae (Laurales): evidence from coding and noncoding chloroplast sequences. *Systematic Biology*, **49**, 579–591.

Renner S.S., Strijk J.S., Strasberg D., & Thébaud C. (2010) Biogeography of the Monimiaceae (Laurales): a role for East Gondwana and long-distance dispersal, but not West Gondwana. *Journal of Biogeography*, **37**, 1227–1238.

Richards P.W. (1973) Africa, the "Odd Man Out." *Tropical forest ecosystems in Africa and South America a comparative review* (ed. by B.J. Meggers, E.S. Ayensu, and W.D. Duckworth), pp. 1–26. Smithsonian Inst. Press, Washington.

Richardson J.E., Pennington R.T., Pennington T.D., & Hollingsworth P.M. (2001) Rapid diversification of a species-rich genus of Neotropical rain forest trees. *Science*, **293**, 2242–2245.

Rohde K. (1992) Latitudinal gradients in species diversity: the search for the primary cause. *Oikos*, **65**, 514–527.

Romdal T.S., Araújo M.B., & Rahbek C. (2012) Life on a tropical planet: niche conservatism and the global diversity gradient. *Global Ecology and Biogeography*, **22**, 344–350.

Ronquist F. (1997) Dispersal-Vicariance Analysis: A New Approach to the Quantification of Historical Biogeography. *Systematic Biology*, **46**, 195–203.

Ronquist F. & Huelsenbeck J.P. (2003) MrBayes 3: Bayesian phylogenetic inference under mixed models. *Bioinformatics*, **19**, 1572–1574.

Ronquist F., Teslenko M., van der Mark P., Ayres D.L., Darling A., Höhna S., Larget B., Liu L., Suchard M.A., & Huelsenbeck J.P. (2012) MrBayes 3.2: efficient Bayesian phylogenetic inference and model choice across a large model space. *Systematic Biology*, **61**, 539–542.

Rosenzweig M.L. (1995) *Species Diversity in Space and Time.* Cambridge University Press, Cambridge.

Rull V. (2011) Neotropical biodiversity: timing and potential drivers. *Trends in Ecology & Evolution*, **26**, 508–513.

Sanderson M.J. (1997) A nonparametric approach to estimating divergence times in the absence of rate constancy. *Molecular Biology and Evolution*, **14**, 1218–1231.

Sang T., Crawford D., & Stuessy T. (1997) Chloroplast DNA phylogeny, reticulate evolution, and biogeography of *Paeonia* (Paeoniaceae). *American Journal of Botany*, **84**, 1120–1136.

Sanmartín I. & Ronquist F. (2004) Southern Hemisphere Biogeography Inferred by Event-Based Models: Plant versus Animal Patterns. *Systematic Biology*, **53**, 216–243.

Sanmartín I., Wanntorp L., & Winkworth R.C. (2007) West Wind Drift revisited: testing for directional dispersal in the Southern Hemisphere using event-based tree fitting. *Journal of Biogeography*, **34**, 398–416.

Särkinen T., Pennington R.T., Lavin M., Simon M.F., & Hughes C.E. (2011) Evolutionary islands in the Andes: persistence and isolation explain high endemism in Andean dry tropical forests. *Journal of Biogeography*, **39**, 884–900.

Sarmiento G. (1986) Ecological features of climate in high tropical mountains. *High Altitude Tropical Biogeography* (ed. by F. Vuilleumier and M. Monasterio), pp. 11–45. Oxford University Press, New York.

Sauquet H. (2013) A practical guide to molecular dating. *Comptes Rendus Palevol*, **12**, 355–367.

Savolainen V., Anstett M.-C., Lexer C., Hutton I., Clarkson J.J., Norup M.V., Powell M.P., Springate D., Salamin N., & Baker W.J. (2006) Sympatric speciation in palms on an oceanic island. *Nature*, **441**, 210–213.

Schaal B.A. & Olsen K.M. (2000) Gene genealogies and population variation in plants. *Proceedings of the National Academy of Sciences of the United States of America*, **97**, 7024–7029.

Schaal B.A., Hayworth D.A., Olsen K.M., Rauscher J.T., & Smith W.A. (1998) Phylogeographic studies in plants: problems and prospects. *Molecular Ecology*, **7**, 465–474.

Schemske D.W. (2009) Biotic interactions and speciation in the tropics. *Speciation and Patterns of Diversity* (ed. by R.K. Butlin, J.R. Bridle, and D. Schutler), pp. 219–239. Cambridge University Press, Cambridge.

Schwarz G. (1978) Estimating the Dimension of a Model. *The Annals of Statistics*, **6**, 461–464.

Scotland R.W. & Sanderson M.J. (2004) The significance of few versus many in the tree of life. *Science*, **303**, 643–643.

Seberg O. (1988) Taxonomy, phylogeny, and biogeography of the genus *Oreobolus* R.Br. (Cyperaceae), with comments on the biogeography of the South Pacific continents. *Botanical Journal of the Linnean Society*, **96**, 119–195.

Shaw J., Lickey E.B., Beck J.T., Farmer S.B., Liu W., Miller J., Siripun K.C., Winder C.T., Schilling E.E., & Small R.L. (2005) The tortoise and the hare II: relative utility of 21 noncoding chloroplast DNA sequences for phylogenetic analysis. *American Journal of Botany*, **92**, 142–166.

Shaw J., Lickey E.B., Schilling E.E., & Small R.L. (2007) Comparison of whole chloroplast genome sequences to choose noncoding regions for phylogenetic studies in Angiosperms: the tortoise and the hare III. *American Journal of Botany*, **94**, 275–288.

Shevenell A.E., Kennett J.P., & Lea D.W. (2004) Middle Miocene Southern Ocean Cooling and Antarctic Cryosphere Expansion. *Science*, **305**, 1766–1770.

Siegert M.J. (2008) Antarctic subglacial topography and ice-sheet evolution. *Earth Surface Processes and Landforms*, **33**, 646–660.

Silvertown J., McConway K., Gowing D., Dodd M., Fay M.F., Joseph J.A., & Dolphin K. (2006) Absence of phylogenetic signal in the niche structure of meadow plant communities. *Proceedings of the Royal Society B: Biological Sciences*, **273**, 39–44.

Simpson B.B. (1975) Pleistocene changes in the flora of the high tropical Andes. *Paleobiology*, **1**, 273–294.

Simpson B.B. & Todzia C.A. (1990) Patterns and processes in the development of the high Andean flora. *American Journal of Botany*, **77**, 1419–1432.

Sklenář P., Dušková E., & Balslev H. (2011) Tropical and Temperate: evolutionary history of Páramo flora. *The Botanical Review*, **77**, 71–108.

Sklenář P., Hedberg I., & Cleef A.M. (2014) Island biogeography of tropical alpine floras. *Journal of Biogeography*, **41**, 287–297.

Sklenář P., Kučerová A., Macek P., & Macková J. (2012) The frost-resistance mechanism in páramo plants is related to geographic origin. *New Zealand Journal of Botany*, **50**, 391–400.

Sklenář P., Luteyn J.L., Ulloa C.U., Jorgensen P.M., & Dillon M.O. (2005) *Flora genérica de los páramos.* The New York Botanical Garden Press, New York.

Slingsby J.A., Britton M.N., & Verboom G.A. (2014) Ecology limits the diversity of the Cape flora: Phylogenetics and diversification of the genus *Tetraria*. *Molecular Phylogenetics and Evolution*, **72**, 61–70.

Smith J. & Cleef A.M. (1988) Composition and origins of the world's tropicalpine floras. *Journal of Biogeography*, **15**, 631–645.

Smith S.Y., Collinson M.E., Simpson D.A., Rudall P.J., Marone F., & Stampanoni M. (2009) Elucidating the affinities and habitat of ancient, widespread Cyperaceae: *Volkeria messelensis* gen. et sp. nov., a fossil mapanioid sedge from the Eocene of Europe. *American Journal of Botany*, **96**, 1506–1518.

Solt M.L. & Wurdack J.J. (1980) Chromosome numbers in the Melastomataceae. *Phytologia*, **47**, 199–220.

Stamatakis A. (2014) RAxML version 8: a tool for phylogenetic analysis and post-analysis of large phylogenies. *Bioinformatics*, **30**, 1312–1313.

Starr J.R., Harris S.A., & Simpson D.A. (2003) Potential of the 5′ and 3′ Ends of the Intergenic Spacer (IGS) of rDNA in the Cyperaceae: New Sequences for Lower - Level Phylogenies in Sedges with an Example from *Uncinia* Pers. *International Journal of Plant Sciences*, **164**, 213–227.

Sun Y., He X., & Glenny D. (2014) Transantarctic disjunctions in Schistochilaceae (Marchantiophyta) explained by early extinction events, post-Gondwanan radiations and palaeoclimatic changes. *Molecular Phylogenetics and Evolution*, **76**, 189–201.

Swenson U. & Bremer K. (1997) Pacific biogeography of the Asteraceae genus *Abrotanella* (Senecioneae, Blennospermatinae). *Systematic Botany*, **22**, 493–508.

Taberlet P., Gielly L., Pautou G., & Bouvet J. (1991) Universal primers for amplification of three non-coding regions of chloroplast DNA. *Plant Molecular Biology*, **17**, 1105–1109.

Tate J.A. & Simpson B.B. (2003) Paraphyly of *Tarasa* (Malvaceae) and diverse origins of the polyploid species. *Systematic Botany*, **28**, 723–737.

Teacher A.G.F. & Griffiths D.J. (2011) HapStar: automated haplotype network layout and visualization. *Molecular Ecology Resources*, **11**, 151–153.

Templeton A.R. (1998) Nested clade analyses of phylogeographic data: testing hypotheses about gene flow and population history. *Molecular Ecology*, **7**, 381–397.

Tremetsberger K., Urtubey E., Terrab A., Baeza C.M., Ortiz M.Á., Talavera M., König C., Temsch E.M., Kohl G., Talavera S., & Stuessy T.F. (2009) Pleistocene refugia and polytopic replacement of diploids by tetraploids in the Patagonian and Subantarctic plant *Hypochaeris incana* (Asteraceae, Cichorieae). *Molecular Ecology*, **18**, 3668–3682.

Turchetto-Zolet A.C., Pinheiro F., Salgueiro F., & Palma-Silva C. (2013) Phylogeographical patterns shed light on evolutionary process in South America. *Molecular Ecology*, **22**, 1193–1213.

van der Hammen T. (1974) The Pleistocene changes of vegetation and climate in tropical South America. *Journal of Biogeography*, **1**, 3–26.

van der Hammen T. & Cleef A.M. (1986) Development of the high Andean Páramo flora and vegetation. *High Altitude Tropical Biogeography* (ed. by F. Vuilleumier and M. Monasterio), pp. 153–201. Oxford University Press, New York.

Verboom G.A. (2006) A phylogeny of the schoenoid sedges (Cyperaceae: Schoeneae) based on plastid DNA sequences, with special reference to the genera found in Africa. *Molecular Phylogenetics and Evolution*, **38**, 79–89.

Verboom G.A., Linder H.P., Forest F., Hoffmann V., Bergh N.G., & Cowling R.M. (2014) Cenozoic assembly of the Greater Cape flora. *Fynbos: Ecology, Evolution, and Conservation of a Megadiverse Region* (ed. by N. Allsopp, J.F. Colville, and G.A. Verboom), pp. 93–118. Oxford University Press, Oxford.

Viljoen J.-A., Muasya A.M., Barrett R.L., Bruhl J.J., Gibbs A.K., Slingsby J.A., Wilson K.L., & Verboom G.A. (2013) Radiation and repeated transoceanic dispersal of Schoeneae (Cyperaceae) through the southern hemisphere. *American Journal of Botany*, **100**, 2494–2508.

Weir J.T. & Schluter D. (2007) The latitudinal gradient in recent speciation and extinction rates of birds and mammals. *Science*, **315**, 1574–1576.

White F. (1981) The history of the Afromontane archipelago and the scientific need for its conservation. *African Journal of Ecology*, **19**, 33–54.

Wiens J.J. & Graham C.H. (2005) Niche Conservatism: Integrating Evolution, Ecology, and Conservation Biology. *Annual Review of Ecology, Evolution, and Systematics*, **36**, 519–539.

Wiens J.J., Ackerly D.D., Allen A.P., Anacker B.L., Buckley L.B., Cornell H.V., Damschen E.I., Jonathan Davies T., Grytnes J.-A., Harrison S.P., Hawkins B.A., Holt R.D., McCain C.M., & Stephens P.R. (2010) Niche conservatism as an emerging principle in ecology and conservation biology. *Ecology Letters*, **13**, 1310–1324.

Wilmé L., Goodman S.M., & Ganzhorn J.U. (2006) Biogeographic evolution of Madagascar's microendemic biota. *Science*, **312**, 1063–1065.

Winkworth R.C., Hennion F., Prinzing A., & Wagstaff S.J. (2015) Explaining the disjunct distributions of austral plants: the roles of Antarctic and direct dispersal routes. *Journal of Biogeography*, **42**, 1197–1209.

Wondimu T., Gizaw A., Tusiime F.M., Masao C.A., Abdi A.A., Gussarova G., Popp M., Nemomissa S., & Brochmann C. (2013) Crossing barriers in an extremely fragmented system: two case studies in the afro-alpine sky island flora. *Plant Systematics and Evolution*, **300**, 415–430.

Wright D.H. (1983) Species-energy theory: an extension of species-area theory. *Oikos*, **41**, 496–506.

Wurdack J.J. (1953) A revision of the genus *Brachyotum* (Tibouchineae–Melastomataceae). *Memoirs of the New York Botanical Garden*, **8**, 343–407.

Yang Z. (1994) Maximum likelihood phylogenetic estimation from DNA sequences with variable rates over sites: approximate methods. *Journal of molecular evolution*, **39**, 306–314.

Yu Y., Harris A.J., Blair C., & He X. (2015) RASP (Reconstruct Ancestral State in Phylogenies): A tool for historical biogeography. *Molecular Phylogenetics and Evolution*, **87**, 46–49.

Zachos J., Pagani M., Sloan L., Thomas E., & Billups K. (2001) Trends, rhythms, and aberrations in global climate 65 Ma to present. *Science*, **292**, 686–693.

Zhang X., Marchant A., Wilson K.L., & Bruhl J.J. (2004) Phylogenetic relationships of *Carpha* and its relatives (Schoeneae, Cyperaceae) inferred from chloroplast *trn*L intron and *trn*L–*trn*F intergenic spacer sequences. *Molecular Phylogenetics and Evolution*, **31**, 647–657.

Zhang Y.-X., Zeng C.-X., & Li D.-Z. (2012) Complex evolution in Arundinarieae (Poaceae: Bambusoideae): Incongruence between plastid and nuclear GBSSI gene phylogenies. *Molecular Phylogenetics and Evolution*, **63**, 777–797.

Zuckerkandl E. & Pauling L. (1962) Molecular disease, evolution and genetic heterogeneity. *Horizons in Biochemistry* (ed. by M. Kasha and B. Pullman), pp. 189–225. Academic Press, New York.

APPENDIX A. SUPPLEMENTARY INFORMATION OF CHAPTER TWO

Table S2.1. List of samples with voucher information or Genbank accession numbers. Total numbers of samples per analysis are given at the end. PR, phylogenetic reconstruction; DTE, divergence time estimation.

Taxon	Genbank accession numbers (ITS/*trn*L-F)	Voucher	PR – ITS	PR – *trn*L-F	PR - combined	DTE
Arthrostylis aphylla	AY506757/AY506700		+	+	+	+
Becquerelia cymosa	-/KF553496			+	+	+
Calyptrocarya sp.	KF553442/-		+		+	+
Capeobolus brevicaulis	KF553443 /DQ058303		+	+	+	+
Carex magellanica	AY278292/AY757521		+	+	+	+
Carpha alpina	DQ385557/AY230010		+	+	+	+
Carpha glomerata	KF553444/AY230024		+	+	+	+
Carpha capitellata var. bracteosa	-/KF553497			+	+	+
Caustis dioica	-/KF553498			+	+	+
Chrysitrixcapensis	-/AY344171			+	+	+
Cladium mariscus	-/AY344172			+	+	+
Costularia arundinacea	-/AY230036			+	+	+
Costularia laxa	DQ450465/DQ456955		+	+	+	+

Taxon	Genbank accession numbers (ITS/*trn*L-F)	Voucher	PR – ITS	PR – *trn*L-F	PR - combined	DTE
Costularia leucocarpa	-/KF553499			+	+	+
Costularia nervosa	-/AY230032			+	+	+
Costularia pantopoda	-/KF553500			+	+	+
Costularia pantopoda var. baronii	-/KF553501			+	+	+
Costularia sp1	-/KF553502			+	+	+
Costularia sp2	-/KF553503			+	+	+
Costularia sp3	-/KF553504			+	+	+
Cyathochaeta avenacea	-/KF553505			+	+	+
Cyathochaeta diandra	-/AY230042			+	+	+
Cyathocoma bachmannii	-/EF178604			+	+	+
Cyathocoma hexandra	-/DQ058304			+	+	+
Cyperus rigidifolius	-/AY040600			+	+	+
Epischoenus cernuus	-/KF553506			+	+	+
Epischoenus quadrangularis	-/DQ058311			+	+	+
Epischoenus villosus	-/KF553507			+	+	+
Diplacrum caricinum	AB261688/-		+		+	+
Eriophorum vaginatum	AY242008/AY757692		+	+	+	+
Evandra aristata	KF553446/KF553508		+	+	+	+
Ficinia paradoxa	KF553447/DQ058317		+	+	+	+
Gahnia aspera	AB261676/-		+		+	+
Gahnia aspera subsp. globosa	-/AF285073			+	+	+
Gahnia baniensis	-/DQ058302			+	+	+
Gahnia trifida	-/KF553509			+	+	+
Gahnia tristis	AB261677 (ITS2)/KF553510		+	+	+	+

Taxon	Genbank accession numbers (ITS/*trn*L-F)	Voucher	PR – ITS	PR – *trn*L-F	PR - combined	DTE
Hypolytrum nemorum	AY242046/AJ577325		+	+	+	+
Lagenocarpus alboniger	KF553448/KF553511		+	+	+	+
Lepidosperma aff. filiforme	KF553449/AF285074		+	+	+	+
Lepidosperma laterale	DQ385587/KF553512		+	+	+	+
Lepidosperma longitudinale	KF553450/KF553513		+	+	+	+
Lepidosperma tortuosum	KF553451/KF553514		+	+	+	+
Machaerina iridifolia	-/KF553515			+	+	+
Machaerina juncea	-/KF553516			+	+	+
Machaerina mariscoides	-/DQ058300			+	+	+
Machaerina rubiginosa	AB261679/KF553517		+	+	+	+
Mapaniacuspidata	-/DQ058297			+	+	+
Mesomelaena pseudostygia	-/DQ058301			+	+	+
Mesomelaena tetragona	-/KF553518			+	+	+
Morelotia gahniiformis	KF553452/KF553519		+	+	+	+
Neesenbeckia punctoria	KF553453/DQ058306		+	+	+	+
Oreobolus acutifolius	DQ450466/DQ456956		+	+	+	+
O. ambiguus		Vink16142A	+		+	+
O. cleefii	DQ450467/DQ456957		+	+	+	+
O. cleefii		MG143	+	+	+	+
O. cleefii		MG144	+	+	+	+
O. cleefii		MG157	+	+	+	+
O. cleefii		MG158	+	+	+	+
O. cleefii		MG197	+	+	+	+
O. cleefii		MG198	+	+	+	+

Taxon	Genbank accession numbers (ITS/*trn*L-F)	Voucher	PR – ITS	PR – *trn*L-F	PR - combined	DTE
O. cleefii		MG199	+	+	+	+
O. cleefii		MG200	+	+	+	+
O. cleefii		MG202	+	+	+	+
O. cleefii		MG231	+	+	+	+
O. cleefii		MG233	+	+	+	+
O. cleefii		MG234	+	+	+	+
O. cleefii		MG235	+	+	+	+
O. cleefii		Cleef6276	+	+	+	+
O. distichus	DQ450468/DQ456958		+	+	+	+
O. distichus	-/AY230030			+		
O. ecuadorensis	DQ450469/DQ456959		+	+	+	+
O. ecuadorensis		Balslev1062	+	+	+	+
O. ecuadorensis		Balslev69137	+	+	+	+
O. ecuadorensis		HolmNielsen20905		+	+	
O. ecuadorensis		HolmNielsen24360	+	+	+	+
O. ecuadorensis		Laegaard101157	+	+	+	+
O. ecuadorensis		Laegaard101594	+	+	+	+
O. ecuadorensis		Laegaard101764	+	+	+	+
O. ecuadorensis		Laegaard101865	+	+	+	+
O. ecuadorensis		Laegaard102080	+	+	+	+
O. ecuadorensis		Laegaard19396	+	+	+	+
O. ecuadorensis		Laegaard20566	+	+	+	+
O. ecuadorensis		Laegaard20596	+	+	+	+
O. ecuadorensis		Laegaard20968	+	+	+	+

Taxon	Genbank accession numbers (ITS/*trn*L-F)	Voucher	PR – ITS	PR – *trn*L-F	PR - combined	DTE
O. ecuadorensis		Laegaard21508	+	+	+	+
O. ecuadorensis		Laegaard53490	+	+	+	+
O. ecuadorensis		Laegaard53588	+		+	
O. ecuadorensis		Laegaard53802A	+	+	+	+
O. ecuadorensis		Laegaard54455	+	+	+	+
O. ecuadorensis		Laegaard54571	+	+	+	+
O. ecuadorensis		Laegaard54734	+	+	+	+
O. ecuadorensis		Laegaard54853	+	+	+	+
O. ecuadorensis		Laegaard54873	+	+	+	+
O. ecuadorensis		Laegaard55305	+	+	+	+
O. ecuadorensis		Laegaard55534	+	+	+	+
O. ecuadorensis		Laegaard55549	+	+	+	+
O. ecuadorensis		Laegaard55550	+	+	+	+
O. ecuadorensis		Laegaard55764	+	+	+	+
O. ecuadorensis		Laegaard70067	+		+	
O. ecuadorensis		Laegaard70294a	+		+	
O. ecuadorensis		Laegaard71008	+	+	+	+
O. ecuadorensis		Laegaard71077	+	+	+	+
O. ecuadorensis		Ollgaard38114	+		+	
O. ecuadorensis		Ollgaard8665	+	+	+	+
O. ecuadorensis		Ollgaard8845	+	+	+	+
O. ecuadorensis		Renvoize4966	+	+	+	+
O. ecuadorensis		Renvoize5072	+	+	+	+
O. ecuadorensis		Smith12554	+		+	

Taxon	Genbank accession numbers (ITS/*trn*L-F)	Voucher	PR – ITS	PR – *trn*L-F	PR - combined	DTE
O. furcatus	DQ450470/DQ456960		+	+	+	+
O. goeppingeri		Balslev23930	+		+	
O. goeppingeri	DQ450471/DQ456961		+	+	+	+
O. goeppingeri		Holm571	+		+	
O. goeppingeri		Keating147	+		+	
O. goeppingeri		Kuhbier0276	+		+	
O. goeppingeri		Laegaard101185	+	+	+	+
O. goeppingeri		Laegaard101765	+	+	+	+
O. goeppingeri		Laegaard102047	+	+	+	+
O. goeppingeri		Laegaard102396	+	+	+	+
O. goeppingeri		Laegaard102477	+	+	+	+
O. goeppingeri		Laegaard103089	+	+	+	+
O. goeppingeri		Laegaard18599	+		+	
O. goeppingeri		Laegaard18697	+		+	
O. goeppingeri		Laegaard19216	+		+	
O. goeppingeri		Laegaard19291	+		+	
O. goeppingeri		Laegaard19438	+		+	
O. goeppingeri		Laegaard19472	+		+	
O. goeppingeri		Laegaard19960	+	+	+	+
O. goeppingeri		Laegaard20269	+	+	+	+
O. goeppingeri		Laegaard20521A	+	+	+	+
O. goeppingeri		Laegaard20672	+	+	+	+
O. goeppingeri		Laegaard20804	+		+	
O. goeppingeri		Laegaard20917	+	+	+	+

Taxon	Genbank accession numbers (ITS/*trn*L-F)	Voucher	PR – ITS	PR – *trn*L-F	PR - combined	DTE
O. goeppingeri		Laegaard20967	+	+	+	+
O. goeppingeri		Laegaard21015	+	+	+	+
O. goeppingeri		Laegaard21558	+	+	+	+
O. goeppingeri		Laegaard21573	+	+	+	+
O. goeppingeri		Laegaard22247	+	+	+	+
O. goeppingeri		Laegaard53479	+		+	
O. goeppingeri		Laegaard53622	+		+	
O. goeppingeri		Laegaard53632	+		+	
O. goeppingeri		Laegaard53655	+		+	
O. goeppingeri		Laegaard53670	+		+	
O. goeppingeri		Laegaard53750	+		+	
O. goeppingeri		Laegaard53777	+		+	
O. goeppingeri		Laegaard54145	+		+	
O. goeppingeri		Laegaard54412	+	+	+	+
O. goeppingeri		Laegaard54421	+	+	+	+
O. goeppingeri		Laegaard54495	+	+	+	+
O. goeppingeri		Laegaard54986	+	+	+	+
O. goeppingeri		Laegaard55048	+		+	
O. goeppingeri		Laegaard55105	+		+	
O. goeppingeri		Laegaard55132	+		+	
O. goeppingeri		Laegaard55239	+	+	+	+
O. goeppingeri		Laegaard55420	+		+	
O. goeppingeri		Laegaard55440	+	+	+	+
O. goeppingeri		Laegaard55763	+	+	+	+

Taxon	Genbank accession numbers (ITS/*trn*L-F)	Voucher	PR – ITS	PR – *trn*L-F	PR - combined	DTE
O. goeppingeri		Laegaard70120	+		+	
O. goeppingeri		Laegaard70381	+	+	+	+
O. goeppingeri		Laegaard70382	+	+	+	+
O. goeppingeri		Laegaard71079	+	+	+	+
O. goeppingeri		Laegaard71446	+	+	+	+
O. goeppingeri		Laegaard71570	+		+	
O. goeppingeri		Lewis3792	+	+	+	+
O. goeppingeri		LFT039		+	+	
O. goeppingeri		LFT047	+	+	+	+
O. goeppingeri		MG121	+	+	+	+
O. goeppingeri		MG140	+	+	+	+
O. goeppingeri		MG154	+	+	+	+
O. goeppingeri		MG169	+	+	+	+
O. goeppingeri		MG182	+	+	+	+
O. goeppingeri		MG183	+	+	+	+
O. goeppingeri		MG201	+	+	+	+
O. goeppingeri		MG203	+	+	+	+
O. goeppingeri		MG215	+	+	+	+
O. goeppingeri		MG217		+	+	
O. goeppingeri		MG220		+	+	
O. goeppingeri		MG221	+	+	+	+
O. goeppingeri		MG222	+	+	+	+
O. goeppingeri		MG248	+	+	+	
O. goeppingeri		MG268	+	+	+	+

Taxon	Genbank accession numbers (ITS/*trn*L-F)	Voucher	PR – ITS	PR – *trn*L-F	PR - combined	DTE
O. goeppingeri		MG278	+	+	+	+
O. goeppingeri		MG297	+	+	+	+
O. goeppingeri		MG316	+	+	+	
O. goeppingeri		MG327	+		+	
O. goeppingeri		MG344	+	+	+	+
O. goeppingeri		MG353	+		+	
O. goeppingeri		Ollgaard100642	+	+	+	+
O. goeppingeri		Ollgaard38270	+		+	
O. goeppingeri		Ollgaard57764	+		+	
O. goeppingeri		Ollgaard58074	+		+	
O. goeppingeri		Ollgaard74262	+	+	+	+
O. goeppingeri		Ollgaard8353	+		+	
O. goeppingeri		Ollgaard90622	+		+	
O. goeppingeri		Ollgaard90629	+	+	+	+
O. goeppingeri		Ollgaard90987	+	+	+	+
O. goeppingeri		Ollgaard98603	+	+	+	+
O. goeppingeri		Renvoize4924	+	+	+	+
O. goeppingeri		Renvoize5018	+		+	
O. goeppingeri		Sklenar1888	+	+	+	+
O. goeppingeri		Weber1764	+		+	
O. kuekenthalii	AY242047/EF178536		+	+	+	+
O. obtusangulus		DollenzTBPA1073	+	+	+	+
O. obtusangulus		DollenzTBPA1157	+	+	+	+
O. obtusangulus		DollenzTBPA1273	+	+	+	+

Taxon	Genbank accession numbers (ITS/*trn*L-F)	Voucher	PR – ITS	PR – *trn*L-F	PR - combined	DTE
O. obtusangulus		Dudley1184A	+	+	+	+
O. obtusangulus		Dudley241	+	+	+	+
O. obtusangulus		Gardner4167	+	+	+	+
O. obtusangulus		Goodall1788	+	+	+	+
O. obtusangulus		Goodall2237	+	+	+	+
O. obtusangulus		Goodall3365	+	+	+	+
O. obtusangulus		Goodall3697	+	+	+	+
O. obtusangulus		Goodall4813	+	+	+	+
O. obtusangulus		Goodall691	+		+	
O. obtusangulus		Jaramillo7701	+	+	+	+
O. obtusangulus		Kubitzki429	+		+	
O. obtusangulus		Laegaard102656	+	+	+	+
O. obtusangulus		Laegaard12537	+	+	+	+
O. obtusangulus		Laegaard12774	+	+	+	+
O. obtusangulus		Laegaard13509	+	+	+	+
O. obtusangulus		Laegaard19102	+	+	+	+
O. obtusangulus		Laegaard19300	+	+	+	+
O. obtusangulus		Laegaard19432	+	+	+	+
O. obtusangulus		Laegaard20559	+	+	+	+
O. obtusangulus		Laegaard20697	+	+	+	+
O. obtusangulus		Laegaard20814	+	+	+	+
O. obtusangulus		Laegaard20969	+	+	+	+
O. obtusangulus		Laegaard21502	+	+	+	+
O. obtusangulus		Laegaard21534	+	+	+	+

Taxon	Genbank accession numbers (ITS/*trn*L-F)	Voucher	PR – ITS	PR – *trn*L-F	PR - combined	DTE
O. obtusangulus		Laegaard21581	+	+	+	+
O. obtusangulus		Laegaard53130	+	+	+	+
O. obtusangulus		Laegaard53802B	+		+	
O. obtusangulus		Laegaard54144	+	+	+	+
O. obtusangulus		Laegaard54411	+	+	+	+
O. obtusangulus		Laegaard54420	+	+	+	+
O. obtusangulus		Laegaard54915	+	+	+	+
O. obtusangulus		Laegaard54963	+	+	+	+
O. obtusangulus		Laegaard54973D	+		+	
O. obtusangulus		Laegaard55003	+		+	
O. obtusangulus		Laegaard70102	+		+	
O. obtusangulus		Larsen17	+	+	+	+
O. obtusangulus		Moore1931	+	+	+	+
O. obtusangulus		Moore2817	+	+	+	+
O. obtusangulus		Moore749	+	+	+	+
O. obtusangulus		MooreTBPA1545	+	+	+	+
O. obtusangulus		MooreTBPA1617	+	+	+	+
O. obtusangulus		MooreTBPA1813	+	+	+	+
O. obtusangulus		Nicora7279	+	+	+	+
O. obtusangulus		Ollgaard38530	+		+	
O. obtusangulus		Ollgaard8547	+		+	
O. obtusangulus		Pisano3461	+		+	
O. obtusangulus		Pisano3773	+		+	
O. obtusangulus		Pisano3971	+		+	

Taxon	Genbank accession numbers (ITS/*trn*L-F)	Voucher	PR – ITS	PR – *trn*L-F	PR - combined	DTE
O. obtusangulus		Pisano5124	+	+	+	+
O. obtusangulus		Pisano5286	+	+	+	+
O. obtusangulus		Pisano5383	+	+	+	+
O. obtusangulus		Pisano5451	+	+	+	+
O. obtusangulus		Pisano5940	+		+	
O. obtusangulus		Pisano6091	+		+	
O. obtusangulus		PisanoTBPA2040	+	+	+	+
O. obtusangulus		PisanoTBPA2836	+	+	+	+
O. obtusangulus		Renvoize5007	+	+	+	+
O. obtusangulus		Roivainen690	+	+	+	+
O. oligocephalus	DQ450473/DQ456963		+	+	+	+
O. oligocephalus	-/AY230031			+		
O. oxycarpus	DQ450474/DQ456964		+	+	+	+
O. pectinatus	DQ450475/DQ456965		+	+	+	+
O. pectinatus	DQ385589/-		+			
O. pumilio	DQ450476/DQ456966		+	+	+	+
O. pumilio	-/AY230029			+		
O. sp.		Chaverri1093	+	+	+	+
O. strictus	DQ450478/DQ456968		+	+	+	+
O. strictus	DQ385590/-		+			
O. venezuelensis	DQ450479/DQ456969		+	+	+	+
O. venezuelensis		Cleef6746A	+		+	
O. venezuelensis		Cleef6787	+		+	
O. venezuelensis		Cleef6838	+	+	+	+

Taxon	Genbank accession numbers (ITS/*trn*L-F)	Voucher	PR – ITS	PR – *trn*L-F	PR - combined	DTE
O. venezuelensis		Cleef8438	+		+	
O. venezuelensis		Cleef9174	+	+	+	+
O. venezuelensis		Jorgensen61989	+	+	+	+
O. venezuelensis		Kubitzki430	+		+	
O. venezuelensis		Laegaard102476	+	+	+	+
O. venezuelensis		Laegaard103087	+	+	+	+
O. venezuelensis		Laegaard17466	+	+	+	+
O. venezuelensis		Laegaard17538	+	+	+	+
O. venezuelensis		Laegaard17552	+	+	+	+
O. venezuelensis		Laegaard18508	+		+	
O. venezuelensis		Laegaard19962	+	+	+	+
O. venezuelensis		Laegaard20520B	+		+	
O. venezuelensis		Laegaard20682	+	+	+	+
O. venezuelensis		Laegaard20918	+	+	+	
O. venezuelensis		Laegaard53613	+		+	
O. venezuelensis		Laegaard53621	+		+	
O. venezuelensis		Laegaard53758	+		+	
O. venezuelensis		Laegaard53770	+		+	
O. venezuelensis		Laegaard53779	+		+	
O. venezuelensis		Laegaard54405	+	+	+	+
O. venezuelensis		Laegaard55200	+		+	
O. venezuelensis		Laegaard70380	+	+	+	+
O. venezuelensis		Laegaard71157	+	+	+	+
O. venezuelensis		Ollgaard58308	+		+	

Taxon	Genbank accession numbers (ITS/*trn*L-F)	Voucher	PR – ITS	PR – *trn*L-F	PR - combined	DTE
O. venezuelensis		Ollgaard74264	+	+	+	+
O. venezuelensis		Ollgaard90623	+	+	+	+
O. venezuelensis		Ollgaard90628	+	+	+	+
O. venezuelensis		Sklenar7012	+	+	+	+
Pseudoschoenus inanis	-/KF553520			+	+	+
Ptilothrix deusta	KF553454/AY230041		+	+	+	+
Rhynchospora rugosa subsp. brownii	KF553455/AY230043		+	+	+	+
Schoenus bifidus	KF553456/KF553521		+	+	+	+
Schoenus caespititius	-/KF553522			+	+	+
Schoenus curvifolius	KF553457/KF553523		+	+	+	+
Schoenus efoliatus	KF553458/KF553524		+	+	+	+
Schoenus grandiflorus	KF553459/KF553525		+	+	+	+
Schoenus nigricans	KF553460/DQ058310		+	+	+	+
Schoenus nitens	KF553461/KF553526		+	+	+	+
Schoenus pennisetis	-/KF553527			+	+	+
Schoenus rigens	GU386455/KF553528		+	+	+	+
Scleria distans	KF553462/DQ058299		+	+	+	+
Tetraria bolusii	-/DQ058315			+	+	+
Tetraria capillaris	DQ385604/KF553529		+	+	+	+
Tetraria compacta	-/DQ058313			+	+	+
Tetraria compar	-/DQ058312			+	+	+
Tetraria crassa	-/DQ058314			+	+	+
Tetraria cuspidata	-/DQ419865			+	+	+
Tetraria exilis	-/DQ419866			+	+	+

Taxon	Genbank accession numbers (ITS/*trn*L-F)	Voucher	PR – ITS	PR – *trn*L-F	PR - combined	DTE
Tetraria flexuosa	-/DQ419859			+	+	+
Tetraria involucrata	-/DQ419852			+	+	+
Tetraria microstachys	-/DQ058307			+	+	+
Tetraria natalensis	KF553542 /DQ058305		+	+	+	+
Tetraria nigrovaginata	-/DQ419857			+	+	+
Tetraria octandra	-/KF553531			+	+	+
Tetraria picta	-/DQ419867			+	+	+
Tetraria sylvatica	-/DQ419864			+	+	+
Tetraria triangularis	-/DQ419853			+	+	+
Tetraria ustulata	-/DQ419861			+	+	+
Tetraria variabilis	-/KF553530			+	+	+
Trianoptiles capensis	KF553463/KF553532		+	+	+	+
Tricostularia pauciflora	-/AY23003			+	+	+
TOTAL			281	267	333	261

Figure S2.4. Tree with the best likelihood score obtained from *trn*L-F. Refer to the digital folder of Supplementary Information.

Figure S2.5. Tree with the best likelihood score obtained from ITS. Refer to the digital folder of Supplementary Information.

Figure S2.6. Maximum clade credibility tree obtained from the Bayesian analysis based on *trn*L-F. Refer to the digital folder of Supplementary Information.

Figure S2.7. Maximum clade credibility tree obtained from the Bayesian analysis based on ITS. Refer to the digital folder of Supplementary Information.

APPENDIX B. SUPPLEMENTARY INFORMATION OF CHAPTER THREE

Table S3.1. List of samples including voucher and population. Total numbers of samples per analysis are given at the end. Hap-ITS, haplotype networks for ITS; hap-cpDNA, haplotype networks for the concatenated plastid region (*trn*L-F, *trn*H-*psb*A and *rpl*32-*trn*L); * Genbank accession numbers.

Taxon	Voucher	Population	Pop Nº	Hap-ITS	Hap-cpDNA	Species tree (*BEAST)
Oreobolus cleefii	MG197	COCUY	2	+		+
O. cleefii	MG198	COCUY	2	+	+	+
O. cleefii	MG199	COCUY	2	+	+	+
O. cleefii	MG200	COCUY	2	+	+	+
O. cleefii	MG202	COCUY	2	+	+	+
O. cleefii	MG143	LA RUSIA	3	+	+	+
O. cleefii	MG144	LA RUSIA	3	+	+	+
O. cleefii	MG157	TOTA-BIJAGUAL	5	+	+	+
O. cleefii	MG158	TOTA-BIJAGUAL	5	+		+
O. cleefii	Cleef6276	GUERRERO	7	+		+
O. cleefii	DQ450467(ITS)/DQ456957(*trn*L-F)*	CHINGAZA	8	+		+
O. cleefii	MG231	AZUFRAL	11	+	+	+
O. cleefii	MG233	AZUFRAL	11	+		+

Taxon	Voucher	Population	Pop Nº	Hap-ITS	Hap-cpDNA	Species tree (*BEAST)
O. cleefii	MG234	AZUFRAL	11	+		+
O. cleefii	MG235	AZUFRAL	11	+	+	+
O. ecuadorensis	Laegaard55764	VOLCAN CHILES	12	+	+	+
O. ecuadorensis	Laegaard101157	COTOCACHI	14		+	+
O. ecuadorensis	Ollgaard8665	COTOCACHI	14	+	+	+
O. ecuadorensis	Balslev1062	COTOPAXI	15	+		+
O. ecuadorensis	Balslev69137	COTOPAXI	15		+	+
O. ecuadorensis	HolmNielsen24360	COTOPAXI	15	+	+	+
O. ecuadorensis	Laegaard101594	COTOPAXI	15		+	+
O. ecuadorensis	Laegaard101764	COTOPAXI	15	+		+
O. ecuadorensis	Laegaard102080	COTOPAXI	15		+	+
O. ecuadorensis	Laegaard53490	COTOPAXI	15		+	+
O. ecuadorensis	Laegaard54455	COTOPAXI	15	+	+	+
O. ecuadorensis	Laegaard54571	COTOPAXI	15		+	+
O. ecuadorensis	Laegaard54734	COTOPAXI	15	+	+	+
O. ecuadorensis	Laegaard54853	COTOPAXI	15	+	+	+
O. ecuadorensis	Laegaard54873	COTOPAXI	15	+	+	+
O. ecuadorensis	Laegaard55534	COTOPAXI	15		+	+
O. ecuadorensis	Laegaard55549	COTOPAXI	15	+		+
O. ecuadorensis	Laegaard55550	COTOPAXI	15		+	+
O. ecuadorensis	Ollgaard8845	COTOPAXI	15	+	+	+
O. ecuadorensis	Laegaard19396	LLANGANATI	16		+	+
O. ecuadorensis	Laegaard55305	ALAO-HUAMBOYA	17	+	+	+
O. ecuadorensis	Laegaard71008	ALAO-HUAMBOYA	17	+	+	+
O. ecuadorensis	Ollgaard38114	ALAO-HUAMBOYA	17	+		+
O. ecuadorensis	HolmNielsen20905	PARAMO DE LAS CAJAS	18		+	+

Taxon	Voucher	Population	Pop Nº	Hap-ITS	Hap-cpDNA	Species tree (*BEAST)
O. ecuadorensis	Laegaard20968	PARAMO DE LAS CAJAS	18	+	+	+
O. ecuadorensis	Laegaard21508	PARAMO DE LAS CAJAS	18	+	+	+
O. ecuadorensis	Laegaard53802A	PARAMO DE LAS CAJAS	18		+	+
O. ecuadorensis	Laegaard70067	PARAMO DE LAS CAJAS	18	+		+
O. ecuadorensis	Laegaard101865	CUENCA-LOJA	20		+	+
O. ecuadorensis	Laegaard20566	CUENCA-LOJA	20	+	+	+
O. ecuadorensis	Laegaard20596	CUENCA-LOJA	20	+	+	+
O. ecuadorensis	Laegaard53588	CUENCA-LOJA	20			+
O. ecuadorensis	Laegaard70294a	CUENCA-LOJA	20	+		+
O. ecuadorensis	Laegaard71077	CUENCA-LOJA	20	+	+	+
O. ecuadorensis	Renvoize4966	CAJAMARCA	22	+	+	+
O. ecuadorensis	Renvoize5072	HUASCARAN	23	+	+	+
O. ecuadorensis	Smith12554	HUASCARAN	23	+		+
O. goeppingeri	Holm571	CHIRRIPO	1			+
O. goeppingeri	Kuhbier0276	CHIRRIPO	1			+
O. goeppingeri	Weber1764	CHIRRIPO	1	+		+
O. goeppingeri	Chaverri1093	CHIRRIPO	1	+		+
O. goeppingeri	MG169	COCUY	2	+	+	+
O. goeppingeri	MG182	COCUY	2		+	+
O. goeppingeri	MG183	COCUY	2	+	+	+
O. goeppingeri	MG201	COCUY	2	+	+	+
O. goeppingeri	MG140	LA RUSIA	3	+		+
O. goeppingeri	MG248	IGUAQUE	4	+	+	+
O. goeppingeri	MG154	TOTA-BIJAGUAL	5	+		+
O. goeppingeri	MG316	TOTA-BIJAGUAL	5	+	+	+
O. goeppingeri	MG327	RABANAL	6	+		+

Taxon	Voucher	Population	Pop Nº	Hap-ITS	Hap-cpDNA	Species tree (*BEAST)
O. goeppingeri	MG344	RABANAL	6	+	+	+
O. goeppingeri	MG268	GUERRERO	7	+		+
O. goeppingeri	DQ450471/DQ456961*	CHINGAZA	8	+		+
O. goeppingeri	MG121	CHINGAZA	8	+	+	+
O. goeppingeri	MG353	CHINGAZA	8	+		+
O. goeppingeri	LFT039	SUMAPAZ	9			+
O. goeppingeri	LFT047	SUMAPAZ	9	+	+	+
O. goeppingeri	MG278	SUMAPAZ	9	+	+	+
O. goeppingeri	MG297	SUMAPAZ	9	+		+
O. goeppingeri	MG203	PURACE	10	+	+	+
O. goeppingeri	MG215	PURACE	10	+	+	+
O. goeppingeri	MG217	PURACE	10			+
O. goeppingeri	MG220	PURACE	10			+
O. goeppingeri	MG221	PURACE	10	+	+	+
O. goeppingeri	MG222	AZUFRAL	11	+	+	+
O. goeppingeri	Balslev23930	VOLCAN CHILES	12	+		+
O. goeppingeri	Laegaard54986	VOLCAN CHILES	12			+
O. goeppingeri	Laegaard55763	VOLCAN CHILES	12	+		+
O. goeppingeri	Laegaard71446	VOLCAN CHILES	12	+		+
O. goeppingeri	Ollgaard8353	VOLCAN CHILES	12	+		+
O. goeppingeri	Sklenar1888	VOLCAN CHILES	12	+		+
O. goeppingeri	Laegaard54412	MIRADOR	13	+	+	+
O. goeppingeri	Laegaard54421	MIRADOR	13	+	+	+
O. goeppingeri	Laegaard101185	COTOCACHI	14	+		+
O. goeppingeri	Laegaard53479	COTOCACHI	14			+
O. goeppingeri	Laegaard54495	COTOCACHI	14	+	+	+

Taxon	Voucher	Population	Pop Nº	Hap-ITS	Hap-cpDNA	Species tree (*BEAST)
O. goeppingeri	Ollgaard100642	COTOCACHI	14	+	+	+
O. goeppingeri	Laegaard101765	COTOPAXI	15	+		+
O. goeppingeri	Laegaard54145	COTOPAXI	15	+		+
O. goeppingeri	Laegaard19438	LLANGANATI	16	+		+
O. goeppingeri	Laegaard19472	LLANGANATI	16	+		+
O. goeppingeri	Laegaard55420	ALAO-HUAMBOYA	17	+		+
O. goeppingeri	Laegaard55440	ALAO-HUAMBOYA	17	+		+
O. goeppingeri	Ollgaard38270	ALAO-HUAMBOYA	17	+		+
O. goeppingeri	Laegaard20967	PARAMO DE LAS CAJAS	18	+	+	+
O. goeppingeri	Laegaard21015	PARAMO DE LAS CAJAS	18	+	+	+
O. goeppingeri	Laegaard55048	PARAMO DE LAS CAJAS	18			+
O. goeppingeri	Laegaard55105	PARAMO DE LAS CAJAS	18			+
O. goeppingeri	Laegaard70120	PARAMO DE LAS CAJAS	18			+
O. goeppingeri	Laegaard19291	CUENCA-LIMON	19	+		+
O. goeppingeri	Laegaard20804	CUENCA-LIMON	19	+		+
O. goeppingeri	Laegaard102047	CUENCA-LOJA	20	+		+
O. goeppingeri	Laegaard102396	CUENCA-LOJA	20	+		+
O. goeppingeri	Laegaard18697	CUENCA-LOJA	20	+		+
O. goeppingeri	Laegaard20672	CUENCA-LOJA	20	+	+	+
O. goeppingeri	Laegaard55132	CUENCA-LOJA	20			+
O. goeppingeri	Laegaard55239	CUENCA-LOJA	20	+		+
O. goeppingeri	Laegaard70381	CUENCA-LOJA	20	+	+	+
O. goeppingeri	Laegaard70382	CUENCA-LOJA	20	+		+
O. goeppingeri	Laegaard71079	CUENCA-LOJA	20	+		+
O. goeppingeri	Laegaard71570	CUENCA-LOJA	20	+		+
O. goeppingeri	Ollgaard57764	CUENCA-LOJA	20			+

Taxon	Voucher	Population	Pop Nº	Hap-ITS	Hap-cpDNA	Species tree (*BEAST)
O. goeppingeri	Ollgaard90987	CUENCA-LOJA	20	+	+	+
O. goeppingeri	Ollgaard98603	CUENCA-LOJA	20	+		+
O. goeppingeri	Keating147	PODOCARPUS	21			+
O. goeppingeri	Laegaard102477	PODOCARPUS	21	+		+
O. goeppingeri	Laegaard103089	PODOCARPUS	21	+	+	+
O. goeppingeri	Laegaard18599	PODOCARPUS	21	+		+
O. goeppingeri	Laegaard19216	PODOCARPUS	21	+		+
O. goeppingeri	Laegaard19960	PODOCARPUS	21	+		+
O. goeppingeri	Laegaard20269	PODOCARPUS	21	+		+
O. goeppingeri	Laegaard20521A	PODOCARPUS	21	+		+
O. goeppingeri	Laegaard20917	PODOCARPUS	21	+		+
O. goeppingeri	Laegaard21558	PODOCARPUS	21	+	+	+
O. goeppingeri	Laegaard21573	PODOCARPUS	21	+		+
O. goeppingeri	Laegaard53622	PODOCARPUS	21			+
O. goeppingeri	Laegaard53632	PODOCARPUS	21	+		+
O. goeppingeri	Laegaard53655	PODOCARPUS	21	+		+
O. goeppingeri	Laegaard53670	PODOCARPUS	21			+
O. goeppingeri	Laegaard53750	PODOCARPUS	21			+
O. goeppingeri	Laegaard53777	PODOCARPUS	21	+		+
O. goeppingeri	Lewis3792	PODOCARPUS	21	+		+
O. goeppingeri	Ollgaard58074	PODOCARPUS	21	+		+
O. goeppingeri	Ollgaard74262	PODOCARPUS	21	+	+	+
O. goeppingeri	Ollgaard90622	PODOCARPUS	21	+		+
O. goeppingeri	Ollgaard90629	PODOCARPUS	21	+	+	+
O. goeppingeri	Laegaard22247	CAJAMARCA	22	+		+
O. goeppingeri	Renvoize4924	CAJAMARCA	22	+		+

Taxon	Voucher	Population	Pop Nº	Hap-ITS	Hap-cpDNA	Species tree (*BEAST)
O. goeppingeri	Renvoize5018	CAJAMARCA	22	+		+
O. obtusangulus	Kubitzki429	SUMAPAZ	9	+		+
O. obtusangulus	Laegaard21534	VOLCAN CHILES	12	+	+	+
O. obtusangulus	Laegaard53130	VOLCAN CHILES	12		+	+
O. obtusangulus	Laegaard54915	VOLCAN CHILES	12	+	+	+
O. obtusangulus	Laegaard54963	VOLCAN CHILES	12	+	+	+
O. obtusangulus	Laegaard54973D	VOLCAN CHILES	12	+		+
O. obtusangulus	Ollgaard8547	VOLCAN CHILES	12	+		+
O. obtusangulus	Laegaard54411	MIRADOR	13		+	+
O. obtusangulus	Laegaard54420	MIRADOR	13	+	+	+
O. obtusangulus	Jaramillo7701	COTOPAXI	15	+	+	+
O. obtusangulus	Laegaard54144	COTOPAXI	15	+	+	+
O. obtusangulus	Laegaard19432	LLANGANATI	16	+	+	+
O. obtusangulus	Ollgaard38530	LLANGANATI	16	+		+
O. obtusangulus	Laegaard55003	CHIMBORAZO	17			+
O. obtusangulus	Laegaard102656	PARAMO DE LAS CAJAS	18	+	+	+
O. obtusangulus	Laegaard20969	PARAMO DE LAS CAJAS	18	+	+	+
O. obtusangulus	Laegaard21502	PARAMO DE LAS CAJAS	18	+	+	+
O. obtusangulus	Laegaard53802B	PARAMO DE LAS CAJAS	18	+		+
O. obtusangulus	Laegaard70102	PARAMO DE LAS CAJAS	18			+
O. obtusangulus	Laegaard19300	CUENCA-LIMON	19	+	+	+
O. obtusangulus	Laegaard20814	CUENCA-LIMON	19	+	+	+
O. obtusangulus	Larsen17	CUENCA-LIMON	19	+	+	+
O. obtusangulus	Laegaard19102	CUENCA-LOJA	20	+	+	+
O. obtusangulus	Laegaard20559	CUENCA-LOJA	20	+	+	+
O. obtusangulus	Laegaard20697	CUENCA-LOJA	20	+	+	+

Taxon	Voucher	Population	Pop Nº	Hap-ITS	Hap-cpDNA	Species tree (*BEAST)
O. obtusangulus	Laegaard21581	PODOCARPUS	21	+	+	+
O. obtusangulus	Renvoize5007	CAJAMARCA	22	+	+	+
O. obtusangulus	Gardner4167	VALDIVIA	24	+	+	+
O. obtusangulus	Pisano5940	FIORDO PEEL	25	+	+	+
O. obtusangulus	Pisano6091	FIORDO PEEL	25	+		+
O. obtusangulus	Moore749	MALVINAS	26	+	+	+
O. obtusangulus	Laegaard12537	PNN NAHUEL HUAPI	27			+
O. obtusangulus	Laegaard12774	PNN NAHUEL HUAPI	27	+		+
O. obtusangulus	Laegaard13509	PNN NAHUEL HUAPI	27	+	+	+
O. obtusangulus	DollenzTBPA1073	MAGALLANES	28	+	+	+
O. obtusangulus	DollenzTBPA1157	MAGALLANES	28	+	+	+
O. obtusangulus	DollenzTBPA1273	MAGALLANES	28	+		+
O. obtusangulus	MooreTBPA1545	MAGALLANES	28	+	+	+
O. obtusangulus	MooreTBPA1617	MAGALLANES	28	+	+	+
O. obtusangulus	MooreTBPA1813	MAGALLANES	28	+		+
O. obtusangulus	Pisano3773	MAGALLANES	28	+		+
O. obtusangulus	Pisano3971	MAGALLANES	28	+		+
O. obtusangulus	Pisano5451	MAGALLANES	28	+	+	+
O. obtusangulus	PisanoTBPA2040	MAGALLANES	28	+		+
O. obtusangulus	PisanoTBPA2836	MAGALLANES	28	+	+	+
O. obtusangulus	Dudley241	TIERRA DEL FUEGO	29	+		+
O. obtusangulus	Goodall1788	TIERRA DEL FUEGO	29	+	+	+
O. obtusangulus	Goodall2237	TIERRA DEL FUEGO	29	+	+	+
O. obtusangulus	Goodall3365	TIERRA DEL FUEGO	29	+		+
O. obtusangulus	Goodall3697	TIERRA DEL FUEGO	29	+		+
O. obtusangulus	Goodall4813	TIERRA DEL FUEGO	29	+	+	+

Taxon	Voucher	Population	Pop Nº	Hap-ITS	Hap-cpDNA	Species tree (*BEAST)
O. obtusangulus	Goodall691	TIERRA DEL FUEGO	29	+		+
O. obtusangulus	Moore1931	TIERRA DEL FUEGO	29	+	+	+
O. obtusangulus	Moore2817	TIERRA DEL FUEGO	29	+	+	+
O. obtusangulus	Roivainen690	TIERRA DEL FUEGO	29	+		+
O. obtusangulus	Dudley1184A	ISLA DE LOS ESTADOS	30	+		+
O. obtusangulus	Nicora7279	ISLA DE LOS ESTADOS	30	+	+	+
O. obtusangulus	Pisano3461	ISLA NAVARINO	31	+		+
O. obtusangulus	Pisano5124	CABO DE HORNOS	32	+	+	+
O. obtusangulus	Pisano5286	CABO DE HORNOS	32	+	+	+
O. obtusangulus	Pisano5383	CABO DE HORNOS	32	+	+	+
O. venezuelensis	Cleef9174	COCUY	2	+		+
O. venezuelensis	Cleef6746A	LA RUSIA	3	+		+
O. venezuelensis	Cleef6787	LA RUSIA	3			+
O. venezuelensis	Cleef6838	LA RUSIA	3	+	+	+
O. venezuelensis	DQ450479/DQ456969*	CHINGAZA	8	+		+
O. venezuelensis	Laegaard17466	CHINGAZA	8	+	+	+
O. venezuelensis	Cleef8438	SUMAPAZ	9	+		+
O. venezuelensis	Kubitzki430	SUMAPAZ	9	+		+
O. venezuelensis	Laegaard17538	SUMAPAZ	9	+	+	+
O. venezuelensis	Laegaard17552	SUMAPAZ	9	+	+	+
O. venezuelensis	Laegaard54405	MIRADOR	13	+	+	+
O. venezuelensis	Jorgensen61989	COTOPAXI	15		+	+
O. venezuelensis	Laegaard20682	CUENCA-LOJA	20	+	+	+
O. venezuelensis	Laegaard70380	CUENCA-LOJA	20	+	+	+
O. venezuelensis	Laegaard71157	CUENCA-LOJA	20		+	+
O. venezuelensis	Laegaard102476	PODOCARPUS	21	+		+

Taxon	Voucher	Population	Pop Nº	Hap-ITS	Hap-cpDNA	Species tree (*BEAST)
O. venezuelensis	Laegaard103087	PODOCARPUS	21	+	+	+
O. venezuelensis	Laegaard18508	PODOCARPUS	21			+
O. venezuelensis	Laegaard19962	PODOCARPUS	21	+		+
O. venezuelensis	Laegaard20520B	PODOCARPUS	21			+
O. venezuelensis	Laegaard20918	PODOCARPUS	21	+	+	+
O. venezuelensis	Laegaard53613	PODOCARPUS	21	+		+
O. venezuelensis	Laegaard53621	PODOCARPUS	21	+		+
O. venezuelensis	Laegaard53758	PODOCARPUS	21	+		+
O. venezuelensis	Laegaard53770	PODOCARPUS	21	+		+
O. venezuelensis	Laegaard53779	PODOCARPUS	21	+		+
O. venezuelensis	Laegaard55200	PODOCARPUS	21	+		+
O. venezuelensis	Ollgaard58308	PODOCARPUS	21	+		+
O. venezuelensis	Ollgaard74264	PODOCARPUS	21	+	+	+
O. venezuelensis	Ollgaard90623	PODOCARPUS	21	+	+	+
O. venezuelensis	Ollgaard90628	PODOCARPUS	21	+	+	+
O. venezuelensis	Sklenar7012	PODOCARPUS	21	+		+
TOTAL				197	118	237

APPENDIX C. SUPPLEMENTARY INFORMATION OF CHAPTER FOUR

Table S4.1. List of samples with voucher information/Genbank accessions numbers and population number. Total numbers of samples per analysis are given at the end. Hap-ETS, haplotype network for ETS; hap-cpDNA, haplotype networks for the concatenated plastid region (*trn*G/*rpl*32-*trn*L); PR, phylogenetic reconstruction.

Taxon	Population	Pop Nº	Genbank accession numbers (ITS/*acc*D-*psa*I/*psb*K-*psb*L)	Voucher	Hap-ETS	Hap-cpDNA	PR Castratella (ETS/*trn*G/*rpl*32-*trn*L)	PR Melastomeae (ITS/*acc*D-*psa*I/*psb*K-*psb*L)
Castratella piloselloides	COCUY	1		MG167	+	+	+	
C. piloselloides	COCUY	1		MG188	+	+	+	+
C. piloselloides	LA RUSIA	2		MG141	+	+	+	
C. piloselloides	IGUAQUE	3		MG247	+	+	+	+
C. piloselloides	TOTA-BIJAGUAL	4		MG150	+	+	+	+
C. piloselloides	TOTA-BIJAGUAL	4		MG308	+	+	+	+
C. piloselloides	TOTA-BIJAGUAL	4		MG317	+	+	+	+
C. piloselloides	RABANAL	5		MG328	+	+	+	+
C. piloselloides	RABANAL	5		MG345	+	+	+	+
C. piloselloides	GUERRERO	6		MG239	+	+	+	+

Taxon	Population	Pop Nº	Genbank accession numbers (ITS/*acc*D-*psa*I/*psb*K-*psb*L)	Voucher	Hap-ETS	Hap-cpDNA	PR Castratella (ETS/*trn*G/*rpl*32-*trn*L)	PR Melastomeae (ITS/*acc*D-*psa*I/*psb*K-*psb*L)
C. piloselloides	GUERRERO	6		MG270	+	+	+	+
C. piloselloides	CHINGAZA	7		MG108	+			
C. piloselloides	CHINGAZA	7		MG122	+			
C. piloselloides	CHINGAZA	7		MG352	+	+	+	
C. piloselloides	SUMAPAZ	8		LFT035	+	+	+	+
C. piloselloides	SUMAPAZ	8		MG282	+	+	+	+
C. piloselloides	SUMAPAZ	8		MG301	+			
C. rosea	COCUY	1		Cleef4735	+	+	+	
Bucquetia glutinosa				MCG-246			+	
B. glutinosa				MCG-281			+	
Chaetolepis cufodontisii				Michelangeli1160			+	+
C. lindeniana				Michelangeli1268			+	+
C. microphylla				Michelangeli1224			+	+
Acanthella sprucei			JQ730036/JQ730247/JQ730456					+
Aciotis acuminifolia			JQ730037/JQ730248/JQ730457					+
Aciotis circaeifolia			JQ730038/JQ730249/JQ730458					+
Aciotis indecora			JQ730039/JQ730250/JQ730459					+
Aciotis paludosa			JQ730040/JQ730251/JQ730460					+
Aciotis purpurascens			JQ730041/JQ730252/JQ730461					+
Aciotis rubricaulis			JQ730042/JQ730253/JQ730462					+

Taxon	Population	Pop Nº	Genbank accession numbers (ITS/*acc*D-*psa*I/*psb*K-*psb*L)	Voucher	Hap-ETS	Hap-cpDNA	PR Castratella (ETS/*trn*G/*rpl*32-*trn*L)	PR Melastomeae (ITS/*acc*D-*psa*I/*psb*K-*psb*L)
Acisanthera alsinaefolia			JQ730043/JQ730254/JQ730463					+
Acisanthera hedyotidea			JQ730044/JQ730255/JQ730464					+
Acisanthera quadrata			JQ730045/JQ730256/JQ730465					+
Amphorocalyx multiflorus			JQ730046/JQ730257/JQ730466					+
Amphorocalyx rupestris			JQ730047/JQ730258/JQ730467					+
Antherotoma naudinii			JQ730048/JQ730259/-					+
Appendicularia thymifolia			JQ730049/JQ730260/JQ730468					+
Arthrostemma ciliatum 1			DQ985619/-/-					+
Arthrostemma ciliatum 2			AY460429/-/-					+
Arthrostemma primaevum			JQ730050/JQ730261/JQ730469					+
Brachyotum benthamianum			JQ730051/JQ730262/JQ730470					+
Brachyotum confertum			JQ730052/JQ730263/JQ730471					+
Brachyotum fictum			JQ730053/JQ730264/JQ730472					+
Brachyotum fraternum			JQ730054/JQ730265/JQ730473					+
Brachyotum harlingii			JQ730055/JQ730266/JQ730474					+
Brachyotum incrassatum			JQ730056/JQ730267/JQ730475					+
Brachyotum ledifolium			JQ730057/JQ730268/JQ730476					+
Brachyotum lindenii			JQ730058/JQ730269/JQ730477					+
Brachyotum microdon			JQ730059/JQ730270/JQ730478					+
Brachyotum rostratum			JQ730060/JQ730271/JQ730479					+

Taxon	Population	Pop Nº	Genbank accession numbers (ITS/*acc*D-*psa*I/*psb*K-*psb*L)	Voucher	Hap-ETS	Hap-cpDNA	PR Castratella (ETS/*trn*G/*rpl*32-*trn*L)	PR Melastomeae (ITS/*acc*D-*psa*I/*psb*K-*psb*L)
Bucquetia glutinosa			JQ730061/JQ730272/JQ730480					+
Cambessedesia espora			JQ730062/JQ730273/JQ730481					+
Cambessedesia hilariana			JQ730063/JQ730274/JQ730482					+
Castratella piloselloides			JQ730064/JQ730275/JQ730483					+
Centradenia grandifolia			JQ730065/JQ730276/-					+
Centradenia inaequilateralis			JQ730066/JQ730277/JQ730484					+
Chaetolepis cufodontisii			JQ730067/JQ730278/JQ730485					+
Chaetolepis microphylla			JQ730068/JQ730279/JQ730486					+
Chaetostoma armatum			JQ730069/JQ730280/JQ730487					+
Comolia microphylla			JQ730070/JQ730281/JQ730488					+
Comolia sertularia			JQ730071/JQ730282/JQ730489					+
Comolia vernicosa			JQ730072/JQ730283/JQ730490					+
Desmocelis villosa			JQ730073/JQ730284/JQ730491					+
Dichaetanthera africana			JQ730074/JQ730285/JQ730492					+
Dichaetanthera oblongifolia			JQ730075/JQ730286/JQ730493					+
Dionycha bojeri			JQ730076/JQ730287/JQ730494					+
Dissotis cf. phaeotricha			JQ730078/JQ730288/JQ730495					+
Dissotis multiflora			JQ730077/JQ730289/JQ730496					+
Eriocnema fulva			EF418811 /JQ730290/JQ730497					+

Taxon	Population	Pop Nº	Genbank accession numbers (ITS/*acc*D-*psa*I/*psb*K-*psb*L)	Voucher	Hap-ETS	Hap-cpDNA	PR Castratella (ETS/*trn*G/*rpl*32-*trn*L)	PR Melastomeae (ITS/*acc*D-*psa*I/*psb*K-*psb*L)
Ernestia confertiflora			JQ730079/JQ730291/JQ730498					+
Ernestia glandulosa			JQ730080/JQ730292/JQ730499					+
Ernestia pullei			JQ730081/JQ730293/JQ730500					+
Ernestia tenella			JQ730082/JQ730294/JQ730501					+
Fritzchia erecta			JQ730083/JQ730295/JQ730502					+
Graffenrieda latifolia			AY460450 /JQ730296/JQ730503					+
Graffenrieda moritziana			AY460451/JQ730297/JQ730504					+
Guyonia ciliata			JQ730084/-/-					+
Heterocentron elegans			JQ730085/JQ730298/JQ730505					+
Heterocentron muricatum			JQ730086/JQ730299/JQ730506					+
Heterocentrum subtriplinervium			JQ730087/JQ730300/JQ730507					+
Heterotis decumbens			JQ730088/JQ730301/JQ730508					+
Heterotis rotundifolia			JQ730089/JQ730302/-					+
Itatiaia cleistopetala			JQ730090/JQ730303/JQ730509					+
Lavoisiera imbricata			JQ730091/JQ730304/JQ730510					+
Lavoisiera mucorifera			JQ730092/JQ730305/JQ730511					+
Lavoisiera pulchella			JQ730093/JQ730306/JQ730512					+
Macairea pachyphylla			JQ730094/-/-					+
Macairea radula			JQ730095/JQ730307/JQ730513					+
Macairea thyrsiflora			JQ730096/JQ730308/JQ730514					+

Taxon	Population	Pop Nº	Genbank accession numbers (ITS/*acc*D-*psa*I/*psb*K-*psb*L)	Voucher	Hap-ETS	Hap-cpDNA	PR Castratella (ETS/*trn*G/*rpl*32-*trn*L)	PR Melastomeae (ITS/*acc*D-*psa*I/*psb*K-*psb*L)
Marcetia acerosa			JQ730097/-/JQ730515					+
Marcetia eimeariana			JQ730098/JQ730309/JQ730516					+
Marcetia ericoides			JQ730099/JQ730310/JQ730517					+
Marcetia harleyi			JQ730100/-/JQ730518					+
Marcetia latifolia			JQ730101/-/JQ730519					+
Marcetia taxifolia			JQ730102/JQ730311/JQ730520					+
Melastoma affine			GQ265878 /-/-					+
Melastoma candidum			JQ730103/JQ730312/JQ730521					+
Melastoma denticulatum			JQ730104/JQ730313/JQ730522					+
Melastoma dodecandrum			GQ265883/-/-					+
Melastoma intermedium			GQ265883/-/-					+
Melastoma malabathricum			JQ730105/JQ730314/JQ730523					+
Melastoma sanguineum			JQ730106/JQ730315/JQ730524					+
Meriania longifolia			AY460454/JQ730316/JQ730525					+
Miconia dodecandra			AY460506/JQ730317/JQ730526					+
Miconia tomentosa			EF418905 /JQ730318/JQ730527					+
Microlepis oleaefolia			JQ730107/JQ730319/JQ730528					+
Monochaetum bonplandii			JQ730108/JQ730320/JQ730529					+
Monochaetum discolor			JQ730109/JQ730321/JQ730530					+
Monochaetum humboldtianum			JQ730110/JQ730322/JQ730531					+
Monochaetum meridense			JQ730111/JQ730323/JQ730532					+

Taxon	Population	Pop Nº	Genbank accession numbers (ITS/*acc*D-*psa*I/*psb*K-*psb*L)	Voucher	Hap-ETS	Hap-cpDNA	PR Castratella (ETS/*trn*G/*rpl*32-*trn*L)	PR Melastomeae (ITS/*acc*D-*psa*I/*psb*K-*psb*L)
Monochaetum polyneuron			JQ730112/JQ730324/JQ730533					+
Monochaetum tenellum			AY460432 /-/-					+
Monochaetum uribei			JQ730113/JQ730325/JQ730534					+
Monochaetum volcanicum			JQ730114/JQ730326/JQ730535					+
Nepsera aquatica			JQ730115/JQ730327/JQ730536					+
Osbeckia australiana			JQ730116/JQ730328/JQ730537					+
Osbeckia courtallensis			JQ730117/-/-					+
Osbeckia nepalensis			JQ730118/JQ730329/JQ730538					+
Osbeckia stellata			JQ730119/JQ730330/JQ730539					+
Pachyloma huberioides			JQ730120/JQ730331/JQ730540					+
Physeterostemon tomasii			JQ730121/JQ730332/JQ730541					+
Pilocosta campanensis			JQ730122/JQ730333/JQ730542					+
Pilocosta nana			JQ730123/JQ730334/JQ730543					+
Pilocosta nubicola			JQ730124/JQ730335/JQ730544					+
Pilocosta oerstedii			JQ730125/JQ730336/JQ730545					+
Pterogastra divaricata			JQ730126/JQ730337/JQ730546					+
Pterogastra minor			JQ730127/JQ730338/JQ730547					+
Pterolepis alpestris			JQ730128/JQ730339/JQ730548					+
Pterolepis glomerata			JQ730129/JQ730340/JQ730549					+
Pterolepis parnasiifolia			JQ730130/JQ730341/JQ730550					+

Taxon	Population	Pop Nº	Genbank accession numbers (ITS/*acc*D-*psa*I/*psb*K-*psb*L)	Voucher	Hap-ETS	Hap-cpDNA	PR Castratella (ETS/*trn*G/*rpl*32-*trn*L)	PR Melastomeae (ITS/*acc*D-*psa*I/*psb*K-*psb*L)
Pterolepis repanda			JQ730131/JQ730342/JQ730551					+
Pterolepis rotundifolia			JQ730132/JQ730343/JQ730552					+
Pterolepis sp			JQ730133/JQ730344/JQ730553					+
Rhexia alifanus			DQ985623 /-/-					+
Rhexia aristosa			JQ730134/JQ730345/JQ730554					+
Rhexia cubensis			DQ985627/-/-					+
Rhexia lutea			DQ985628 /-/-					+
Rhexia mariana			JQ730135/-/JQ730555					+
Rhexia nuttallii			DQ985634/-/-					+
Rhexia parviflora			DQ985636/-/-					+
Rhexia petiolata			DQ985637/-/-					+
Rhexia salicifolia			DQ985639/-/-					+
Rhexia virginica			JQ730136/JQ730346/JQ730556					+
Rhynchanthera bracteata			JQ730137/JQ730347/JQ730557					+
Rhynchanthera grandiflora			JQ730138/JQ730348/JQ730558					+
Rhynchanthera serrulata			AY460435 /JQ730349/JQ730559					+
Rousseauxia andringitrensis			JQ730139/JQ730350/JQ730560					+
Rousseauxia minimifolia			JQ730140/JQ730351/JQ730561					+
Sandemania hoehnei			JQ730141/JQ730352/JQ730562					+
Siphanthera hostmanii			JQ730142/JQ730353/JQ730563					+
Svitramia hatschbachii			JQ730143/JQ730354/JQ730564					+
Svitramia minor			JQ730144/JQ730355/JQ730565					+

Taxon	Population	Pop Nº	Genbank accession numbers (ITS/*acc*D-*psa*I/*psb*K-*psb*L)	Voucher	Hap-ETS	Hap-cpDNA	PR Castratella (ETS/*trn*G/*rpl*32-*trn*L)	PR Melastomeae (ITS/*acc*D-*psa*I/*psb*K-*psb*L)
Svitramia pulchra			JQ730145/JQ730356/JQ730566					+
Svitramia sp			JQ730146/JQ730357/JQ730567					+
Svitramia sp			JQ730147/JQ730358/JQ730568					+
Svitramia wurdackiana			JQ730148/JQ730359/JQ730569					+
Tibouchina aemula			JQ730149/JQ730360/JQ730570					+
Tibouchina alpestris			JQ730150/JQ730361/JQ730571					+
Tibouchina angustifolia			JQ730151/JQ730362/JQ730572					+
Tibouchina arborea			JQ730152/JQ730363/JQ730573					+
Tibouchina arenaria			JQ730153/JQ730364/JQ730574					+
Tibouchina aspera			JQ730154/JQ730365/JQ730575					+
Tibouchina aspera var. asperrima			JQ730155/JQ730366/JQ730576					+
Tibouchina axillaris			JQ730156/JQ730367/JQ730577					+
Tibouchina barnebyana			JQ730157/JQ730368/-					+
Tibouchina benthamiana			JQ730158/JQ730369/JQ730578					+
Tibouchina bicolor			JQ730159/JQ730370/JQ730579					+
Tibouchina bipenicillata			JQ730160/JQ730371/JQ730580					+
Tibouchina blanchetiana			JQ730161/JQ730372/-					+
Tibouchina boudetii			JQ730162/JQ730373/JQ730581					+
Tibouchina breedlovei			JQ730163/JQ730374/JQ730582					+
Tibouchina candolleana			JQ730164/JQ730375/JQ730583					+

Taxon	Population	Pop Nº	Genbank accession numbers (ITS/*acc*D-*psa*I/*psb*K-*psb*L)	Voucher	Hap-ETS	Hap-cpDNA	PR Castratella (ETS/*trn*G/*rpl*32-*trn*L)	PR Melastomeae (ITS/*acc*D-*psa*I/*psb*K-*psb*L)
Tibouchina cardinalis			JQ730165/JQ730376/JQ730584					+
Tibouchina castellenis			JQ730166/JQ730377/JQ730585					+
Tibouchina cerastifolia			JQ730167/-/JQ730586					+
Tibouchina chamaecistus			JQ730168/JQ730378/JQ730587					+
Tibouchina ciliaris			JQ730169/-/JQ730588					+
Tibouchina cinerea			JQ730170/JQ730379/JQ730589					+
Tibouchina citrina			JQ730171/JQ730380/JQ730590					+
Tibouchina clavata			JQ730172/JQ730381/JQ730591					+
Tibouchina clidemiodes			JQ730173/JQ730382/-					+
Tibouchina clinopodifolia			JQ730174/JQ730383/JQ730592					+
Tibouchina confertiflora			JQ730175/JQ730384/JQ730593					+
Tibouchina corymbosa			JQ730176/JQ730385/JQ730594					+
Tibouchina cristata			JQ730177/JQ730386/JQ730595					+
Tibouchina cryptadena			JQ730178/JQ730387/JQ730596					+
Tibouchina dubia			JQ730179/JQ730388/JQ730597					+
Tibouchina estrellensis			JQ730180/JQ730389/JQ730598					+
Tibouchina fissinervia			JQ730181/JQ730390/JQ730599					+
Tibouchina fothergillae			JQ730182/JQ730391/JQ730600					+
Tibouchina foveolata			JQ730183/JQ730392/JQ730601					+
Tibouchina fraterna			JQ730184/JQ730393/JQ730602					+

Taxon	Population	Pop Nº	Genbank accession numbers (ITS/*acc*D-*psa*I/*psb*K-*psb*L)	Voucher	Hap-ETS	Hap-cpDNA	PR Castratella (ETS/*trn*G/*rpl*32-*trn*L)	PR Melastomeae (ITS/*acc*D-*psa*I/*psb*K-*psb*L)
Tibouchina frigidula			JQ730185/JQ730394/JQ730603					+
Tibouchina gardneriana			JQ730186/JQ730395/JQ730604					+
Tibouchina gayana			JQ730187/JQ730396/JQ730605					+
Tibouchina geitneriana			JQ730188/JQ730397/JQ730606					+
Tibouchina gleasoniana			JQ730189/-/JQ730607					+
Tibouchina gracilis			JQ730190/JQ730398/JQ730608					+
Tibouchina granulosa			JQ730191/JQ730399/JQ730609					+
Tibouchina grossa			JQ730192/JQ730400/JQ730610					+
Tibouchina heteromalla			JQ730193/JQ730401/JQ730611					+
Tibouchina hieracioides			JQ730194/JQ730402/JQ730612					+
Tibouchina hospita			JQ730195/JQ730403/JQ730613					+
Tibouchina inopinata			JQ730196/JQ730404/JQ730614					+
Tibouchina itatiaiae			JQ730197/JQ730405/JQ730615					+
Tibouchina kleinii			JQ730198/JQ730406/JQ730616					+
Tibouchina laevicaulis			JQ730199/JQ730407/JQ730617					+
Tibouchina laxa			JQ730200/JQ730408/JQ730618					+
Tibouchina lepidota			JQ730201/JQ730409/JQ730619					+
Tibouchina lindeniana			JQ730202/JQ730410/JQ730620					+
Tibouchina llanorum			JQ730203/JQ730411/JQ730621					+

Taxon	Population	Pop Nº	Genbank accession numbers (ITS/*acc*D-*psa*I/*psb*K-*psb*L)	Voucher	Hap-ETS	Hap-cpDNA	PR Castratella (ETS/*trn*G/*rpl*32-*trn*L)	PR Melastomeae (ITS/*acc*D-*psa*I/*psb*K-*psb*L)
Tibouchina longifolia			JQ730204/JQ730412/JQ730622					+
Tibouchina macrochiton			JQ730205/JQ730413/JQ730623					+
Tibouchina manicata			JQ730206/JQ730414/JQ730624					+
Tibouchina martialis			JQ730207/JQ730415/JQ730625					+
Tibouchina martiusiana			JQ730208/JQ730416/JQ730626					+
Tibouchina melanocalyx			JQ730209/JQ730417/JQ730627					+
Tibouchina microphylla			JQ730210/JQ730418/JQ730628					+
Tibouchina minor			JQ730211/JQ730419/JQ730629					+
Tibouchina mollis			JQ730212/JQ730420/JQ730630					+
Tibouchina mutabilis			JQ730213/JQ730421/JQ730631					+
Tibouchina naudiniana			JQ730214/JQ730422/JQ730632					+
Tibouchina nodosa			JQ730215/JQ730423/JQ730633					+
Tibouchina octopetala			JQ730216/JQ730424/JQ730634					+
Tibouchina oreophilla			JQ730217/JQ730425/JQ730635					+
Tibouchina ornata			JQ730218/JQ730426/JQ730636					+
Tibouchina papyrus			JQ730219/JQ730427/JQ730637					+
Tibouchina pendula			JQ730220/JQ730428/JQ730638					+
Tibouchina pereirae			JQ730221/JQ730429/JQ730639					+
Tibouchina pulchra			JQ730222/JQ730430/JQ730640					+

Taxon	Population	Pop Nº	Genbank accession numbers (ITS/*acc*D-*psa*I/*psb*K-*psb*L)	Voucher	Hap-ETS	Hap-cpDNA	PR Castratella (ETS/*trn*G/*rpl*32-*trn*L)	PR Melastomeae (ITS/*acc*D-*psa*I/*psb*K-*psb*L)
Tibouchina radula			JQ730223/JQ730431/JQ730641					+
Tibouchina ramboi			JQ730224/JQ730432/JQ730642					+
Tibouchina salviaefolia			JQ730225/JQ730433/JQ730643					+
Tibouchina sebastianopolitana			JQ730226/JQ730434/JQ730644					+
Tibouchina sellowiana			JQ730227/JQ730435/JQ730645					+
Tibouchina semidecandra			JQ730228/JQ730436/JQ730646					+
Tibouchina sp			JQ730229/JQ730437/JQ730647					+
Tibouchina sp ined1			JQ730230/JQ730438/JQ730648					+
Tibouchina sp ined2			JQ730231/JQ730439/JQ730649					+
Tibouchina sp ined3			JQ730232/JQ730440/JQ730650					+
Tibouchina stenocarpa			JQ730233/JQ730441/JQ730651					+
Tibouchina striphnocalyx			JQ730234/JQ730442/JQ730652					+
Tibouchina trichopoda			JQ730235/JQ730443/JQ730653					+
Tibouchina urceolaris			JQ730236/JQ730444/JQ730654					+
Tibouchina ursina			JQ730237/JQ730445/JQ730655					+
Tibouchina valtherii			JQ730238/JQ730446/JQ730656					+
Tibouchina velutina			JQ730239/JQ730447/JQ730657					+
Tibouchina wurdackii			JQ730240/JQ730448/JQ730658					+
Tibouchina aegopogon			JQ730241/JQ730449/JQ730659					+

Taxon	Population	Pop Nº	Genbank accession numbers (ITS/*acc*D-*psa*I/*psb*K-*psb*L)	Voucher	Hap-ETS	Hap-cpDNA	PR Castratella (ETS/*trn*G/*rpl*32-*trn*L)	PR Melastomeae (ITS/*acc*D-*psa*I/*psb*K-*psb*L)
Tibouchina trinervia			JQ730242/JQ730450/JQ730660					+
Tibouchinopsis mirabilis			JQ730243/JQ730451/JQ730661					+
Trembleya laniflora			AY553744 /-/-					+
Trembleya parviflora			JQ730244/JQ730452/JQ730662					+
Trembleya pentagona			AY553745 /-/-					+
Tristemma coronatum			JQ730245/JQ730453/JQ730663					+
Tristemma hirtum			JQ730246/JQ730454/JQ730664					+
Tristemma littorale			JQ730247/JQ730455/JQ730665					+
Tristemma mauritianum			JQ730248/JQ730456/JQ730666					+
TOTAL					18	15	20	249

Table S4.2. Sample numbers discriminated by geographic origin and altitudinal distribution.

	Tropical				Temperate				TOTAL
	Páramo endemic	Neotropical	Pantropical	Total	Austral-Antarctic	Holarctic	Pantemperate	Total	
Subpáramo	-	23	5	28	1	1	1	3	31
Páramo	10	139	30	179	21	27	34	82	261
Superpáramo	6	33	3	42	9	10	27	46	88
TOTAL	16	195	38	249	31	38	61	131	380

Table S4.3. Test statistics and *p*-values calculated for differences in species richness in relation to geographic origin and altitudinal distribution for the complete Páramo flora. *p*-values in **bold** are significant at the 5% level; n/a, not applicable.

COMPARISON	Kruskal-Wallis test	Conover-Inman test (post-hoc multiple comparison test)
Species richness between elements of tropical and temperate origin	$p = 0.293$	n/a
Species richness amongst the six geographic categories within elements of tropical and temperate origin (Páramo endemic, Neotropical, Pantropical, Austral-Antarctic, Holarctic and Pantemperate)	$p = 0.536$	n/a
Species richness between elements of tropical and temperate origin within Subpáramo	$p = 0.935$	n/a
Species richness between elements of tropical and temperate origin within Páramo	$p = 0.073$	n/a
Species richness between elements of tropical and temperate origin within Superpáramo	$p = 0.386$	n/a
Species richness amongst the six geographic categories within elements of tropical and temperate origin within Subpáramo	$p = 0.578$	n/a
Species richness amongst the six geographic categories within elements of tropical and temperate origin within Páramo	$p = 0.187$	n/a
Species richness amongst the six geographic categories within elements of tropical and temperate origin within Superpáramo	$p = 0.095$	n/a
Species richness amongst altitudinal categories (Subpáramo, Páramo, Superpáramo) within elements of tropical origin	**$p < 0.001$**	**Páramo > Subpáramo ($p < 0.001$)**
		Superpáramo > Páramo ($p < 0.001$)
		Superpáramo > Subpáramo ($p < 0.001$)
Species richness amongst altitudinal categories (Subpáramo, Páramo, Superpáramo) within elements of temperate origin	**$p < 0.001$**	Páramo – Subpáramo ($p = 0.225$)
		Superpáramo > Páramo ($p < 0.001$)
		Superpáramo > Subpáramo ($p = 0.003$)
Species richness amongst altitudinal categories within Páramo endemic elements	$p = 0.956$	n/a
Species richness amongst altitudinal categories within Neotropical elements	**$p < 0.001$**	**Páramo > Subpáramo ($p < 0.001$)**
		Superpáramo > Páramo ($p < 0.001$)
		Superpáramo > Subpáramo ($p < 0.001$)
Species richness amongst altitudinal categories within Pantropical elements	**$p < 0.001$**	**Páramo > Subpáramo ($p = 0.009$)**
		Páramo – Superpáramo ($p = 0.510$)
		Superpáramo > Subpáramo ($p = 0.024$)
Species richness amongst altitudinal categories within Austral-Antarctic elements	$p = 0.453$	n/a
Species richness amongst altitudinal categories within Holarctic elements	**$p = 0.002$**	Páramo – Subpáramo ($p = 0.896$)
		Superpáramo > Páramo ($p < 0.001$)
		Subpáramo – Superpáramo ($p = 0.189$)

Species richness amongst altitudinal categories within Pantemperate elements	***p* < 0.001**	Páramo – Subpáramo (*p* = 0.357)
		Superpáramo > Páramo (*p* < 0.001)
		Superpáramo > Subpáramo (*p* = 0.020)